

# **Advanced water soluble BODIPY dyes: Synthesis and application**

Songlin NIU



UMR 7515 CNRS - UDS

Laboratory of Organic Chemistry and Advanced Spectroscopy,

Doctoral School of Chemistry, University of Strasbourg

Strasbourg

France

Thesis submitted to the University of Strasbourg for the  
degree of doctor of philosophy

July 2011



## Examining Committee

Dr. Olivier MAURY

Dr. Pei YU

Dr. Maurice GOELDNER

Dr. Gilles ULRICH

Dr. Raymond ZIESSEL

External rapporteur

External rapporteur

External examiner

Supervisor

Supervisor



*To Cheng Ting*



# Acknowledgements

This dissertation describes the work effectuated at the Laboratory of Organic Chemistry and Advanced spectroscopy at European Engineering School of Chemistry of Strasbourg (University of Strasbourg) from autumn 2007 until summer 2011. During this time I had the pleasure of meeting and working with a lot of great people from whom I learned so much, and who have had a deep influence on my work and my life for the past years.

The greatest scientific influence has naturally come from my two supervisors: Dr. Raymond Ziessel and Dr. Gilles Ulrich. I am very grateful to Dr. Raymond Ziessel for giving me the opportunity to join his team and do a PhD. Over the years, it has been an inspiration to witness his enthusiasm and vigorous manner for chemical science. The scientific influence of Dr. Gilles Ulrich is apparent in much of the work presented in here. I spent three excellent years under his guidance and I do really appreciate his good humor and vast scientific knowledge. My work would have been much harder without his competent advices, enthusiasm and confidence. It was reassuring to know that his office door was always open for me when the experiments became excessively frustrating. I would also like to express my gratitude towards both supervisors for always giving me the freedom to pursue my own ideas, at my own pace.

I grateful acknowledge the scholarship fund provided by the program of Égide, which was run by the French Ministry of Foreign Affairs to provide support for foreign students to pursue their studies in France.

I would like to thank Dr. Antoinette de Nicola for the care and useful advices she selflessly provided, and especially, for the fruits that she fed me everyday during my redaction. It is heartwarming and I really appreciate it a lot.

I would like to thank also Dr. Michel Schmidt for providing excellent work on NMR experiments as well as his amicableness.

I would also like to thank Pr. Pierre-Yves Renard, Dr. Anthony Romieu and their PhD student Cédrik Massif at group COBRA at Rouen University for their excellent work on post-functionalizing, purifying and especially labeling our BODIPY dyes on bio-molecules.

I would also like to thank Dr. Alberto Barsella and Dr. Alex Boeglin at IPCMS for their hard working on EFISHG measurements and the following computational calculations, as well as the interesting discussions we had on nonlinear optics.

All the present and past members of LCOSA lab – thank you all so much for the memorable experience we had together during the past three and a half years. Franck, Loïc, Steph, Pascal, Soumya, “Grand” Alex, Jub, Batcha, Matthieu, Charlotte, “P’ti” Alex, Sandra, Thomas, Denis, Julien, Delphine, Alexandra, Elodie, Arnaud, Mus, Séb... It has been a great pleasure for me to work with you guys.

I can not thank enough all the friends I have been luck to make since I arrived in France. You have made my life different and made Strasbourg a significant and memorable place for me in the years to come.

A special thanks to my friends Luo Hongteng, Cheng Ting and Chen Zhao, thanks for your support and understanding through all these years.

Finally, we would like to thank my parents for their sacrifices, unconditional love, and support which have enabled me to pursue my crazy ideas.

---

# Table of contents

|   |    |
|---|----|
| <b>CHAPTER I</b> .....  | 1  |
| General introduction .....  | 1  |
| 1.1. Photoluminescence.....   | 1  |
| 1.1.1. Light absorption – Formation of excited state .....                  | 1  |
| 1.1.2. The excited state.....   | 4  |
| 1.2. Organic long emission wavelength fluorophores.....                     | 5  |
| 1.2.1. Fluoresceins .....   | 6  |
| 1.2.2. Rhodamines.....  | 7  |
| 1.2.3. Cyanines.....  | 7  |
| 1.2.4. BODIPY.....  | 8  |
| 1.3. Water-solubilization strategies for BODIPY dyes.....                   | 10 |
| 1.3.1. Nucleophilic substitution on halogenated BODIPY .....                | 10 |
| 1.3.2. Introduction of hydrophilic peptide linkers .....                    | 11 |
| 1.3.3. Introduction of oligo (polyethylene glycol) methyl ether (PEG).....  | 13 |
| 1.3.4. Sulfonation of BODIPY via electrophilic substitution .....           | 13 |
| 1.4. Thesis objective and outline.....                                      | 15 |
| Bibliography.....   | 18 |
| <br>  |    |
| <b>CHAPTER II</b> .....   | 23 |
| New insights into the water-solubilization of BODIPY dyes .....             | 23 |
| 1.1 Introduction .....  | 23 |
| 1.2 Incorporation of benzenesulfonic acid group.....                        | 24 |
| 1.2.1 Introduction of benzenesulfonic ester. ....                           | 24 |
| 1.2.2 Cleavage of the protection group. ....                                | 27 |
| 1.2.3 Optical properties of the sulfonyl/sulfonic ester BODIPYs.....        | 28 |
| 1.3 Introduction of sulfobetaine onto the BODIPY core .....                 | 30 |
| 1.3.1 Direct introduction of sulfobetaine via cross coupling reaction. .... | 30 |
| 1.3.1.1 Optical properties of <b>19</b> .....                               | 31 |
| 1.3.2 Post-synthetic introduction of sulfobetaine.....                      | 32 |
| 1.3.2.1 X-ray analysis of sulfobetaine pyrene <b>21</b> .....               | 33 |
| 1.3.2.2 Optical properties of sulfobetaine pyrene. ....                     | 34 |
| 1.3.3 Post-synthetic introduction of sulfobetaines onto BODIPY core. ....   | 36 |

---

|   |  |    |
|---|--|----|
| 1.3.3.1   | Synthesis of $\beta$ -pyrrolic sulfobetaine BODIPY.....                    | 36 |
| 1.3.3.2   | Optical properties of the $\beta$ -sulfobetaine BODIPY.....                | 37 |
| 1.3.4   | Synthesis of boron-ethynyl-substitued sulfobetaine BODIPY.....             | 38 |
| 1.3.4.1   | Optical properties of BODIPY <b>27</b> .....                               | 39 |
| 1.4   | Functionalization of sulfobetaine BODIPY dye.....                          | 40 |
| 1.4.1   | Synthesis of the BODIPY <b>29</b> .....                                    | 40 |
| 1.4.1.1   | Optical properties of the dye <b>29</b> .....                              | 40 |
| 1.4.2   | Synthesis of the ester BODIPY <b>30</b> .....                              | 41 |
| 1.4.3   | Synthesis of a watersoluble ‘cassette’ BODIPY.....                         | 43 |
| 1.4.4   | Synthesis of ester pyrene <b>33</b> .....                                  | 44 |
| 1.4.4.1   | Optical properties of the pyrene <b>33</b> .....                           | 44 |
| 1.4.5   | Synthesis of the ester pyrene BODIPY <b>35</b> .....                       | 45 |
| 1.4.5.1   | <sup>1</sup> H NMR characterisation of ester pyrene BODIPY <b>35</b> ..... | 46 |
| 1.4.5.2   | Optical properties of compound <b>35</b> .....                             | 47 |
| 1.4.6   | Synthesis of the acid compound <b>36</b> .....                             | 48 |
| 1.5   | Conclusion.....  | 49 |
|   | Reference.....   | 50 |
|   |  |    |
| CHAPTER III   | .....  | 53 |
| Synthesis of Water-soluble Red-emitting BODIPY dyes | .....  | 53 |
| 1.1.  | Introduction.....  | 53 |
| 1.1.1.  | Commercial available water-soluble red-emitting fluorophores.....          | 53 |
| 1.1.2.  | Red-emitting BODIPY.....   | 55 |
| 1.1.3.  | Distyryl-BODIPY dyes.....  | 56 |
| 1.1.4.  | Water-solubilization of distyryl BODIPYs.....                              | 58 |
| 1.2.  | Synthesis of the distyryl BODIPYs.....                                     | 59 |
| 1.2.1.  | Synthesis of distyryl BODIPY <b>40</b> .....                               | 59 |
| 1.2.1.1.  | Photophysical properties of the dye <b>40</b> .....                        | 60 |
| 1.2.2.  | Synthesis of distyryl BODIPY <b>46</b> .....                               | 62 |
| 1.2.2.1.  | Photophysical properties of the dye <b>46</b> .....                        | 63 |
| 1.2.3.  | Synthesis of distyryl BODIPY <b>50</b> .....                               | 64 |
| 1.2.3.1.  | Optical properties of the dye <b>50</b> .....                              | 64 |
| 1.2.4.  | Synthesis of distyryl BODIPY <b>55</b> .....                               | 65 |
| 1.2.4.1.  | <sup>1</sup> H NMR analysis of compound <b>55</b> .....                    | 67 |

---

|                   |  |     |
|-------------------|--|-----|
| 1.2.4.2.          | Photophysical properties of compound <b>55</b> .....                     | 67  |
| 1.3.              | Results and Discussion.....  | 68  |
| 1.3.1.            | Biological labeling evaluation of the distyryl BODIPYs.....              | 70  |
| 1.3.2.            | Two photon absorption and cell imaging application.....                  | 73  |
| 1.3.2.1           | TPA evaluation of the dye <b>55</b> . ....                               | 73  |
| 1.3.2.2.          | Two-photon excitation and fluorescence cell imaging .....                | 75  |
| 1.4.              | Conclusion .....   | 75  |
|                   | References.....  | 77  |
| <br>              |  |     |
| <b>CHAPTER IV</b> | .....  | 83  |
| 1.1               | General.....   | 83  |
| 1.1.1             | Push-pull chromophore for nonlinear optical (NLO) material .....         | 83  |
| 1.1.2             | New insight into BODIPY based push-pull chromophores .....               | 85  |
| 1.2               | Synthesis of BODIPY-bridged push-pull chromophores.....                  | 86  |
| 1.2.1             | Synthesis of chromophores <b>62</b> and <b>65</b> . ....                 | 86  |
| 1.2.1.1           | Optical properties of the push-pull chromophores.....                    | 88  |
| 1.2.1.2           | Electrochemical properties of compound <b>62</b> . ....                  | 93  |
| 1.2.2             | Synthesis of tetracyanobuta-1,3-dienes (TCBDs) BODIPY.....               | 94  |
| 1.2.2.1           | X-ray structure of compound <b>68</b> . ....                             | 95  |
| 1.2.2.2           | The synthesis of the TCBDs chromophores <b>71</b> and <b>72</b> .....    | 96  |
| 1.2.2.3           | Optical properties of the TCBDs-BODIPYs.....                             | 96  |
| 1.2.2.4           | Electrochemical properties of the TCBDs dyes .....                       | 97  |
| 1.2.3             | Synthesis of mono-styryl TCBDs BODIPY .....                              | 100 |
| 1.2.3.1           | Identification of the mono-styryl BODIPYs.....                           | 102 |
| 1.2.3.2           | X-ray analysis of compound <b>75</b> . ....                              | 106 |
| 1.2.3.3           | Optical properties of the asymmetric mono-styryls .....                  | 106 |
| 1.2.4             | Synthesis of TCBDs compound <b>74</b> .....                              | 109 |
| 1.2.4.1           | Optical properties of compound <b>74</b> .....                           | 110 |
| 1.2.4.2           | Electrochemical properties of compounds <b>73</b> and <b>74</b> . ....   | 111 |
| 1.2.5             | The hyperpolarizabilities of the push-pull chromophores .....            | 112 |
| 1.2.5.1           | Studies of resonance effect on the hyperpolarizability of the TCBDs..... | 115 |
| 1.3               | Conclusion .....   | 116 |
|                   | References.....  | 118 |

---

|  |     |
|--|-----|
| <b>Conclusion and Perspective</b> .....                | 123 |
| <b>Experimental</b> .....                              | 125 |
| General Methods. ....                                  | 125 |
| CHAPTER II.....  | 126 |
| CHAPTER III .....                                      | 144 |
| CHAPTER IV .....                                       | 159 |
| <b>Appendix</b> .....                                  | 167 |
| A. Crystallographic data .....                         | 167 |
| B. Publication/Patent produced during the thesis ..... | 170 |

# CHAPTER I

## General introduction

Since the invention of confocal microscopy and more advanced instruments such as Zewail's femtosecond ( $\times 10^{-15}$  sec) spectroscopy developed in the 1990's, the fluorescence has been widely used as a sensitive analytical technique in the domain of environmental detection, medicine, pharmacy and life sciences. The biological labelling is one of the most studied domains in the life sciences, thanks to those advances in engineering of imaging devices and development in chemistry of imaging probes. The development of fluorescent probes that are suitable for specific applications in biological conditions is crucial in those researches. The main theme of this thesis is to develop a set of water-soluble fluorophores as molecular probes for biological labeling applications. This work was based on the functionalization of 4,4-difluoro-4-bora-3a,4a-diaza-s-indacene (BODIPY) as fluorescent framework, in order to introduce water solubility and functional groups to: (i) tune the color; (ii) to graft the probes to bio-molecules; (iii) to increase the dipole moment in the ground and excited states...

### 1.1. Photoluminescence

Photoluminescence is an optical property of a substance which absorbs photons (via electromagnetic radiation) and then releases these photons radiatively.<sup>1</sup> In this process, an electronically excited state is formed rapidly after the absorption of light, and then dissipates by emission of photons or heat. Photoluminescence is formally divided into two categories, fluorescence and phosphorescence, depending on the nature of the excited states.<sup>2</sup> The background information about the process of photoluminescence will be discussed in the following section.

#### 1.1.1. Light absorption – Formation of excited state

##### Absorption of light

The transition of an electron of a molecule from HOMO to LUMO induced by radiation can be regarded as a change in state.<sup>3</sup> The energy required for such electronic transition lies in the range of 60 to 150 kcal mole<sup>-1</sup> which corresponding to the 200 - 800 nm wavelength window (Figure 1).

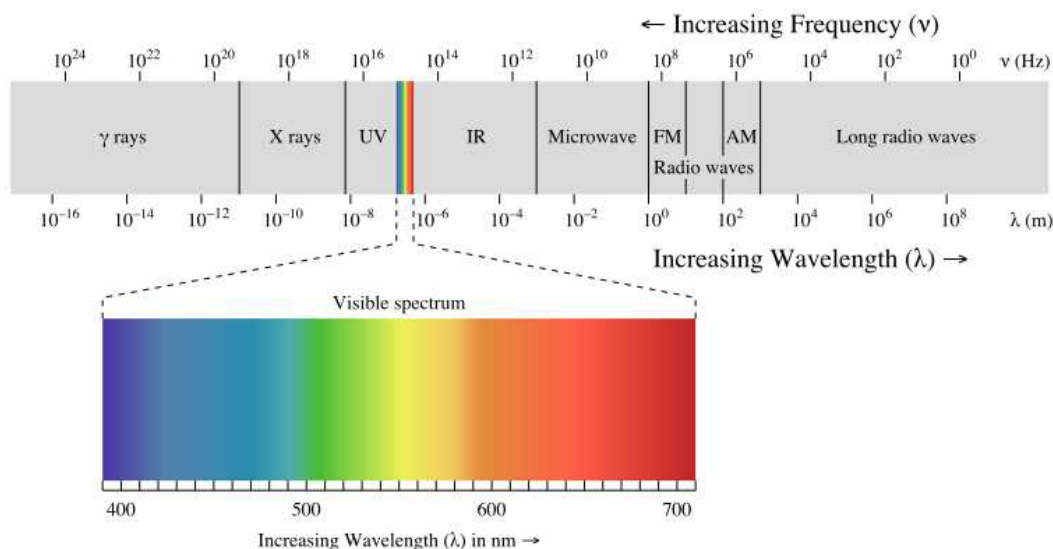


**Figure 1. Electromagnetic spectrum and the visible region.**

## Molar absorption coefficient

The intensity of the absorption as a function of wavelength, measured by UV/Visible absorption spectroscopy is depending on the molar absorption coefficient  $\epsilon$  at a defined wavelength. The absorption coefficient is the measurement of the probability of an electronic transition from ground to excited state at a given wavelength. If the  $\epsilon$  is greater than  $10^5 \text{ M}^{-1} \cdot \text{cm}^{-1}$ , then the transition is fully allowed; whereas the  $\epsilon$  is below  $100 \text{ M}^{-1} \cdot \text{cm}^{-1}$ , then the transition is forbidden which indicates that the probability of transition is very weak. The in-between area, for  $\epsilon$  values between  $10^2$  and  $10^4 \text{ M}^{-1} \cdot \text{cm}^{-1}$ , corresponds to transitions that are “partially” allowed. The quantum mechanical rules are based primarily on two components — spin and symmetry. If the transition involves a change of spin (*e.g.* singlet to triplet) then the transition is forbidden. The symmetry component examines the symmetry between the ground and excited state, and depending on these symmetries the transition will be allowed or forbidden. Hence, if a transition is spin-forbidden, symmetry allowed, then the probability is very weak, and  $\epsilon$  values will be  $<100$ . But the transition is spin-allowed and symmetry forbidden, then the molar absorption coefficient may be observed between  $10^2$  and  $10^4 \text{ M}^{-1} \cdot \text{cm}^{-1}$ .

## Electronic absorption spectra

The form of the electronic absorption spectrum is related to the value of  $\epsilon$  at each wavelength. However, for an individual electronic transition, the transitions between vibrational levels of each orbital may be more intense than others. These transitions are governed by the Franck-Condon principle: “In the very short time required for an electronic transition to take place (about  $10^{-15}$  sec),

the atoms in a molecule do not have time to change position appreciably.” Since the electronic transitions take place so quickly, the molecule will be in the same molecular configuration and vibrational kinetic energy in the excited state than in the ground state. As a result, all electronic transitions are indicated by a vertical line on the Morse potential diagram of the ground and excited states (Figure 2. left).

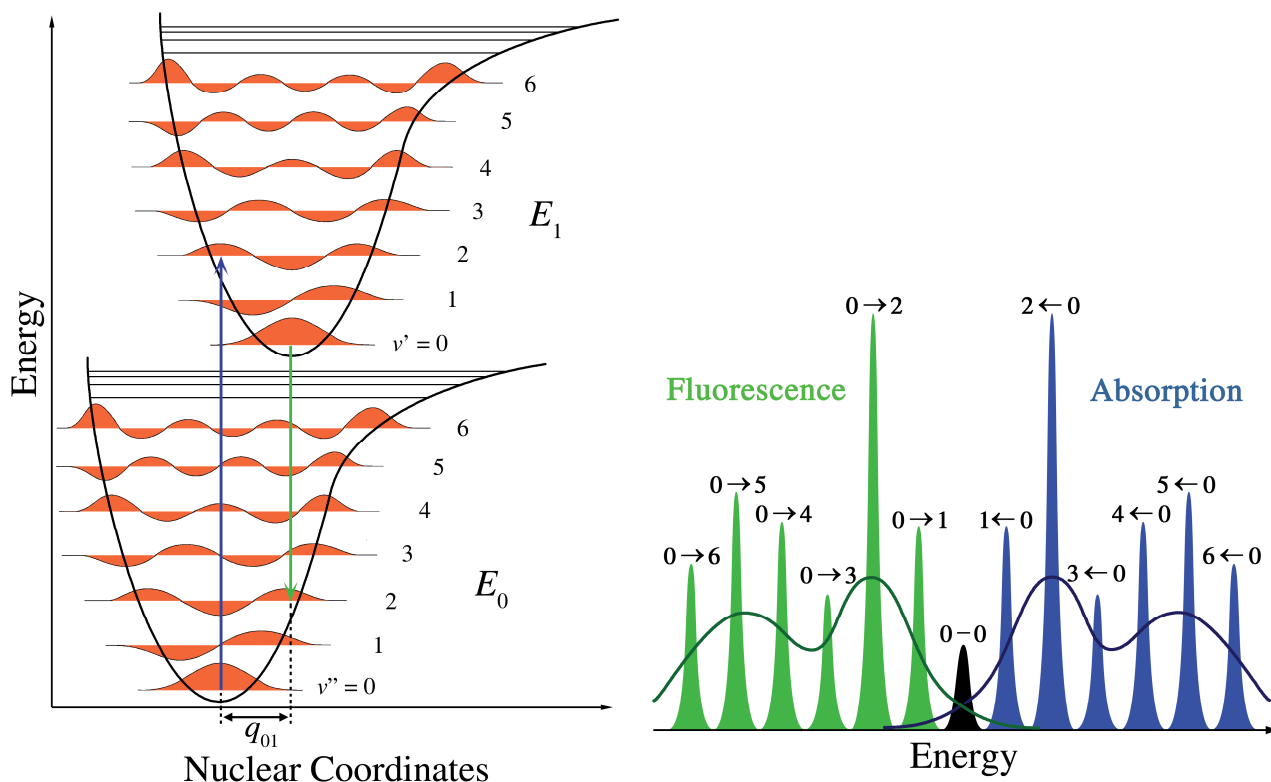


Figure 2. Left, Franck-Condon principle diagram for the transition between ground and excited states. Right, electronic absorption and fluorescence emission spectra. <sup>5</sup>

There is no change in internuclear distance during the transition. However, the electron configuration of the new state may result in a shift of the equilibrium position of the nuclei constituting the molecule. This shift in nuclear coordinates between the ground and the first excited state is indicated as  $q_{01}$  (Figure 2. left). The probability of transition that the molecule can end up in any particular vibrational level is proportional to the square of the (vertical) overlap of the vibrational wave functions of the original and final state. Therefore the most probable transition between the ground and excited states will be the one where the wavefunctions overlap the most in the vertical line. The most favourable overlap is the ground state vibrational level  $v = 0$  and the excited state vibrational level  $v = 2$ . The differences in wavelength at which the peaks occur represent the energy differences of the vibrational levels in the excited state of the molecule (Figure 2. right). However, the fine structure of the narrow lines can only be observed in the spectra of

dilute gases. In liquids and solids, the absorption spectra are essentially a line drawn covering the tops of the individual transition peaks and resulting in the broad curves.

In addition, the Franck–Condon principle can be applied equally to absorption and to fluorescence emission spectra, in the diagrams the molecule in the electronic excited state quickly relax to the lowest vibrational level, and from there can decay to the ground state via photon emission. The details of these relaxation processes will be discussed in the following section.

### 1.1.2. The excited state

#### The Jablonski diagram

After a photon is absorbed by a molecule promoting the transition of an electron from the HOMO to the LUMO, the excited state is formed. However, this state is energetically unstable and usually short-lived; the absorbed energy will be quickly released. Between the absorption of photon to form the excited state and the relaxation of energy to return to the ground state, a series of processes consequently occur, which could be illustrated by the Jablonski diagram (Figure 3).

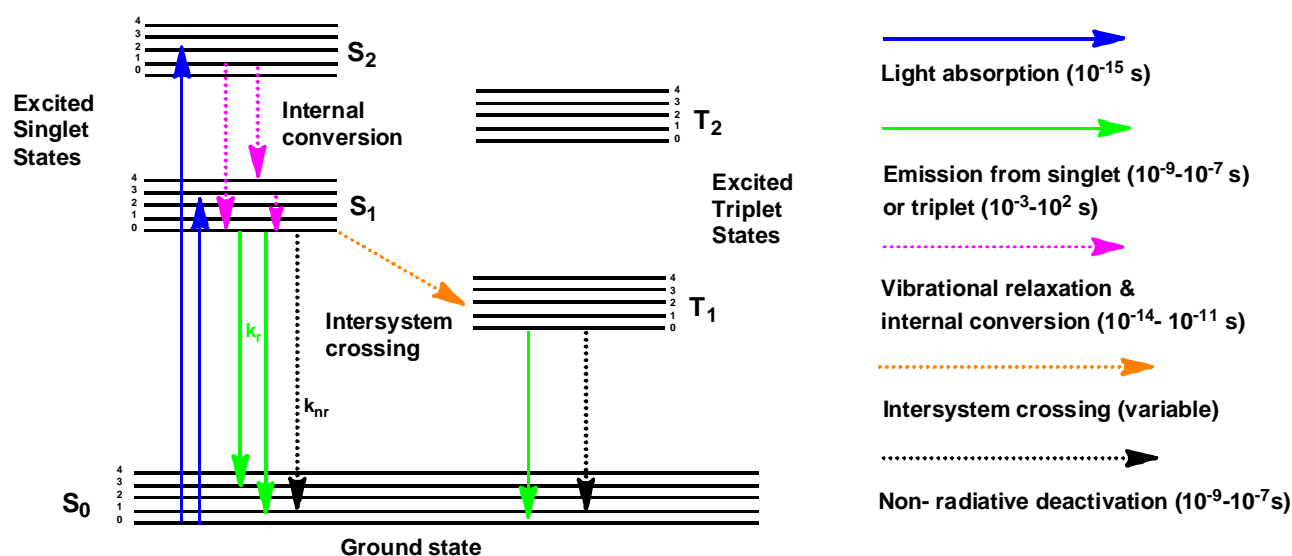


Figure 3. Jablonski diagram for a molecule upon excitation.

The Jablonski diagram illustrates upon excitation the molecular electronic states and the energy transitions between them. Following light absorption, an electron is promoted to the higher vibrational level of  $S_1$  or  $S_2$ . The electron in the upper vibrational levels rapidly relaxes to the lowest vibrational level  $S_1$ . This process is called internal conversion and generally occurs within  $10^{-12}$  s or less. Then the electron returns to the ground state by releasing a photon (fluorescence) or by nonradiative deactivation. The return of electron to the ground state typically occurs to a higher

excited vibrational ground state level which can be illustrated by the vibrational structures (Figure 2. left). It is noteworthy that the emission process happens from the lowest vibrational state  $S_1$ . The emission spectra and fluorescence quantum yields are generally independent of the excitation wavelength, known as Kasha's rule.<sup>6</sup> Therefore, the emission spectra are the mirror image of  $S_0 \rightarrow S_1$  absorption and not of the total absorption spectra (Figure 2. right).

The electron in the  $S_1$  state can also undergo a spin conversion to the first triplet state  $T_1$ . The conversion of  $S_1$  to  $T_1$  is called intersystem crossing, and it is forbidden in the idealized conditions; however, in reality such transition can be favored by the presence of a heavy atom on the molecule or present in the solvent. Emission from  $T_1$  is termed phosphorescence, and is generally shifted to longer wavelengths (lower energy region) relative to the fluorescence. In addition, the rate constants for triplet emission are several orders of magnitude smaller than those of fluorescence, which can last for several microseconds or even longer.

### Fluorescence lifetime and quantum yield

The fluorescence quantum yield  $\phi$  and lifetime  $\tau$  are the most important characteristic of a fluorophore. Quantum yield is the ratio of the number of photons emitted to the number of photons absorbed, which can be determined by two factors, the radiative rate  $k_r$  and non-radiative rate  $k_{nr}$ . In practice, the fluorescence quantum yields are determined by comparison with standard fluorophore with known quantum yield. The determination of the quantum yield is generally accomplished by comparison of the wavelength integrated intensity of the unknown dye with respect to the standard.<sup>7</sup>

$$\phi = \frac{k_r}{k_r + k_{nr}}$$

The lifetime of the excited state is defined by the average time the molecule stays in its excited state and is represented by the equation below. The lifetime can be determined by calculating the average time in the excited state by time-resolved measurements. New technologies were developed based on these measurements which provide information that are not available from the steady-state data, such as fluorescence lifetime imaging microscopy (FLIM) for biological cell imaging, where the image contrast is based on the lifetime in each region of the sample.<sup>8</sup>

$$\tau = \frac{1}{k_r + k_{nr}}$$

## 1.2. Organic long emission wavelength fluorophores

During the last 20 years there has been a remarkable growth in the use of fluorescence in life science. Fluorescence is now a dominant methodology used extensively in biotechnology for

medical diagnostics.<sup>9-11</sup> Fluorescence detection is highly sensitive, and there is no longer the need for the expense and difficulties of handling radioactive tracers for biochemical measurements. Nowadays thousands of organic fluorophores have been discovered and developed. In the following section, we will give a brief overview of the well-known organic fluorophore families which usually emit beyond 500 nm; the chemical classes discussed comprise fluoresceins, rhodamines, cyanines, and 4,4-difluoro-4-bora-3a,4a-diaza-s-indacene (BODIPY) dyes.<sup>12</sup>

### 1.2.1. Fluoresceins

Fluorescein is a polycyclic fluorophore that belong to the xanthene class of dyes,<sup>13</sup> with absorption and fluorescence maxima in the visible region ( $\lambda_{\text{abs}}$  490 nm and  $\lambda_{\text{em}}$  512 nm, in water). Fluorescein is one of the most common used fluorophore in bio-labelling.<sup>14</sup> It can be synthesized from phthalic anhydride and 1,3-dihydroxy-benzene in presence of zinc chloride via a Friedel-Craft reaction (Figure 4).<sup>15,16</sup>

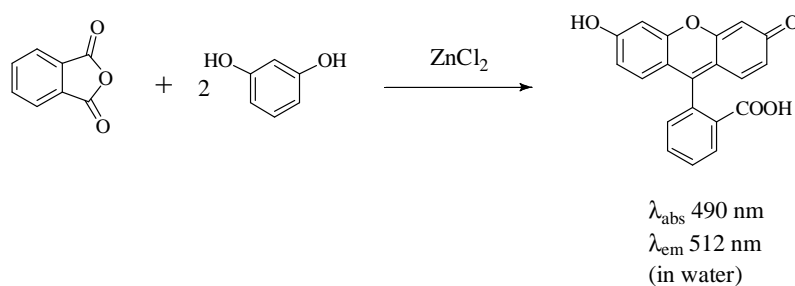


**Figure 4. Synthesis of Fluorescein.**

Relatively high molar extinction coefficient, high fluorescence quantum yield, and good water-solubility were observed for fluorescein dyes, these remarkable properties make them important molecular probes in biolabelling applications. However, the fluoresceins have some disadvantages as well: high rate of photobleaching;<sup>17,18</sup> absorption/emission pH-dependency;<sup>19</sup> relatively broad emission spectra;<sup>20</sup> tendency of self-quenching after bioconjugation.<sup>21,22</sup>

In addition, there are many fluorescein derivatives. For example, fluorescein isothiocyanate, often abbreviated as FITC, is the original fluorescein molecule functionalized with an isothiocyanate group (-N=C=S), replacing a hydrogen atom on the bottom ring of the structure. This derivative is reactive towards amine groups of proteins to form a thiourea linkage.<sup>23,24</sup> A succinimidyl-ester functional group attached to the fluorescein core, creating NHS-fluorescein, forms another common amine-reactive derivative, yielding more stable adducts.

### 1.2.2. Rhodamines

The rhodamine dyes are well known as fluorescence markers in biology such as rhodamine 6G, Texas red, and rhodamine B. They belong to the xanthene class of dyes as well. The rhodamine

dyes generally have strong absorption and emission spectra in the visible region, compare with fluoresceins dyes the rhodamine dyes are more photostable and less sensible to pH.<sup>25</sup> The rhodamine dyes have been widely used as biolabelling maker, photosensitizers and laser dyes.<sup>26,27</sup> However, poor water-solubility of rhodamines dyes limits their applications in biolabelling applications. In 2006, Burgess and co-workers synthesized a rhodamine dye which processes four carboxylic acid to promote water solubility and facilitate conjugation to proteins (Figure 5).<sup>28</sup>

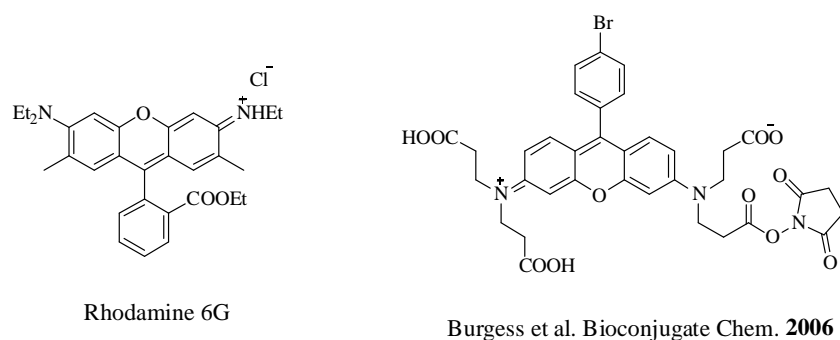


**Figure 5. Structures of Rhodamine dyes.**

### 1.2.3. Cyanines

The cyanine dye is one of the most commonly used long-wavelength fluorophore family in bioconjugation. The basic structure of cyanine dyes includes two aromatic or heterocyclic rings linked by a polymethine chain with conjugated carbon-carbon double bonds.<sup>12</sup> The cyanine dyes are the most familiar long wavelength fluorophores, with emission spectra in the 600-900 nm range; and high extinction coefficient ( $> 100000 \text{ M}^{-1} \cdot \text{cm}^{-1}$ ).<sup>29</sup> The cyanine dyes are widely used in biolabelling applications,<sup>14,30,31</sup> and cell imaging.<sup>9,31</sup> However, the cyanine dyes have also some drawbacks, such as poor water solubility, low quantum yield (usually  $< 25\%$ ), tendency to aggregate in aqueous conditions. In 2008, Romieu and co-worker developed a new synthetic route to improve the cyanine dye's water solubility by introducing a polysulfonate peptide linker (Figure 6).<sup>32</sup>

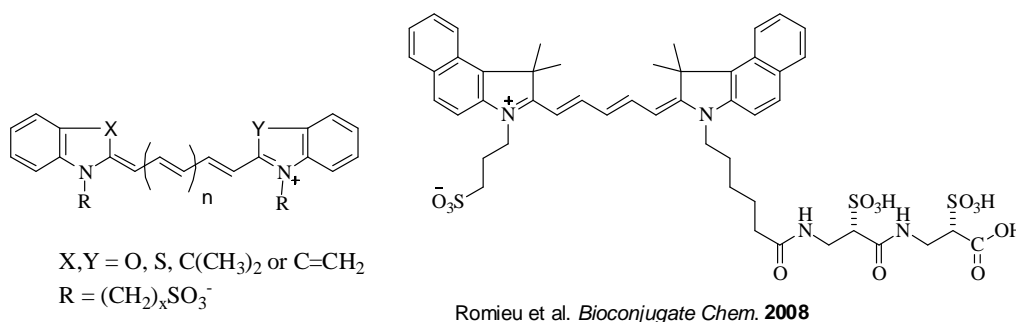


**Figure 6. Basic structure of cyanine dye and the Cy 5.5 analogue NIR 5.5-ws.**

### 1.2.4. BODIPYs

The fluorophore BODIPY is a registered trademark of Molecular Probes, the molecular structure is based on the 4,4-difluoro-4-bora-3a,4a-diaza-s-indacene platform (Figure 7), and the name was derived from BOron DIPYrromethenes.<sup>14</sup>

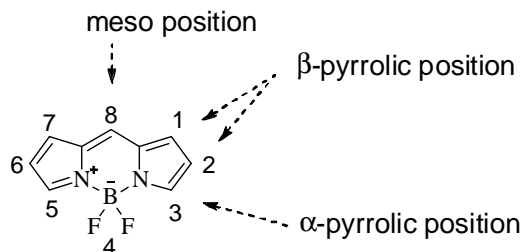


**Figure 7. General structure of BODIPY.**

BODIPY dyes were first synthesized in 1968 by Treibs and Kreuzer,<sup>33</sup> but only until 90's the BODIPY dyes began to attract the attention of biochemist and biologist as a new candidate for fluorescence makers. BODIPY dyes have been considered as substitute for fluoresceins and rhodamines. 8-substitued BODIPY dyes can be easily obtained via condensation of acyl chlorides with pyrroles, followed by complexation with  $\text{BF}_3 \cdot \text{Et}_2\text{O}$  in the presence of a base giving BODIPY derivatives in satisfactory yields (Figure 8).<sup>34,35</sup>

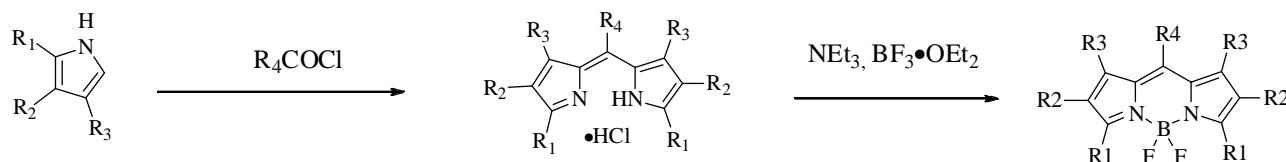


**Figure 8. Synthesis of BODIPY dye.**

Depending on precise post-functionalization on the BODIPY core at meso,  $\alpha,\beta$ -pyrrolic or even at the 4 position, the emission maximum of BODIPY dyes extend in the 510-800 nm range (Figure 9).<sup>36,37</sup> BODIPY dyes have the additional advantage of high extinction coefficients ( $\epsilon > 50,000$ ), high fluorescence quantum yield ( $\phi > 70\%$ ), sharp emission peak, insensitivity to solvent polarity and pH, good photostability and chemical stability. Furthermore, not only their absorption /emission spectra, but also their electrochemical signatures can be tuned by modification of the pyrrolic core.<sup>36-38</sup> All these remarkable properties enable the BODIPY based dyes to be applied in wide applications, such as molecular biolabelling,<sup>12,39</sup> cell imaging,<sup>40,41</sup> chemical sensors,<sup>40,42,43</sup> two photon absorption,<sup>44-46</sup> dye sensitized and bulk heterojunction solar cells.<sup>47-50</sup>

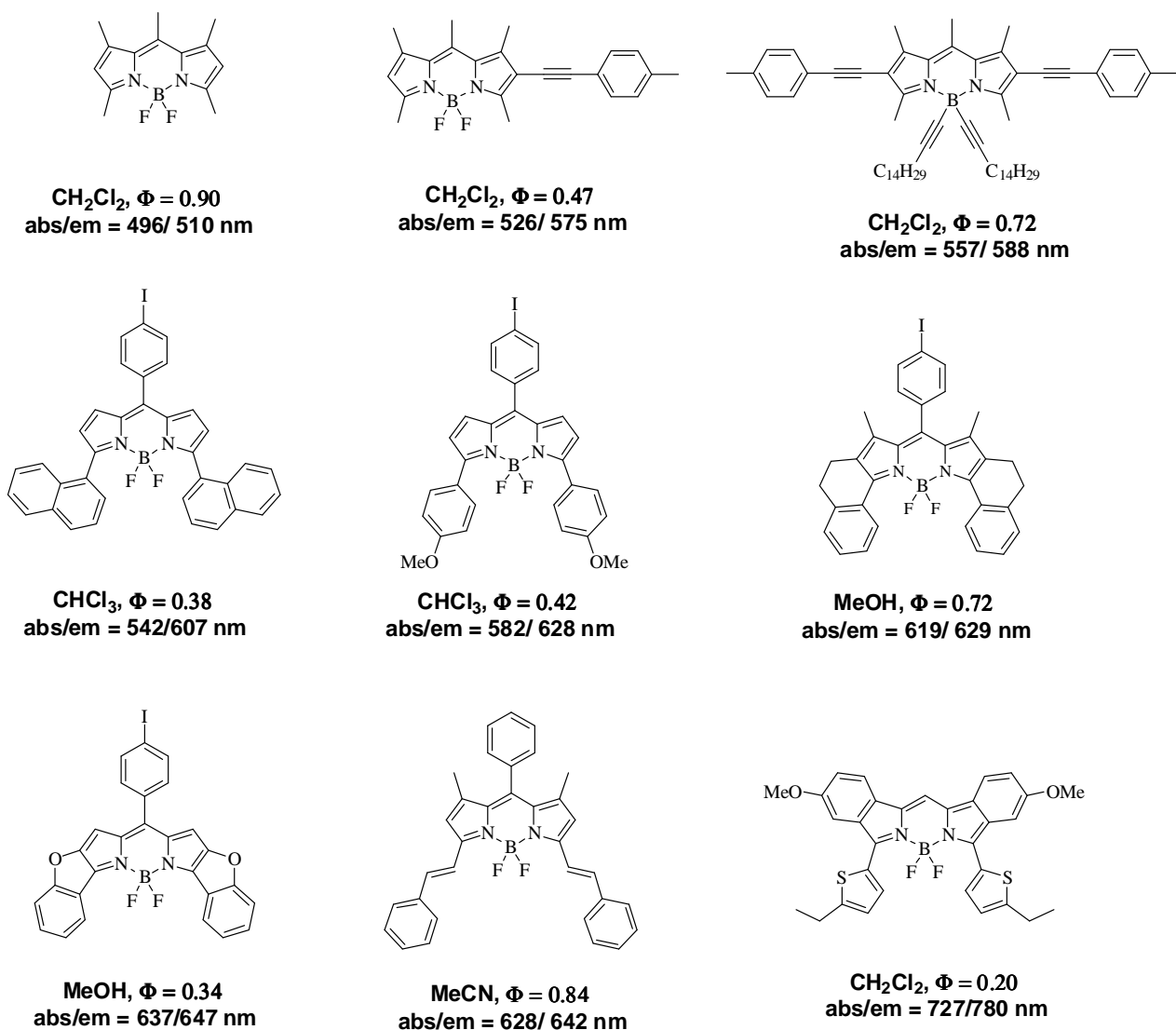


Figure 9. Structures of several BODIPY dyes and their optical properties.

A common drawback for BODIPY dyes is that the Stokes shift is too small for optimum use in flow cytometry and fluorescence microscopy.<sup>51,52</sup> Nevertheless, the Stokes shifts of the BODIPY dyes could be virtually improved by covalent attachment of an ancillary light absorber to the BODIPY core to form an energy transfer cassette.<sup>52-54</sup> However, the hydrophobic nature of BODIPY core is much more problematic for applications in biological labeling. A good water-solubility is necessary for the fluorescent probe to be used in biological conditions. However, self-quenching or aggregation in water is the main problem for such dyes to be used as molecular probes. Nowadays, only a few commercial BODIPY dyes soluble in water and possessing an additional functional group for biolabelling are available.<sup>14</sup> Meanwhile, the synthetic strategies that could conveniently provide a series of water-soluble BODIPY dyes which are suitable for bioconjugation are still limited. We will give an overview of these available strategies in the following section.

## 1.3. Water-solubilization strategies for BODIPY dyes

### 1.3.1. Nucleophilic substitution on halogenated BODIPY

The presence of good leaving groups, such as chlorides at the 3,5 position of the BODIPY core, allows introducing functional groups onto the BODIPY scaffold via  $S_NAr$  reactions (Figure 10a).<sup>55,56</sup> In 2008 Burgess and coworker synthesized water soluble BODIPY dyes by successive introduction of two adequate groups on the BODIPY core (Figure 10b).<sup>57</sup> This strategy was also applied by Jiao and others for the synthesis of BODIPY dyes for use in aqueous conditions.<sup>58,59</sup>

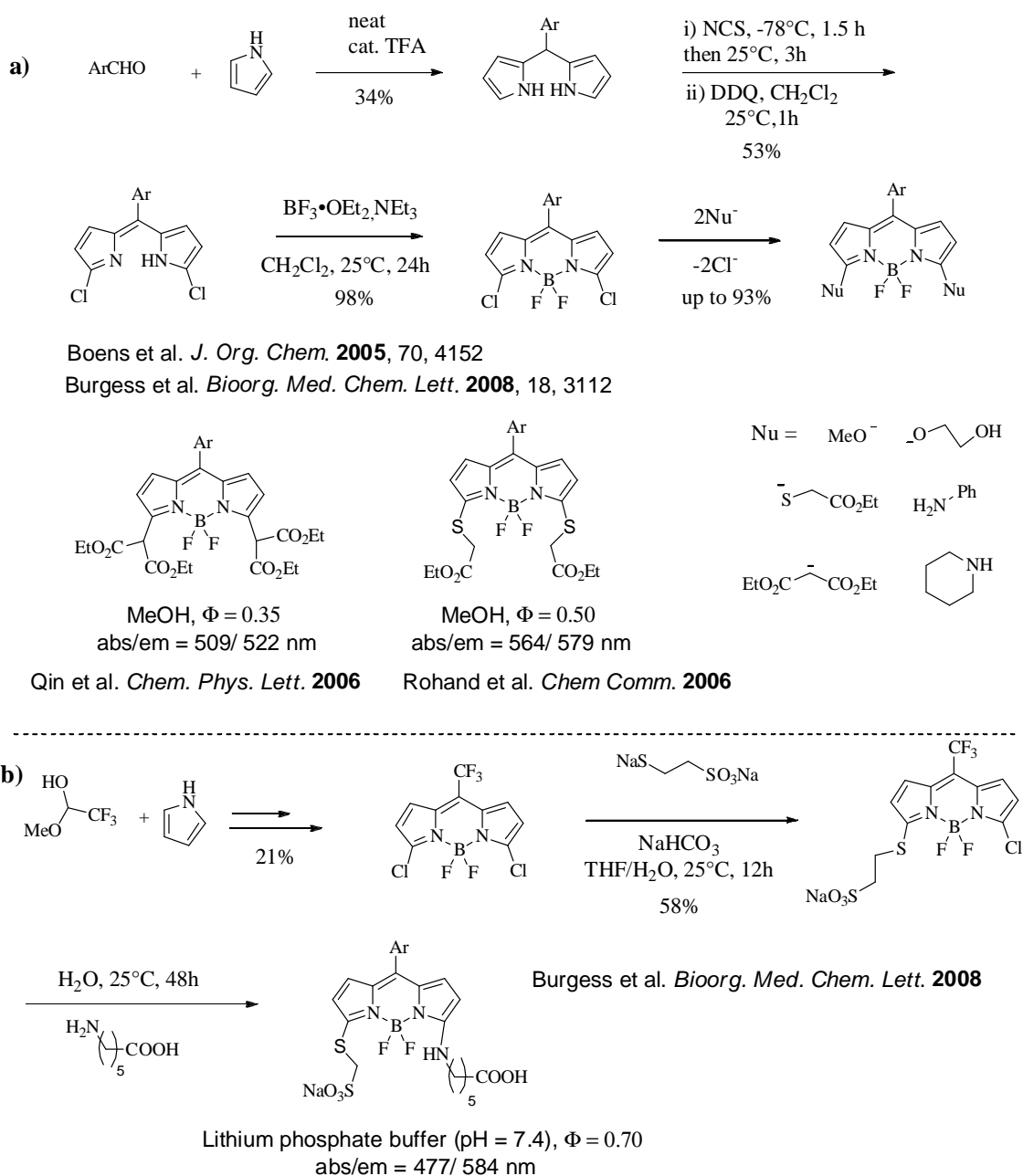


**Figure 10. Synthesis of water soluble BODIPY via nucleophilic substitution reactions.**

### 1.3.2. Introduction of hydrophilic peptide linkers

The enhanced water solubility can also be achieved by introduction of a hydrophilic dipeptide linker between the BODIPY core and the reactive succinimidyl ester group. The hydrophilic dipeptide linker group can be introduced on the BODIPY scaffold which carrying a carboxylic acid group.<sup>60,61</sup> In this strategy, the carboxylic acid BODIPY dye was prepared by a condensation reaction of a functionalized pyrrole, which was then activated by *N*-hydroxysuccinimidyl (NHS) to form the NHS ester BODIPY derivatives. The prepared dipeptide was then introduced onto the BODIPY scaffold via an acylation with the NHS BODIPY. Followed by a second carboxylic acid activation with NHS in DMF, the dipeptide NHS ester BODIPY derivative was ready for the bioconjugation (Figure 11).

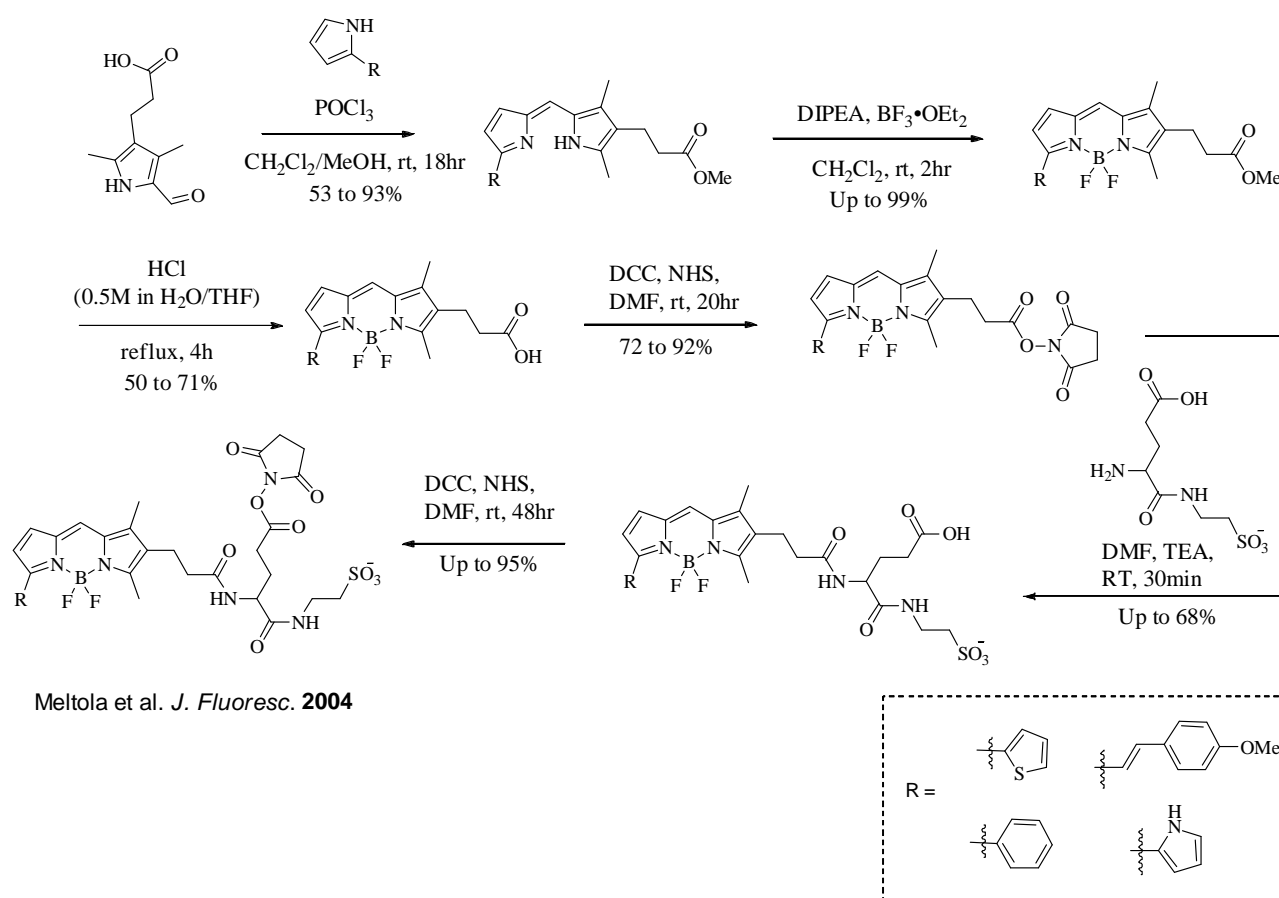


**Figure 11. Introduction of sulfonated peptide linker onto the BODIPY at  $\beta$ -pyrrolic position.**

In 2009, Romieu and coworkers prepared a disulfonated peptide linker and introduced it to the BODIPY dye carrying a carboxylic acid at the meso position (Figure 12a).<sup>62</sup> The disulfonated linker ( $\alpha$ -sulfo- $\beta$ -alanine)<sub>2</sub> was prepared from the coupling between two  $\alpha$ -sulfo- $\beta$ -alanine units.<sup>32</sup> The sulfonation of  $\beta$ -alanine with oleum (25%) gave the racemic  $\alpha$ -sulfo- $\beta$ -alanine in 54%. Followed by the protection of the N-terminal the amino group with fluorenylmethyloxycarbonyl (Fmoc) derivative gave the Fmoc- $\alpha$ -sulfo- $\beta$ -alanine in 95% yield. Then the carboxylic acid group was

converted into the corresponding NHS ester before coupling with the second  $\alpha$ -sulfo- $\beta$ -alanine to give the Fmoc-disulfonated peptide linker. Ultimately, deprotection of the Fmoc group with diethylamine performed in DMF gave the free amine disulfonated linker in 87%.

Similar strategy was also applied by Brellier et al in 2010, using the moiety of nitrilotriacetic acid as water-solubilization group (Figure 12b).<sup>63</sup>

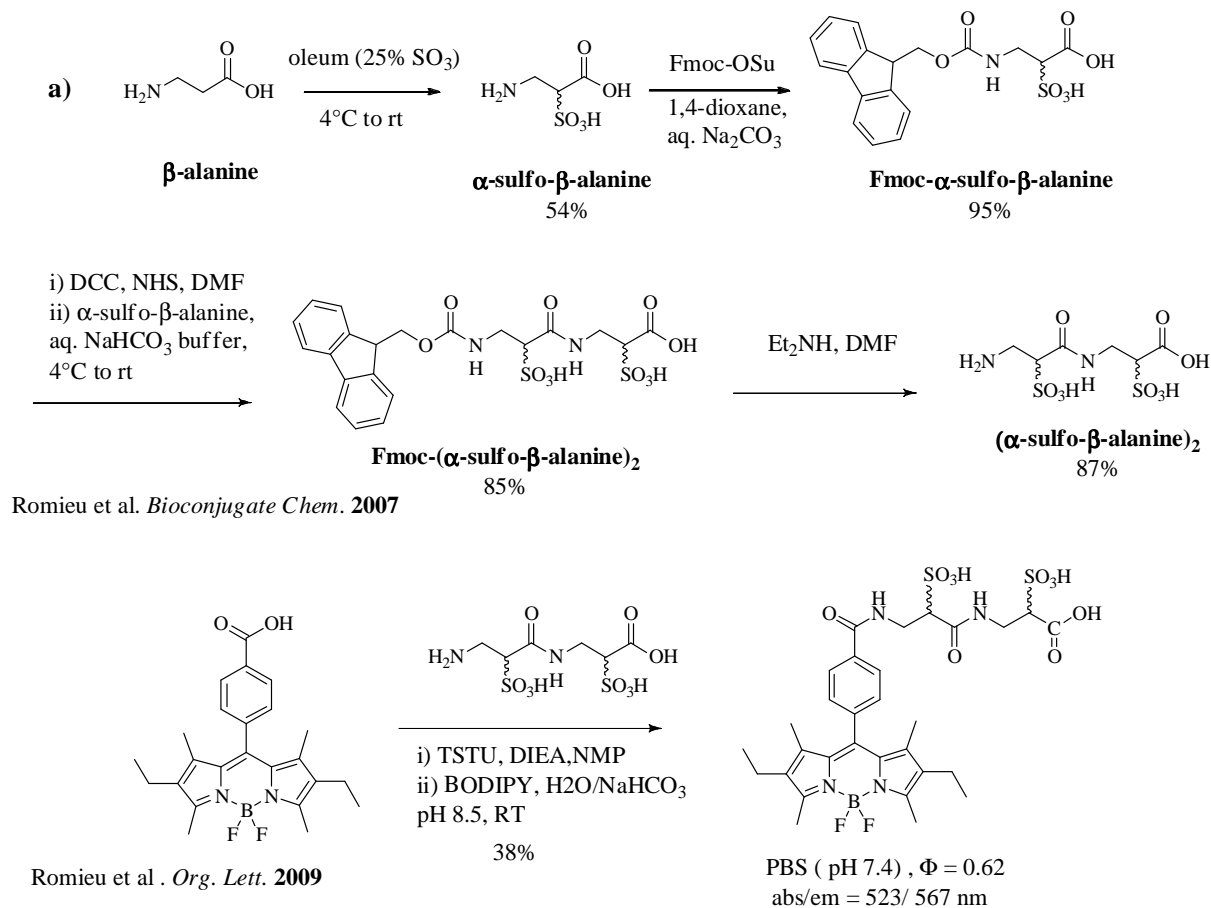
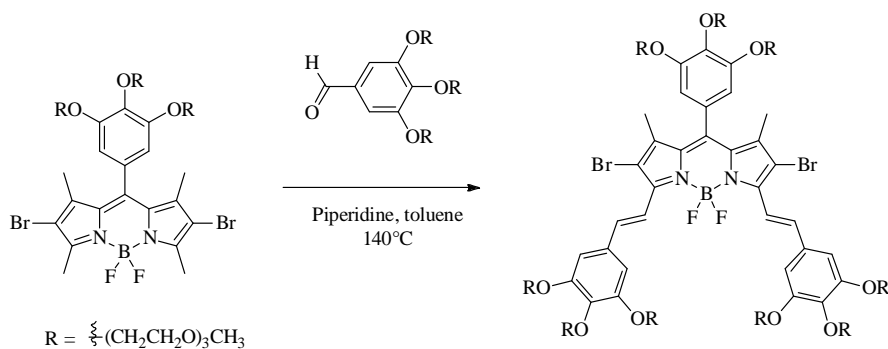


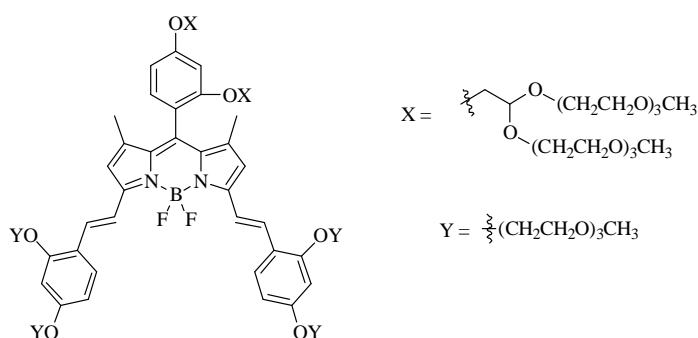
Figure 12. Introduction of polypeptide linker at meso position of BODIPY dye.

### 1.3.3. Introduction of oligo (polyethylene glycol) methyl ether (PEG)

Incorporation of branched PEG onto BODIPY dyes could also effectively enhance enthalpic interactions of BODIPY dyes with water, and significantly increase the water solubility of the dyes. Moreover, the induced steric hindrance by PEG could significantly reduce the formation of aggregates. Owing to the amphiphilic nature of PEG, introduction of the PEG groups onto BODIPY scaffold leads to a series of amphiphilic BODIPY dyes which are soluble in both water and organic solvents (Figure 13).<sup>64-67</sup>



Atilgan et al. *Chem. Comm.* **2006**.



Zhu et al. *Org. Lett.* **2010**.

**Figure 13. Structures of PEG BODIPY dyes.**

### 1.3.4. Sulfonation of BODIPY via electrophilic substitution

In 1969, it was reported by Treibs and Kreuzer that the BODIPY derivatives which are free of substituents at the 2,6 positions could undergo electrophilic substitution in presence of chlorosulfonic acid, which gives the corresponding mono or di sulfonated BODIPY dyes.<sup>68</sup> In the 90's, four 2,6 position sulfonated BODIPY derivatives were synthesized by Boyer and coworkers (Figure 14a). The sulfonated BODIPYs are highly water soluble and introduction of sulfonate groups doesn't affect the optical properties of the BODIPY dyes.<sup>69,70</sup> In 2008, Burgess and coworker restudied and developed this synthesis by introduction of an additional functional group at

the meso position of BODIPY core which allows the dye to be conjugated with proteins (Figure 14b).<sup>57,71</sup>

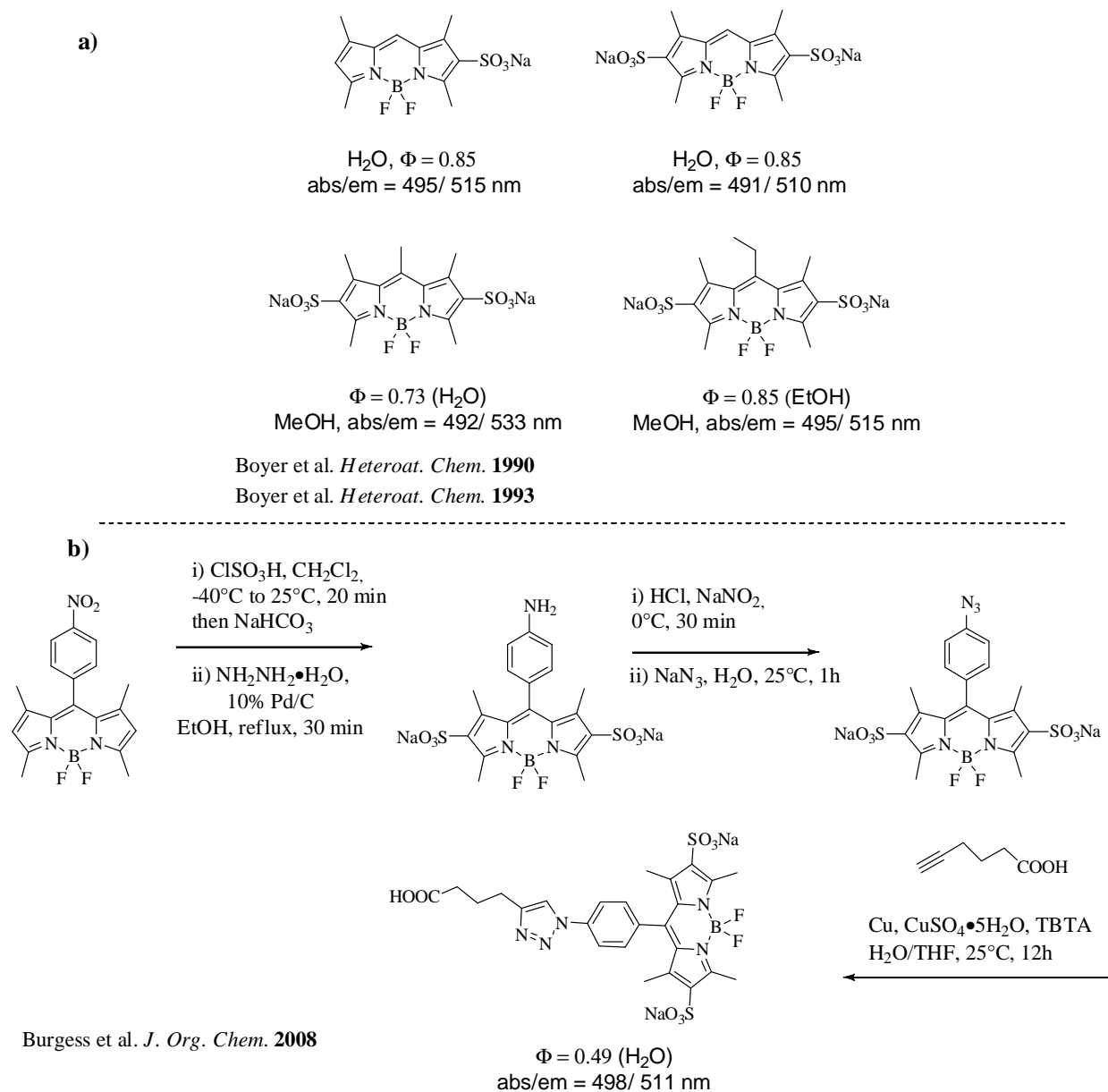


**Figure 14. Sulfonation of BODIPY dyes.**

In addition, introduction of carboxylic,<sup>72,73</sup>  $\alpha$ -galactosylceramide,<sup>74</sup> betaine<sup>75</sup> or nucleotide<sup>61</sup> onto BODIPY core could also increase the dyes' water solubility. Moreover, the carboxylic acid group is sensitive to the pH of the environment; hence it might be useful as a tool for visualizing the variety of reactions in living cells. However, the enhancement of water-solubility of the corresponding dye by these strategies was rather modest.

## 1.4. Thesis objective and outline

Despite the existing strategies discussed above which allow improving the water solubility of certain BODIPY dyes, some of these require multi-step synthesis or harsh experimental conditions (e.g. using chlorosulfonic acid). Furthermore, most of these protocols can hardly be applied to more conjugated BODIPY dyes emitting in the red region of the electromagnetic spectrum in the 600 to 700 nm range. Therefore, the main theme of this thesis is to develop a general strategy without the inconveniences mentioned above.

In Chapter II, a two-step protocol was developed for the synthesis of water soluble BODIPY dyes. The protocol involves successive introduction of zwitterionic sulfobetaines as water solubilization groups onto the BODIPY scaffold in two separated processes. This strategy allows converting the hydrophobic BODIPYs to the corresponding water soluble dyes without hurting their optical properties. Afterwards, the introduction of functional group (ester, functionalized pyrene moiety) onto the BODIPY core was successfully performed, via a palladium-catalyzed carboalkoxylation or cross-coupling reaction with the aryl iodide derivatives (Figure 15).

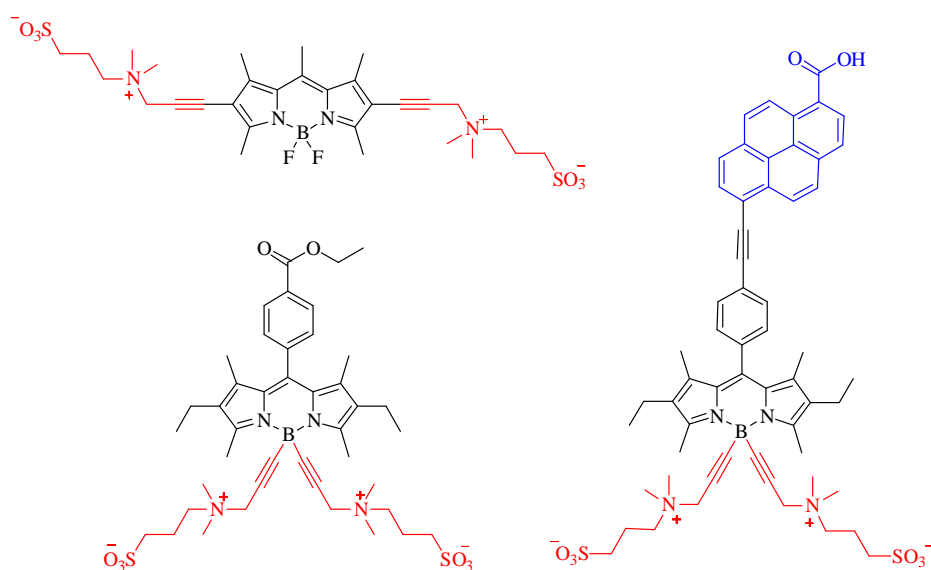


**Figure 15. Structures of sulfobetaine BODIPY dyes.**

In Chapter III, using the two-step water solubilization protocol, a set of water-soluble red-emitting distyryl BODIPY dyes were designed and synthesized for bioconjugation applications (Figure 16). The optical properties of these dyes were evaluated under the simulated physiological conditions (i.e., phosphate buffered saline (PBS), pH 7.5) with emission wavelength in the 641 to 657 nm range and quantum yields from 38 to 4%. Afterwards, the bioconjugation of the distyryl BODIPY dyes **A**, **B**, and **C** with protein bovine serum albumin (BSA) or monoclonal antibody (mAb) 12CA5 was effectuated under physiological conditions. The preliminary results show that it is possible to

get red-emitting fluorescent protein conjugates by using the newly synthesized water-soluble distyryl BODIPY dyes. Furthermore, the fluorescence emission of these bio-conjugates is observed in aqueous buffers without adding aggregate disrupting additives.

According to the recent research on the two-photon absorption of distyryl BODIPY derivatives,<sup>46</sup> the two-photon absorption (TPA) ability of the synthesized water-soluble distyryl BODIPY dye **D** was evaluated in water and remarkable TPA properties of the dye were observed. Afterwards, two-photon excited (TPE) fluorescence microscopy and fluorescence lifetime imaging microscopy (FLIM) experiments were then carried out with the HeLa living cells with our synthesized water-soluble red-emitting BODIPY dye **D** in biological conditions. The TPE and FLIM images demonstrate that the dye can internalize within the cell without using additional solvents. The experiments demonstrated no cytotoxicity of the dye to HeLa cells. Furthermore, the coloration of the cytoplasm of the cell was observed but not the nucleus, which might be an important characteristic for further bio-labeling studies.

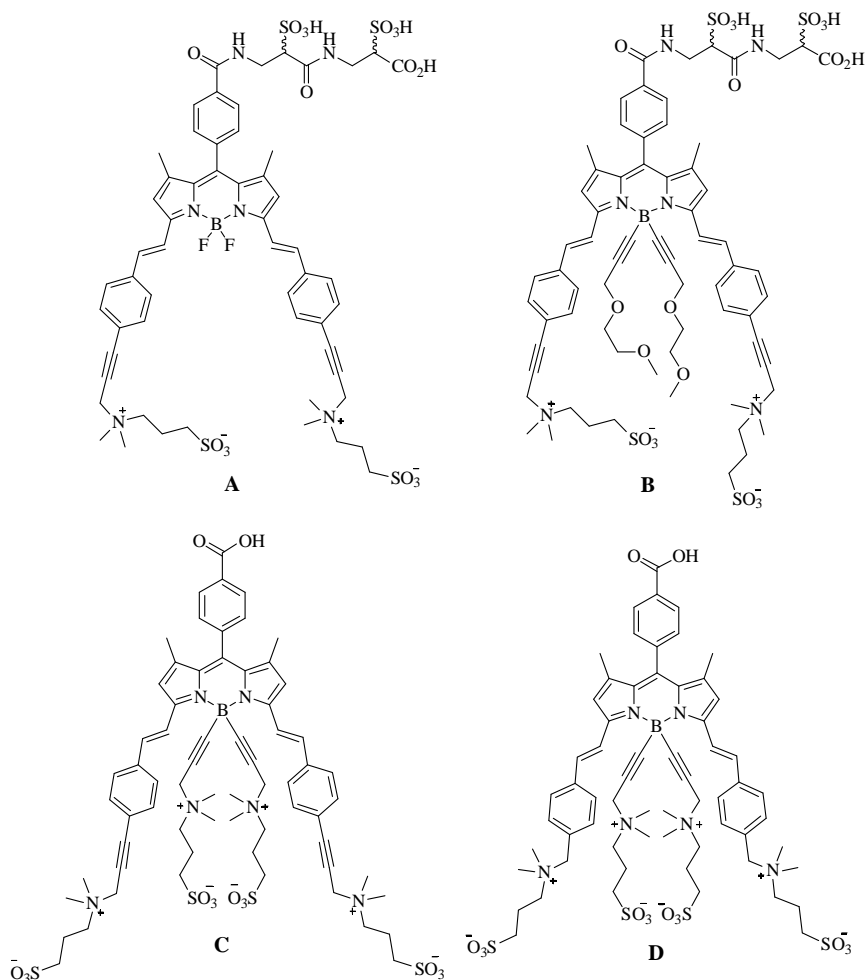
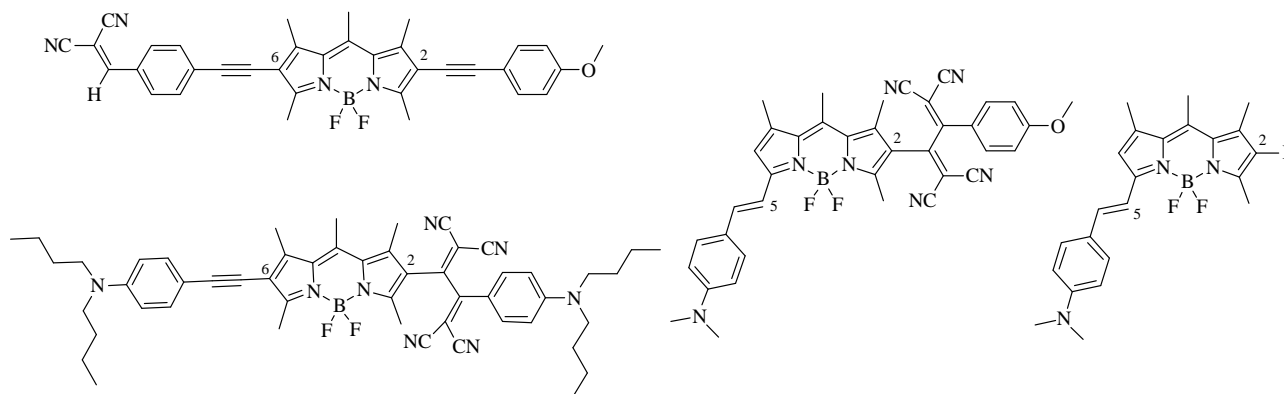


Figure 16. Structures of water soluble red emitting BODIPY dyes.

In Chapter IV, we investigated BODIPY bridged push-pull chromophores. The BODIPY bridged push-pull system was designed and synthesized from a BODIPY platform, an electron donor group

and an electron acceptor group was consecutively conjugated at the 2 and 6 positions of the BODIPY core. In this molecular architecture, an induced dipole moment is expected due to the asymmetric charge distribution of  $\pi$ -electrons along the conjugated molecular axis. The optical and electrochemical properties of the BODIPY bridged push-pull chromophores, as well as the nonlinear optical (NLO) properties were investigated and compared.

Interestingly, it was observed that the Knoevenagel condensation of a 2-position-substituted BODIPY with an electron-rich benzaldehyde gives principally regioselective monostyryl BODIPYs. The condensation occurs only at the 5-position and such regioselectivity was observed in several similar reactions and confirmed with a series of compounds (Figure 17).



**Figure 17. Structures of BODIPY based push-pull chromophores.**

In order to improve the ICT strength along the BODIPY molecular axis, the strong electron withdrawing group 1,1,4,4-tetracyanobuta-1,3-dienes (TCBDs) derivatives was introduced onto the BODIPY scaffold by reacting the ethynyl-linked BODIPYs with tetracyanoethene (TCNE). The ethynyl group undergoes [2+2] cycloaddition and subsequent retro-ring-opening reaction leading to the TCBDs residue. The non-planarity of the TCBDs residue with the BODIPY platform efficiently prevents the formation of aggregates and hence provides a good solubility of the dyes in common solvents. This could be a good feature for the push-pull chromophores. Furthermore, the optical and electrochemical properties of the TCBDs BODIPY dyes were fully investigated and discussed.

Ultimately, the hyperpolarizability of selected push-pull compounds was evaluated by EFISHG measurement. The TCBDs compounds show interesting NLO response. In addition, the interesting electrochemical properties (especially in reduction steps); the strong CT absorption band in the 500-700 nm range; as well as good solubility in common solvent; the TCBDs BODIPY dyes have are potential candidates for the study of bulk heterojunction solar cells.

## Bibliography

- (1) Lakowicz, J. R. *Principles of fluorescence spectroscopy*; Springer, 2006.
- (2) Turro, N. J.; Ramamurthy, V.; Scaiano, J. C. *Modern molecular photochemistry of organic molecules*; University Science Books, 2010.
- (3) Drago, R. S. *Physical methods in chemistry*; Saunders, 1977.
- (4) Michael Seery : Light Absorption and Fate of Excited State.  
<http://photochemistryportal.net/home/index.php/2009/08/24/light-absorption-and-fate-of-excited-state/>
- (5) Franck, J.; Dymond, E. G. *Transactions of the Faraday Society* **1926**, *21*, 536.
- (6) Kasha, M. *Discussions of the Faraday Society* **1950**, *9*, 14.
- (7) Weber, G.; Teale, F. W. J. *Transactions of the Faraday Society* **1957**, *53*, 646.
- (8) Kobayashi, H.; Ogawa, M.; Alford, R.; Choyke, P. L.; Urano, Y. *Chem. Rev.* **2009**, *110*, 2620.
- (9) Bates, M.; Huang, B.; Dempsey, G. T.; Zhuang, X. *Science* **2007**, *317*, 1749.
- (10) Marks, K. M.; Nolan, G. P. *Nat Meth* **2006**, *3*, 591.
- (11) Kawahashi, Y.; Doi, N.; Takashima, H.; Tsuda, C.; Oishi, Y.; Oyama, R.; Yonezawa, M.; Miyamoto-Sato, E.; Yanagawa, H. *Proteomics* **2003**, *3*, 1236.
- (12) Gonçalves, M. S. T. *Chem. Rev.* **2009**, *109*, 190.
- (13) Lide, D.; Milne, G. W. A. *Handbook of Data on Organic Compounds: Compounds 10001-15600 Cha-Hex*; CRC Press, 1994.
- (14) Haugland, R. P.; Gregory, J.; Spence, M. T. Z.; Johnson, I. D. *Handbook of fluorescent probes and research products*; Molecular Probes, 2002.
- (15) von Bayer, A. *Chem. Ber.* **1871**, *5*, 255.
- (16) Sun, W.-C.; Gee, K. R.; Klaubert, D. H.; Haugland, R. P. *J. Org. Chem.* **1997**, *62*, 6469.
- (17) Song, L.; Hennink, E. J.; Young, I. T.; Tanke, H. J. *Biophys. J.* **1995**, *68*, 2588.
- (18) Saylor, J. *Experiments in Fluids* **1995**, *18*, 445.
- (19) Geisow, M. J. *Exp. Cell Res.* **1984**, *150*, 29.
- (20) Martin, M. M.; Ware, W. R. *J. Phys. Chem* **1978**, *82*, 2770.
- (21) Egawa, Y.; Hayashida, R.; Seki, T.; Anzai, J.-i. *Talanta* **2008**, *76*, 736.
- (22) Lakowicz, J. R.; Malicka, J.; D'Auria, S.; Gryczynski, I. *Anal. Biochem.* **2003**, *320*, 13.

- (23) Twining, S. S. *Anal. Biochem.* **1984**, *143*, 30.
- (24) Hoffmann, C.; Leroy-Dudal, J.; Patel, S.; Gallet, O.; Pauthe, E. *Anal. Biochem.* **2008**, *372*, 62.
- (25) Zondervan, R.; Kulzer, F.; Kol'chenk, M. A.; Orrit, M. *J. Phys. Chem. A* **2004**, *108*, 1657.
- (26) Costela, A.; Florido, F.; Garcia-Moreno, I.; Duchowicz, R.; Amat-Guerri, F.; Figuera, J. M.; Sastre, R. *Appl. Phys. B: Lasers Opt.* **1995**, *60*, 383.
- (27) Amat-Guerri, F.; Costela, A.; Figuera, J. M.; Florido, F.; Sastre, R. *Chem. Phys. Lett.* **1993**, *209*, 352.
- (28) Bandichhor, R.; Petrescu, A. D.; Vespa, A.; Kier, A. B.; Schroeder, F.; Burgess, K. *Bioconjugate Chem.* **2006**, *17*, 1219.
- (29) Berlier, J. E.; Rothe, A.; Buller, G.; Bradford, J.; Gray, D. R.; Filanoski, B. J.; Telford, W. G.; Yue, S.; Liu, J.; Cheung, C.-Y.; Chang, W.; Hirsch, J. D.; Beechem, J. M.; Haugland, R. P.; Haugland, R. P. *J. Histochem. Cytochem.* **2003**, *51*, 1699.
- (30) Ernst, L. A.; Gupta, R. K.; Mujumdar, R. B.; Waggoner, A. S. *Cytometry* **1989**, *10*, 3.
- (31) Escobedo, J. O.; Rusin, O.; Lim, S.; Strongin, R. M. *Curr. Opin. Chem. Biol.* **2010**, *14*, 64.
- (32) Romieu, A.; Brossard, D.; Hamon, M.; Outaabout, H.; Portal, C.; Renard, P.-Y. *Bioconjugate Chem.* **2007**, *19*, 279.
- (33) Treibs, A.; Kreuzer, F. H. *Justus Liebigs Ann. Chem.* **1968**, *718*, 208.
- (34) Littler, B. J.; Miller, M. A.; Hung, C.-H.; Wagner, R. W.; O'Shea, D. F.; Boyle, P. D.; Lindsey, J. S. *J. Org. Chem.* **1999**, *64*, 1391.
- (35) Baruah, M.; Qin, W.; Basarić, N.; De Borggraeve, W. M.; Boens, N. *J. Org. Chem.* **2005**, *70*, 4152.
- (36) Ulrich, G.; Ziessel, R.; Harriman, A. *Angew. Chem., Int. Ed.* **2008**, *47*, 1184.
- (37) Loudet, A.; Burgess, K. *Chem. Rev.* **2007**, *107*, 4891.
- (38) Ziessel, R.; Retailleau, P.; Elliott, K. J.; Harriman, A. *Chemistry – A European Journal* **2009**, *15*, 10369.
- (39) Rostron, J. P.; Ulrich, G.; Retailleau, P.; Harriman, A.; Ziessel, R. *New J. Chem.* **2005**, *29*, 1241.
- (40) Peng, X.; Du, J.; Fan, J.; Wang, J.; Wu, Y.; Zhao, J.; Sun, S.; Xu, T. *J. Am. Chem. Soc.* **2007**, *129*, 1500.
- (41) Zheng, Q.; Xu, G.; Prasad, P. *Chemistry – A European Journal* **2008**, *14*, 5812.
- (42) Zeng, L.; Miller, E. W.; Pralle, A.; Isacoff, E. Y.; Chang, C. J. *J. Am. Chem. Soc.* **2005**, *128*, 10.
- (43) Bozdemir, O. A.; Guliyev, R.; Buyukcakir, O.; Selcuk, S.; Kolemen, S.; Gulseren, G.; Nalbantoglu, T.; Boyaci, H.; Akkaya, E. U. *J. Am. Chem. Soc.* **2010**, *132* (23), pp 8029.

- (44) Zheng, Q.; He, G. S.; Prasad, P. N. *Chem. Phys. Lett.* **2009**, *475*, 250.
- (45) Zhang, D.; Wang, Y.; Xiao, Y.; Qian, S.; Qian, X. *Tetrahedron* **2009**, *65*, 8099.
- (46) Didier, P.; Ulrich, G.; Mely, Y.; Ziessel, R. *Org. Biomol. Chem.* **2009**, *7*, 3639.
- (47) Rousseau, T.; Cravino, A.; Bura, T.; Ulrich, G.; Ziessel, R.; Roncali, J. *J. Mater. Chem.* **2009**, *19*, 2298.
- (48) Rousseau, T.; Cravino, A.; Bura, T.; Ulrich, G.; Ziessel, R.; Roncali, J. *Chemical Communications* **2009**, 1673.
- (49) Erten-Ela, S.; Yilmaz, M. D.; Icli, B.; Dede, Y.; Icli, S.; Akkaya, E. U. *Org. Lett.* **2008**, *10*, 3299.
- (50) Kolemen, S.; Cakmak, Y.; Erten-Ela, S.; Altay, Y.; Brendel, J.; Thelakkat, M.; Akkaya, E. U. *Org. Lett.* **2010**, *12*(17), pp 3812.
- (51) Qin, W.; Baruah, M.; Van der Auweraer, M.; De Schryver, F. C.; Boens, N. *J. Phys. Chem. A* **2005**, *109*, 7371.
- (52) Ulrich, G.; Goze, C.; Guardigli, M.; Roda, A.; Ziessel, R. *Angew. Chem., Int. Ed.* **2005**, *44*, 3694.
- (53) Ziessel, R.; Goze, C.; Ulrich, G.; Césario, M.; Retailleau, P.; Harriman, A.; Rostron, J. P. *Chemistry – A European Journal* **2005**, *11*, 7366.
- (54) Ziessel, R.; Ulrich, G.; Elliott, K.; Harriman, A. *Chemistry – A European Journal* **2009**, *15*, 4980.
- (55) Qin, W.; Rohand, T.; Baruah, M.; Stefan, A.; der Auweraer, M. V.; Dehaen, W.; Boens, N. *Chem. Phys. Lett.* **2006**, *420*, 562.
- (56) Rohand, T.; Baruah, M.; Qin, W.; Boens, N.; Dehaen, W. *Chemical Communications* **2006**, 266.
- (57) Li, L.; Han, J.; Nguyen, B.; Burgess, K. *J. Org. Chem.* **2008**, *73*, 1963.
- (58) Jiao, L.; Li, J.; Zhang, S.; Wei, C.; Hao, E.; Vicente, M. G. H. *New J. Chem.* **2009**, *33*, 1888.
- (59) Dilek, Ö.; Bane, S. L. *Bioorg. Med. Chem. Lett.* **2009**, *19*, 6911.
- (60) Meltola, N. J.; Wahlroos, R.; Soini, A. E. *J. Fluoresc.* **2004**, *14*, 635.
- (61) Gießler, K.; Griesser, H.; Göhringer, D.; Sabirov, T.; Richert, C. *Eur. J. Org. Chem.* **2010**, 3611.
- (62) Niu, S. L.; Ulrich, G.; Ziessel, R.; Kiss, A.; Renard, P.-Y.; Romieu, A. *Org. Lett.* **2009**, *11*, 2049.
- (63) Brellier, M.; Duportail, G.; Baati, R. *Tetrahedron Lett.* **2010**, *51*, 1269.
- (64) Atilgan, S.; Ekmekci, Z.; Dogan, A. L.; Guc, D.; Akkaya, E. U. *Chemical Communications* **2006**, 4398.

- 
- (65) Atilgan, S.; Ozdemir, T.; Akkaya, E. U. *Org. Lett.* **2008**, *10*, 4065.
- (66) Zhu, S.; Zhang, J.; Vegesna, G.; Luo, F.-T.; Green, S. A.; Liu, H. *Org. Lett.* **2010**, *13*, 438.
- (67) Zhu, S.; Zhang, J.; Vegesna, G. K.; Pandey, R.; Luo, F.-T.; Green, S. A.; Liu, H. *Chemical Communications* **2011**, *47*, 3508.
- (68) Treibs, A.; Kreuzer, F.-H. *Justus Liebigs Ann. Chem.* **1968**, *718*, 208.
- (69) Shah, M.; Thangaraj, K.; Soong, M.-L.; Wolford, L. T.; Boyer, J. H.; Politzer, I. R.; Pavlopoulos, T. G. *Heteroat. Chem.* **1990**, *1*, 389.
- (70) Boyer, J. H.; Haag, A. M.; Sathyamoorthi, G.; Soong, M. L.; Thangaraj, K.; Pavlopoulos, T. G. *Heteroat. Chem.* **1993**, *4*, 39.
- (71) Han, J.; Gonzalez, O.; Aguilar-Aguilar, A.; Pena-Cabrera, E.; Burgess, K. *Org. Biomol. Chem.* **2009**, *7*, 34.
- (72) Komatsu, T.; Urano, Y.; Fujikawa, Y.; Kobayashi, T.; Kojima, H.; Terai, T.; Hanaoka, K.; Nagano, T. *Chem. Commun.* **2009**, 7015.
- (73) Tasior, M.; Murtagh, J.; Frimannsson, D. O.; McDonnell, S. O.; O'Shea, D. F. *Org. Biomol. Chem.* **2009**, *8*, 522.
- (74) Vo-Hoang, Y.; Micouin, L.; Ronet, C.; Gachelin, G.; Bonin, M. *ChemBioChem* **2003**, *4*, 27.
- (75) Hornillos, V.; Carrillo, E.; Rivas, L.; Amat-Guerri, F.; Acuña, A. U. *Bioorg. Med. Chem. Lett.* **2008**, *18*, 6336.



## CHAPTER II

# New insights into the water-solubilization of BODIPY dyes

### 1.1 Introduction

An important constraint on organic fluorescent compounds to be used in biological research as molecular probes is a good water-solubility of the molecule. The BODIPY dyes have been known for their remarkable optical properties including, high extinction coefficients, high quantum yield, sharp absorption/emission bands, and high photo-stability. However, the poor water-solubility limits their applications as biological probes. Up to now only a limit number of BODIPY dyes that are water-soluble enough to be used in aqueous conditions, and even so the inconvenient synthetic routes made it difficult to be widely applied. Therefore, it was important to find out a new method that allows improving water-solubility of BODIPY dyes. Moreover, the simplicity of the synthesis procedures as well as compatibility with the functional groups on the BODIPY core should also be considered. Keeping those requirements in consideration, our recent studies on the water-solubilization of BODIPY dyes will be discussed in the following paragraphs.

The most common way to improve the water-solubility of organic compound is to introduce sulfonate groups onto the compound's scaffold. This method has been widely applied on the family of Rhodamine dyes for biological molecular probes.<sup>1,2</sup> Sulfonation of BODIPY core by concentrated chlorosulfonic acid can be carried out at the 2,6 position and gives the corresponding mono and disulfonated BODIPY dyes, which has been reported by Boyer and others.<sup>3,4</sup> In literature, several water-soluble BODIPY dyes suitable for further bio-conjugation were successfully synthesized and isolated. However, the poor compatibilities of such harsh experimental conditions with other functional groups (such as double bond, triple band, aldehyde ...) limit its applications.

We first attempted to incorporate a preformed benzenesulfonic acid group onto a BODIPY scaffold in order to improve its water-solubility. The synthesis involves introduction of benzenesulfonic ester groups onto BODIPY's scaffold via a soft coupling reaction; followed by a cleavage reaction of the ester group to generate benzenesulfonic acid as watersolubilization group.<sup>5</sup> By this method a series of benzenesulfonic ester BODIPY derivatives were successfully synthesized. However, the cleavage

of the protection group is more problematic. In addition, the amphiphilic nature of the generated benzenesulfonic acid BODIPY results in formation of aggregates in water and leads to undesired fluorescence quenching.<sup>6-9</sup> In the meantime, we were also working on the second approach by post-synthetic introduction of sulfobetaine group<sup>10</sup> onto the BODIPY core. In this approach, the zwitterionic sulfobetaine group was generated in two separated steps. The precursor dimethylamino groups were introduced at first onto the BODIPY core at different position; and alkylation reaction of the dimethylamino BODIPY derivatives with 1,3-propanesultone in organic solvent gave the water-soluble BODIPY dyes. This strategy was successfully applied on several BODIPY derivatives and gave the corresponding water-soluble dyes with both high fluorescent quantum yield (0.60-0.80) and satisfactory overall yields. Soon afterwards a functionalized pyrene group was grafted in meso-position of the water-soluble BODIPY derivative by cross coupling reaction in order to provide a larger virtual Stokes' shift to the dye and a functional group for bio-conjugation.<sup>11-14</sup> These strategies are now developed in the following sections.

## 1.2 Incorporation of benzenesulfonic acid group

### 1.2.1 Introduction of benzenesulfonic ester.

The benzenesulfonate ester is commonly used as leaving group in organic chemistry.<sup>15,16</sup> However in our case, the benzenesulfonyl derivatives are used to generate the sulfonic acid as water solubilization group. The benzenesulfonic ester group was primarily introduced onto the BODIPY core via a cross coupling reaction, and then the cleavage of the ester group generates the benzenesulfonic acid BODIPY derivatives (Figure 1). By this method the synthesis can be conveniently carried out in the mild organic conditions and allows us to avoid the problem of the reagent solubility.

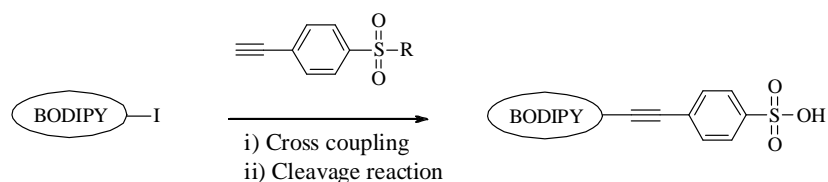
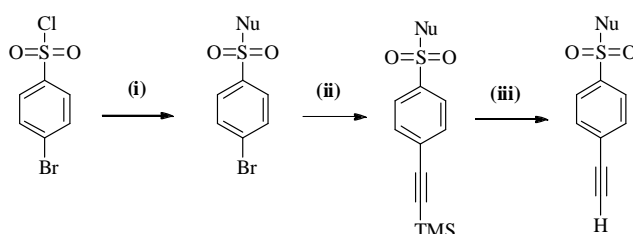


**Figure 1. Introduction of benzenesulfonic acid.**

A series of benzenesulfonic ester and benzenesulfonyl derivatives (Figure 2) were prepared from 4-bromophenylsulfonyl chloride according to Scheme 1. More importantly, the use of pyrrole or indole as protection group in the case of N-benzenesulfonyl-pyrrole **3** and N-benzenesulfonyl-indole **4**, could efficiently keep the sulfonyl group intact during the Grignard reaction.<sup>17</sup>



**Scheme 1.** Keys: (i) isobutanol, 2,6-lutidine, 1,2-dichloroethane, RT, 70%; or pyrrole, NaH, THF, RT, 76%; or isoindole, NaH, THF, RT, 67%. (ii) TMSacetylene, TEA, benzene, [Pd(PPh<sub>3</sub>)<sub>2</sub>Cl<sub>2</sub>] (0.06 mol%), CuI (0.1 mol%), 50°C, 8% to 94%. (iii) KF, methanol, RT, 83% to 97%.

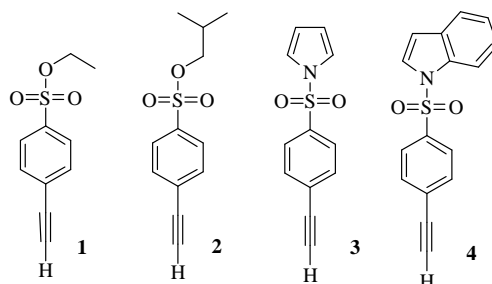


**Figure 2.** Protected sulfonate/sulfonyl compounds 1-4.

The synthesized sulfonate ester / sulfonyl derivatives were introduced in pseudo-meso position of 8-(4-iodophenyl)-BODIPY **5** via a Sonogashira cross coupling reaction.<sup>14,18-20</sup> The cross coupling reaction of the aromatic halide with terminal alkyne was promoted by low-valent Pd (0) in standard condition and gave compounds **6** to **8** in 62 to 91% (Figure 3).

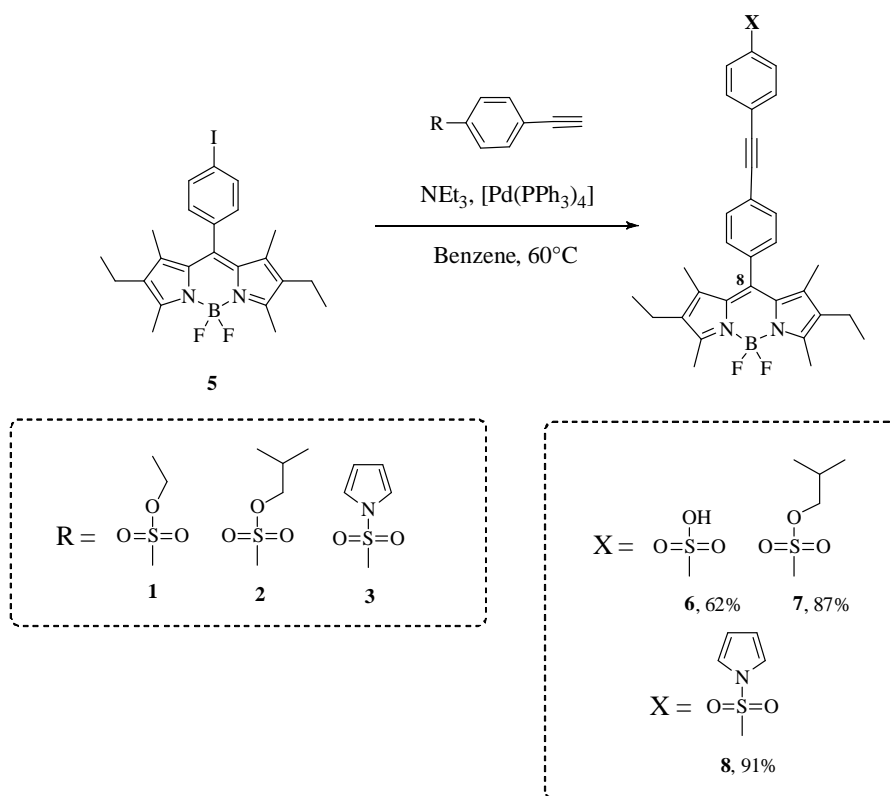


**Figure 3.** Synthesis of sulfonate ester **6**, **7**, **8**.

It is particularly noteworthy that in the synthesis of compound **6**, the generated ethyl sulfonic acid ester was hydrolyzed during the reaction and precipitated from the organic solvent. The sulfonic acid **6** is water-soluble but its fluorescence is totally quenched, but restored by addition of MeOH/EtOH solvent. This fluorescence quenching behavior of the amphiphilic structural molecule in water has widely been discussed in the literature,<sup>21,22</sup> as the consequence of formation of aggregate or micelle. Sometimes detergents or alcohol solvent was added to prevent the formation of aggregate and to restore the fluorescence,<sup>22</sup> but such procedure is not always favorable especially in protein labeling and live-cell imaging experiments.

We also introduced the protected sulfonate groups in  $\beta$ -pyrrolic positions of BODIPY dye, the efficient cross-coupling with the 2-iodo BODIPY **9a**<sup>23</sup> provided the substituted dyes **10-12** in excellent isolated yields (Figure 4).

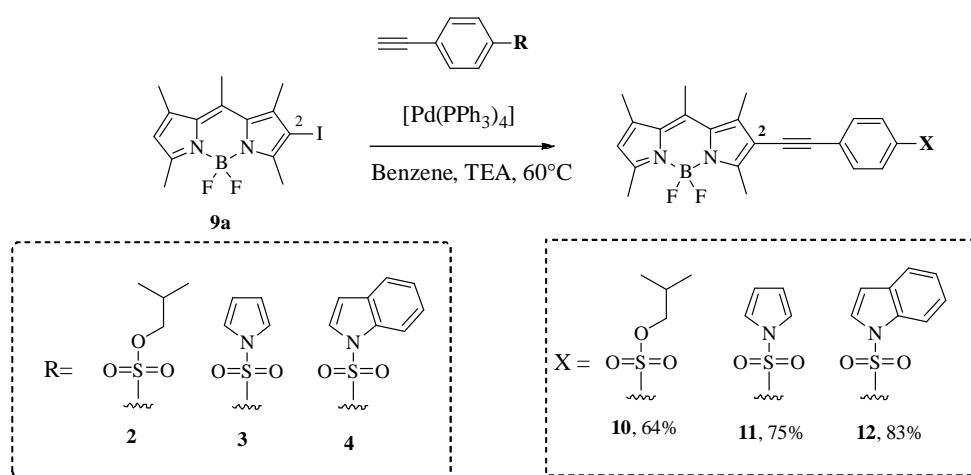


**Figure 4. Structures of compounds 10-12.**

As mentioned previously, the pyrrole or indole protected sulfonic derivatives **3** and **4** could resist to the Grignard reagents. It is noteworthy that the replacement of the fluorides on boron in the 4 position of BODIPY by alkyne-Grignard reagents could effectively generate the corresponding boron-ethynyl-substituted BODIPY (*E*-BODIPY),<sup>24</sup> which have been extensively studied.<sup>14,19,25</sup> Following this approach, the sulfonyl-pyrrole/indole Grignard reagent were prepared from compounds **3** and **4** with EtMgBr in anhydrous THF at 60°C, the resulting anions were then transferred via cannula to an anhydrous THF solution of the BODIPYs, and gave the boron substituted dyes **13** and **14** in 72% and 66% isolated yields, respectively (Figure 5).

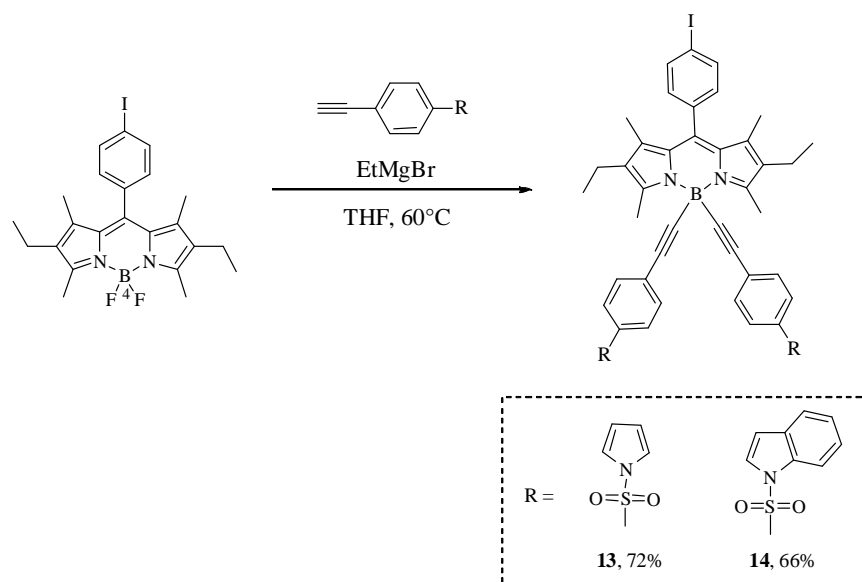


Figure 5. Synthesis of the boron-ethynyl-substituted BODIPY dyes **13** and **14**.

### 1.2.2 Cleavage of the protection group.

The cleavage reaction of the protection groups appeared to be more problematic. According to literature the deprotection of N-tosylated indoles could be smoothly achieved in presence of cesium carbonate in mixture of THF/MeOH at room temperature to give free indole and *p*-MePhSO<sub>3</sub>H.<sup>16,17</sup>

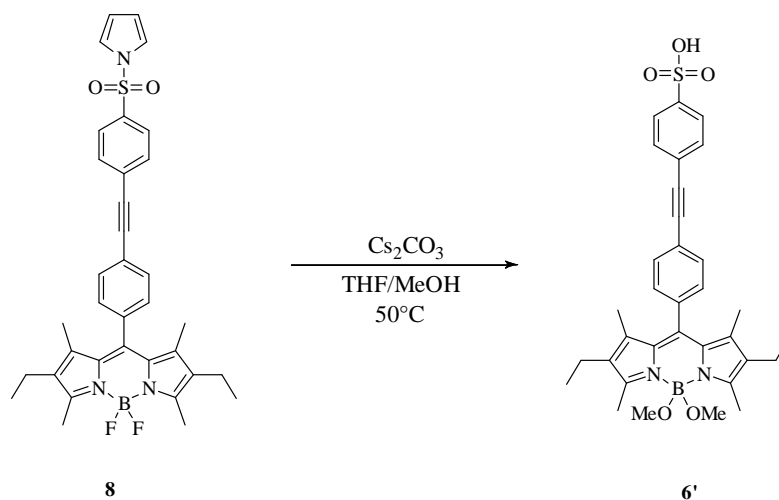
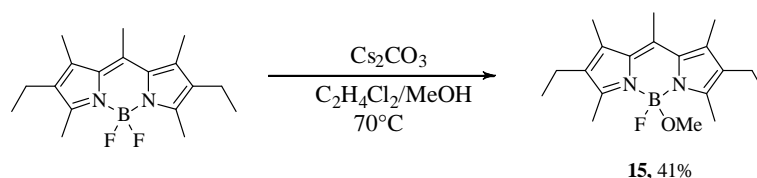


Figure 6. Deprotection of compound **8**.

In our case, the deprotection of N-pyrrole sulfonyl **8** gave the sulfonate **6'** which was confirmed by the mass spectrometry analysis (Figure 6). The fluorine atoms are substituted by MeOH via nucleophilic attack on boron, the similar reaction had also been reported.<sup>26</sup> Moreover, the decomposition of the dye was observed when the reaction is heated over 60°C. Additional attempts confirmed that the BODIPY dye decomposes in the mixture of THF/MeOH in presence of cesium carbonate over 60°C, but not in the mixture of C<sub>2</sub>H<sub>4</sub>Cl<sub>2</sub>/MeOH. We carried out the reaction with

2,6-diethyl-1,3,5,7,8-pentamethyl-4-bora-3a,4a-diaza-s-indacene dissolved in the mixture of  $C_2H_4Cl_2/MeOH$  in presence of  $Cs_2CO_3$  and stirred at  $70^\circ C$  for 10 hours, the mono-substituted compound was isolated after purification in 41% of yield (Figure 7). The fact that mono-substitution of fluorine atom of BODIPY<sup>27</sup> with alcohol in such mild condition might be useful for the synthesis BODIPY dye with an asymmetric boron.<sup>28,29</sup> But indeed, more investigations are still needed.



**Figure 7. Mono-fluoride substitution of BODIPY.**

Then we focused on the deprotection of pyrrole/indole-sulfonyl compounds **13** and **14**. The deprotection of compound **13** was effectuated in the mixture of  $MeOH/C_2H_4Cl_2$  at  $70^\circ C$  for 10 h. Compound **16** was analyzed by mass spectrometry and microanalysis (Figure 8). However, probably due to the amphiphilic nature **16** the poor solubility in common solvent makes the  $^1H$  NMR analysis very difficult. For **14**, the deprotection seems even more problematic. Therefore, the deprotection reaction was only achieved in the case of **16**. In solution, without accurate measurement, the compound **16** shows little water solubility; under UV light no fluorescence was observed by naked eye. Thus, we decided to turn our attentions to an alternative strategy to improve the water-solubility of BODIPY dyes.

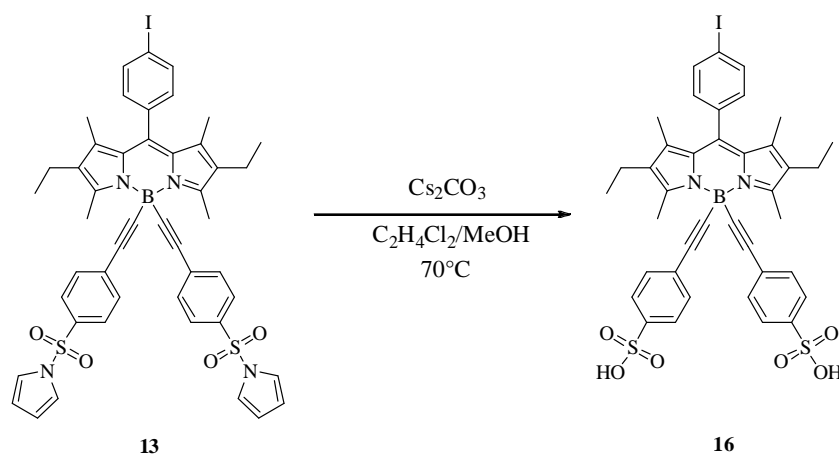


**Figure 8. Deprotection of the pyrrole-sulfonyl compound 13.**

### 1.2.3 Optical properties of the sulfonyl/sulfonic ester BODIPYs.

The optical properties of the synthesized sulfonyl/sulfonic ester BODIPYs were evaluated and the spectroscopic data were collected in Table 1. In solution, all compounds show a strong  $S_0 \rightarrow S_1$  ( $\pi$

$\rightarrow\pi^*$ ) transition about  $\lambda \approx 524$  nm with an absorption coefficient of  $54000\text{-}103000\text{ M}^{-1}\text{cm}^{-1}$ , unambiguously assigned to the boradiazaindacene chromophore.<sup>18,30</sup> At higher energy the weaker and broad bands centered about 380 nm, can be attributed to the  $S_0 \rightarrow S_2$  ( $\pi \rightarrow \pi^*$ ) transition of the BODIPY moiety.<sup>18,30</sup> For **13**, the stronger and structureless absorption band around 230-300 nm can be attributed to the  $\pi \rightarrow \pi^*$  transitions of the ethynyl and N-pyrrole-benzenesulfonyl moiety, which is comparable to the absorption spectra of the ethynyl-aryl-substituted BODIPY dyes (Figure 9).<sup>14</sup> By irradiation at 480 nm, all the sulfonyl/sulfonic ester BODIPYs show intense sharp emission peak around 534-548 nm with fluorescence quantum yield reaching 48-82%. In addition, the cross coupling reaction at 2 position of the BODIPY core induces a bathochromic shift about 40 nm for compounds **10**, **11** and **12**, compare to the 4,4-difluoro-1,3,5,7,8-pentamethyl-4-bora-3a,4a-diaza-s-indacene (BODIPY 493/503);<sup>31</sup> whereas the introduction of the benzenesulfonyl moieties in 8 position or by substitution of fluorides at the 4 position of BODIPY does not cause such bathochromic shift.<sup>13,19</sup>

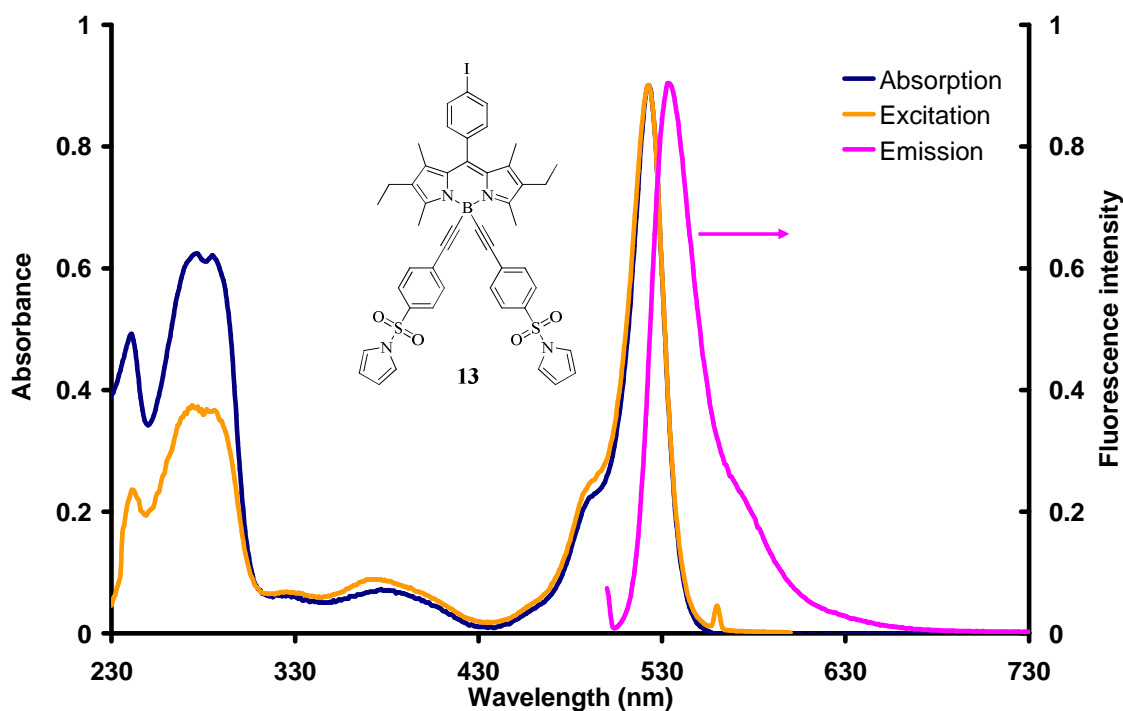


Figure 9. Absorption, emission and excitation spectra of compound **13** in  $\text{CH}_2\text{Cl}_2$ .

**Table 1. Optical properties of the selected BODIPY dyes.**

| Compound                               | $\lambda_{\text{abs}}$ (nm) | $\epsilon$ ( $M^{-1}\cdot\text{cm}^{-1}$ ) | $\lambda_{\text{em}}$ (nm) | $\phi$ (%) <sup>a</sup> | $\tau$ (ns) | $k_r$ ( $10^7\text{s}^{-1}$ ) | $k_{nr}$ ( $10^7\text{s}^{-1}$ ) |
|--|-----------------------------|--|----------------------------|-------------------------|-------------|-------------------------------|----------------------------------|
| <b>6</b> (EtOH)                        | 524                         | 54100                                      | 537                        | 66                      | 4.3         | 15.3                          | 7.9                              |
| <b>7</b> ( $\text{CH}_2\text{Cl}_2$ )  | 527                         | 65000                                      | 542                        | 48                      | 5.1         | 9.4                           | 10.2                             |
| <b>8</b> ( $\text{CH}_2\text{Cl}_2$ )  | 527                         | 92600                                      | 541                        | 64                      | 5.5         | 11.6                          | 6.5                              |
| <b>10</b> ( $\text{CH}_2\text{Cl}_2$ ) | 523                         | 67000                                      | 548                        | 78                      | 4.5         | 17.3                          | 4.9                              |
| <b>11</b> ( $\text{CH}_2\text{Cl}_2$ ) | 523                         | 48000                                      | 548                        | 79                      | 3.9         | 20.3                          | 5.4                              |
| <b>12</b> ( $\text{CH}_2\text{Cl}_2$ ) | 523                         | 71500                                      | 548                        | 74                      | 5.1         | 14.5                          | 5.1                              |
| <b>13</b> ( $\text{CH}_2\text{Cl}_2$ ) | 522                         | 103000                                     | 534                        | 50                      | 6.9         | 7.2                           | 7.2                              |
| <b>14</b> ( $\text{CH}_2\text{Cl}_2$ ) | 523                         | 54000                                      | 534                        | 82                      | 6.4         | 12.8                          | 2.8                              |

a) Quantum yield determined in dilute solution ( $1 \times 10^{-6} \text{M}$ ) using rhodamine 6G as reference ( $\phi_F = 0.78$  in water,  $\lambda_{\text{exc}} = 488 \text{ nm}$ ).<sup>32</sup> All  $\phi_F$  are corrected for changes in refractive index. b)  $k_r$  and  $k_{nr}$  were calculated using the following equations:  $k_r = \phi_F/\tau$ ,  $k_{nr} = (1-\phi_F)/\tau$ .

## 1.3 Introduction of sulfobetaine onto the BODIPY core

### 1.3.1 Direct introduction of sulfobetaine via cross coupling reaction.

Therefore, employing more efficient water-solubilization group is the crucial point to improve BODIPY dye's water solubility. The betaine groups are widely used as a tool in biology and biochemistry to improve the solubilization of drugs or protein in water.<sup>33-36</sup> The betaine is a neutral zwitterionic compound which has a positive charged group (such as quaternary ammonium or a phosphonium cation) and a negative charged group (such as carbonate or sulfonate anion) which may not be adjacent to the cationic site (Figure 10). The zwitterionic character makes the betaine highly soluble in water. In addition, the intracellular accumulation of betaines does not perturb enzyme function, protein structure and membrane integrity.<sup>37</sup> Moreover, in biological systems many betaines serve as organic osmolytes that protect cells against osmotic stress, drought, high salinity or high temperature.<sup>38-41</sup>

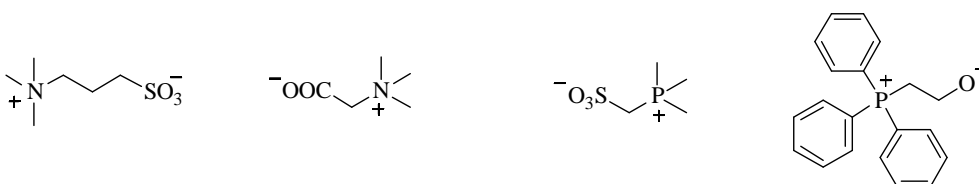


**Figure 10. Several molecular structures of betaine derivatives.**

The sulfobetaine can be obtained by quaternization of a tertiary amine group with 1,3 propasultone according to literature procedures.<sup>42,43</sup> The ethynyl-sulfobetaine (Figure 11) was conveniently prepared from 1-(N,N-dimethylamino)-prop-2-yne with 1,3 propasultone in toluene at rt. The generated sulfobetaine compound precipitated from toluene during the course of the reaction, and a centrifugation gave the product pure as a white powder.

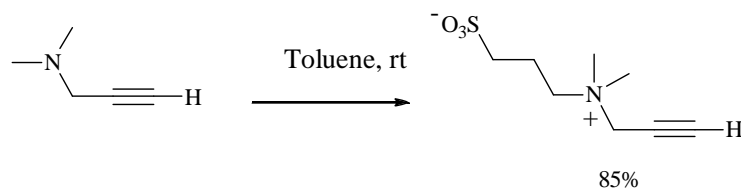


**Figure 11. The formation of sulfobetaine.**

The ethynyl-sulfobetaine can easily be linked to 8-iodophenyl-BODIPY derivatives through the Sonogashira cross-coupling reaction in DMF catalyzed by low valent Pd(0) (Figure 12). The compound **18** and **19** were purified by flash chromatography on silica and obtained in 70% and 30% yields respectively.

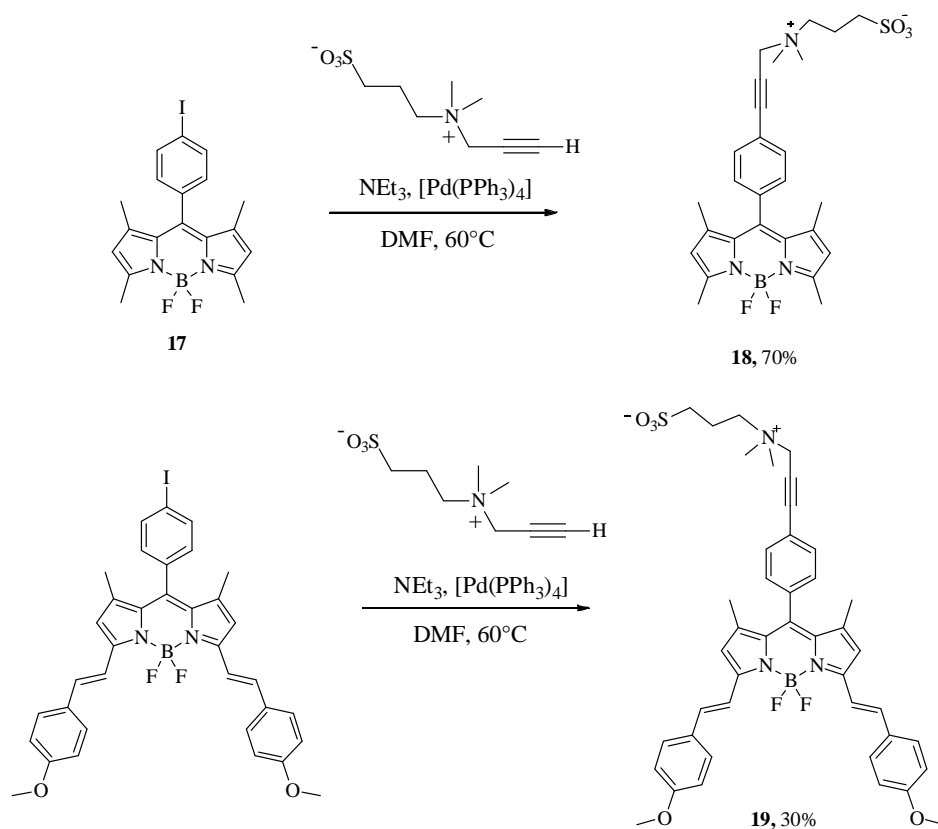


**Figure 12. Synthesis of the compounds 18 and 19.**

### 1.3.1.1 Optical properties of **19**.

The optical properties of the sulfobetaine BODIPY **18** and **19** were evaluated and the spectroscopic data were collected in Table 2. For **18**, the dye is slightly soluble in water. The evaluation was carried out in both water and EtOH.<sup>30</sup> However, the fluorescence quantum yield is rather low due to aggregation. Such aggregation totally disappeared in EtOH, indicating the amphiphilic nature of the dye. For the blue dye **19**, in EtOH solution, the spectra of the dye correspond very closely with those of distyryl BODIPY derivatives (Figure 13).<sup>44,45</sup> In the absorption spectra, the lowest energy

absorption maxima centered at 643 nm corresponds to the  $S_0 \rightarrow S_1$  ( $\pi \rightarrow \pi^*$ ) transition of the BODIPY core with an absorption coefficient of  $47000 \text{ M}^{-1}\text{cm}^{-1}$ . In addition, a small hypsochromic shift about 7 nm was observed for this absorption bands in comparison with the excitation spectra (excited at 664 nm), probably due to the tendency of the dye to aggregate in EtOH. The absorption band centered at 371 nm can be assigned to the  $\pi \rightarrow \pi^*$  transitions of the conjugated styryl moieties.<sup>46</sup> The results indicated that these two first sulfobetaine BODIPYs are not highly soluble in water and tend to form aggregates due to their amphiphilic character. Thus, it appeared necessary to introduce hydrophilic substituents onto the aromatic core of the dyes.

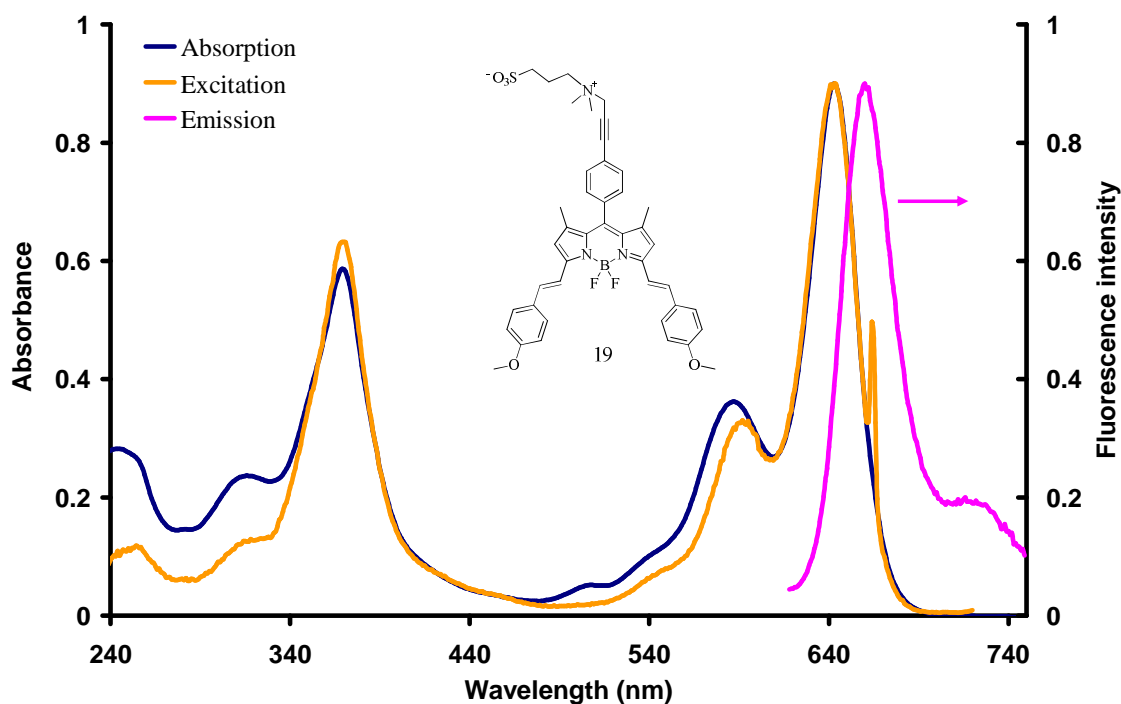


Figure 13. Absorption, emission and excitation spectra of dye 19 in EtOH.

Table 2. Optical properties of compounds 18 and 19.

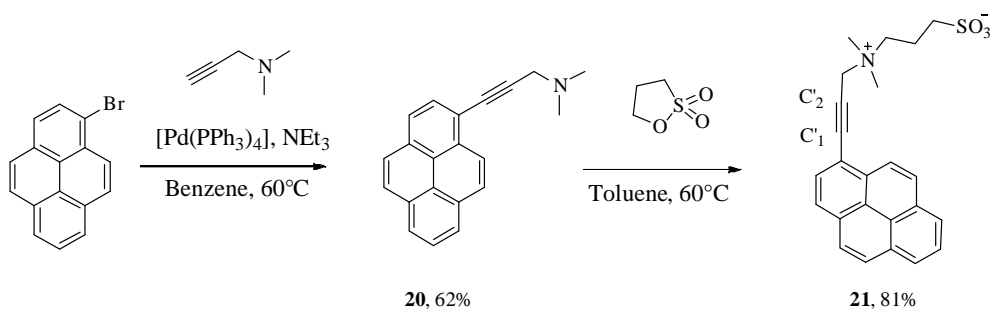
| Compound                           | $\lambda_{\text{abs}}$ (nm) | $\epsilon$ ( $\text{M}^{-1}\cdot\text{cm}^{-1}$ ) | $\lambda_{\text{em}}$ (nm) | $\phi$ (%) <sup>a</sup> | $\tau$ (ns) | $k_r$ ( $10^7 \text{ s}^{-1}$ ) | $k_{\text{nr}}$ ( $10^7 \text{ s}^{-1}$ ) |
|------------------------------------|-----------------------------|---|----------------------------|-------------------------|-------------|---------------------------------|---|
| <b>18</b> (EtOH)                   | 501                         | 77600   | 512                        | 43                      | 2.6         | 16.5                            | 21.9                                      |
| <b>18</b> ( $\text{H}_2\text{O}$ ) | 496                         | 75500   | 511                        | 20                      | 3.2         | 6.3                             | 25.0                                      |
| <b>19</b> (EtOH)                   | 643                         | 47000   | 660                        | 60                      | 4.7         | 12.8                            | 8.5                                       |

a) Quantum yield was determined in dilute solution ( $1 \times 10^{-6} \text{ M}$ ) using rhodamine 6G ( $\phi_F = 0.78$  in water,  $\lambda_{\text{exc}} = 488 \text{ nm}$ ) or cresyl violet as reference ( $\phi_F = 0.51$  in EtOH,  $\lambda_{\text{exc}} = 578 \text{ nm}$ ).<sup>32</sup> All  $\phi_F$  are corrected for changes in refractive index. b)  $k_r$  and  $k_{\text{nr}}$  were calculated using the following equations:  $k_r = \phi_F/\tau$ ,  $k_{\text{nr}} = (1-\phi_F)/\tau$ .

### 1.3.2 Post-synthetic introduction of sulfobetaine.

In order to prove the generality of the previously developed method, the sulfobetaine group was

introduced to a large aromatic chromophore pyrene. The pyrene and its derivatives have been widely used and studied as fluorescent dyes in biology.<sup>47-49</sup> It will be useful to improve its water solubility, hence a similar two step protocol was designed to solubilise the pyrene in water: (i) use 1-dimethylamino-2-propyne cross-coupling; and (ii) quaternization of the dimethylanimo derivative with 1,3-propane sultone in apolar condition provides the zwitterionic fragment (betaine). Both steps are straightforward and compounds **20** and **21** were obtained in excellent yields, providing a water soluble pyrene **21** (Scheme 2).



**Scheme 2. Synthesis of pyrene 21.**

### 1.3.2.1 X-ray analysis of sulfobetaine pyrene **21**.

Single crystals of **21** suitable for X-ray analysis was grown by slow diffusion of the saturated Et<sub>2</sub>O vapour into a solution of **21** in mixture of MeOH/H<sub>2</sub>O. The x-ray analysis confirmed the expected structure (Figure 14), with a C ≡ C distance of 1.185 Å and the puckered sulfobetaine chain folded back towards the pyrene ring. The mean plane of the sulfobetaine chain lies close to that of the ethynylpyrene unit, the quaternary-N and sulfonate-S atoms lying approximately 1 Å to opposite sides of this plane.

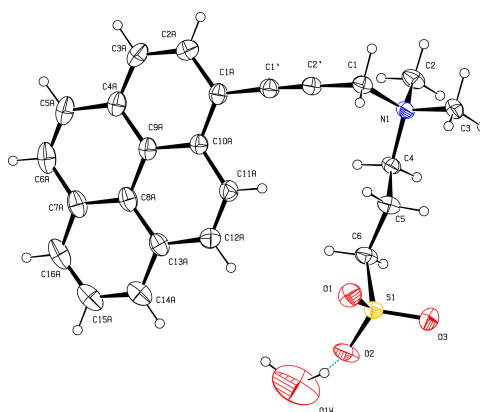


**Figure 14. Single crystal structure of 21, displacement ellipsoids are drawn at the 30% probability level and H atoms are shown as small spheres of arbitrary radii.**

Interestingly, one molecule H<sub>2</sub>O per pyrene unit was observed in the lattice. Note that there is also a short contact of O1W to C16A of 3.266 Å, though the (water) oxygen atom lies well out of the plane of the ring and thus the interaction may be of π⋯O character. This water molecules is clearly

involved in H-bonding to sulfonate-O2 ( $O\cdots O$  2.803 Å) and has another short contact of 3.319 Å to C2 in an adjacent column. Moreover, within the lattice, the molecules form columnar stacks parallel to  $a$  (Figure 15) with the pyrene substituent orientation alternating down the column. The pyrene plane is inclined at  $20.5^\circ$  to axis- $a$  and alternates in orientation from one column to the next. While  $\pi$ -stacking is commonly observed in the solid state structure of pyrene and its derivatives,<sup>13,50</sup> and , in the present case, the rings in the columns down to axis- $a$  are close to parallel (mean dihedral  $2.5^\circ$ ) and separated by only 3.5 Å, consistent with such an interaction, analysis of the structure using Hirshfeld surfaces generated with crystal CrystalExplorer<sup>51</sup> indicates that  $\pi$ -stacking is less important than interactions of the peripheral hydrogen atoms probably involving  $CH\cdots O$  bonding (note that there is some evidence that the ethyne unit is involved in interaction with an adjacent pyrene ring).

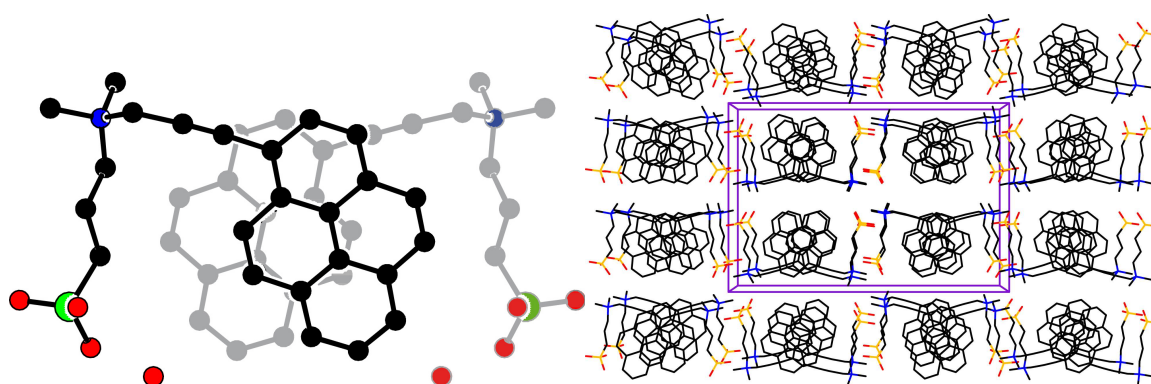


Figure 15. Left side. Non-centrosymmetric  $\pi$ -stacked pairs viewed down the axis- $a$ . In grey, molecule at position  $x-1/2, y, 1/2-z$ ; hydrogen atoms are omitted for clarity. Right side. Enlarged view of the crystal packing down the axis- $a$ . The water molecules are omitted for clarity.

Thus, within a column, there are intermolecular contacts such that C16A is 3.502 Å from (sulfonate) O3, with C6A 3.596 Å from the same oxygen, while between columns, again the same sulfonate-O has a contact to C5A of 3.502 Å. In any case, the Hirshfeld surface properties indicate that strongest lattice interactions are those between the zwitterionic arms, which from head-to-tail arrays (i.e., anti-parallel alignment of the dipoles) in columns also parallel to  $a$ . interactions between the formally oppositely charged ammonium and sulfonate centres appear again to be mediated through  $CH\cdots O$  interaction.

### 1.3.2.2 Optical properties of sulfobetaine pyrene.

The optical properties of the water soluble sulfobetaine pyrene **21** were then investigated in both water and DMF and the data were collected in Table 3. Generally speaking, no significant difference was observed in both solvents. In solution, the electronic absorption spectrum of **21** exhibits characteristic  $\pi-\pi^*$  transitions corresponding to the different  $S_3$ ,  $S_2$  and  $S_1$  excited states

respectively from high to low energy (Figure 16).<sup>13</sup> In the emission spectra, the strong emission peak was observed centred at 385 nm, corresponding to the emission of the pyrene moiety. This emission spectrum mirrors that of the absorption which is typical of a singlet excited state. The excitation spectra match the absorption spectra allowing concluding that all the transitions contribute to this emission. However, the significantly weaker values of extinction coefficient observed in water ( $\epsilon$ , 30600) compared with that of in DMF ( $\epsilon$ , 39000) is probably due to the presence of aggregates in solvents (Table 3). Despite all that, the efficient solvation of the zwitterionic unit has proved to be sufficient to give overall solubility to the hydrophobic compounds. Furthermore, this two-step sulfobetaine pyrene synthesis allows establishing a new synthetic route to incorporate efficiently and conveniently a sulfobetaine moiety to a chromophore under mild operation conditions.

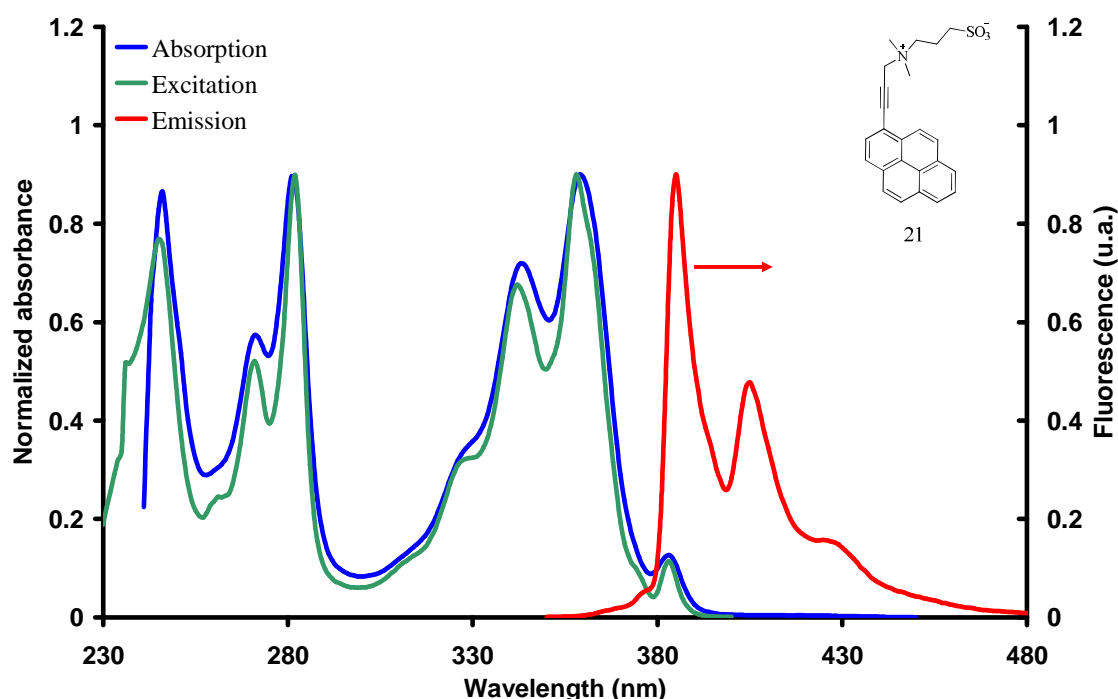


Figure 16. Absorption, emission and excitation spectra of dye 21 in Water.

Table 3. Optical data of sulfobetaine pyrene 21.

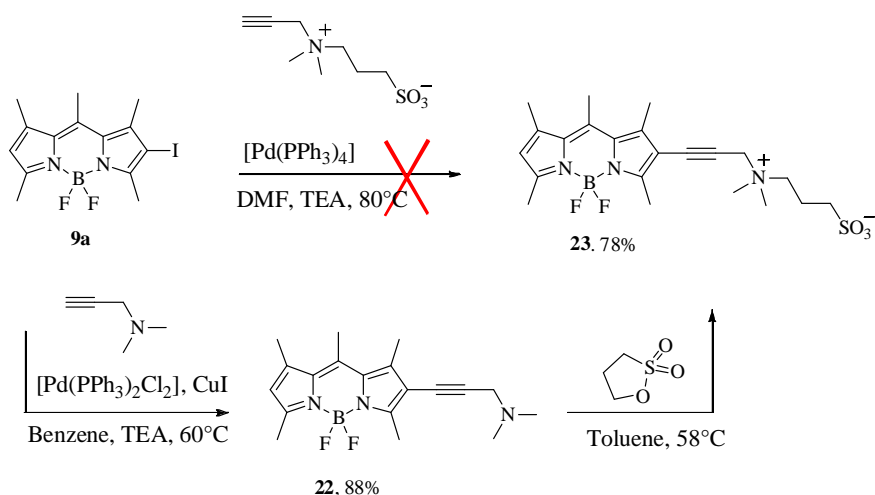
| Compound                    | $\lambda_{\text{abs}}$ (nm) | $\epsilon$ ( $\text{M}^{-1} \cdot \text{cm}^{-1}$ ) | $\lambda_{\text{em}}$ (nm) | $\phi$ (%) | $\tau$ (ns) | $k_{\text{r}}$ ( $10^7 \text{s}^{-1}$ ) | $k_{\text{nr}}$ ( $10^7 \text{s}^{-1}$ ) |
|-----------------------------|-----------------------------|---|----------------------------|------------|-------------|---|--|
| 21 ( $\text{H}_2\text{O}$ ) | 359                         | 30600   | 385/405                    | 32         | 11.6        | 2.8                                     | 5.9                                      |
| 21 (DMSO)                   | 365                         | 39000   | 387/407                    | 38         | 17.4        | 2.2                                     | 3.6                                      |

a) Quantum yield determined in dilute solution ( $1 \times 10^{-6} \text{M}$ ) using quinine sulfate as reference ( $\phi_{\text{F}} = 0.55$  in  $1 \text{M H}_2\text{SO}_4$ ,  $\lambda_{\text{exc}} = 366 \text{ nm}$ ).<sup>32</sup> All  $\phi_{\text{F}}$  are corrected for changes in refractive index. b)  $k_{\text{r}}$  and  $k_{\text{nr}}$  were calculated using the following equations:  $k_{\text{r}} = \phi_{\text{F}}/\tau$ ,  $k_{\text{nr}} = (1-\phi_{\text{F}})/\tau$ .

### 1.3.3 Post-synthetic introduction of sulfobetaines onto BODIPY core.

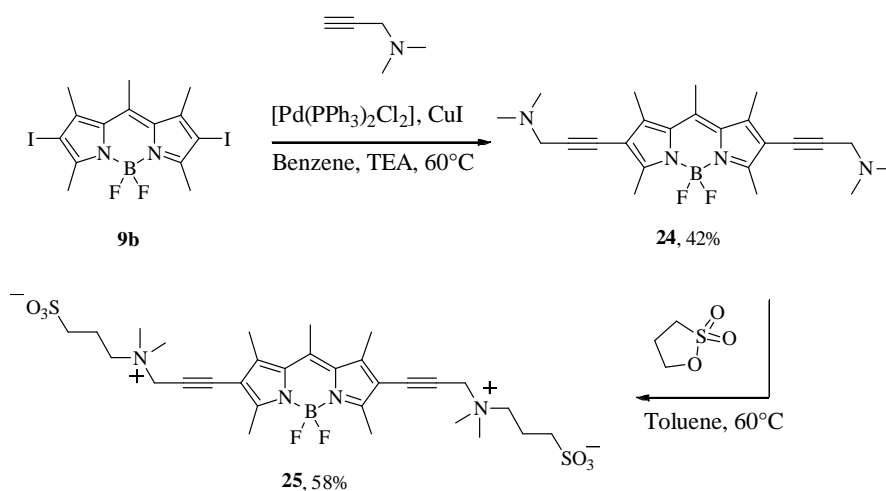
#### 1.3.3.1 Synthesis of $\beta$ -pyrrolic sulfobetaine BODIPY.

Following the two steps synthesis protocol described above, the cross coupling of 1-dimethylamino-2-propyne with the BODIPY **9a**<sup>23</sup> afforded compound **22** in 82% yield. Then the subsequent alkylation with 1,3-propanesultone provided the sulfobetaine BODIPY dye **23** in 78% yield. The use of a non-polar solvent allows the sulfobetaine dye to precipitate from the solvent during the course of the reaction, and then isolation is feasible by a simple centrifugation without additional treatments. It is noteworthy that direct cross coupling of the ethynylsulfobetaine with the BODIPY **9a** in DMF did not give the target betaine BODIPY **23**, but a rather complicated mixture of highly coloured and non-fluorescent compounds that were difficult to separate properly.



Scheme 3. Synthesis of BODIPY dye **23**.

Using the 2,6-diiodo-tetramethyl BODIPY dye **9b**,<sup>23</sup> the disulfobetaine BODIPY dye **25** was conveniently synthesized following the same protocol.



Scheme 4. Synthesis of BODIPY dye **25**.

### 1.3.3.2 Optical properties of the $\beta$ -sulfobetaine BODIPY.

The photophysical properties of the  $\beta$ -sulfobetaine BODIPY dyes **23** and **25** were evaluated and the data were collected in Table 4. For **23**, the optical properties were evaluated in both H<sub>2</sub>O and DMSO (Figure 17). In order to avoid the overestimation of the fluorescence quantum yield due to the low solubility of the dye in H<sub>2</sub>O, only the data measured in DMSO were given in Table 4. In solution, the dye **23** exhibits similar spectral properties as standard BODIPYs.<sup>30</sup> A blue shift about 5 nm was observed in both absorption and emission spectra in H<sub>2</sub>O, compared with those in DMSO. For the dye **25**, the optical properties were evaluated under simulated physiological condition [i.e., phosphate-buffered saline (PBS), pH 7.3] (Figure 18). In PBS solution, the electronic absorption spectrum of **25** exhibits BODIPY characteristic: the narrow and sharp absorption peak at 521nm is typical of S<sub>0</sub> → S<sub>1</sub> transition. In emission, the intense emission peak is centered at 540 nm with a high quantum yield of 82 %. The excitation spectra match the absorption spectra proving the absence of aggregates. In addition, the quaternization of the dye **24** with 1,3-propanesultone results in a hypsochromic shift about 22 nm in both absorption and emission spectra, and a higher quantum yield.

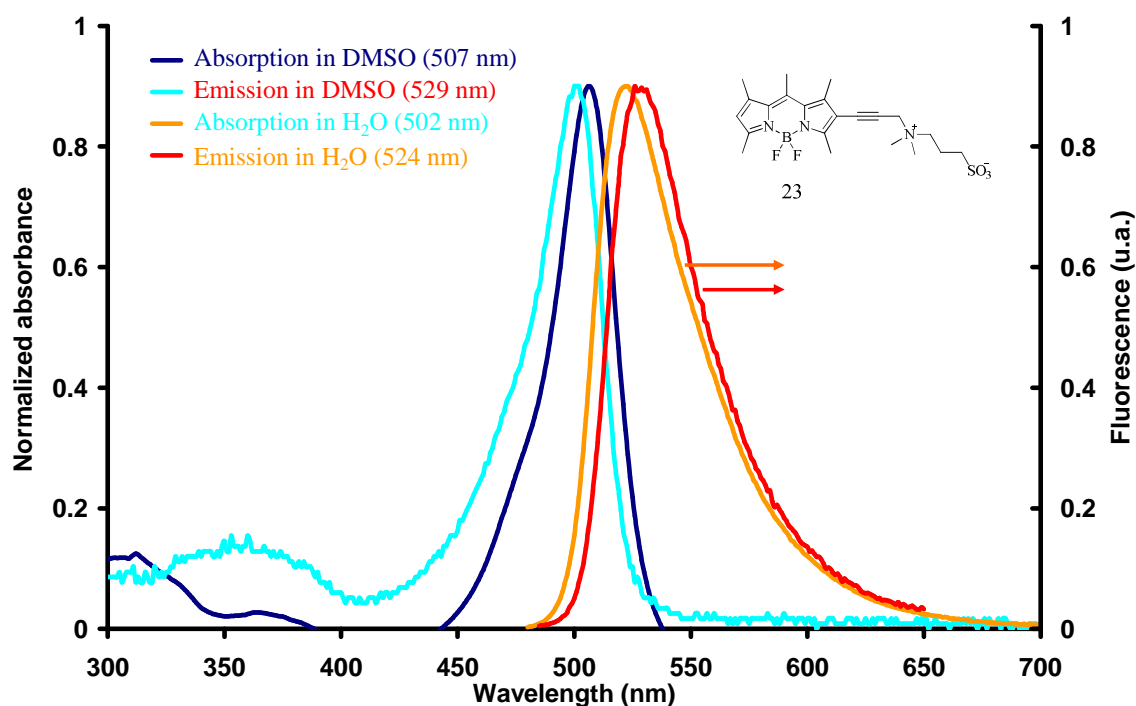


Figure 17. Normalized absorption and emission spectra of compound **23** in H<sub>2</sub>O and DMSO, respectively.

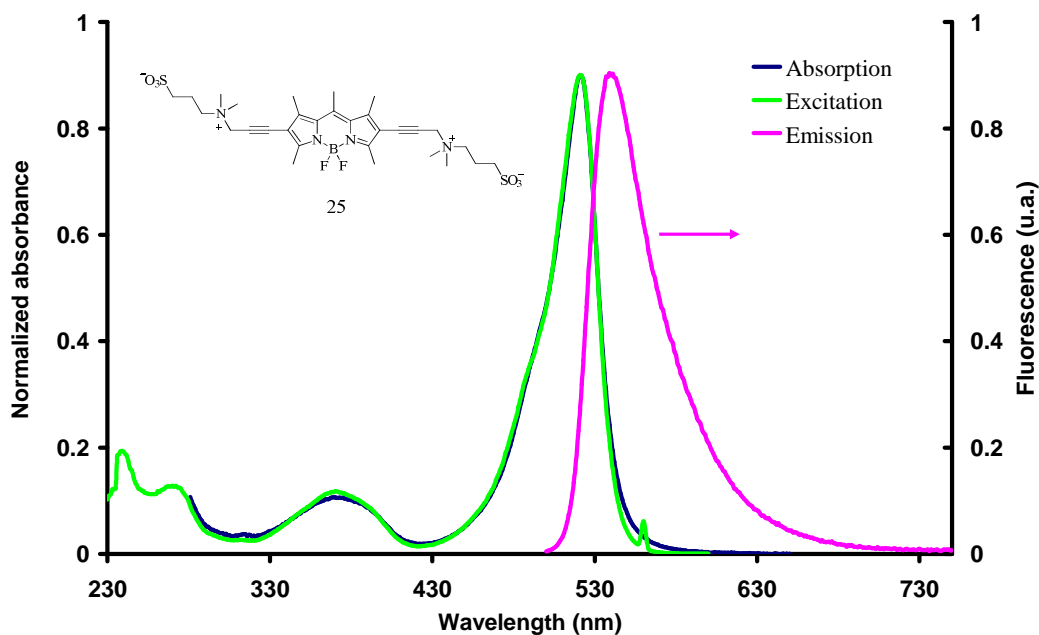


Figure 18. Absorption, emission and excitation spectra of compound 25 in PBS.

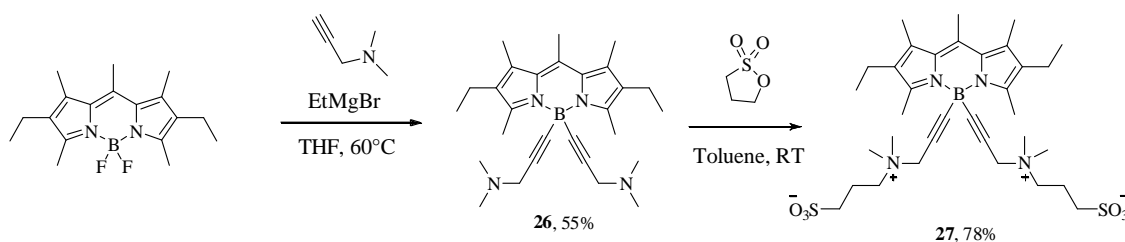
Table 4. Optical properties of the  $\beta$ -sulfobetaine BODIPY dyes.

| Compound                        | $\lambda_{\text{abs}}$ (nm) | $\epsilon$ ( $\text{M}^{-1} \cdot \text{cm}^{-1}$ ) | $\lambda_{\text{em}}$ (nm) | $\phi$ (%) <sup>a</sup> | $\tau$ (ns) | $k_r$ ( $10^7 \text{s}^{-1}$ ) | $k_{\text{nr}}$ ( $10^7 \text{s}^{-1}$ ) |
|---------------------------------|-----------------------------|---|----------------------------|-------------------------|-------------|--------------------------------|--|
| 23 (DMSO)                       | 506                         | 44700   | 529                        | 80                      | 7.2         | 11.1                           | 2.8                                      |
| 24 ( $\text{CH}_2\text{Cl}_2$ ) | 543                         | 38000   | 565                        | 54                      | -           | -                              | -  |
| 25 (PBS)                        | 521                         | 58800   | 540                        | 82                      | 5.1         | 16.1                           | 3.5                                      |

a) Quantum yield determined in dilute solution ( $1 \times 10^{-6} \text{M}$ ) using rhodamine 6G as reference ( $\phi_F = 0.78$  in water,  $\lambda_{\text{exc}} = 488 \text{ nm}$ ).<sup>32</sup> All  $\phi_F$  are corrected for changes in refractive index. b)  $k_r$  and  $k_{\text{nr}}$  were calculated using the following equations:  $k_r = \phi_F/\tau$ ,  $k_{\text{nr}} = (1-\phi_F)/\tau$ .

### 1.3.4 Synthesis of boron-ethynyl-substituted sulfobetaine BODIPY.

Finally, this two steps synthesis was applied to graft sulfobetaine residues onto boron using the corresponding ethynyl Grignard reagent (Scheme 5). In the synthesis of dye **27**, the dimethylamino moieties were successfully introduced onto boron by replacing the fluorides with the Grignard reagent of 1-(N,N-dimethylamino)-prop-2-yne. Then the quaternization of the boron-ethynyl-substituted dimethylamino BODIPY **26** with 1,3-propanesultone gave the boron-ethynyl-substituted sulfobetaine BODIPY dye **27** which precipitate during the course of the reaction.



Scheme 5. Synthesis of BODIPY 27.

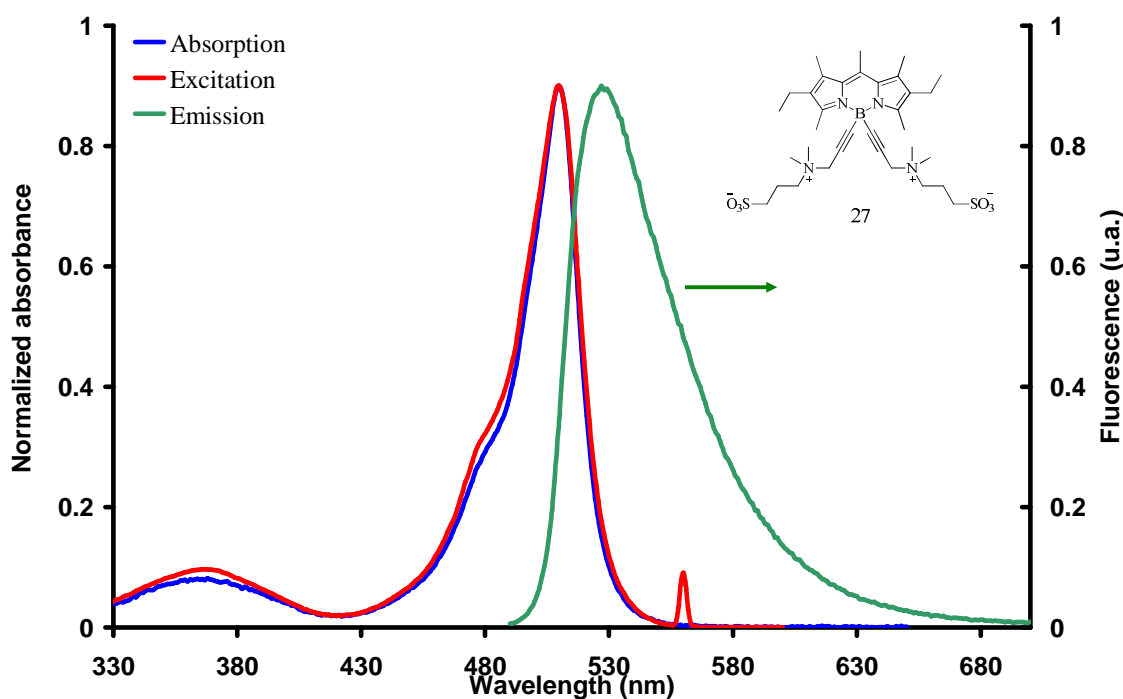
## 1.3.4.1 Optical properties of BODIPY 27.

The BODIPY 27 was found highly water-soluble, its optical properties were evaluated in pure water and the data were collected in Table 5. In solution, the electronic absorption spectrum exhibits the characteristic strong  $S_0 \rightarrow S_1$  ( $\pi \rightarrow \pi^*$ ) transition absorption peak at 510 nm with a molar absorption coefficients of  $63000 \text{ M}^{-1}\text{cm}^{-1}$ , unambiguously assigned to the boradiazaindacene chromophore (Figure 19). The weaker and broad absorption bands is centered at 368 nm can be attributed to the  $S_0 \rightarrow S_2$  ( $\pi \rightarrow \pi^*$ ) transition of the BODIPY core. The intense emission peak centered at 528 nm with a high quantum yield of 81% and a fluorescence lifetime of 9.2 ns are in keeping with a singlet excited state. In addition, the excitation spectra match perfectly the absorption spectra proving the absence of aggregates. Interestingly, in aqueous condition the sulfobetaine moieties on the boron does not affect the BODIPY's optical properties regarding to the non-boron-substituted BODIPYs.<sup>52</sup>

Table 5. Optical properties of BODIPY dyes 26 and 27.

| Compound                        | $\lambda_{\text{abs}}$ (nm) | $\epsilon$ ( $\text{M}^{-1}\cdot\text{cm}^{-1}$ ) | $\lambda_{\text{em}}$ (nm) | $\phi$ (%) <sup>a</sup> | $\tau$ (ns) | $k_r$ ( $10^7 \text{ s}^{-1}$ ) | $k_{nr}$ ( $10^7 \text{ s}^{-1}$ ) |
|---------------------------------|-----------------------------|---|----------------------------|-------------------------|-------------|---------------------------------|------------------------------------|
| 26 ( $\text{CH}_2\text{Cl}_2$ ) | 515                         | 69400   | 532                        | 40                      | 9.4         | 4.3                             | 6.4                                |
| 27 ( $\text{H}_2\text{O}$ )     | 510                         | 63300   | 528                        | 81                      | 9.2         | 8.8                             | 2.1                                |

a) quantum yield determined in dilute solution ( $1 \times 10^{-6} \text{ M}$ ) using rhodamine 6G as reference ( $\phi_F = 0.78$  in water,  $\lambda_{\text{exc}} = 488 \text{ nm}$ ).<sup>32</sup> All  $\phi_F$  are corrected for changes in refractive index. b)  $k_r$  and  $k_{nr}$  were calculated using the following equations:  $k_r = \phi_F/\tau$ ,  $k_{nr} = (1-\phi_F)/\tau$ .

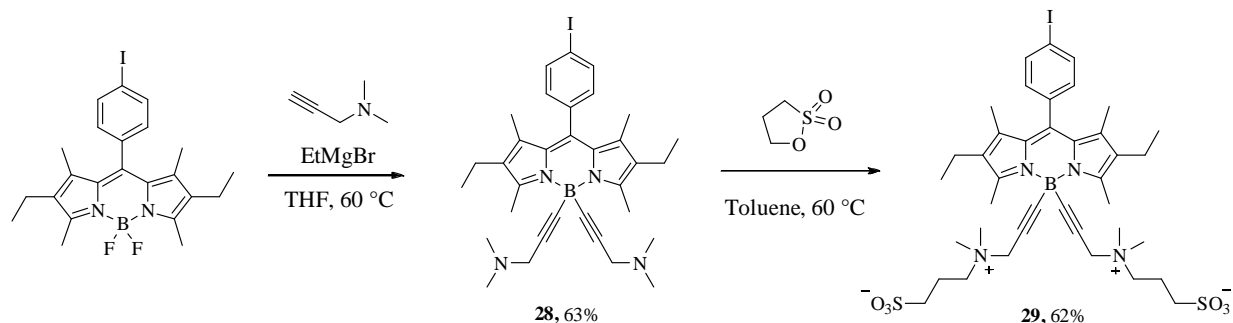
Figure 19. Absorption, emission and excitation spectra of dye 27 in  $\text{H}_2\text{O}$ .

## 1.4 Functionalization of sulfobetaine BODIPY dye.

So far, we have established new synthetic routes for water-solubilisation of the BODIPY dyes using sulfobetaine residues in different circumstances. The two-step sulfobetaine BODIPY synthesis is required to first graft the N,N-dimethylamino-2-propyne fragment either on the dipyrromethene core or on the boron and then quaternize the tertiary amine centre with 1,3-propasultone. Interestingly, in all cases the optical properties are retained with respect to the non-substituted BODIPYs. This protocol may open the door for the engineering of fluorescent dyes in aqueous medium, and to the engineering of a vast range of new water-soluble BODIPY derivatives. By extension of these protocols, we were particularly interested in engineering water-soluble BODIPY dyes suitable for applications in fluorescent labelling. Therefore we moved on to the introduction of a functional group to the BODIPY scaffold, which allows grafting the dye specifically onto proteins or peptides.

### 1.4.1 Synthesis of the BODIPY **29**.

Following the two step synthesis protocol, the iodophenyl BODIPY **29** was synthesized with satisfactory overall yields according to Scheme 6.



**Scheme 6. Synthesis of the BODIPY **29**.**

#### 1.4.1.1 Optical properties of the dye **29**.

The optical properties of the BODIPY **29** were evaluated in both PBS (phosphate-buffered saline (PBS), pH 7.3) and ethanol, and the data were collected in Table 6. The absorption spectra of the dye **29** in PBS exhibit two absorption peaks at 519 and 567 nm, the latter transition is characteristic of an aggregate which disappears in EtOH solvent (Figure 20). Nevertheless, in emission spectra a single emission peak was observed in both PBS and EtOH at about 532 nm with quantum yields of 61% and 71%, respectively. Note that in PBS the excitation at 567 nm does not cause any fluorescence of the dye. Moreover, the excitation spectra of the dye in both PBS and EtOH do not perfectly match the absorption spectra in EtOH. The disaccord between the absorption and emission

spectra of the dye in PBS is likely regarded in the following way. In aqueous condition the aggregation of the BODIPY dye observed in absorption is more likely non-emissive, therefore in emission and excitation spectra, only the emissive monomer of BODIPY dye was observed. In addition, the rather low extinction coefficient of the dye in PBS is probably due to the formation of aggregate in aqueous condition.

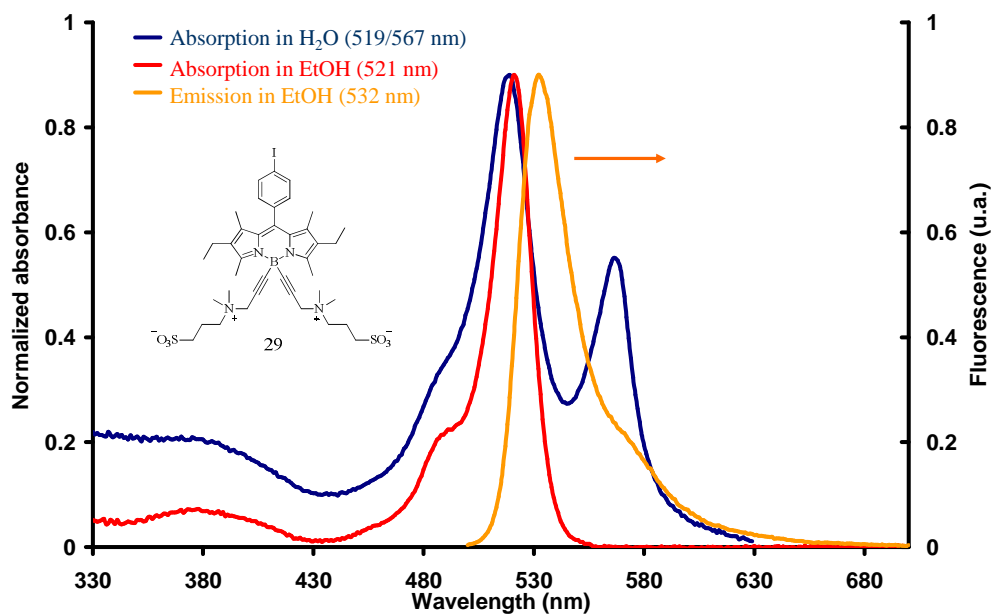
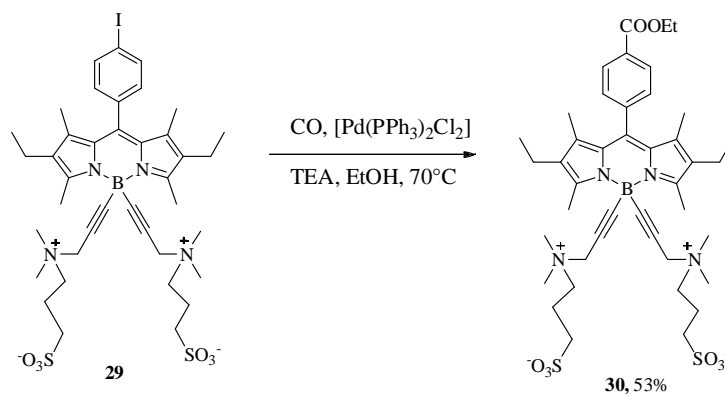


Figure 20. Normalized absorption and emission spectra of **29** in H<sub>2</sub>O and EtOH.

#### 1.4.2 Synthesis of the ester BODIPY **30**.

According to the literature and the know-how of the laboratory, a functional benzoic acid ester group could easily be formed from the aromatic halide through a carboalkoxylation reaction promoted by a catalytic amount of [Pd(PPh<sub>3</sub>)<sub>2</sub>Cl<sub>2</sub>].<sup>53-55</sup> The ethyl ester **30** was formed in situ by reacting the aromatic iodide **29** dissolved in ethanol (served as both reagent and solvent), with carbon monoxide at 70°C at atmospheric pressure in presence of a tertiary amine as base and 5% of [Pd(PPh<sub>3</sub>)<sub>2</sub>Cl<sub>2</sub>] (Scheme 7). The generated ester group is a stable functional group that is suitable for the storage of the dye, and can be easily converted to the carboxylic acid by saponification. The carboxylic acid functional group can be activated using sulfonate succinimide reagents and then linked to amino groups on proteins or DNA-derivatives.<sup>56</sup>

The optical properties of **30** were evaluated in ethanol and the optical data were collected in Table 6. In solution, the optical spectra of **30** were comparable with those of dye **29**. The introduction of an ethyl ester group doesn't affect its spectral properties (Figure 21). However, the drop of extinction coefficient ( $\epsilon$ ) and quantum yield ( $\phi$ ) were both observed, probably due to the formation of dimer in solvent.



Scheme 7. Synthesis of the ester BODIPY 30.

Table 6. Optical properties of BODIPY 28, 29 and 30.

| Compound                               | $\lambda_{\text{abs}}$ (nm) | $\epsilon$ ( $\text{M}^{-1} \cdot \text{cm}^{-1}$ ) | $\lambda_{\text{em}}$ (nm) | $\phi$ (%) <sup>a</sup> | $\tau$ (ns) | $k_r$ ( $10^7 \text{ s}^{-1}$ ) | $k_{\text{nr}}$ ( $10^7 \text{ s}^{-1}$ ) |
|--|-----------------------------|---|----------------------------|-------------------------|-------------|---------------------------------|---|
| <b>28</b> ( $\text{CH}_2\text{Cl}_2$ ) | 521                         | 57000   | 532                        | 48                      | 6.6         | 7.3                             | 7.9                                       |
| <b>29</b> ( $\text{H}_2\text{O}$ )     | 519/567                     | 28000/16800   | 530                        | 61                      | 7.0         | 8.7                             | 5.6                                       |
| <b>29</b> ( $\text{EtOH}$ )            | 521                         | 80100   | 532                        | 75                      | 7.2         | 10.4                            | 3.5                                       |
| <b>30</b> ( $\text{EtOH}$ )            | 521                         | 15400   | 532                        | 47                      | -           | -                               | -   |

a) Quantum yield determined in dilute solution ( $1 \times 10^{-6} \text{ M}$ ) using rhodamine 6G as reference ( $\phi_F = 0.78$  in water,  $\lambda_{\text{exc}} = 488 \text{ nm}$ ).<sup>32</sup> All  $\phi_F$  are corrected for changes in refractive index. b)  $k_r$  and  $k_{\text{nr}}$  were calculated using the following equations:  $k_r = \phi_F/\tau$ ,  $k_{\text{nr}} = (1-\phi_F)/\tau$ .

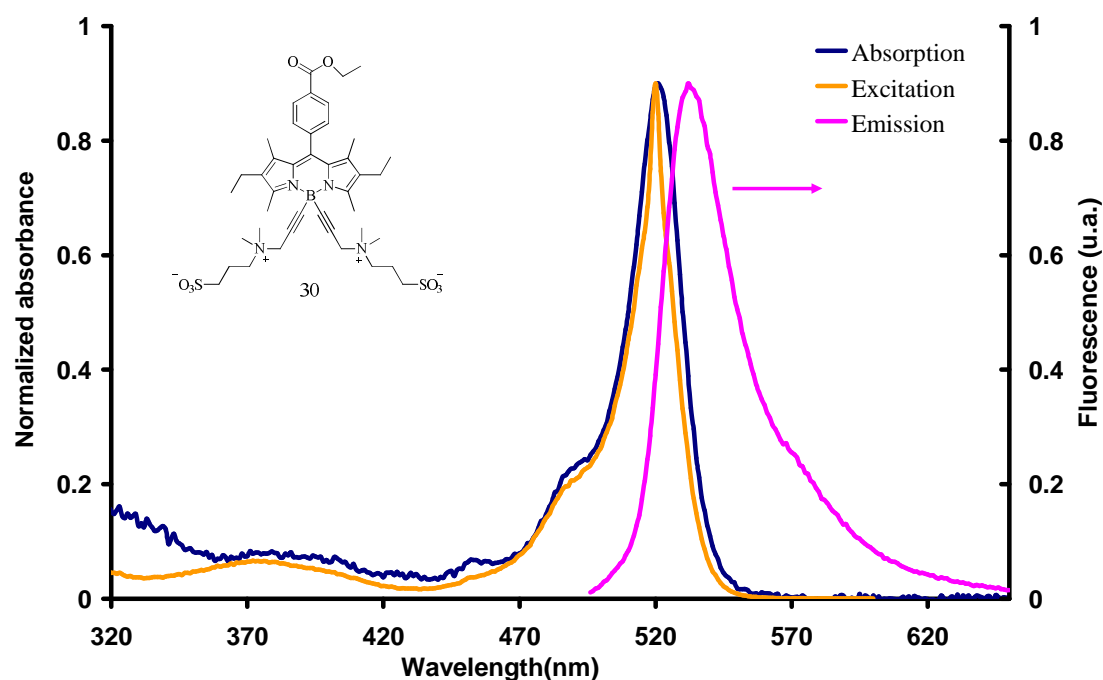


Figure 21. Normalized absorption, emission and excitation spectra of 30 in EtOH.

### 1.4.3 Synthesis of a watersoluble ‘cassette’ BODIPY.

The water-soluble dye **30** with an additional ester group for the bioconjugation was synthesized and its optical properties were evaluated. However, the relatively small Stokes' shift (the difference between the absorption and emission maxima) of BODIPY dye might be disadvantageous in biological labeling experiments. A narrow-band filter will be needed to analyze the emission spectrum and to separate them from the excitation source, which will consequently result in an extra cost during the use of the apparatus and a loss of experimental sensitivities.<sup>57</sup>

A common approach to enhance the Stokes's shift, at least in a virtual sense, is to make use of electronic energy transfer between two dyes tethered together via a covalent link; one taking the role of energy donor and the other being the acceptor.<sup>13,25,58</sup> According to recent researches, grafting of a pyrene unit onto the 8-meso position of BODIPY scaffold can effectively enhance the virtual Stokes's shift of the dye.<sup>13</sup>

Therefore, a new synthetic route was designed to enhance the Stokes' shifts of the dye (Figure 22). The retro-synthesis consisted of two parts: the first involves in functionalization of the pyrene unit with a terminal ethynyl group for the cross coupling and an additional functional group for the bioconjugation; and then the functionalized pyrene unit will be introduced onto the BODIPY scaffold. The pyrene moiety serves as the energy donor and functional group for bioconjugation, while BODIPY moiety is the energy acceptor and light emitter.

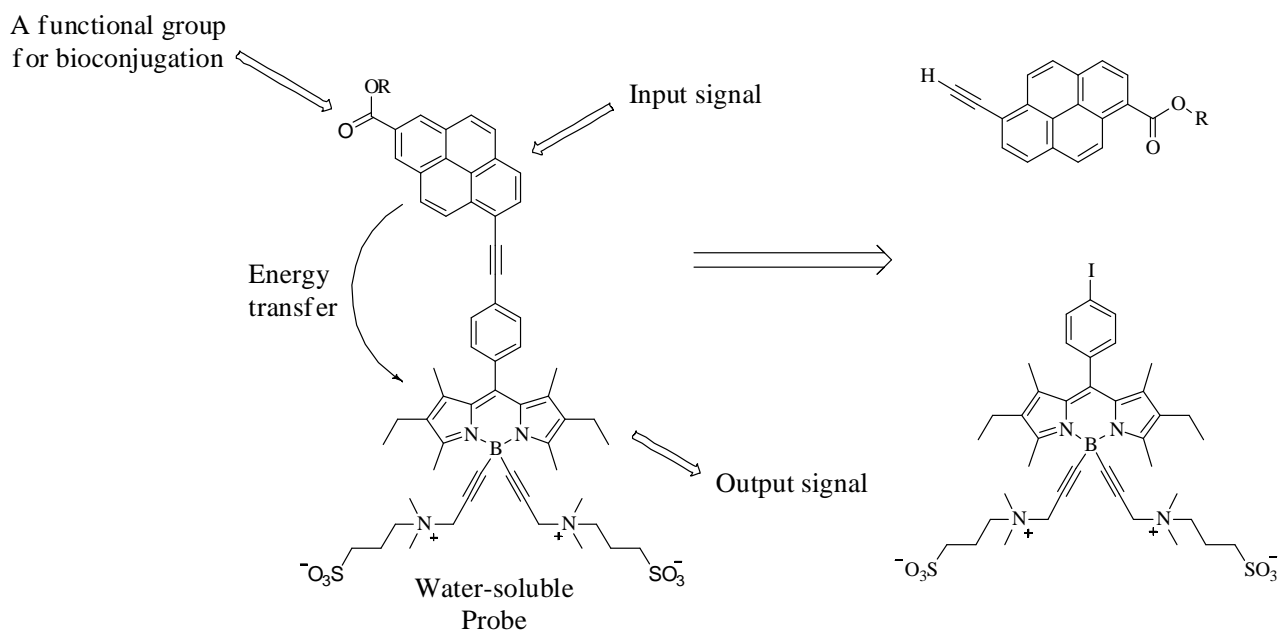
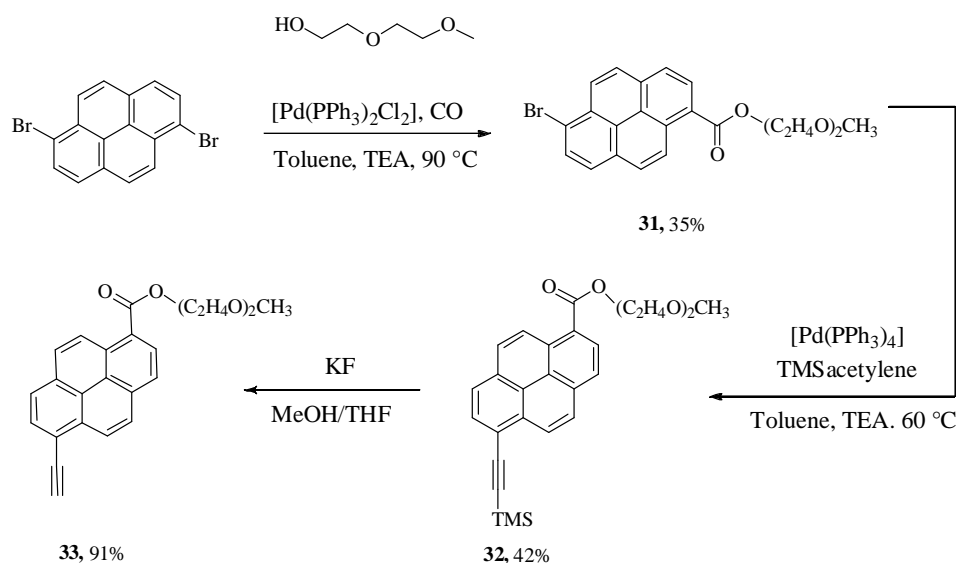


**Figure 22. Retro-synthesis of the pyrene sulfobetaine BODIPY cassette.**

### 1.4.4 Synthesis of ester pyrene **33**.

The 1,6-dibromopyrene was used as starting material,<sup>59</sup> a carboalkoxylation reaction was carried out under standard condition to convert the aromatic bromide into ester group and gave the mono-ester pyrene **31** in 35% isolated yield. The diethylene glycol monomethyl ether was used as the nucleophilic alcohol in order to facilitate the purification of the yielded mono-ester pyrene from the di-ester pyrene and starting material. Followed by a Sonogashira cross-coupling reaction the pyrene **31** was converted to TMS-ethynyl pyrene **32**. The trimethylsilyl protecting group was then removed by using KF in a methanol/THF mixture to give the acetylene pyrene **33** (Scheme 8).



**Scheme 8. Synthesis of pyrene **33**.**

#### 1.4.4.1 Optical properties of the pyrene **33**.

The optical properties of pyrene **33** were evaluated in  $\text{CH}_2\text{Cl}_2$  and the data were collected in Table 7. In solution, the electronic absorption spectrum exhibit three characteristic absorption bands centered at 369, 296, and 240 nm, safely assigned to the  $\pi$ - $\pi^*$  transitions of pyrene- moiety. However, the lowest energy absorption bands centered at about 369 nm is less structured, probably due to the overlapping between  $S_0 \rightarrow S_1$  transition of the pyrene and the  $\pi$ - $\pi^*$  transition localized on the alkyne fragment. A well structured characteristic of pyrene emission band was observed centered at 400 and 422 nm with a quantum yield of 59%. The excitation spectrum matches the absorption spectrum and confirms that all the transitions are involved in the emission spectra.

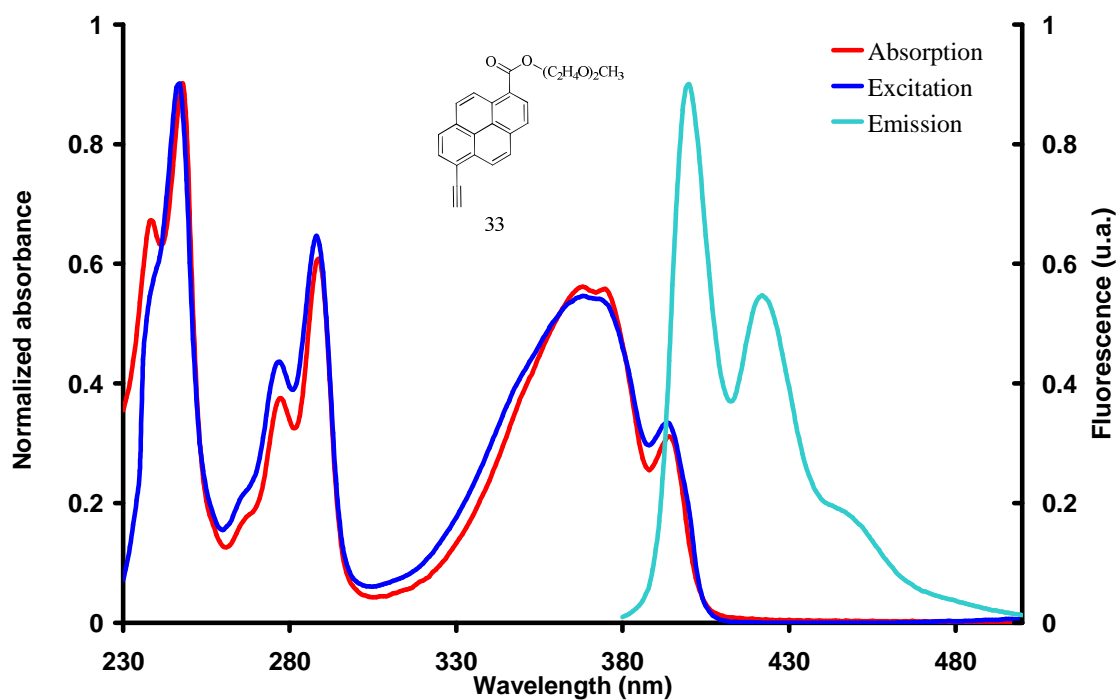
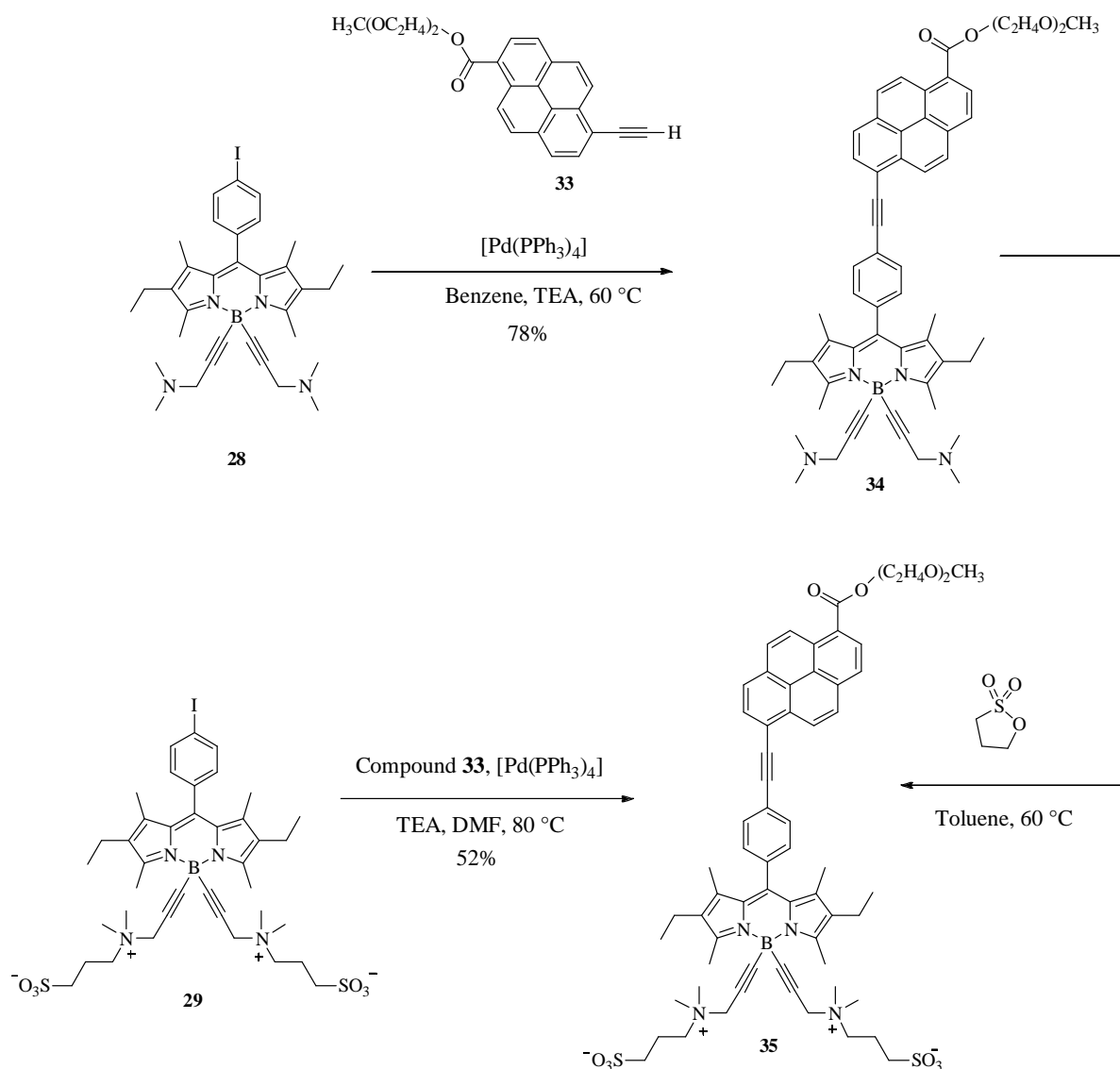


Figure 23. Absorption, emission and excitation spectra of compound **33** in  $\text{CH}_2\text{Cl}_2$ .

#### 1.4.5 Synthesis of the ester pyrene BODIPY **35**.

Dye **35** could be prepared by using two convergent synthetic approaches. The first protocol involved a cross-coupling reaction of BODIPY **28** with acetylene-pyrene **33** via a Sonogashira reaction under standard condition leading to compound **34** in 78% yields. Followed by a quaternization of **34** with 1,3-propanesultone to give the pyrene-sulfobetaine BODIPY **35**. However, the quaternization reaction generated both the mono and the bis-sulfobetaine compounds, which were difficult to be isolated due to similar polarity. Therefore the synthesis was carried out via a cross-coupling reaction of pyrene **33** with the BODIPY dye **29** to afford compound **35** in 52% yields.



Scheme 9. Synthesis of pyrene BODIPY 35.

#### 1.4.5.1 <sup>1</sup>H NMR characterisation of ester pyrene BODIPY 35.

The <sup>1</sup>H NMR spectra of compound **35** was carried out in a mixture of CD<sub>3</sub>OD/CDCl<sub>3</sub>/D<sub>2</sub>O, due to its amphiphilic nature (Figure 24), and confirms its molecular structure. The integration of 8H observed around 9.1-8.5 ppm is attributed to the pyrene subunit; the integration of 2 protons and 2 protons observed at 7.9 and 7.4 ppm is unambiguously attributed to the AB system of phenyl group. The integration of 12H at 3.1 ppm is assigned to the four methyl groups of the ammonium moieties. The integration of 4 protons and 4 protons at 2.25 and 2.4 ppm, respectively, belonging to the methylene groups of the CH<sub>2</sub>-CH<sub>2</sub>-SO<sub>3</sub><sup>-</sup> chains, which confirm the formation of the sulfobetaine residues.

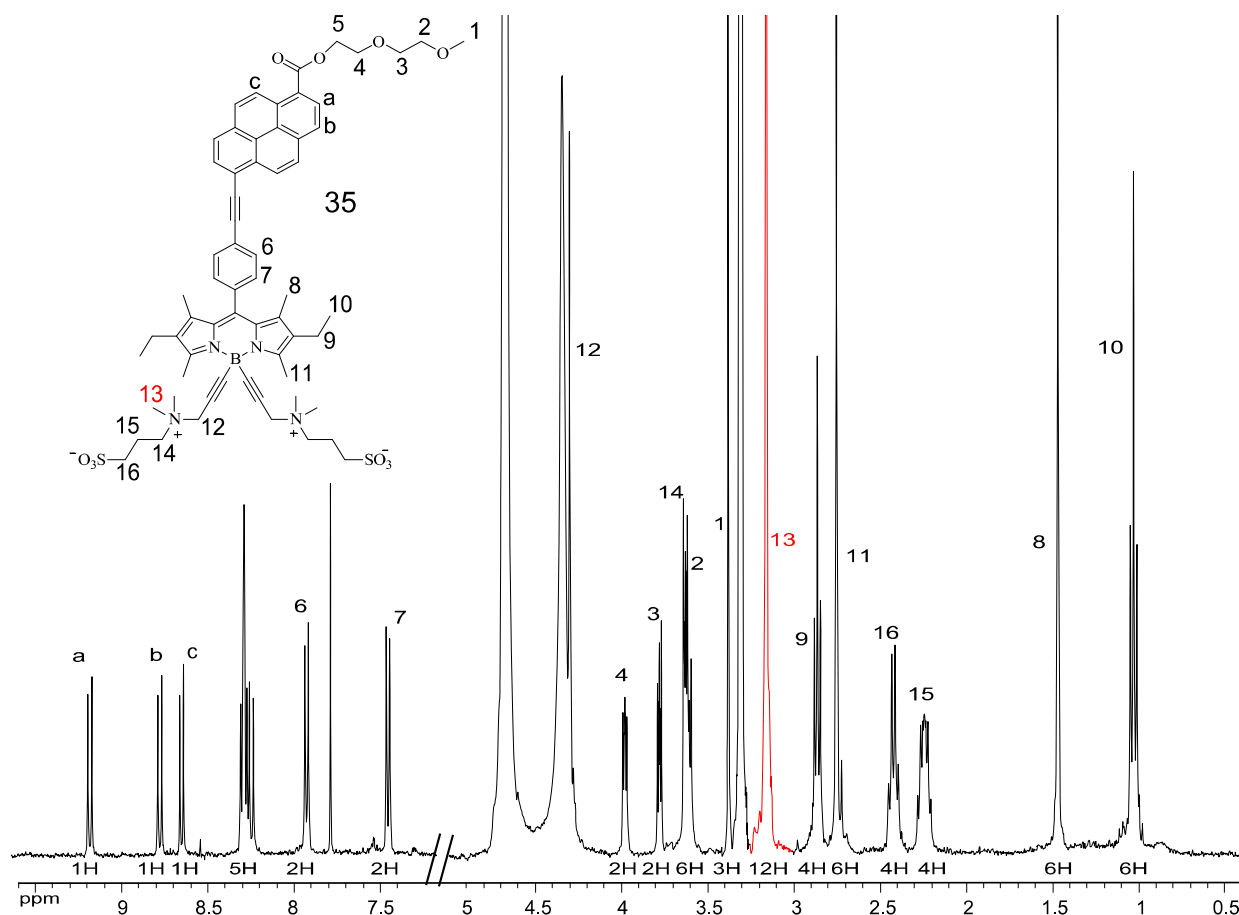


Figure 24.  $^1\text{H}$  NMR 400 MHz spectra of the ester **35** in  $\text{CD}_3\text{OD}/\text{CDCl}_3/\text{D}_2\text{O}$ .

#### 1.4.5.2 Optical properties of compound **35**.

The optical properties of compound **35** were evaluated in EtOH, and the data were collected in Table 7. In absorption spectra, the relatively sharp absorption band centered at 521 nm with a shoulder at 488 nm is safely assigned to the  $S_0$ - $S_1$  transition of BODIPY, with an absorption coefficient of  $57000 \text{ M}^{-1}\text{cm}^{-1}$ . At higher energy region, three broad absorption bands located around 330-430nm and 300 nm can be assigned to the  $(\pi$ - $\pi^*)$  transition localized on the pyrene subunit. By excitation in the BODIPY at 488 nm, a single sharp emission peak was observed centered at 535nm, corresponds to the emission of the BODIPY moiety with a quantum yield of 38%. By excitation in the pyrene absorption region at 370 nm, no residual fluorescence emission was detected within the spectral region of 400-500nm from the pyrene unit, but only the emission peak of BODIPY was detected. The excitation spectrum recorded at 625 nm is in excellent agreement with the absorption spectra, proving that the energy-transfer from the pyrene subunit to the BODIPY moiety is quantitative and very fast.<sup>13</sup> Moreover, the irradiation within the absorption region of BODIPY dye at 498 nm give a quantum yield of 38%, and the irradiation within the absorption region of pyrene unit at 362 nm (where BODIPY moiety has little absorption) provides a similar quantum yield of 38%, indicating a very efficient intramolecular energy transfer. The mechanism of energy transfer

between the pyrene and BODIPY moiety is likely due to a good spectra overlap between the emission of pyrene unit and the  $S_0 \rightarrow S_2$  transition bands of BODIPY moiety localized around 350 nm. Likewise the energy transfer process is in conformity with the frame of the Förster theory based on a dipole-dipole mechanism.<sup>13,25,60</sup>

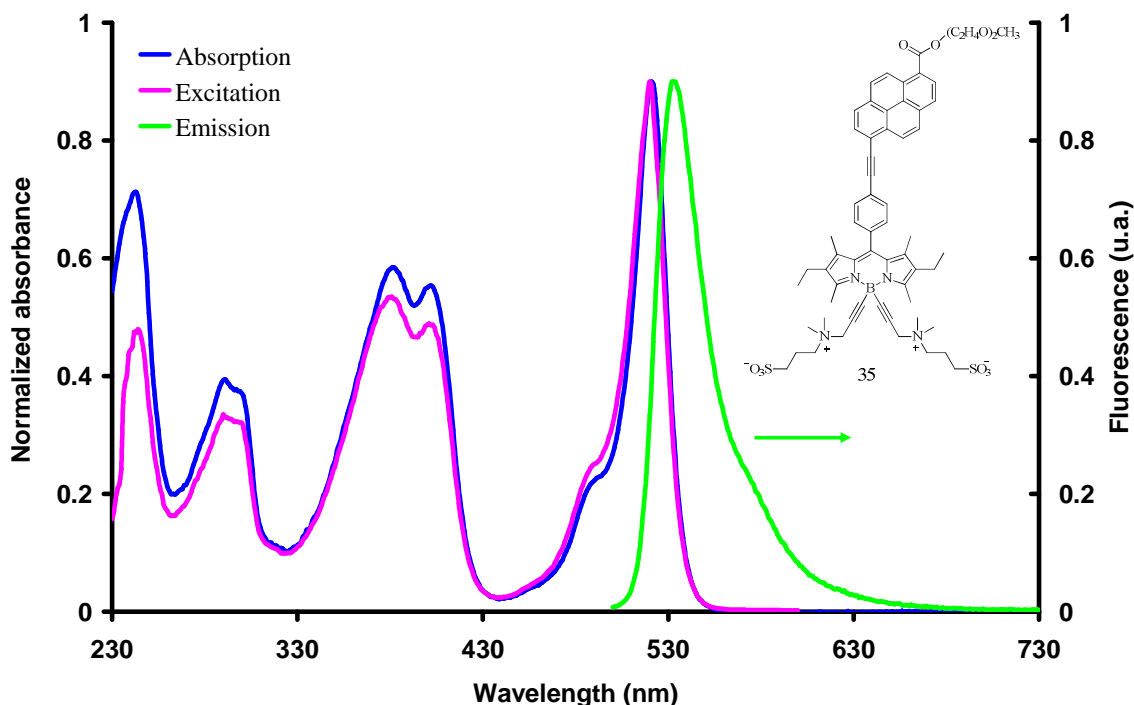


Figure 25. Absorption, emission and excitation spectra of **35** in EtOH.

Table 7. Optical properties of the selected compounds.

| Compound                               | $\lambda_{\text{abs}}$ (nm) | $\epsilon$ ( $\text{M}^{-1} \cdot \text{cm}^{-1}$ ) | $\lambda_{\text{em}}$ (nm) | $\phi$ (%) <sup>a</sup> | $\tau$ (ns) |
|--|-----------------------------|---|----------------------------|-------------------------|-------------|
| <b>33</b> ( $\text{CH}_2\text{Cl}_2$ ) | 394/369                     | 17800/33000   | 400/422                    | 59                      | -           |
| <b>34</b> ( $\text{CH}_2\text{Cl}_2$ ) | 522/404                     | 46900/32400   | 535                        | 54                      | -           |
| <b>35</b> (EtOH)                       | 521/402                     | 57000/35200   | 533                        | 38                      | -           |

a) Quantum yield determined in dilute solution ( $1 \times 10^{-6} \text{M}$ ) using rhodamine 6G ( $\phi_{\text{F}} = 0.78$  in water,  $\lambda_{\text{exc}} = 488$  nm) or quinine sulfate as reference ( $\phi_{\text{F}} = 0.55$  in 1M  $\text{H}_2\text{SO}_4$ ,  $\lambda_{\text{exc}} = 366$  nm).<sup>32</sup> All  $\phi_{\text{F}}$  are corrected for changes in refractive index.

#### 1.4.6 Synthesis of the acid compound **36**.

The saponification of **35** was carried out in EtOH/ $\text{H}_2\text{O}$  in presence of NaOH at room temperature over 10 hours and gave the acid **36** in 30% of isolated yield (Figure 26). Thus, we succeed to produce a partially water soluble cassette dye potentially capable of fluorescing in aqueous media with large virtual stokes shift and carrying an additional functional group for bioconjugation.



## Reference

- (1) Panchuk-voloshina, N.; Haugland, R. P.; Bishop-stewart, J.; Bhalgat, M. K.; Millard, P. J.; Mao, F.; Leung, W.-Y.; Haugland, R. P. *J. Histochem. Cytochem.* **1999**, *47*, 1179.
- (2) Kolmakov, K.; Belov, V.; Bierwagen, J.; Ringemann, C.; Müller, V.; Eggeling, C.; Hell, S. *Chem. Eur. J.* **2009**, *16*, 158.
- (3) Boyer, J. H.; Haag, A. M.; Sathyamoorthi, G.; Soong, M. L.; Thangaraj, K.; Pavlopoulos, T. G. *Heteroat. Chem.* **1993**, *4*, 39.
- (4) Li, L.; Han, J.; Nguyen, B.; Burgess, K. *J. Org. Chem.* **2008**, *73*, 1963.
- (5) Li, Z.; Lier, J. v.; Leznoff, C. C. *Can.J.Chem.* **1999**, *77*, 138.
- (6) Eftink, M. R.; Ghiron, C. A. *Anal. Biochem.* **1981**, *114*, 199.
- (7) Kano, K.; Sato, T.; Yamada, S.; Ogawa, T. *J. Phys. Chem* **1983**, *87*, 566.
- (8) Oshima, J.; Yoshihara, T.; Tobita, S. *Chem. Phys. Lett.* **2006**, *423*, 306.
- (9) Noh, M.; Kim, T.; Lee, H.; Kim, C.-K.; Joo, S.-W.; Lee, K. *Colloids and Surfaces A: Physicochemical and Engineering Aspects* **2010**, *359*, 39.
- (10) King, J. F.; Loosmore, S. M.; Aslam, M.; Lock, J. D.; McGarrity, M. J. *J. Am. Chem. Soc.* **1982**, *104*, 7108.
- (11) Speiser, S. *Chem. Rev.* **1996**, *96*, 1953.
- (12) Jiao, G.-S.; Thoresen, L. H.; Burgess, K. *J. Am. Chem. Soc.* **2003**, *125*, 14668.
- (13) Ziessel, R.; Goze, C.; Ulrich, G.; Césarío, M.; Retailleau, P.; Harriman, A.; Rostron, J. P. *Chemistry – A European Journal* **2005**, *11*, 7366.
- (14) Ulrich, G.; Goze, C.; Guardigli, M.; Roda, A.; Ziessel, R. *Angew. Chem.* **2005**, *117*, 3760.
- (15) De Castro, K. A.; Ko, J.; Park, D.; Park, S.; Rhee, H. *Org. Process Res. Dev.* **2007**, *11*, 918.
- (16) Bajwa, J. S.; Chen, G.-P.; Prasad, K.; Repic, O.; Blacklock, T. J. *Tetrahedron Lett.* **2006**, *47*, 6425.
- (17) Jolicoeur, B.; Chapman, E. E.; Thompson, A.; Lubell, W. D. *Tetrahedron* **2006**, *62*, 11531.
- (18) Ulrich, G.; Ziessel, R. *J. Org. Chem.* **2004**, *69*, 2070.
- (19) Ulrich, G.; Ziessel, R.; Harriman, A. *Angew. Chem., Int. Ed.* **2008**, *47*, 1184.
- (20) Loudet, A.; Burgess, K. *Chem. Rev.* **2007**, *107*, 4891.
- (21) Meltola, N. J.; Wahlroos, R.; Soini, A. E. *J. Fluoresc.* **2004**, *14*, 635.
- (22) Tasior, M.; Murtagh, J.; Frimannsson, D. O.; McDonnell, S. O.; O'Shea, D. F. *Org. Biomol. Chem.* **2009**, *8*, 522.

- (23) Bonardi, L.; Ulrich, G.; Ziessel, R. *Org. Lett.* **2008**, *10*, 2183.
- (24) Goze, C.; Ulrich, G.; Ziessel, R. *Org. Lett.* **2006**, *8*, 4445.
- (25) Goze, C.; Ulrich, G.; Ziessel, R. *J. Org. Chem.* **2007**, *72*, 313.
- (26) Komatsu, T.; Urano, Y.; Fujikawa, Y.; Kobayashi, T.; Kojima, H.; Terai, T.; Hanaoka, K.; Nagano, T. *Chem. Commun.* **2009**, 7015.
- (27) Gabe, Y.; Ueno, T.; Urano, Y.; Kojima, H.; Nagano, T. *Anal. Bioanal. Chem.* **2006**, *386*, 621.
- (28) Li, L.; Nguyen, B.; Burgess, K. *Bioorg. Med. Chem. Lett.* **2008**, *18*, 3112.
- (29) Haeefe, A.; Zedde, C.; Retailleau, P.; Ulrich, G.; Ziessel, R. *Org. Lett.* **2010**, *12*, 1672.
- (30) Qin, W.; Baruah, M.; Van der Auweraer, M.; De Schryver, F. C.; Boens, N. *J. Phys. Chem. A* **2005**, *109*, 7371.
- (31) Fillafer, C.; Friedl, D. S.; Wirth, M.; Gabor, F. *Small* **2008**, *4*, 627.
- (32) Olmsted, J. *J. Phys. Chem* **1979**, *83*, 2581.
- (33) Collins, T.; D'Amico, S.; Georlette, D.; Marx, J. C.; Huston, A. L.; Feller, G. *Anal. Biochem.* **2006**, *352*, 299.
- (34) Gonne, A.; Ernst, R. *Anal. Biochem.* **1978**, *87*, 28.
- (35) Hjelmeland, L. M.; Nebert, D. W.; Osborne, J. C. *Anal. Biochem.* **1983**, *130*, 72.
- (36) Hjelmeland, L. M. *Proc. Natl. Acad. Sci. U. S. A.* **1980**, *77*, 6368.
- (37) Handler, J. S.; Kwon, H. M. *Nephron* **2001**, *87*, 106.
- (38) Le Rudulier, D.; Strom, A. R.; Dandekar, A. M.; Smith, L. T.; Valentine, R. C. *Science* **1984**, *224*, 1064.
- (39) Holmström, K. O.; Somersalo, S.; Mandal, A.; Palva, T. E.; Welin, B. *J. Exp. Bot.* **2000**, *51*, 177.
- (40) Yeo, A. *J. Exp. Bot.* **1998**, *49*, 915.
- (41) Sakamoto, A.; Murata, N. *Plant, Cell & Environment* **2002**, *25*, 163.
- (42) Lowe, A. B.; Billingham, N. C.; Armes, S. P. *Chemical Communications* **1996**, 1555.
- (43) Lowe, A. B.; Vamvakaki, M.; Wassall, M. A.; Wong, L.; Billingham, N. C.; Armes, S. P.; Lloyd, A. W. *Journal of Biomedical Materials Research* **2000**, *52*, 88.
- (44) Dost, Z.; Atilgan, S.; Akkaya, E. U. *Tetrahedron* **2006**, *62*, 8484.
- (45) Ziessel, R.; Ulrich, G.; Harriman, A.; Alamiry, M. A. H.; Stewart, B.; Retailleau, P. *Chemistry – A European Journal* **2009**, *15*, 1359.
- (46) Rurack, K.; Kollmannsberger, M.; Daub, J. *New J. Chem.* **2001**, *25*, 289.

- (47) Somerharju, P. *Chem. Phys. Lipids* **2002**, *116*, 57.
- (48) Schultz, S. G. *Molecular biology of membrane transport disorders*; Plenum Press, 1996.
- (49) Salonen, A.; Knyazev, A.; von Bandel, N.; Degrouard, J.; Langevin, D.; Drenckhan, W. *ChemPhysChem* **2011**, *12*, 150.
- (50) Robertson, J. M.; White, J. G. *J. Chem. Soc.(Lond.)* **1947**, 358.
- (51) Spackman, M. A.; Jayatilaka, D. *CrystEngComm* **2009**, *11*, 19.
- (52) Nepomnyashchii, A. B.; Cho, S.; Rosky, P. J.; Bard, A. J. *J. Am. Chem. Soc.* **2010**, *132*, 17550.
- (53) Schoenberg, A.; Bartoletti, I.; Heck, R. F. *J. Org. Chem.* **1974**, *39*, 3318.
- (54) El-ghayoury, A.; Ziessel, R. *Tetrahedron Lett.* **1998**, *39*, 4473.
- (55) Stille, J. K.; Wong, P. K. *J. Org. Chem.* **1975**, *40*, 532.
- (56) Gee, K. R.; Archer, E. A.; Kang, H. C. *Tetrahedron Lett.* **1999**, *40*, 1471.
- (57) Querner, J.; Wolff, T. *Angew. Chem., Int. Ed.* **2002**, *41*, 3063.
- (58) Goze, C.; Ulrich, G.; Mallon, L. J.; Allen, B. D.; Harriman, A.; Ziessel, R. *J. Am. Chem. Soc.* **2006**, *128*, 10231.
- (59) Grimshaw, J.; Trocha-Grimshaw, J. *Journal of the Chemical Society, Perkin Transactions 1* **1972**, 1622.
- (60) Förster, T. *Radiation Research Supplement* **1960**, *2*, 326.
- (61) Niu, S. L.; Massif, C.; Ulrich, G.; Ziessel, R.; Renard, P.-Y.; Romieu, A. *Org. Biomol. Chem.* **2010**, *9*, 66.

# CHAPTER III

## Synthesis of Water-soluble Red-emitting BODIPY dyes

### 1.1. Introduction

In this chapter, we aimed to design and synthesize a new series of water-soluble BODIPY dyes emitting in the red spectral region, besides an additional functional group for labeling antibodies or proteins.

#### 1.1.1. Commercial available water-soluble red-emitting fluorophores

Generally speaking, the red color to human eyes is the light of wavelengths in the 630-740 nm range and the red/near-infrared from 630 to 900 nm spectral region. In biological labeling, the scattering and absorption of the light by tissues in this spectral region is remarkably reduced, the background signal from cellular autofluorescence (300-550 nm) is also minimized.<sup>1-5</sup> Hence, the red-emitting fluorophores offer a better resolution and contrast in the biological labeling experiments. Therefore the red-emitting dyes are highly demanded in the field of fluorescence-labeling. Red-emitting, high fluorescence quantum yield ( $\theta$ ), high absorption coefficient ( $\epsilon$ ), relatively long lifetimes (1–5 ns), high photostability, good water-solubility, and an additional functional group for bio-conjugation, all these properties are required for an ideal bio-labeling fluorophore.<sup>6-10</sup> In practice, however, all these requirements can hardly be fulfilled by a single molecule.

Commercially available Red-emitting fluorescent dyes such as rhodamine dyes, Texas Red ( $\lambda_{em} = 615$  nm), Alexa 594 ( $\lambda_{em} = 617$  nm), Alexa 633 ( $\lambda_{em} = 647$  nm), Carbocyanine dyes such as Alexa 647 ( $\lambda_{em} = 672$  nm) and Cy 5.5 ( $\lambda_{em} = 694$  nm), Carbopyronine dyes Atto 635 ( $\lambda_{em} = 659$  nm) and Atto 647N ( $\lambda_{em} = 669$  nm) (Chart 1 and Table 1), designed from different chromophore families have been widely used for different biological labeling purposes.<sup>7,9,11</sup> The rhodamine dyes are known for their chemical stability and brightness, a quite number of red-emitting rhodamine dyes

were designed by different chemical modifications. The research aim to shift the emission of the dyes to the red region while keeping their suitable properties for bio-labeling is still under investigation.<sup>7</sup> Alexa 647 dye is similar to the Cy5 dye with respect to absorption maxima, Stokes' shifts, and extinction coefficients, but more stable and shows better performance in bio-labeling analysis according to the literature.<sup>6</sup> On the other hand, the cyanine dyes usually have rather short fluorescence lifetimes of about 1 ns and low quantum yield, which are inconvenient in certain time-resolved fluorescence imaging techniques.<sup>12</sup> The Carbopyronine dye Atto 647N is more photostable with a rather high quantum yield compare with the cyanine dyes, but its low polarity leads to difficulties in biological essays.<sup>13</sup> Recently, new carbopyronine dye has been synthesized and reported with good water-solubility and suitable for bio-conjugation.<sup>8</sup>

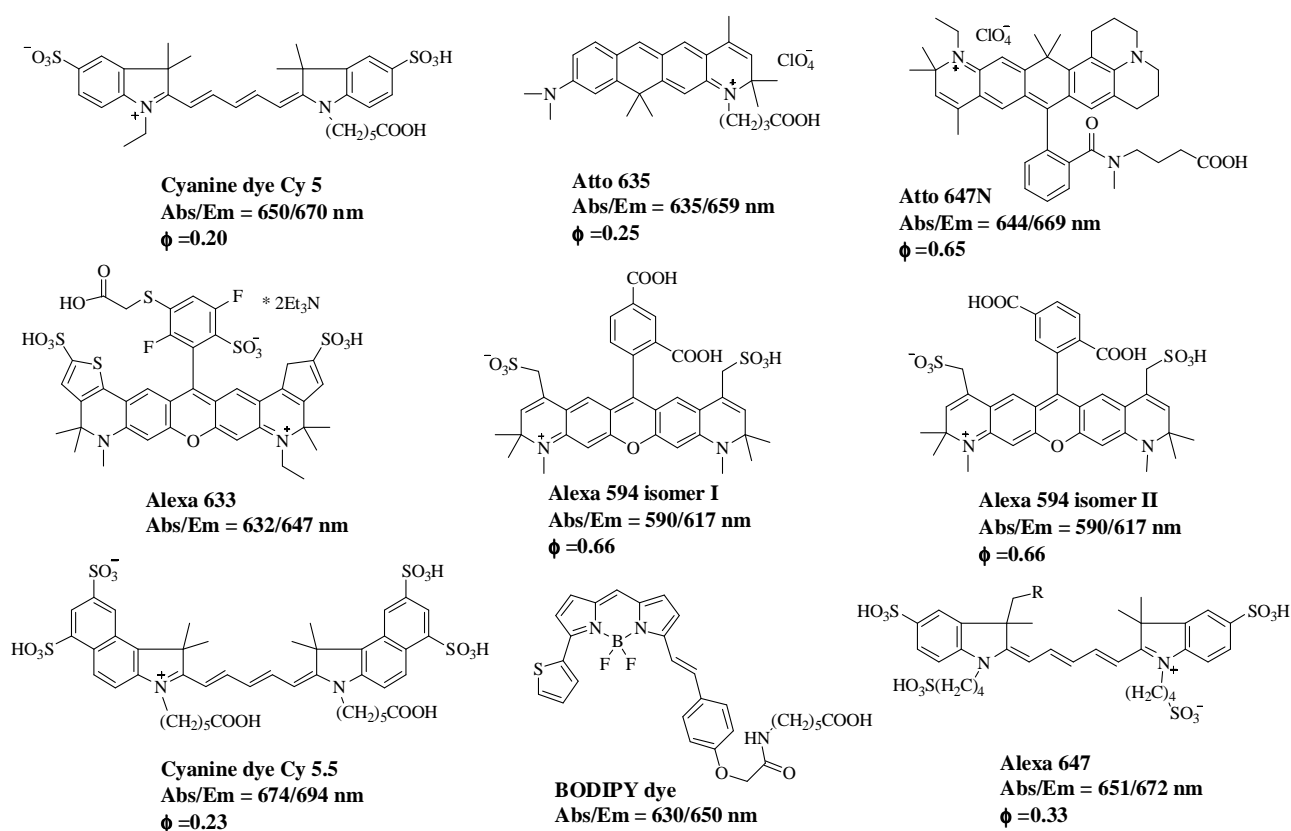


**Chart 1. Structures of the commercially available red-emitting fluorescent dyes.**<sup>9,11,14,15</sup>

Contrary to the cyanine and rhodamine family, only a limited number of water-soluble and bio-conjugable BODIPY derivatives are now available.<sup>16-22</sup> In 2006, Atilgan and coworkers reported the synthesis of the first water-soluble NIR fluorescent BODIPY dye by introduction of several PEG-type linkers onto the 8-*meso*-phenyl and 3,5-distyryl moieties of BODIPY core.<sup>23</sup> Further functionalization with dipicolylamine ligand has enabled them to design a sensitive and selective ratiometric chemosensor for Zn(II) ions.<sup>24</sup> However, the lack of an additional functional group for

bio-conjugation limits their use as a bio-labeling reagent. Anionic and cationic substituted  $\text{BF}_2$ -chelated tetraarylazadipyrrromethene derivatives (aza-BODIPY), bearing sulfonic acid, carboxylic acid or quaternary amine moieties have been synthesized.<sup>25</sup> However, the location of two water-solubilization groups on the same side (top or bottom) of the aza-BODIPY scaffold led to amphiphilic-like structures which are fluorescent only in aqueous solution containing additives that disrupt aggregates.

**Table 1. Optical properties of commercially available red-emitting fluorescent dyes. The data above were cited from the reports<sup>7,9,11,20</sup> or provided by chemical suppliers.<sup>26,27,28</sup>**

| Name                        | $\lambda_{\text{abs}}$ (nm) | $\lambda_{\text{em}}$ (nm) | $\epsilon \times 10^{-5}$ ( $\text{M}^{-1}\text{cm}^{-1}$ ) | $\phi$ (%) | $\tau$ (ns)            | Solubility             | Provider      |
|-----------------------------|-----------------------------|----------------------------|---|------------|------------------------|------------------------|---------------|
| BODIPY <sup>®</sup> 630/650 | 625                         | 640                        | 1.01  | "good"     | 3.9 (H <sub>2</sub> O) | DMSO, MeCN             | Invitrogen    |
| Atto 633                    | 629                         | 657                        | 1.3   | 64         | 3.2 (H <sub>2</sub> O) | DMF, DMSO              | Atto-tec      |
| Atto 635                    | 635                         | 659                        | 1.2   | 25         | 1.9                    | MeCN                   | Atto-tec      |
| Atto 647N                   | 644                         | 669                        | 1.5   | 65         | 3.4                    | DMF, DMSO              | Atto-tec      |
| Alexa <sup>®</sup> 633      | 632                         | 647                        | 1   | -          | 3.2                    | DMSO, H <sub>2</sub> O | Invitrogen    |
| Alexa <sup>®</sup> 647      | 651                         | 672                        | 2.7   | 33         | 1                      | DMSO, H <sub>2</sub> O | Invitrogen    |
| Cy <sup>®</sup> 5           | 647                         | 633                        | 2.5   | 27 (PBS)   | 1 (PBS)                | H <sub>2</sub> O       | GE Healthcare |
| Cy <sup>®</sup> 5.5         | 674                         | 694                        | 1.9   | 23 (PBS)   | 1 (PBS)                | H <sub>2</sub> O       | GE Healthcare |
| Texas Red                   | 589                         | 615                        | 0.85  | -          | 4.2                    | H <sub>2</sub> O       | Sigma-Aldrich |

Recently in 2009, we developed two strategies to introduce the sulfonate groups onto the BODIPY scaffold (discussed in Chapter II) to improve its solubility in water.<sup>29,30</sup> The first one lies on introduction of polysulfonated linkers derived from  $\alpha$ -sulfo- $\beta$ -alanine peptide<sup>9,10</sup> (discussed in chapter I) onto the BODIPY scaffolds by post-synthetic acylation reaction. The second approach is based on the formation of polar zwitterions by the reaction of propargylamine BODIPY derivatives with 1,3-propanesultone. Both methods could be perfectly applied on the green-emitting BODIPY derivatives and enable the dyes to be totally soluble in water without affecting their photo-physical properties. However, the attempt of introducing the polysulfonated linker on the pseudo-meso 8-position of Red-emitting distyryl BODIPY scaffold leads to fluorescence-quenching of the dye in water due to the formation of aggregates as described previously. Thus, in this chapter, we focused on resolving this problem and designing a new range of red-emitting water-soluble BODIPY derivatives for bio-labeling applications.

### 1.1.2. Red-emitting BODIPY

In the last decade, considerable efforts have been dedicated to the functionalization of BODIPY dyes' to more sophisticated one for which the absorption and emission spectrum is shifted to longer wavelengths by extending the aromatic core.

Many Red-emitting BODIPY analogues (Chart 2) were developed by using several approaches: (i) pyrrole-based starting materials leading to more conjugated BODIPY derivatives;<sup>31,32</sup> (ii) aromatic ring-fused BODIPY derivatives;<sup>33-36</sup> (iii) attaching auxochromic substituents to the 3,5-positions of the BODIPY core<sup>37</sup> or by condensation reaction of the 3,5-dimethyl BODIPY derivatives with the nucleophilic benzaldehyde derivatives to give styryl-BODIPY derivatives.<sup>38-40</sup> Among these methods, the 3,5-position substituted di-aryl BODIPY dyes show a bathochromic shift of over 100 nm, but generally have relatively low fluorescence quantum yields due to the flexibility of the aromatic substituent.<sup>41,42</sup>

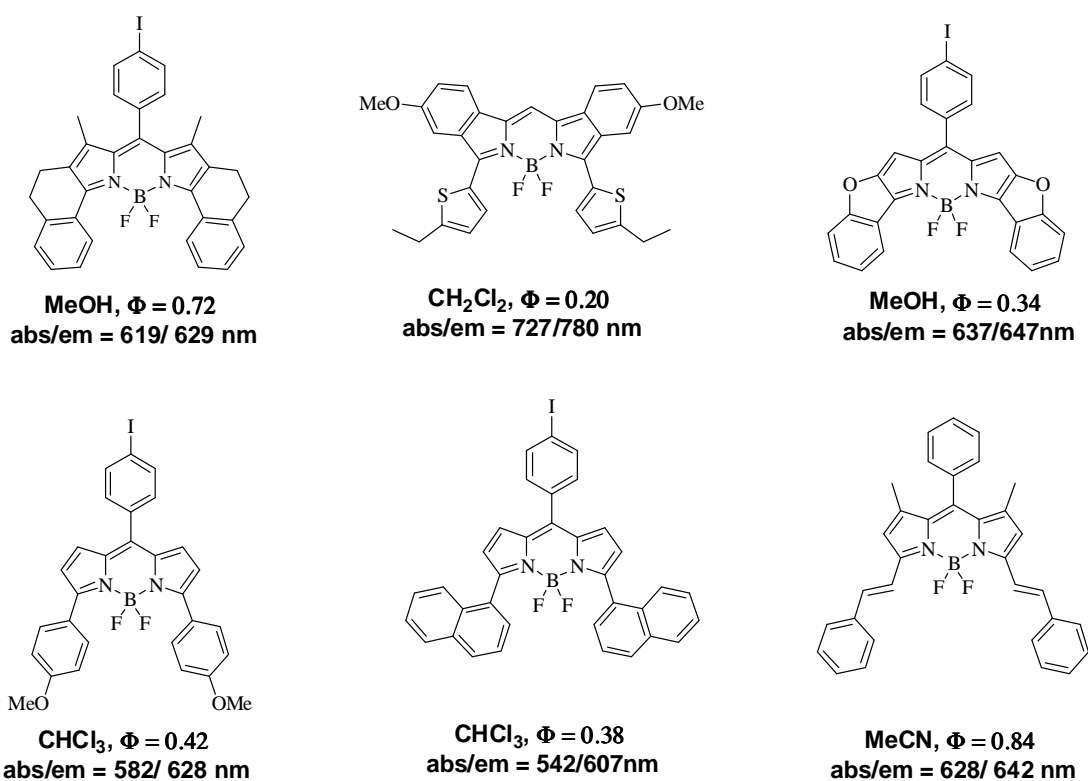


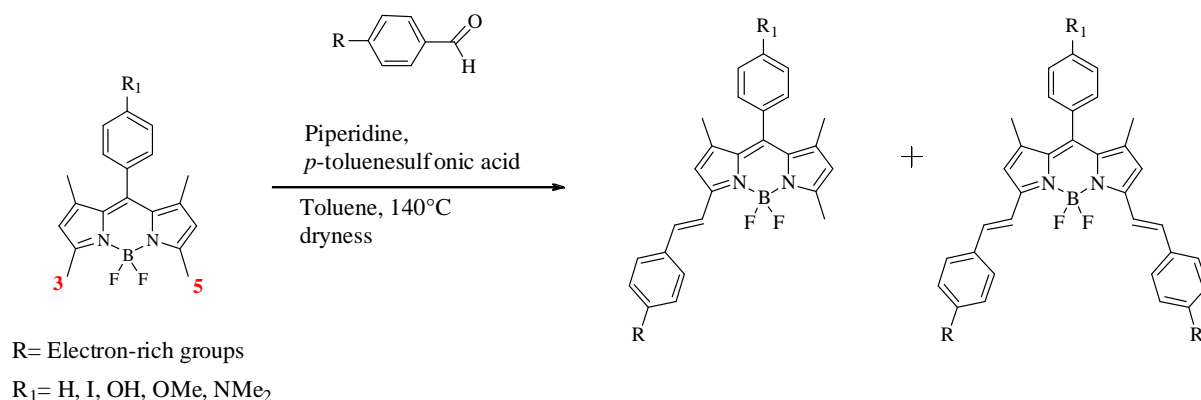
Chart 2. Some Red-emitting BODIPY dyes.<sup>43</sup>

Interestingly, the introduction of styryl substituent at the 3,5-positions of a BODIPY core can bring large bathochromic shifts of the dye by 70-170 nm. Moreover, the rigidified BODIPY scaffold results in higher quantum yields.<sup>44,45</sup>

### 1.1.3. Distyryl-BODIPY dyes

The first distyryl BODIPY was obtained via the condensation reaction of 2-styrylpyrrole<sup>46</sup> with the corresponding aromatic aldehyde.<sup>45</sup> It was discovered later that the methyl groups at 3,5-position of the BODIPY core are nucleophilic enough to participate in Knoevenagel condensation reaction.<sup>47</sup> A mixture of mono- and di-styryl-BODIPY can be obtained by the condensation reaction with the

corresponding aromatic aldehyde derivatives (Scheme 1).<sup>38-40,48,49</sup> Such one-pot reaction is convenient and a less time-consuming approach to extend the  $\pi$ -conjugation of the BODIPY core compared with other methods.



**Scheme 1. Formation of mono- and distyryl BODIPY derivatives.**

The absorption spectrum of such derivatives presents the typical BODIPY features, showing the narrow and intense peak ( $\epsilon = 90,000$  to  $120,000 \text{ M}^{-1} \text{ cm}^{-1}$ ) with the maxima centered around 620-700 nm. A bathochromic shifts about 120-170 nm is observed compared with the conventional BODIPY dyes.<sup>45</sup> The emission peaks of the distyryl BODIPY dyes are centered around 640-700 nm with relatively small Stokes' shifts about 15 nm. In addition, the styryl BODIPY derivatives can be modified by replacement of the fluorides with the ethynyl Grignard reagent to give a new BODIPY family of E-BODIPY with interesting optical properties.<sup>50,51</sup>

In general, the BODIPYs are relatively insensitive to the polarity and pH of the environment.<sup>50,52</sup> However, in last ten years, quite a lot distyryl BODIPY dyes which are sensitive to pH or selective to certain ions in solution have been synthesized and intensively investigated.<sup>38,45,48,53,54</sup> The protonation or ion-binding of the functional group carried by the styryl residues could significantly changes the electronic signature of BODIPY core, leading to large emission spectral shifts or on/off of the fluorescence. These processes are extremely significant and selective that change of fluorescence could be modulated by ions in solution of  $10^{-6}$  to  $10^{-7} \text{ M}^{-1}$  range. The HOMO-LUMO energy gap of the BODIPY can be modified by ion-binding leading to intramolecular charge transfer (ICT) between the BODIPY core and the complexation pocket resulting in large shifts of the absorption/emission spectra. Therefore, the styryl-BODIPY derivatives provide a great future for the applications of digital responses in electronic logic gates.<sup>55-59</sup> Recently, quite a lot of research based on the styryl-BODIPY derivatives was devoted to the fluorescence sensing of metal ions.<sup>24,54,60,61</sup> A prototypical example (A) is given in Chart 3.

Besides, according to the recent searches, the distyryl BODIPY derivatives present also a great potential for the two-photon absorption (TPA) applications.<sup>62,63</sup> In 2009, Didier *et al.* reported the use of distyryl-E-BODIPY dye (compound B) for the two-photon imaging.<sup>64</sup> According to the experiment, the nontoxicity of the dyes to the cells provides a promising future for imaging applications and diagnostic tools.

Furthermore, the high extinction coefficients, good stability, easy functionalization of the styryl-BODIPYs have also attracted some attention in the field of Dye-sensitized solar cells (DSSC),<sup>65-67</sup> (compound C) and bulk heterojunction solar cells (BHJ).<sup>68-70</sup>

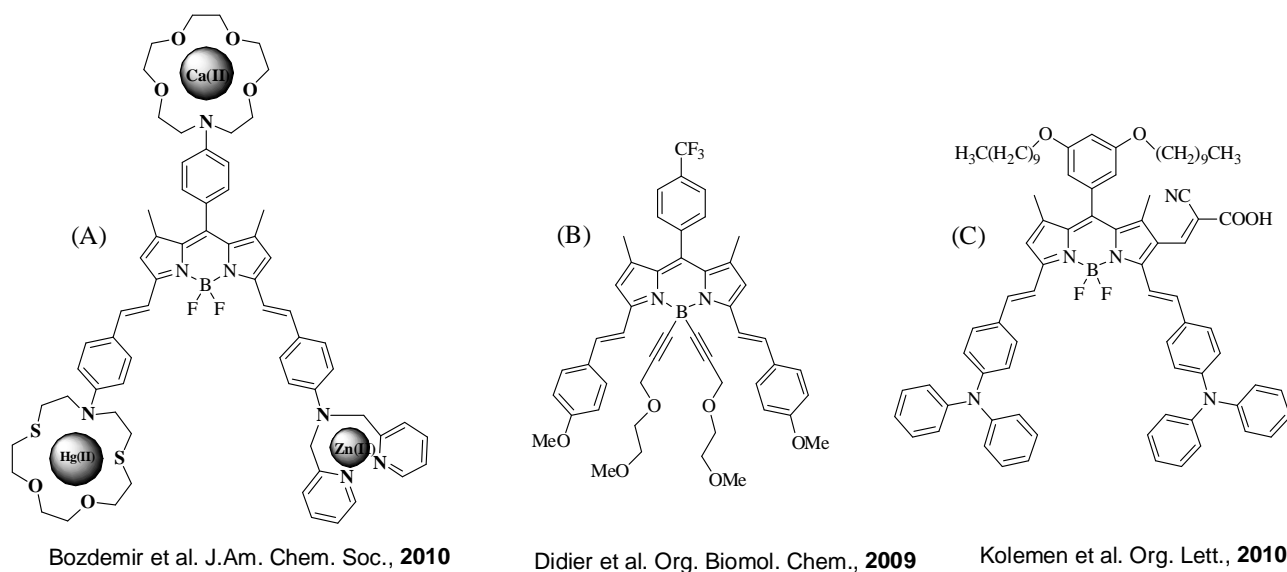


**Chart 3. Some distyryl BODIPY derivatives in different applications.**<sup>55,64,66</sup>

However, the poor water-solubility of the distyryl BODIPY derivatives limits their applications in the field of biological labeling. Therefore, in this chapter we focused on the functionalization of the distyryl BODIPYs in order to improve their water-solubility and introduce an additional functional group to the BODIPY scaffold for fluorescence bio-labeling applications.

#### 1.1.4. Water-solubilization of distyryl BODIPYs

Three complementary approaches were considered to improve the water-solubility of the distyryl BODIPYs, involving introduction of several water-solubilization groups onto the BODIPY scaffold. The first approach involves the formation of the sulfobetaine residues from dimethylamino groups on the styryl moieties. The second approach consists of the substitution of the fluorides of distyryl BODIPY with the appropriate ethynyl Grignard reagent. In this approach, the poly-ethylene-glycol or the sulfobetaine moieties will be introduced onto the boron atom as water-solubilization groups.

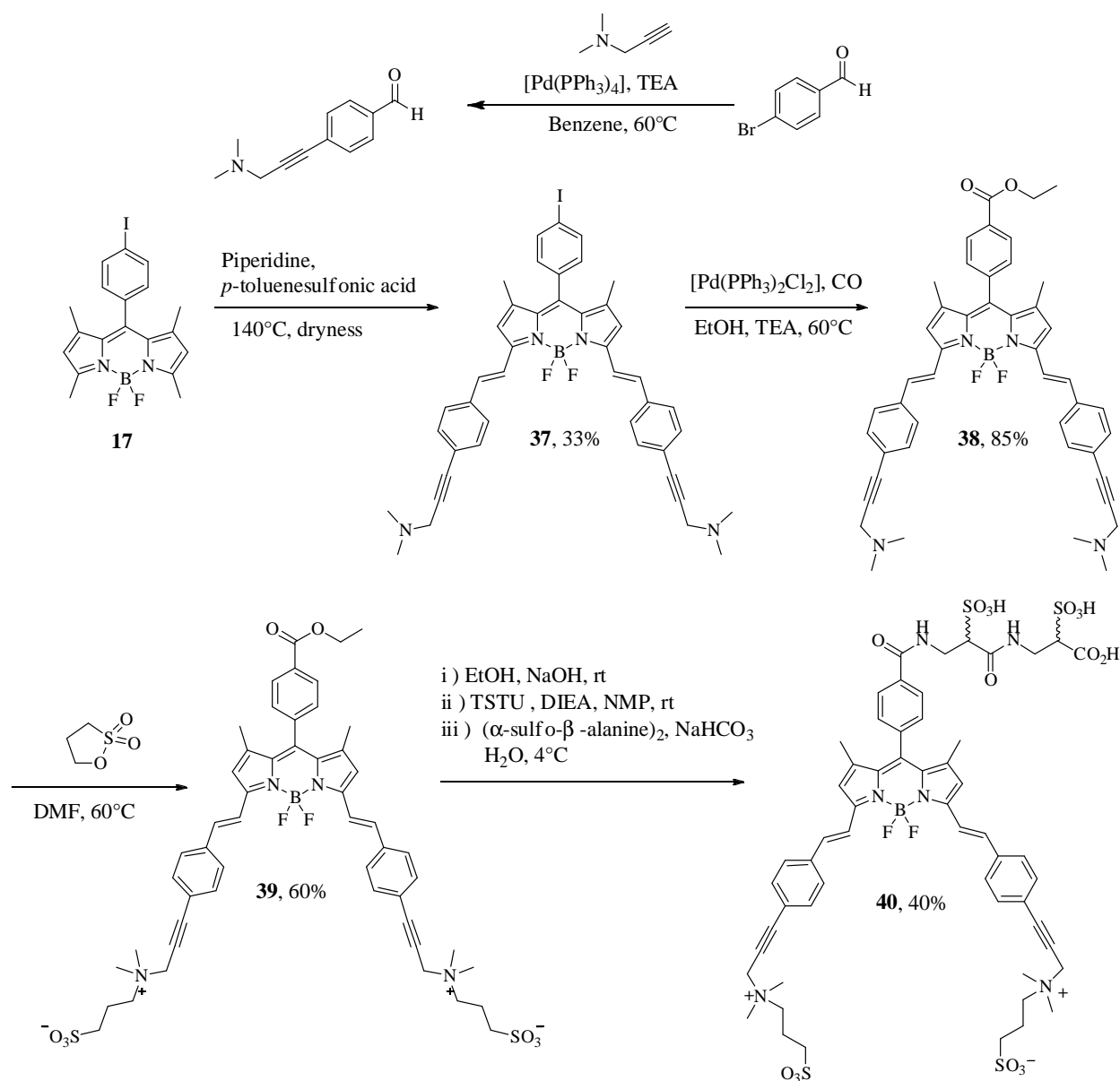
As mentioned above, the functionalization of the distyryl BODIPY involves not only improving the dye's water-solubility, but also the introduction of an additional functional group for the bio-conjugation. Therefore an ethyl ester group is introduced by carboalkoxylation reaction in situ from the aromatic halide group in meso-position of the BODIPY dye. Saponification of the ethyl ester group gives the carboxylic acid derivative. Then the carboxylic acid can be converted into the 'activated' N-hydroxysuccinimidyl (NHS) ester for bio-conjugation with proteins. Furthermore, the activated N-hydroxysuccinimidyl ester derivatives offer a third approach to improve the dye's water-solubility, to which the polysulfonated peptides linker containing an additional carboxylic acid group can be introduced in situ by an alkylation reaction.

## 1.2. Synthesis of the distyryl BODIPYs

The synthesis of the dyes **40** and **46** was achieved thanks the collaboration between our laboratory and the laboratory of Chimie Bio-Organique (COBRA) at the Rouen University. The first part of the synthesis consisted of the formation of polar zwitterions sulfobetaine by reacting the dimethylamine groups of the distyryl BODIPYs with 1,3-propanesultone; The second part involved grafting of the  $\alpha$ -sulfo- $\beta$ -alanine peptide linker to the corresponding distyryl BODIPY scaffold were accomplished by the laboratory COBRA in Rouen.

### 1.2.1. Synthesis of distyryl BODIPY **40**.

The Knoevenagel condensation reaction required the iodophenyl tetramethyl-BODIPY **17** and 4-[3-(dimethylamino)-1-propyn-1-yl]-benzaldehyde as starting materials, reacted in a mixture of toluene and piperidine leading to the blue derivative **37** in 33% yield after careful column chromatography. Use of a carboalkoxylation reaction promoted by low-valent palladium provided quantitatively the ethyl ester **38**.<sup>71,72</sup> Then quaternization of the tertiary amines with 1,3-propanesultone performed in anhydrous DMF at 60°C afforded compound **39**. Finally, saponification of the ethyl ester was performed under standard conditions to give the corresponding carboxylic acid. This BODIPY acid was then converted quantitatively into the corresponding N-hydroxysuccinimidyl (NHS) ester by treatment with peptide coupling uronium reagent O-(N-Succinimidyl)-1,1,3,3-tetramethyl uronium tetrafluoroborate (TSTU) and DIEA in dry NMP.<sup>73,74</sup> Thereafter, the crude mixture of NHS ester was subjected to aminolysis with dipeptide ( $\alpha$ -sulfo- $\beta$ -alanine)<sub>2</sub> in aqueous bicarbonate buffer to give the water-soluble BODIPY dye **40**. RP-HPLC purification using aq. triethylammonium bicarbonate (TEAB) buffer and acetonitrile as eluents, followed by desalting on ion-exchange resin Dowex H<sup>+</sup> provided **40** in a pure form (Scheme 2).

Scheme 2. Synthesis of distyryl BODIPY **40**.

### 1.2.1.1. Photophysical properties of the dye **40**.

The double sulfonated BODIPY dye **40** was found perfectly soluble in water and related aqueous buffers in the concentration range (1  $\mu\text{M}$  to 10 mM) suitable for bio-labeling applications.<sup>75</sup> The optical properties of **40** were evaluated under simulated physiological conditions (i.e., phosphate buffered saline (PBS), pH 7.5). In solution, despite the presence of polysulfonate and sulfobetaine residues on the BODIPY scaffold, the dye shows a tendency to aggregate in aqueous solution. The weak absorption coefficient in the 20000  $\text{M}^{-1}\text{cm}^{-1}$  range and low fluorescence quantum yield (4%) were observed. The hypsochromic shift in absorption maxima at 601 nm is in keeping with the formation of non-emissive H-dimer<sup>30,76</sup> (Figure 1). The adding of protein bovine serum albumin

(BSA) 5% (w/v) as an additive disrupt the aggregation,<sup>10,77</sup> leading to a better quantum yield of 20% (Figure 2). (Postscript: The weight percent (w/v) is: [Mass of solute (g) / Volume of solution (ml)] x 100).

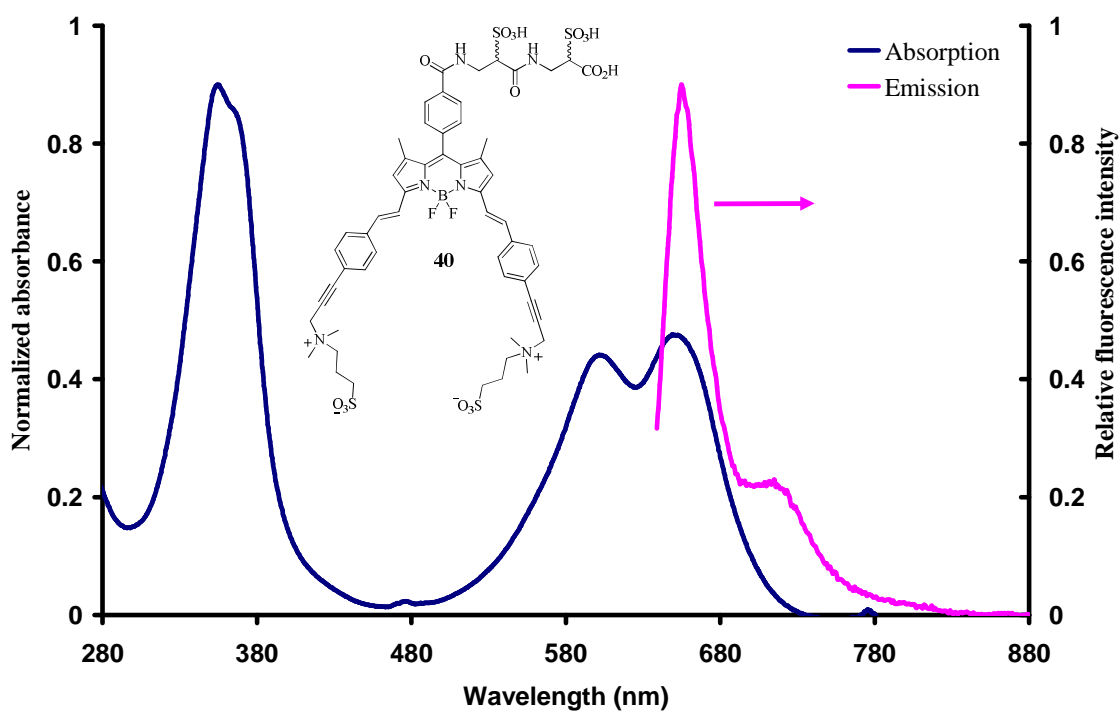


Figure 1. Normalized absorption and fluorescence emission spectra of 40 in PBS.

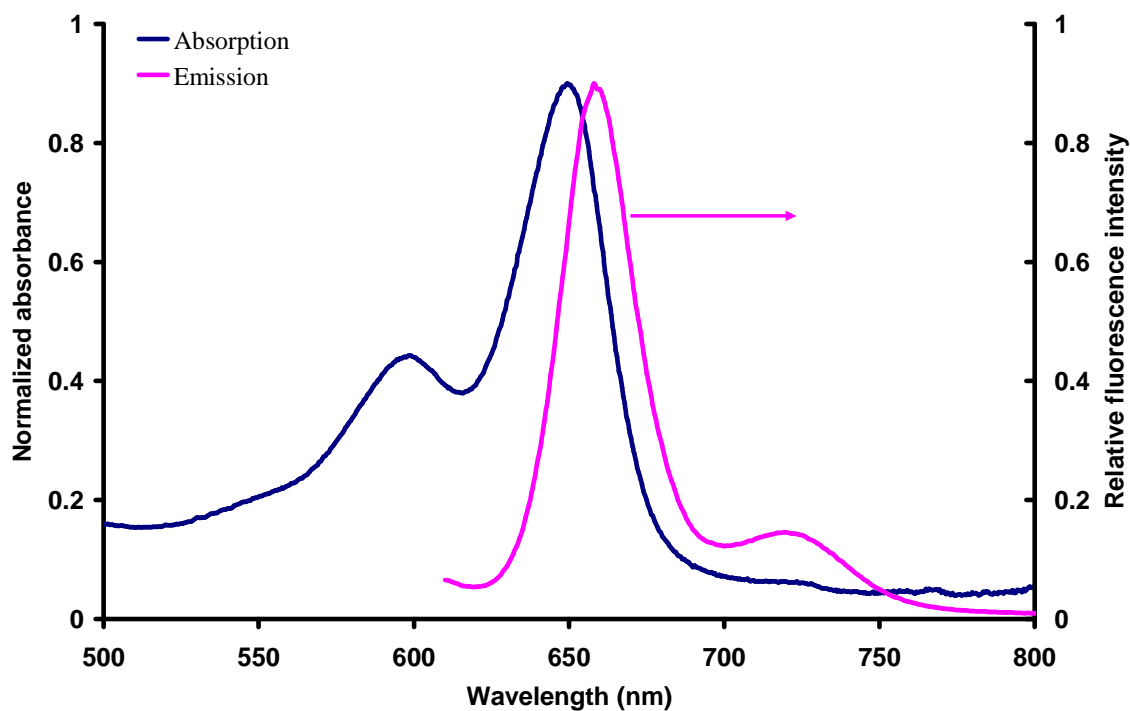
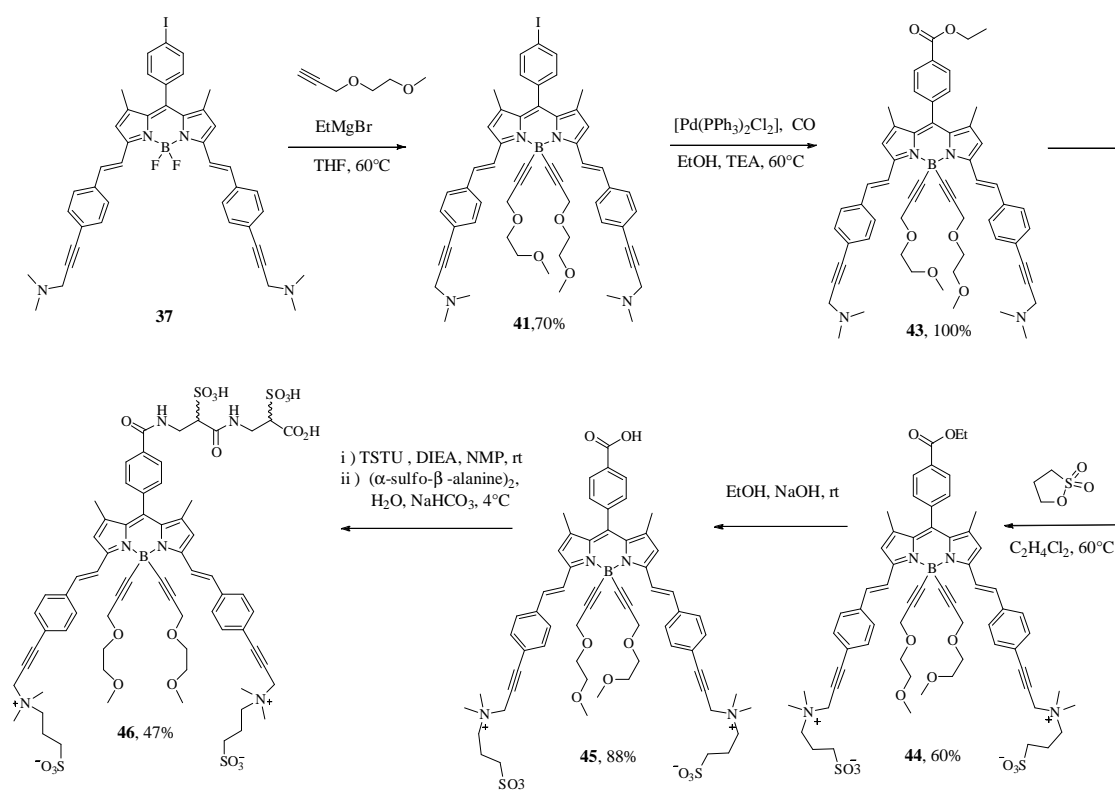


Figure 2. Normalized absorption and fluorescence emission spectra of 40 in PBS containing 5% (w/v) BSA.

1.2.2. Synthesis of distyryl BODIPY **46**.

In order to prevent the tendency of aggregation formation, one ideal choice was to increase the steric hindrance of the dye by substitution of boron center with ethylene fragments. Therefore, short ethyleneglycole (EG) chains were introduced to BODIPY core to improve the dye's water-solubility and prevent the formation of aggregation in water.<sup>24,64</sup> Compound **46** was prepared from the starting material **37**. The synthesis involved the use of the Grignard reagent of 4,7-dioxa-oct-1-yne in THF allowing substitution of fluorine atoms, leading to derivative **41** in 70% isolated yield. Then a carboalkoxylation reaction promoted by low-valent palladium provided quantitatively the ethyl ester **43**. The next step involved quaternarisation of the tertiary amines with an excess of 1,3-propanesultone in 1,2-dichloroethane. The resulting precipitate was centrifuged and purified to provide the sulfobetaine **44** in 60%. Finally, saponification of the ethyl ester was performed under standard conditions to give the acid **45**. Notice that the reverse order for the two-reaction sequence (*i.e.*, saponification followed by sulfonation with 1,3-propanesultone) did not provide the expected derivative dye **45**. Then BODIPY carboxylic acid was converted quantitatively into the corresponding *N*-hydroxysuccinimidyl (NHS) ester. Thereafter, the crude mixture of NHS ester was subjected to aminolysis with dipeptide ( $\alpha$ -sulfo- $\beta$ -alanine)<sub>2</sub> in aq. bicarbonate buffer to give the water-soluble BODIPY dye **46**.

Scheme 3. Synthesis of distyryl BODIPY **46**.

1.2.2.1. Photophysical properties of the dye **46**.

The optical properties of dye **46** were evaluated under simulated physiological conditions (i.e., phosphate buffered saline (PBS), pH 7.5). In solution, the spectra of the dye in the red region correspond very closely with those previously reported for the class of distyryl BODIPY derivatives in organic solvent (Figure 2).<sup>64</sup> In absorption spectra, the lowest energy absorption maxima centered at 642 nm corresponds to the 0-0 band of  $S_0 \rightarrow S_1$  ( $\pi \rightarrow \pi^*$ ) transition of the BODIPY core with an absorption coefficient of  $55100 \text{ M}^{-1}\text{cm}^{-1}$ . The shoulder centered at about 590nm can be attributed to the 0-1 vibrational band of same transition.<sup>44</sup> The strong absorption band with the absorption coefficient of  $76800 \text{ M}^{-1}\text{cm}^{-1}$  centered at 366 nm can probably be assigned to the  $\pi \rightarrow \pi^*$  transition of the styryl moieties and the overlapped  $S_0 \rightarrow S_2$  ( $\pi \rightarrow \pi^*$ ) transition band of the BODIPY core.<sup>45</sup> In emission, in contrast to the BODIPY dye **40**, the diethyleneglycol-substituted E-BODIPY **46** exhibits strong fluorescence emission centered at 657 nm, with a fluorescence quantum yield of 22%. In addition, the absence of aggregation was also confirmed by the excitation spectrum (the excitation spectrum is missing due to the optical measurement was carried out at Rouen university; However, it was provided separately in ESI of the published article<sup>78</sup>), indicating that the substitution by the diethyleneglycol residues efficiently prevents the aggregation of the dye in aqueous condition.

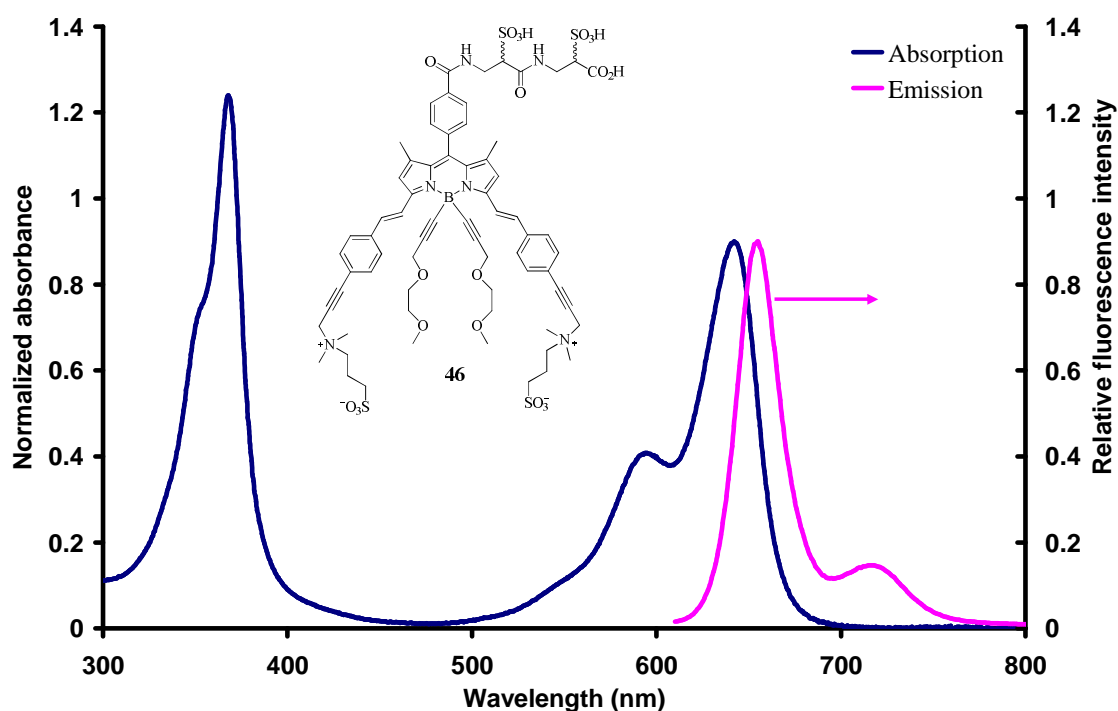
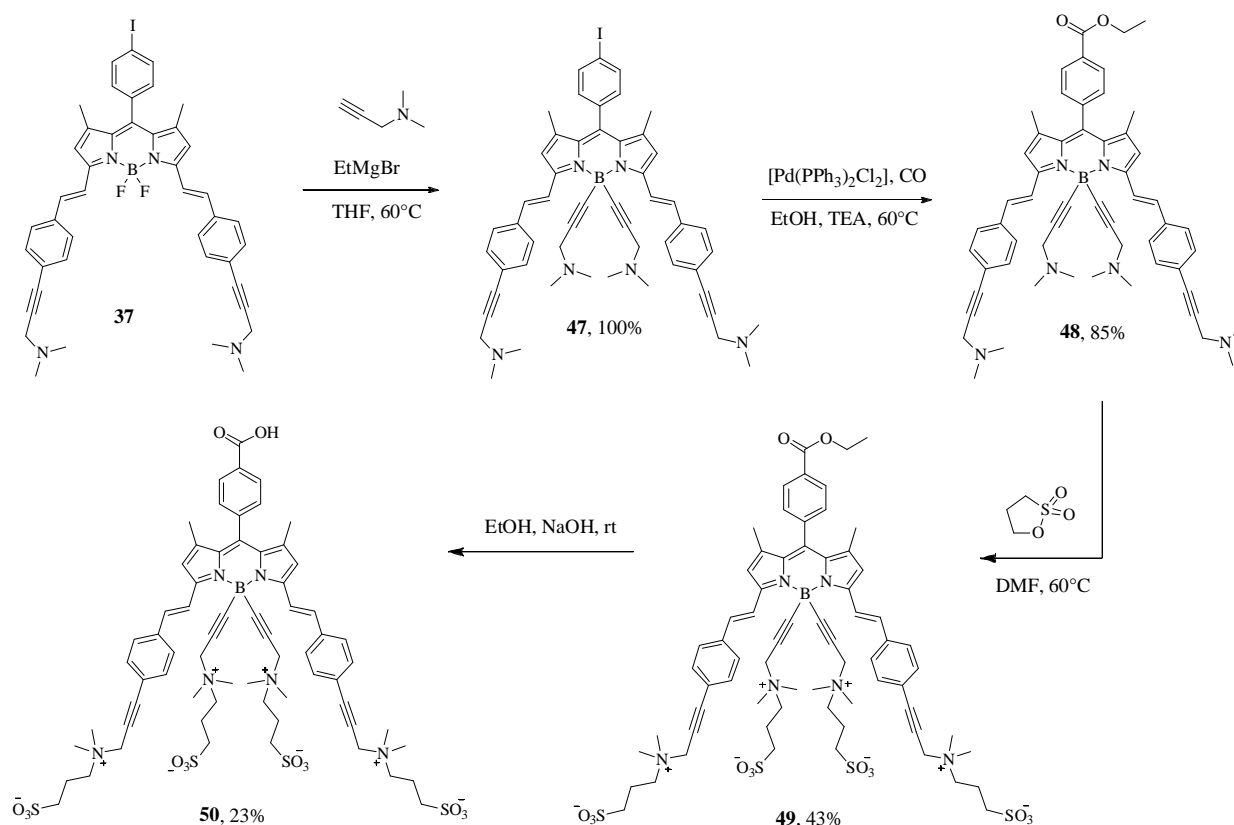


Figure 3. Normalized absorption and fluorescence emission spectra of **46** in PBS.

### 1.2.3. Synthesis of distyryl BODIPY **50**.

According to the synthesis of **46**, the alkynyl Grignard reagent of ethyleneglycol (EG) was replaced by N,N-dimethylamino propyne in order to provide two extra pairs of sulfobetaine. The substitution of **37** with the Grignard reagent of dimethylamino propyne in THF provided quantitatively the E-BODIPY derivative **47**. Then a carboalkoxylation reaction promoted by low-valent palladium gave the ethyl ester **48** in yield of 85%. The quaternarisation of the tertiary amines with excess amount of 1,3-propanesultone was performed in anhydrous DMF at 60°C, and the purification by a column chromatography on reversed-phase silica gave the ethyl ester **49** in 43%. The saponification of the ethyl ester afforded the carboxylic acid **50** in 23% isolated yield. Interestingly, the compound **50** is already well-soluble in water, so that further post-synthesis with the sulfonated-dipeptide linker is no longer necessary.



Scheme 4. Synthesis of distyryl BODIPY **50**.

#### 1.2.3.1. Optical properties of the dye **50**.

The optical properties of the dye **50** were evaluated as well under the simulated physiological conditions (i.e., phosphate buffered saline (PBS), pH 7.5). As we expected, the formation of four

sulfobetaine residues on the BODIPY scaffold could totally overcome the solubilization of the dye in water. In solution, the spectra of **50** show similar photophysical properties as those of the dye **46**. In UV-Vis absorption spectra, the lowest energy absorption of **50** centered at 641 nm with an absorption coefficient of  $58000 \text{ M}^{-1}\text{cm}^{-1}$ . The strong absorption of the styryl  $\pi \rightarrow \pi^*$  transitions of the phenyl groups was observed at 369 nm. In fluorescence emission, the dye exhibits strong fluorescence emission maximum centered at 657 nm with the fluorescence quantum yield of 25%. In addition, the absorption, emission and excitation spectra confirm the absence of aggregation in aqueous condition (Figure 4). Thus, the formation of four sulfobetaine groups in one step is convenient to overcome the water-solubilization of the red-emitting BODIPY derivatives while maintaining their fluorescence properties.

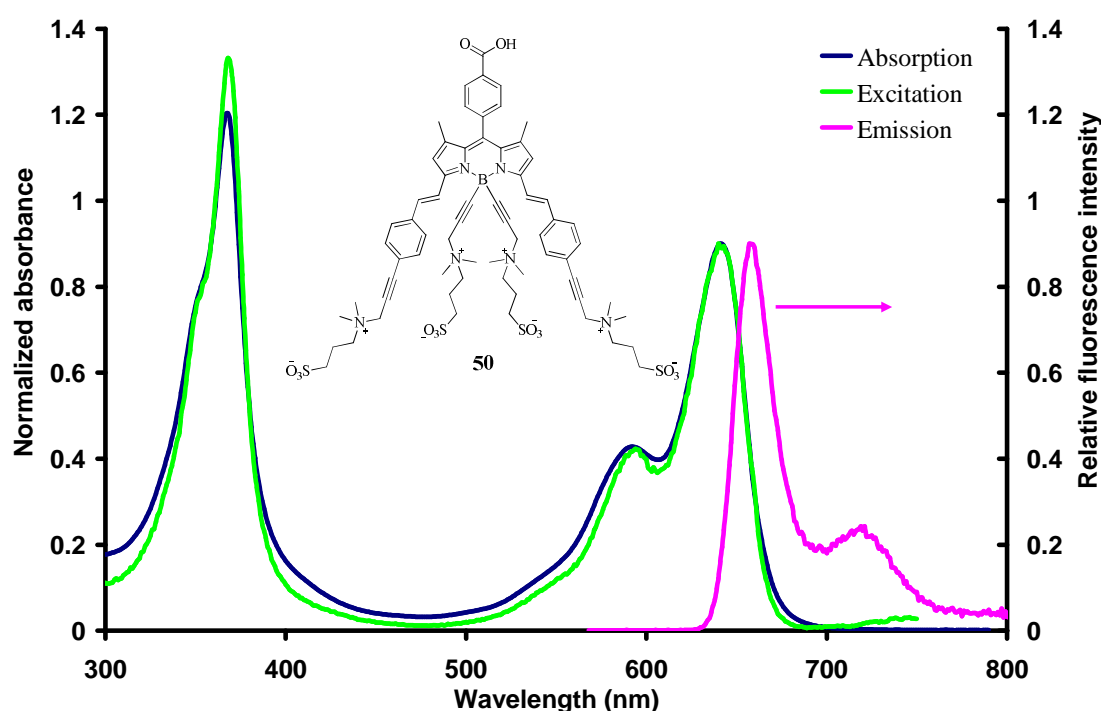
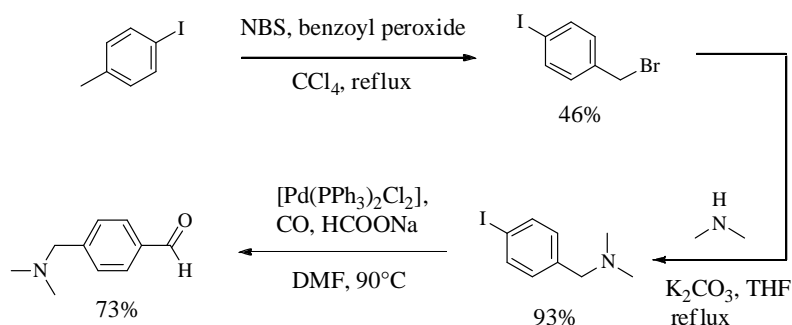


Figure 4. Normalized absorption, emission and excitation spectra of **50** in PBS.

#### 1.2.4. Synthesis of distyryl BODIPY **55**.

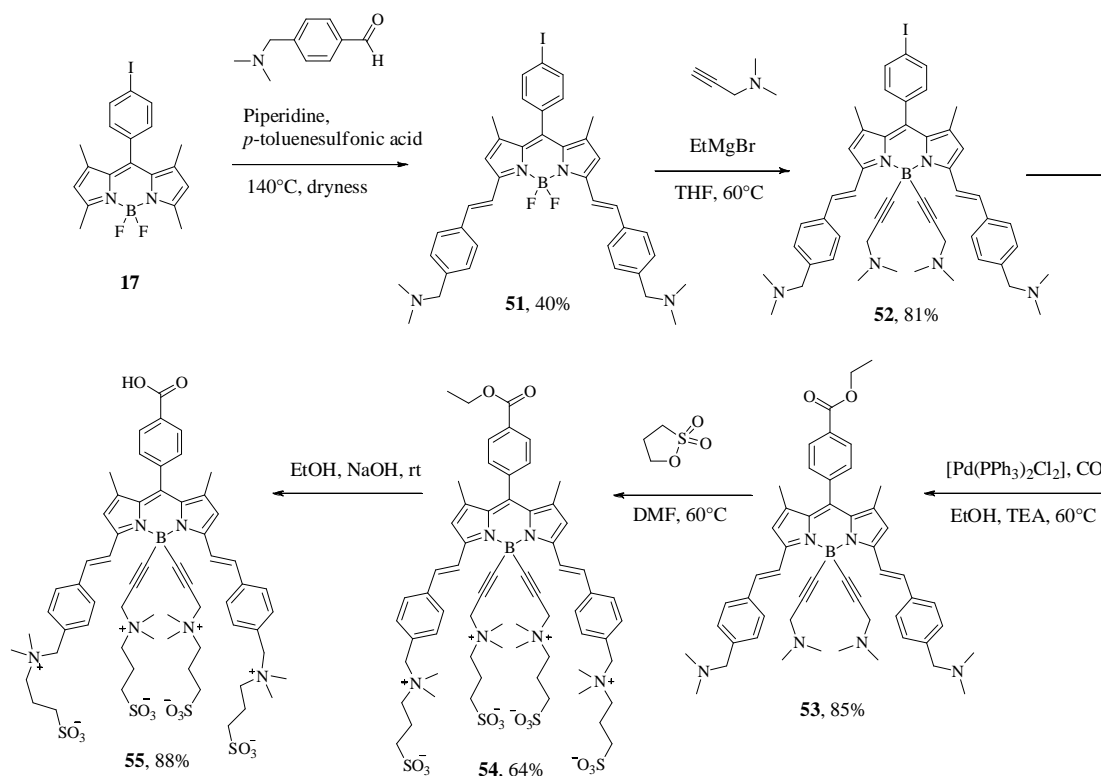
We considered that the low overall yield of the synthesis of **50** (3%) was due to the instability of the ethynylaryl substituents. Thus, we synthesized alternatively 4-[(dimethylamino)methyl]-benzaldehyde in place of the derivative 4-[3-(dimethylamino)-1-propyn-1-yl]-benzaldehyde (Scheme 6). The three step synthesis involved: i) the radical bromination of 4-iodo-toluene to give the 4-iodobenzyl bromide<sup>79</sup> in 47%; ii) followed by a nucleophilic substitution with dimethylamine in THF to afford the N-(4-iodobenzyl) -N,N-dimethylamine in 93%; iii) ultimately, a formylation

reaction promoted by low-valent palladium provided the 4-[(dimethylamino)methyl]-benzaldehyde in 73%.



**Scheme 5. Synthesis of the benzaldehyde derivative.**

A Knoevenagel condensation reaction of the **17** with the benzaldehyde derivative gave the distyryl compound **51** in 40%. The consecutive substitution of fluorine by alkynyl-Grignard reagent of *N,N*-dimethylamino propyne gave the dye **52** in 81%. Followed by a carboalkoxylation reaction providing the ethyl ester **53** in 85%, and a final quaternization of the dimethylamino groups with 1,3-propanesultone in DMF, the resulted residue was purified on a reversed-phase silica gel column chromatography leading to **54** in 64% isolated yield. Ultimately, the saponification of the ethyl ester **54** in EtOH afforded the acid derivative **55** in 88% isolated yield. Thus, this five-step synthesis of **55** provides a 16% overall yield (Scheme 7).



Scheme 6. Synthesis of the distyryl BODIPY **55**.1.2.4.1.  $^1\text{H}$  NMR analysis of compound **55**.

The  $^1\text{H}$  NMR 300MHz spectra of **55** was performed in  $\text{CD}_3\text{OD}/\text{D}_2\text{O}$ . The well-resolved spectrum in Figure 5 represents clearly the characteristic signals of the acid **55**. The integration of 8 protons at 7.92-7.83 ppm is corresponding to the AB system of the phenyl subunits on the distyryl arms; the 4 protons of the benzoic acid group are observed at 8.21 and 7.44 ppm. The dimethyl groups of the quaternary ammonium groups are observed for the double integrations of 12 protons at 3.21 and 3.06 ppm, respectively. The 8 protons at 2.42 and 2.12 ppm are corresponding to the  $\text{CH}_2$  groups of the sulfobetaine residues on the styryl arms and on the boron atom, respectively. In addition, the observed 16Hz proton-proton coupling constant is in keeping with an E conformation of the double bonds, a situation expected based on the type of the condensation.<sup>80</sup>

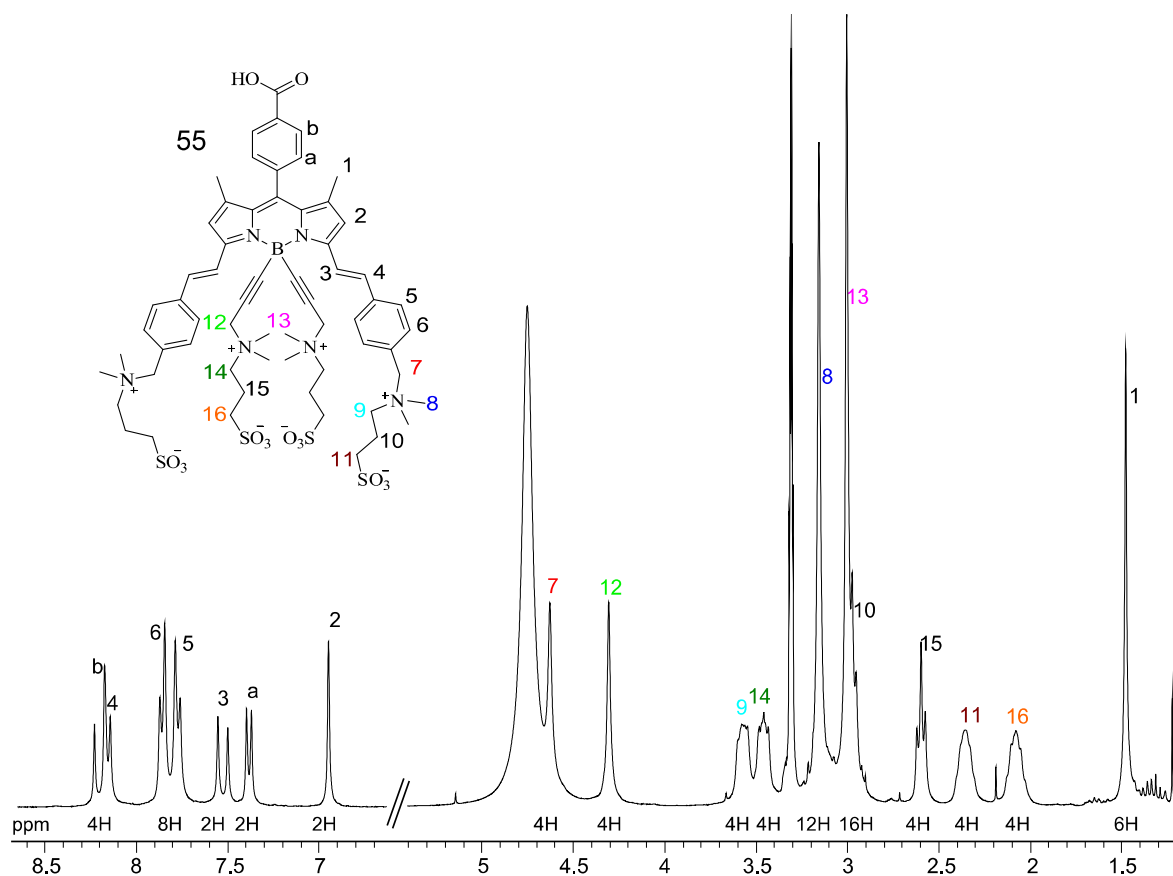


Figure 5.  $^1\text{H}$  NMR 300MHz spectra of **55** in  $\text{CD}_3\text{OD}/\text{D}_2\text{O}$ .

1.2.4.2. Photophysical properties of compound **55**.

The optical properties of **55** were evaluated in pure water. In solution, the carboxylic acid **55** shows

similar optical properties as those of **46** and **50**. In UV-Vis absorption spectra, the lowest energy absorption maxima centered at 628 nm with an absorption coefficient of  $71000 \text{ M}^{-1}\text{cm}^{-1}$ . The strong absorption of the  $\pi \rightarrow \pi^*$  transitions of the phenyl groups was observed at 352 nm. In fluorescence emission, the dye exhibits emission maxima centered at 641 nm with the fluorescence quantum yield of 38%. Once again, the absorption, emission and excitation spectra confirm the absence of aggregation in water (Figure 6). In addition, slight hypsochromic shifts about 14 nm were observed in both absorption and emission spectra of dye **55** compare to the analogue dye **50**, due to the reduced  $\pi$ -conjugation of the BODIPY core. On the other hand, from a chemical point of view the overall yields of the dye **55** were improved to 16% compared to 3% of those of dye **50**; furthermore, the quantum yields of dye **55** (38%) are also superior of those of dye **50** (3%).

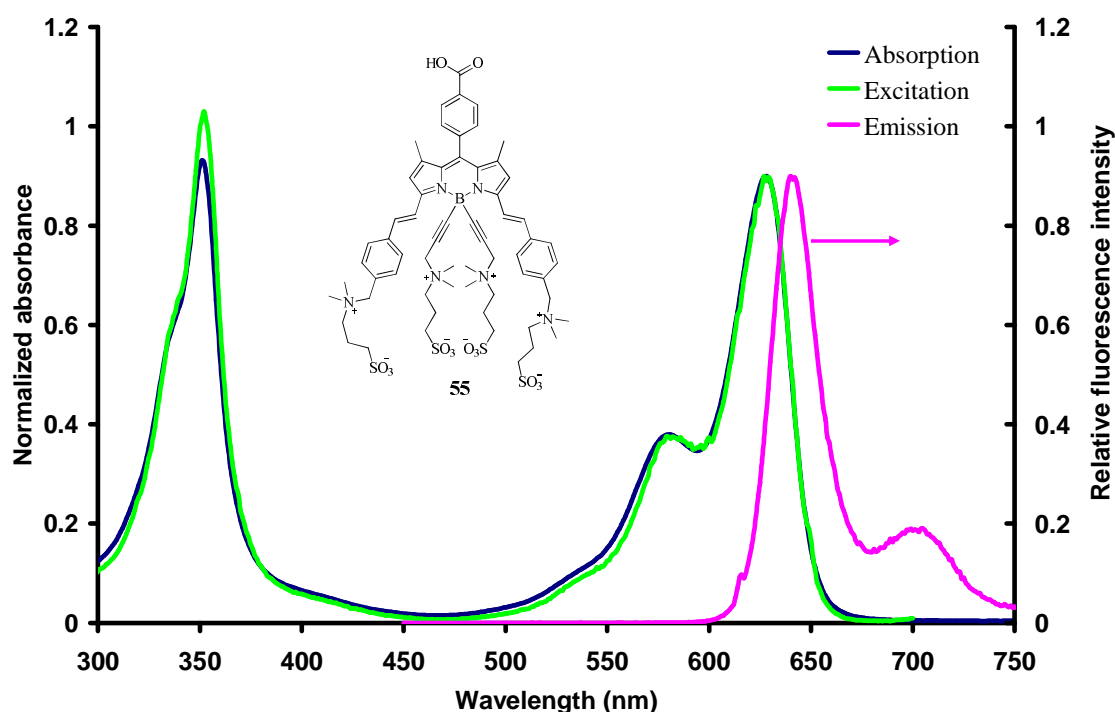
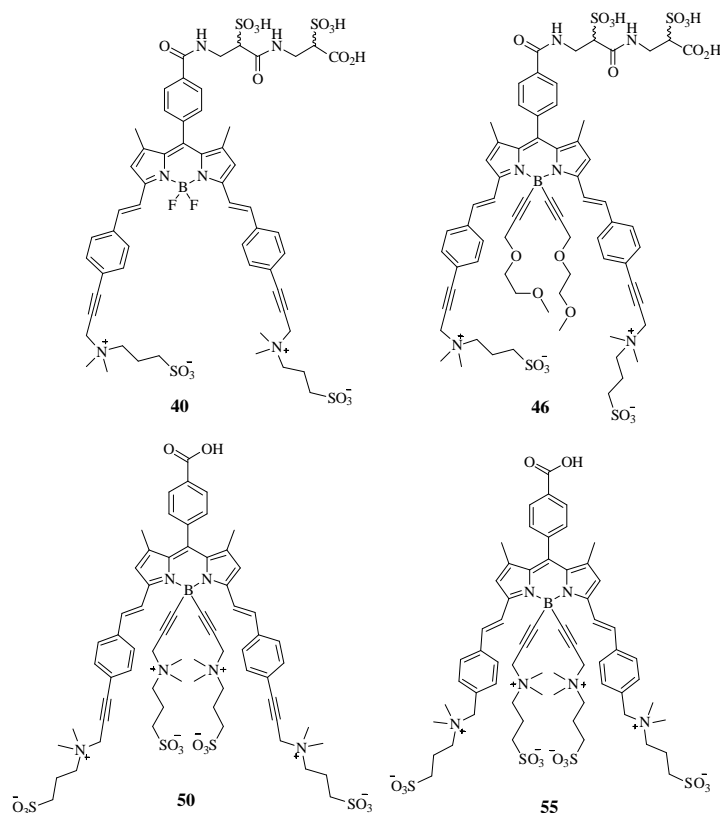


Figure 6. Normalized absorption, emission and excitation spectra of **55** in  $\text{H}_2\text{O}$ .

### 1.3. Results and Discussion

Four water-soluble red-emitting distyryl BODIPY dyes were synthesized and isolated (Figure 7). The distyryl BODIPY dyes and the intermediates were unambiguously characterized by NMR, ESI-MS, and element analysis. Their optical properties were evaluated by UV-Vis absorption and steady-state Fluorescence emission spectra in various solvents. The data were collected in Table 2. The biological labeling evaluation of dyes **40**, **46** and **50** were carried out with the protein bovine serum albumin (BSA) and the monoclonal antibody (mAb) 12CA5 under simulated physiological

conditions. Furthermore, the two photon absorption (TPA) and fluorescence cell imaging experiment were performed with HeLa cells incubated with the dye **55**. Note that the protein labeling has been performed in collaboration with COBRA in Rouen; while the two photon absorption cell imaging was performed in collaboration with Dr. Pascal Didier at the faculty of pharmacy of ULP in Strasbourg. The results will be discussed in the following sections.



**Figure 7.** The structures of water-soluble distyryl BODIPY derivatives.

**Table 2.** Optical properties of distyryl BODIPY dyes.

| Compound (solvent)                     | $\lambda_{\text{abs}}$ (nm) | $\epsilon$ ( $\text{M}^{-1}\cdot\text{cm}^{-1}$ ) | $\lambda_{\text{em}}$ (nm) | $\phi$ (%) <sup>a</sup> | $\tau$ (ns) <sup>b</sup> | $k_r$ ( $10^7\text{s}^{-1}$ ) <sup>c</sup> | $k_{nr}$ ( $10^7\text{s}^{-1}$ ) <sup>c</sup> |
|--|-----------------------------|---|----------------------------|-------------------------|--------------------------|--|---|
| <b>37</b> ( $\text{CH}_2\text{Cl}_2$ ) | 646                         | 110600  | 661                        | 46                      | 5.2                      | 8.8  | 10.4  |
| <b>38</b> ( $\text{CH}_2\text{Cl}_2$ ) | 646                         | 122200  | 659                        | 43                      | 4.6                      | 9.3  | 12.4  |
| <b>40</b> (PBS) <sup>d</sup>           | 649                         | 19300   | 655                        | 4                       | -                        | -  | -   |
| <b>41</b> ( $\text{CH}_2\text{Cl}_2$ ) | 647                         | 108500  | 659                        | 47                      | 4.8                      | 9.8  | 11.0  |
| <b>46</b> (PBS) <sup>d</sup>           | 642                         | 55100   | 657                        | 22                      | -                        | -  | -   |
| <b>47</b> ( $\text{CH}_2\text{Cl}_2$ ) | 648                         | 92200   | 661                        | 26                      | 5.2                      | 5.0  | 14.2  |
| <b>48</b> ( $\text{CH}_2\text{Cl}_2$ ) | 647                         | 83500   | 663                        | 30                      | 4.8                      | 6.3  | 14.6  |
| <b>50</b> (PBS)                        | 641                         | 58000   | 657                        | 25                      | 2.7                      | 9.3  | 27.8  |
| <b>51</b> ( $\text{CH}_2\text{Cl}_2$ ) | 632                         | 64500   | 640                        | 40                      | 6.5                      | 6.2  | 9.2   |
| <b>52</b> (Dioxan)                     | 634                         | 81300   | 645                        | 25                      | 6.3                      | 4.0  | 11.9  |
| <b>53</b> (Dioxan)                     | 634                         | 84200   | 649                        | 36                      | 5.3                      | 6.8  | 12.1  |
| <b>54</b> ( $\text{H}_2\text{O}$ )     | 630                         | 76600   | 643                        | 30                      | 3.4                      | 8.8  | 20.6  |
| <b>54</b> (EtOH)                       | 636                         | 92000   | 646                        | 35                      | 4.5                      | 7.8  | 14.4  |
| <b>55</b> ( $\text{H}_2\text{O}$ )     | 628                         | 71000   | 641                        | 38                      | 3.9                      | 9.7  | 15.9  |

a) Quantum yield determined in diluted solution ( $c \approx 1 \times 10^{-6} \text{M}$ ) using cresyl violet as a reference  $\phi = 0.51$  in ethanol,  $\lambda_{\text{exc}} = 578 \text{ nm}$ .<sup>81</sup> All  $\phi_f$  are corrected for changes in refractive index. b) Lifetime. c)  $k_r = \phi / \tau$ ,  $k_{nr} = (1 - \phi) / \tau$ . d) measured at COBRA in Rouen.

### 1.3.1. Biological labeling evaluation of the distyryl BODIPYs.

Since the water-soluble BODIPY dyes **40**, **46** and **50** are functionalized with a free carboxylic acid group, its ability to label proteins and antibodies through reactions of its active ester with the  $\text{NH}_2$  groups of  $\epsilon$ -lysine residues present in these biopolymers, was considered.<sup>78</sup> The BSA and the monoclonal antibody (mAb) 12CA5 that recognizes the influenza hemagglutinin (HA) epitope tag,<sup>82,83</sup> were chosen as the protein and the antibody respectively for the bio-conjugation experiments. To compare the labelling performances of these novel red-fluorescent markers with those of classic CyDye™ reagents, similar reactions were performed with sulfoindocyanine dye Cy 5.0 under the same experimental conditions. To avoid possible deleterious effects of organic solvents and additives towards mAb (or protein) structure and functional activity, a carboxylic acid activation protocol performed in water and involving the use of 1-ethyl-3-(3-dimethylaminopropyl) carbodiimide (EDC) and sulfo-NHS instead of TSTU/DIEA in a polar aprotic solvent was preferred.<sup>84,85</sup> BSA and anti-HA mAb were labelled through overnight incubation with a 13- and 31-fold molar excess of BODIPY derivatives **40**, **46** and **50** in PBS (pH 7.5) respectively. The resulting protein fluorescent conjugates were purified by size-exclusion chromatography over a Sephadex® G-25 column. Table 3 reports the absorption /emission wavelengths, quantum yields of fluorescent proteins after conjugation in PBS, together with the attached fluorophore to protein molar ratios (F/P), estimated from the relative intensities of protein and dye absorptions. The F/P values achieved with *meso*-derivatised BODIPY dye **46** was significantly higher than those achieved with the dye **40**, **50** and Cy 5.0, indicating a greater reactivity of its sulfo-NHS ester. Indeed, the added ( $\alpha$ -sulfo- $\beta$ -alanine)-dipeptidyl spacer enables to extend the bioconjugable  $\text{CO}_2\text{H}$  group away from sterically hindered di-styryl BODIPY core compare with **50**, thus ensuring a better capability for the acylation of primary amines within proteins, especially under pH neutral conditions. When compared with the non-covalently bound distyryl BODIPY dyes, the absorption maxima of the fluorescent protein conjugates are slightly red-shifted by about 8 nm whereas emission maxima remain unchanged (Table 3). In addition, the conjugated dyes **40** and **50** show the tendency of aggregation by the observation of the blue shift of the absorption maximum, whereas it is less pronounced for the conjugate **46** (Figure 8-10). Such aggregation behavior is likely due to the molecular structure of the dyes.

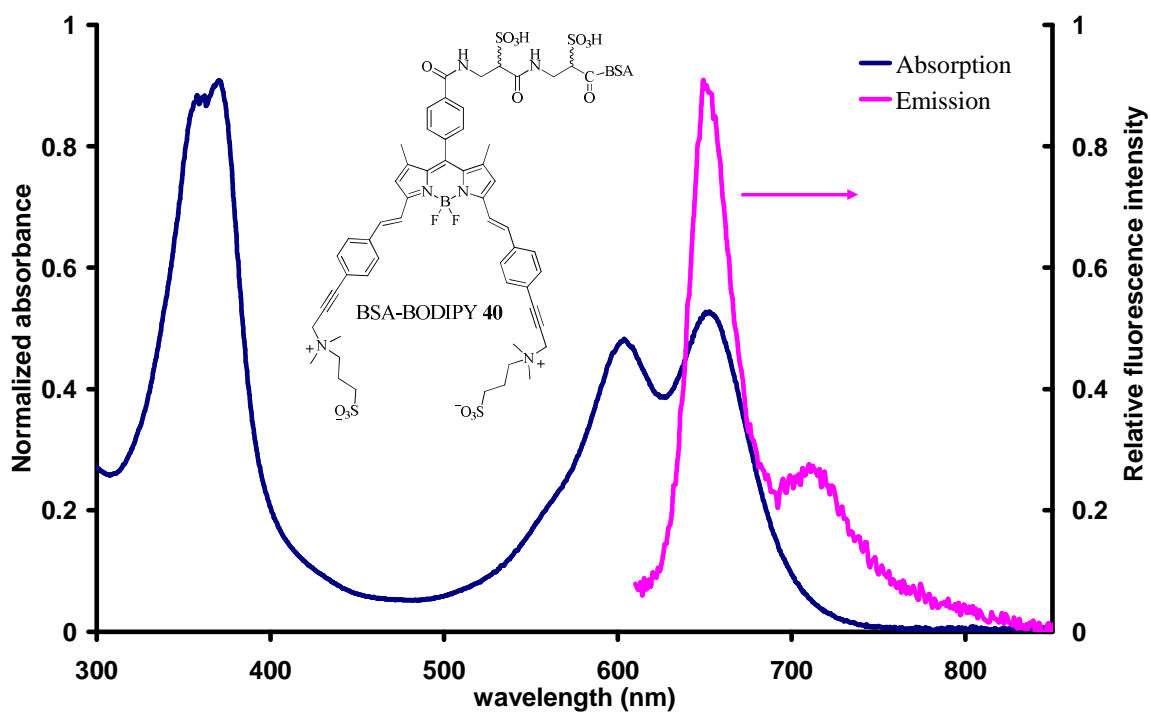


Figure 8. Normalized absorption, emission spectra of BSA-BODIPY 40 in PBS.

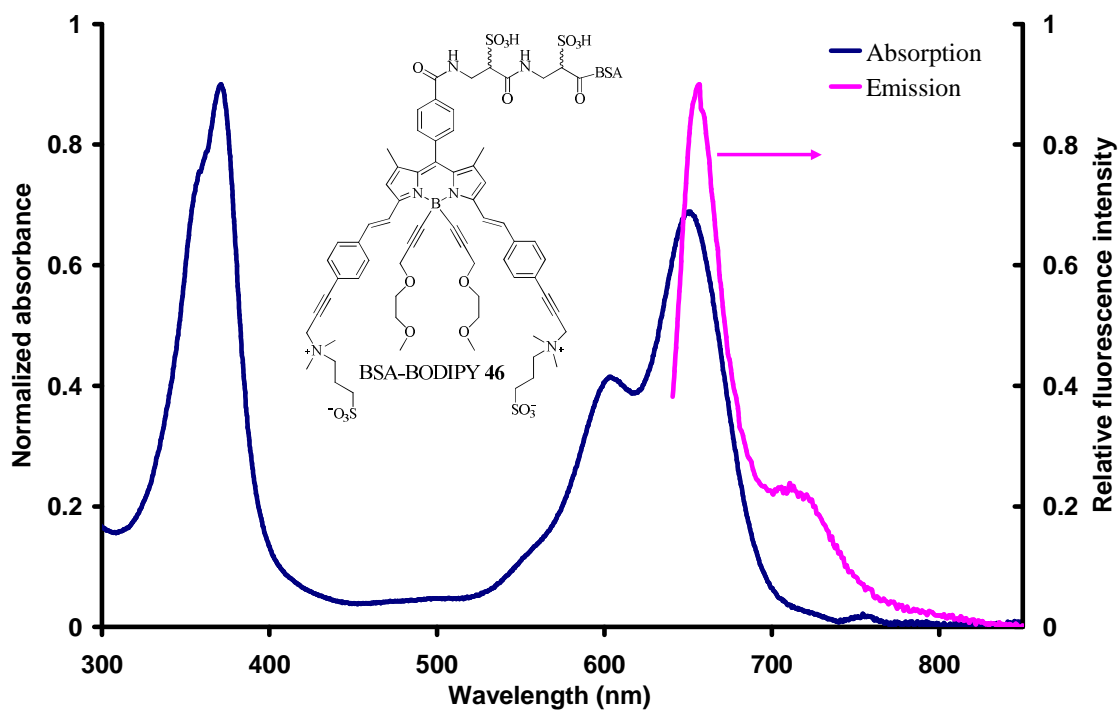


Figure 9. Normalized absorption, emission spectra of BSA-BODIPY 46 in PBS.

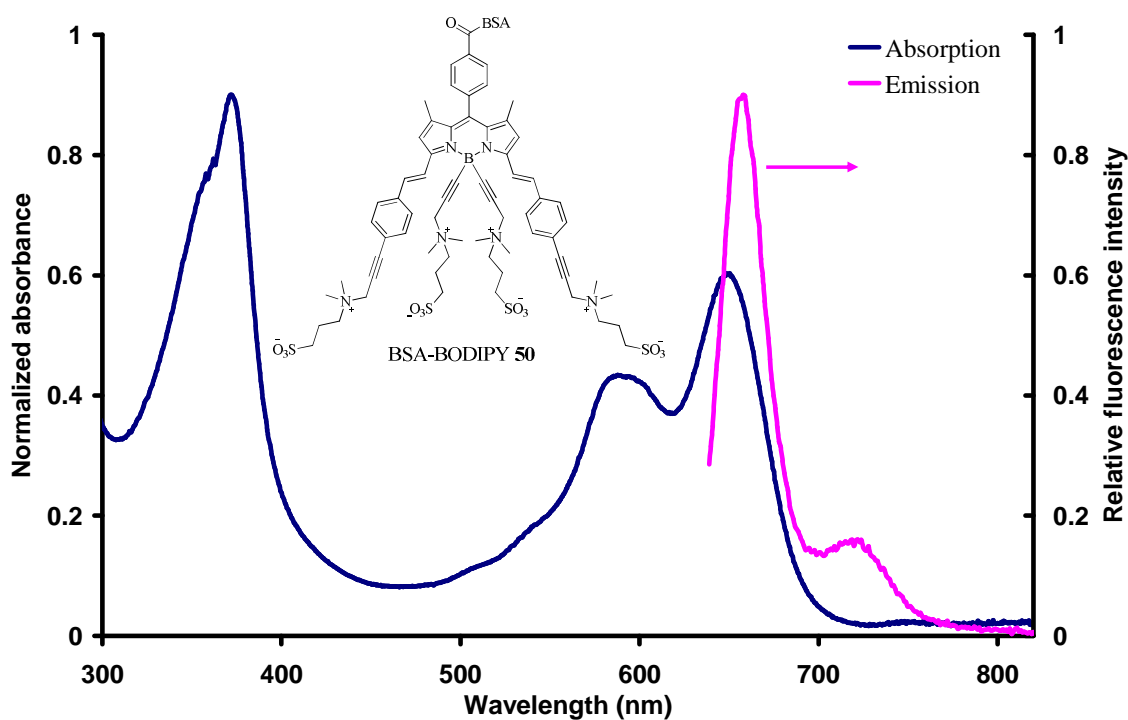


Figure 10. Normalized absorption, emission spectra of BSA-BODIPY 50 in PBS.

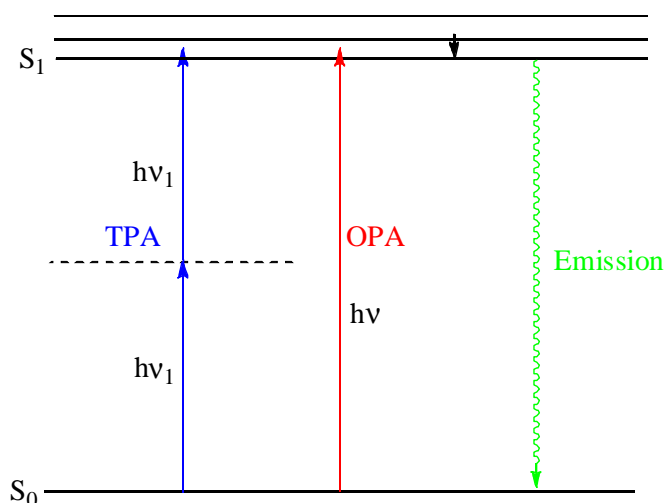
The drop of quantum yield of the conjugated dyes observed after bio-conjugation is likely explained by dye to protein interactions favoring in certain cases electron transfer to specific nucleic bases or dye to dye interactions leading to non-emissive aggregate, in the same manner as observed for DNA biopolymers.<sup>86</sup> We also notice that this binding-induced reduction in emission is also observed with protein-Cy 5.0 conjugates (it is less pronounced for labeled anti-HA mAb) and has been already reported for other bioanalytical relevant fluorescent labels including Cy 5.0, Cy 5.5 and the Alexa Fluor<sup>®</sup> dyes.<sup>87</sup> However, these preliminary results show for the first time that it is possible to get red-emitting fluorescent protein conjugates by using the water-soluble distyryl BODIPY dyes. Furthermore, the fluorescence emission of these bio-conjugates is observed in aq. buffers without adding aggregate disrupting additives.

Table 3. Biolabeling data of dyes 40, 46, 50 and Cy 5.0. a) Fluorophore to protein molar ratios.

| Conjugated dye | $\lambda_{\max}$ , abs (nm) | $\lambda_{\max}$ , em (nm) | $\Phi_F$ (%) | F/P <sup>a</sup> |
|----------------|-----------------------------|----------------------------|--------------|------------------|
| mAb-BODIPY 40  | 369, 601, 649               | 649                        | 3            | 1.3              |
| mAb-BODIPY 46  | 370, 603, 650               | 657                        | 7            | 5.7              |
| mAb-BODIPY 50  | 370, 588, 650               | 659                        | 5            | 3.8              |
| mAb-Cy 5.0     | 610, 650                    | 657                        | 12           | 2.8              |
| BSA-BODIPY 40  | 369, 601, 650               | 651                        | 2            | 2.6              |
| BSA-BODIPY 46  | 372, 603, 651               | 657                        | 6            | 2.3              |
| BSA-BODIPY 50  | 371, 588, 650               | 658                        | 5            | 0.7              |
| BSA-Cy 5.0     | 609, 651                    | 663                        | 3            | 0.7              |

### 1.3.2. Two photon absorption and cell imaging application

As mentioned previously, the distyryl BODIPY dyes has shown great potential in the field of two photon absorption (TPA) applications. The two photon absorption is the optical property of the molecules that being promoted to the excited state by simultaneous absorption of two photons of half the energy (or twice the wavelength) of the corresponding one-photon transition (Figure 11).<sup>88</sup> Different from the one-photon absorption which depends linearly on the intensity of the incident light, the TPA increases with the square of the light intensity, hence the TPA is only observed in intense laser beams, especially focused pulsed lasers. The molecules with TPA property are highly demanded in a range of applications, such as three-dimensional data-storage,<sup>89</sup> optical limiting,<sup>90</sup> photodynamic therapy,<sup>91</sup> and two-photon excited fluorescence microscopy.<sup>63,92,93</sup>



**Figure 11. Energy level diagram for one photon absorption (OPA), two photon absorption (TPA) and fluorescence emission.**

In 2009, our laboratory has reported the use of E-distyryl BODIPY derivatives for two photon absorption cell-imaging application.<sup>64</sup> The studies revealed that the E-distyryl dye is a promising candidate for the TPA imaging application and diagnostic tools. Therefore, the new synthesized water-soluble distyryl BODIPY derivative **55** naturally attracted our attention for the TPA application.

#### 1.3.2.1. TPA evaluation of the dye **55**.

The two-photon absorption cross section  $\delta_{\text{TPA}}$  (in units of  $\text{cm}^4 \cdot \text{s} \cdot \text{photon}^{-1}$ , where  $10^{-50} \text{cm}^4 \cdot \text{s} \cdot \text{photon}^{-1} = 1$  Göppert-Mayer (GM))<sup>94</sup> was determined by using interferometric autocorrelations of the Equation 1.<sup>95</sup>

$$\delta(\omega) = \frac{4\pi^2 \hbar \omega^2}{n^2 c^2} \langle \gamma_I^* \rangle$$

**Equation 1. The two-photon absorption cross section ( $\delta$ ).**

The TPA cross section  $\delta_{\text{TPA}}$  is related to the imaginary part of the diagonal component of the second hyperpolarizability ( $\gamma$ ).<sup>96</sup> Where  $n$  is refractive index of the bulk material,  $\omega$  the frequency of the incident light,  $c$  the speed of light, and the brackets indicate the average over all-possible orientations of the molecule.<sup>95</sup> In the TPA cross section measurement between 735-920 nm, an interferometer was incorporated in the optical path between the laser and the microscope. By applying a slowly varying voltage with a frequency generator of the interferometer, an interference pattern is generated in the focal plane of the microscope. In the two-photon excitation regime, irradiated with a laser the solution of the dye acts as a non-linear medium that allows the measurement of an interferometer autocorrelation from for which it is possible to deduce the TPA cross section of the dye. The TPA cross section spectra is given for the dye **55** in water, as a function of the laser wavelength in Figure 12. Tetramethylrhodamine (TMR) was used as a reference compound. The dye **55** shows high TPA cross section of 491 GM at 735 nm, approximately twice the wavelength of the linear absorption of the  $S_0$ - $S_2$  transition band of the chromophore (Figure 6).<sup>64</sup> This two-photon transition takes place from the ground state  $S_0$  to the lowest excited state with similar geometry, being  $S_2$  in this centrosymmetric system.<sup>97</sup> Note that the dye **55** exhibits a three fold enhancement of the TPA cross section compared to TMR in water (Figure 12).

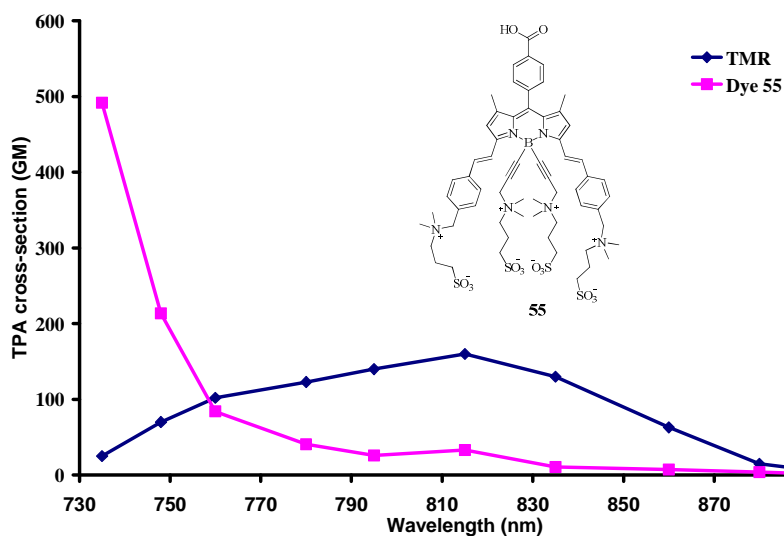


**Figure 12. Two-photon absorption cross section spectra of TMR and dye 55 in water.**

### 1.3.2.2. Two-photon excitation and fluorescence cell imaging

The two-photon excitation (TPE) microscopy and fluorescence lifetime imaging microscopy (FLIM) experiment were performed on HeLa cells in biological conditions. The FLIM is an imaging technique for producing an image based on the differences in the exponential decay rate of the fluorescence,<sup>98</sup> which is largely used in the field of TPE microscopy and multiphoton tomography. The living cells were stained in solution with concentration  $10^{-6}$  M of the dye for 6 h, and then washed several times with a buffer (PBS) solution. The excitation fluorescence and FLIM images have been taken on the same cells by the microscope associated to TPE source (Ti: sapphire laser) by excitation at 750 nm (Figure 13).

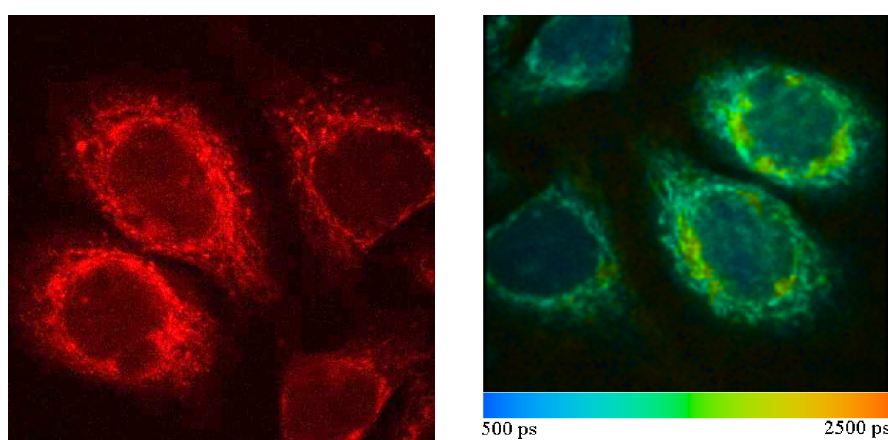


**Figure 13.** HeLa cells were incubated for 6h with the dye **55** in the biological condition. Left, the TPE fluorescence image. Right, the FLIM image with the color code corresponding to 500 to 2500 ps.

The images clearly demonstrate that the dye **55** can penetrate within the living cells in the normal biological conditions. The homogenous coloration of the cytoplasm was observed, but not in the nucleus. Furthermore, the FLIM spectra show mono-exponential fluorescence decay from 500 to 2500 ps. The incubating of the dye causes no change in the cell morphology suggesting lack of significant cytotoxicity. In addition, the dye shows good photostability during the experiments.

## 1.4. Conclusion

In this chapter, we succeeded in introduction of the sulfobetaine groups onto the distyryl BODIPY scaffold by using different approaches to improve the dye's water-solubility while remaining their optical properties in aqueous media. An additional functional group for bio-conjugation is incorporated during the synthesis protocol. Four water-soluble red-emitting distyryl BODIPY dyes were synthesized and isolated, and all of the dyes are found perfectly water-soluble, their optical

properties were evaluated and discussed. The preliminary bio-labelling experiments of dyes **40**, **46**, and **50** were evaluated with protein BSA and monoclonal antibody (mAb) 12CA5 under simulated physiological conditions, the physical and optical properties of the dye **46** and **50** were found similar to those of the commercial available dye Cy 5.0. For the dye **55**, the dye's two-photon absorption property attracts our attention due to its quadrupole structure and the high quantum yield of 38% in water. Interestingly, the dye shows remarkable TPA properties in water compared with the rhodamine dye (TMR). The two-photon excited fluorescence microscopy and the fluorescence lifetime imaging microscopy experiments were carried out with HeLa living cells in biological conditions, and no significant cytotoxicity was observed after 6h of incubation with the dye. The two-photon excited spectra and the FLIM imaging experiments demonstrate that the dye can be internalized within the cell without using additional solvents. Furthermore, the images show the coloration of the cytoplasm of the cell but not the nucleus, which might be an important characteristic for further bio-labeling studies. In addition, the functional carboxylic group of the dye **55** offers the opportunity for selective and specific bio-labeling of biological molecules, which is currently in progress.

## References

- (1) Monici, M. In *Biotechnology Annual Review*; El-Gewely, M. R., Ed.; Elsevier: 2005; Vol. Volume 11, p 227.
- (2) Albers, A. E.; Dickinson, B. C.; Miller, E. W.; Chang, C. J. *Bioorg. Med. Chem. Lett.* **2008**, *18*, 5948.
- (3) Lavis, L. D.; Chao, T.-Y.; Raines, R. T. *ACS Chem. Biol.* **2006**, *1*, 252.
- (4) Lavis, L. D.; Raines, R. T. *ACS Chem. Biol.* **2008**, *3*, 142.
- (5) Escobedo, J. O.; Rusin, O.; Lim, S.; Strongin, R. M. *Curr. Opin. Chem. Biol.* **2010**, *14*, 64.
- (6) Berlier, J. E.; Rothe, A.; Buller, G.; Bradford, J.; Gray, D. R.; Filanoski, B. J.; Telford, W. G.; Yue, S.; Liu, J.; Cheung, C.-Y.; Chang, W.; Hirsch, J. D.; Beechem, J. M.; Haugland, R. P.; Haugland, R. P. *J. Histochem. Cytochem.* **2003**, *51*, 1699.
- (7) Kolmakov, K.; Belov, V.; Bierwagen, J.; Ringemann, C.; Müller, V.; Eggeling, C.; Hell, S. *Chem. Eur. J.* **2009**, *16*, 158.
- (8) Kolmakov, K.; Belov, V. N.; Wurm, C. A.; Harke, B.; Leutenegger, M.; Eggeling, C.; Hell, S. W. *Eur. J. Org. Chem.* **2010**, 3593.
- (9) Romieu, A.; Brossard, D.; Hamon, M.; Outaabout, H.; Portal, C.; Renard, P.-Y. *Bioconjugate Chem.* **2007**, *19*, 279.
- (10) Romieu, A.; Tavernier-Lohr, D.; Pellet-Rostaing, S.; Lemaire, M.; Renard, P. Y. *Tetrahedron Lett.* **2010**, *51*, 3304.
- (11) Bates, M.; Huang, B.; Dempsey, G. T.; Zhuang, X. *Science* **2007**, *317*, 1749.
- (12) Suhling, K.; French, P. M. W.; Phillips, D. *Photochem. Photobiol. Sci.* **2005**, *4*, 13.
- (13) Lasne, D.; Maali, A.; Amarouchene, Y.; Cognet, L.; Lounis, B.; Kellay, H. *Phys. Rev. Lett.* **2008**, *100*, 214502.
- (14) Eggeling, C.; Ringemann, C.; Medda, R.; Schwarzmann, G.; Sandhoff, K.; Polyakova, S.; Belov, V. N.; Hein, B.; von Middendorff, C.; Schonle, A.; Hell, S. W. *Nature (London, U. K.)* **2009**, *457*, 1159.
- (15) The structures of Alexa 647 and Alexa were reported in the Supporting Information of the following report: Bates et al. *Science*, 2007, 317, 1749-1753. The structure of Cy5 and Cy5.5 were reported in: Romieu et al. *Tetrahedron Lett.* 2010, 51, 3304-3308; for the structure of Atto647: see supporting information of the report: Eggeling et al. *Nature*, 2009, 457, 1159-1162.
- (16) Brellier, M.; Duportail, G.; Baati, R. *Tetrahedron Lett.* **2010**, *51*, 1269.
- (17) Dilek, O.; Bane, S. L. *Bioorg. Med. Chem. Lett.* **2009**, *19*, 6911.

- (18) Jiao, L.; Li, J.; Zhang, S.; Wei, C.; Hao, E.; Vicente, M. G. H. *New J. Chem.* **2009**, *33*, 1888.
- (19) Li, L.; Han, J.; Nguyen, B.; Burgess, K. *J. Org. Chem.* **2008**, *73*, 1963.
- (20) Resch-Genger, U.; Grabolle, M.; Cavaliere-Jaricot, S.; Nitschke, R.; Nann, T. *Nat Meth* **2008**, *5*, 763.
- (21) Thivierge, C.; Bandichhor, R.; Burgess, K. *Org. Lett.* **2007**, *9*, 2135.
- (22) Meltola, N. J.; Wahlroos, R.; Soini, A. E. *J. Fluorescence* **2004**, *14*, 635.
- (23) Atilgan, S.; Ekmekci, Z.; Dogan, A. L.; Guc, D.; Akkaya, E. U. *Chemical Communications* **2006**, 4398.
- (24) Atilgan, S.; Ozdemir, T.; Akkaya, E. U. *Org. Lett.* **2008**, *10*, 4065.
- (25) Tasiar, M.; Murtagh, J.; Frimannsson, D. O.; McDonnell, S. O.; O'Shea, D. F. *Org. Biomol. Chem.* **2010**, *8*, 522.
- (26) Lifetime Data of Selected Fluorophores:  
[http://www.iss.com/resources/reference/data\\_tables/LifetimeDataFluorophores.html](http://www.iss.com/resources/reference/data_tables/LifetimeDataFluorophores.html)
- (27) Date for the fluorophore Alexa 647:  
<http://www.invitrogen.com/site/us/en/home/References/Molecular-Probes-The-Handbook/tables/Fluorescence-quantum-yields-and-lifetimes-for-Alexa-Fluor-dyes.html>
- (28) Fluorescence Quantum Yield of Cy 5 :Standards.  
[http://www.iss.com/resources/reference/data\\_tables/FL\\_QuantumYieldStandards.html](http://www.iss.com/resources/reference/data_tables/FL_QuantumYieldStandards.html)
- (29) Niu, S.-L.; Ulrich, G.; Retailleau, P.; Harrowfield, J.; Ziessel, R. *Tetrahedron Lett.* **2009**, *50*, 3840.
- (30) Niu, S. L.; Ulrich, G.; Ziessel, R.; Kiss, A.; Renard, P.-Y.; Romieu, A. *Org. Lett.* **2009**, *11*, 2049.
- (31) Chen, J.; Burghart, A.; Derecskei-Kovacs, A.; Burgess, K. *J. Org. Chem.* **2000**, *65*, 2900.
- (32) Burghart, A.; Kim, H.; Welch, M. B.; Thoresen, L. H.; Reibenspies, J.; Burgess, K.; Bergstrom, F.; Johansson, L. B. A. *J. Org. Chem.* **1999**, *64*, 7813.
- (33) Descalzo, A. B.; Xu, H. J.; Shen, Z.; Rurack, K. *Ann. N. Y. Acad. Sci.* **2008**, *1130*, 164.
- (34) Wada, M.; Ito, S.; Uno, H.; Murashima, T.; Ono, N.; Urano, T.; Urano, Y. *Tetrahedron Lett.* **2001**, *42*, 6711.
- (35) Kang, H. C.; Haugland, R. P. 1995; Vol. US Patent 5,433,896,.
- (36) Wu, Y.; Klaubert, D. H.; Kang, H. C.; Zhang, Y.-z. 1999; Vol. US Patent 6,005,113,.
- (37) Rohand, T.; Qin, W.; Boens, N.; Dehaen, W. *Eur. J. Org. Chem.* **2006**, *2006*, 4658.
- (38) Coskun, A.; Akkaya, E. U. *Tetrahedron Lett.* **2004**, *45*, 4947.
- (39) Coskun, A.; Akkaya, E. U. *J. Am. Chem. Soc.* **2005**, *127*, 10464.

- (40) Dost, Z.; Atilgan, S.; Akkaya, E. U. *Tetrahedron* **2006**, *62*, 8484.
- (41) Thoresen, L. H.; Kim, H.; Welch, M. B.; Burghart, A.; Burgess, K. *Synlett* **1998**, 1276.
- (42) Ortiz, M. J.; Garcia-Moreno, I.; Agarrabeitia, A. R.; Duran-Sampedro, G.; Costela, A.; Sastre, R.; Arbeloa, F. L.; Prieto, J. B.; Arbeloa, I. L. *Phys. Chem. Chem. Phys.* **2010**, *12*, 7804.
- (43) Loudet, A.; Burgess, K. *Chem. Rev.* **2007**, *107*, 4891.
- (44) Qin, W.; Rohand, T.; Dehaen, W.; Clifford, J. N.; Driesen, K.; Beljonne, D.; Van Averbeke, B.; Van der Auweraer, M.; Boens, N. *J. Phys. Chem. A* **2007**, *111*, 8588.
- (45) Rurack, K.; Kollmannsberger, M.; Daub, J. *New J. Chem.* **2001**, *25*, 289.
- (46) Hinz, W.; Jones, R. A.; Anderson, T. *Synthesis* **1996**, *8*, 620.
- (47) Knoevenagel, E. *Ber. Der. Deut. Chem. Gesell.* **1898**, *31*, 2596.
- (48) Rurack, K.; Kollmannsberger, M.; Daub, J. *Angew. Chem., Int. Ed.* **2001**, *40*, 385.
- (49) Haugland, R. P.; Gregory, J.; Spence, M. T. Z.; Johnson, I. D. *Handbook of fluorescent probes and research products*; Molecular Probes, 2002.
- (50) Ulrich, G.; Ziessel, R.; Harriman, A. *Angew. Chem., Int. Ed.* **2008**, *47*, 1184.
- (51) Ulrich, G.; Goze, C.; Guardigli, M.; Roda, A.; Ziessel, R. *Angew. Chem.* **2005**, *117*, 3760.
- (52) Qin, W.; Baruah, M.; Van der Auweraer, M.; De Schryver, F. C.; Boens, N. *J. Phys. Chem. A* **2005**, *109*, 7371.
- (53) Rurack, K.; Triefflinger, C.; Koval'chuck, A.; Daub, J. *Chemistry – A European Journal* **2007**, *13*, 8998.
- (54) Peng, X.; Du, J.; Fan, J.; Wang, J.; Wu, Y.; Zhao, J.; Sun, S.; Xu, T. *J. Am. Chem. Soc.* **2007**, *129*, 1500.
- (55) Bozdemir, O. A.; Guliyev, R.; Buyukcakir, O.; Selcuk, S.; Kolemen, S.; Gulseren, G.; Nalbantoglu, T.; Boyaci, H.; Akkaya, E. U. *J. Am. Chem. Soc.* **2010**, *132* (23), pp 8029.
- (56) Coskun, A.; Deniz, E.; Akkaya, E. U. *Org. Lett.* **2005**, *7*, 5187.
- (57) Silva, A. P. d.; et al. *J. Phys.: Condens. Matter* **2006**, *18*, S1847.
- (58) Raymo, F. M. *Advanced Materials* **2002**, *14*, 401.
- (59) Balzani, V.; Credi, A.; Venturi, M. *ChemPhysChem* **2003**, *4*, 49.
- (60) Guliyev, R.; Coskun, A.; Akkaya, E. U. *J. Am. Chem. Soc.* **2009**, *131*, 9007.
- (61) Cheng, T.; Xu, Y.; Zhang, S.; Zhu, W.; Qian, X.; Duan, L. *J. Am. Chem. Soc.* **2008**, *130*, 16160.
- (62) Bouit, P. A.; Kamada, K.; Feneyrou, P.; Berginc, G.; Toupet, L.; Maury, O.; Andraud, C. *Advanced Materials* **2009**, *21*, 1151.

- (63) Zheng, Q.; Xu, G.; Prasad, P. *Chemistry – A European Journal* **2008**, *14*, 5812.
- (64) Didier, P.; Ulrich, G.; Mely, Y.; Ziessel, R. *Org. Biomol. Chem.* **2009**, *7*, 3639.
- (65) Kumaresan, D.; Thummel, R.; Bura, T.; Ulrich, G.; Ziessel, R. *Chemistry – A European Journal* **2009**, *15*, 6335.
- (66) Kolemen, S.; Cakmak, Y.; Erten-Ela, S.; Altay, Y.; Brendel, J.; Thelakkat, M.; Akkaya, E. U. *Org. Lett.* **2010**, *12(17)*, pp 3812.
- (67) Erten-Ela, S.; Yilmaz, M. D.; Icli, B.; Dede, Y.; Icli, S.; Akkaya, E. U. *Org. Lett.* **2008**, *10*, 3299.
- (68) Rousseau, T.; Cravino, A.; Bura, T.; Ulrich, G.; Ziessel, R.; Roncali, J. *J. Mater. Chem.* **2009**, *19*, 2298.
- (69) Rousseau, T.; Cravino, A.; Bura, T.; Ulrich, G.; Ziessel, R.; Roncali, J. *Chemical Communications* **2009**, 1673.
- (70) Rousseau, T.; Cravino, A.; Ripaud, E.; Leriche, P.; Rihn, S.; De Nicola, A.; Ziessel, R.; Roncali, J. *Chemical Communications* **2010**, *46*, 5082.
- (71) Schoenberg, A.; Bartoletti, I.; Heck, R. F. *J. Org. Chem.* **1974**, *39*, 3318.
- (72) El-ghayoury, A.; Ziessel, R. *Tetrahedron Lett.* **1998**, *39*, 4473.
- (73) Albericio, F.; Carpino, L. A. In *Methods Enzymol.*; Gregg, B. F., Ed.; Academic Press: 1997; Vol. Volume 289, p 104.
- (74) Bannwarth, W.; Knorr, R. *Tetrahedron Lett.* **1991**, *32*, 1157.
- (75) Gonçalves, M. S. T. *Chem. Rev.* **2009**, *109*, 190.
- (76) Tleugabulova, D.; Zhang, Z.; Brennan, J. D. *J. Phys. Chem. B* **2002**, *106*, 13133.
- (77) Takeuchi, T.; Miwa, T. *Chromatographia* **1995**, *40*, 159.
- (78) Niu, S. L.; Massif, C.; Ulrich, G.; Ziessel, R.; Renard, P.-Y.; Romieu, A. *Org. Biomol. Chem.* **2011**, *9*, 66.
- (79) Wilson, A. A.; Dannals, R. F.; Ravert, H. T.; Frost, J. J.; Wagner, H. N. *J. Med. Chem.* **1989**, *32*, 1057.
- (80) Ziessel, R.; Retailleau, P.; Elliott, K. J.; Harriman, A. *Chemistry – A European Journal* **2009**, *15*, 10369.
- (81) Olmsted, J. *J. Phys. Chem* **1979**, *83*, 2581.
- (82) Chidley, C.; Mosiewicz, K.; Johnsson, K. *Bioconjugate Chem.* **2008**, *19*, 1753.
- (83) Maurel, D.; Kniazeff, J.; Mathis, G.; Trinquet, E.; Pin, J.-P.; Ansanay, H. *Anal. Biochem.* **2004**, *329*, 253.
- (84) Gao, Y.; Kyratzis, I. *Bioconjugate Chem.* **2008**, *19*, 1945.

- 
- (85) Debord, J. D.; Lyon, L. A. *Bioconjugate Chem.* **2007**, *18*, 601.
- (86) Rostron, J. P.; Ulrich, G.; Retailleau, P.; Harriman, A.; Ziessel, R. *New J. Chem.* **2005**, *29*, 1241.
- (87) Pauli, J.; Brehm, R.; Spieles, M.; Kaiser, W.; Hilger, I.; Resch-Genger, U. *J. Fluoresc.* **2010**, *20*, 681.
- (88) Pawlicki, M.; Collins, H. A.; Denning, R. G.; Anderson, H. L. *Angew. Chem., Int. Ed.* **2009**, *48*, 3244.
- (89) Kawata, S.; Kawata, Y. *Chem. Rev.* **2000**, *100*, 1777.
- (90) Zheng, Q.; He, G. S.; Prasad, P. N. *Chem. Phys. Lett.* **2009**, *475*, 250.
- (91) Fisher, W. G.; Partridge, W. P.; Dees, C.; Wachter, E. A. *Photochem. Photobiol.* **1997**, *66*, 141.
- (92) Hayek A., B. F., Nicoud J.F., Duperray A., Grichine A., Baldeck P.L., Vial J.-C. *Nonlinear Optics and Quantum Optics* **2006**, *35* 155.
- (93) Zhang, D.; Wang, Y.; Xiao, Y.; Qian, S.; Qian, X. *Tetrahedron* **2009**, *65*, 8099.
- (94) Göppert-Mayer, M. *Annalen der Physik* **2009**, *18*, 466.
- (95) Moreno, J. P.; Kuzyk, M. G. *J. Chem. Phys* **2005**, *123*, 194101.
- (96) Oudar, J. L.; Le Person, H. *Opt. Commun.* **1975**, *15*, 258.
- (97) Albota, M.; Beljonne, D.; Brédas, J.-L.; Ehrlich, J. E.; Fu, J.-Y.; Heikal, A. A.; Hess, S. E.; Kogej, T.; Levin, M. D.; Marder, S. R.; McCord-Maughon, D.; Perry, J. W.; Röckel, H.; Rumi, M.; Subramaniam, G.; Webb, W. W.; Wu, X.-L.; Xu, C. *Science* **1998**, *281*, 1653.
- (98) Chang, C.; Sud, D.; Mycek, M. In *Methods in Cell Biology*; Greenfield, S., David, E. W., Eds.; Academic Press: 2007; Vol. 81, p 495.



# CHAPTER IV

## The BODIPY bridged push-pull chromophores

### 1.1 General introduction

The term “Push-pull” was used to describe conjugated compounds that have an electron donor group (D) and an electron withdrawing (A) group that exhibit intramolecular charge transfer (ICT) through the  $\pi$ -conjugated bridge (also called as D- $\pi$ -A system). The ICT character derives from the molecular push-pull structure and has been largely investigated in a wide range of optical-electrical applications, such as light-emitting devices,<sup>1,2</sup> optical imaging of living tissues,<sup>3,4</sup> nonlinear optical devices,<sup>5,6</sup> and solar cell materials.<sup>7-10</sup> It has been demonstrated that combination of electron donor group and electron withdrawing group could efficiently modify the electronic signatures of the conjugated chromophore,<sup>7,11-13</sup> such as optical properties, electronic states (HOMO/LUMO), and chemical properties. In this chapter, we were interested in functionalization of the BODIPY moiety as the bridge of  $\pi$ -conjugated push-pull chromophores, in order to investigate their linear and nonlinear optical properties as well as the electrochemical properties that arise from the interaction between the conjugated donor and acceptor groups through the BODIPY core.

#### 1.1.1 Push-pull chromophore for nonlinear optical (NLO) material

The nonlinear optics (NLO) is one of the most intensively investigated properties of push-pull chromophores. The push-pull structural molecules (Chart 1) usually possess large ground-state dipole moments ( $\mu$ ) and the second order susceptibilities (also called the first hyperpolarizability)<sup>14</sup> ( $\beta$ ), the latter plays a dominant role in contributions to the observed optical nonlinear responses.<sup>15,16</sup> The organic molecules with NLO properties that are capable of manipulating electric fields, especially photonic signals are valuable for the development of novel materials in telecommunications, information storage, optical switching, as well as frequency doubling of incident irradiation. Therefore, in both theory and synthesis, extensive research efforts have been devoted on push-pull chromophores in order to obtain molecules with large first hyperpolarizabilities for the NLO applications.<sup>5,17-23</sup>

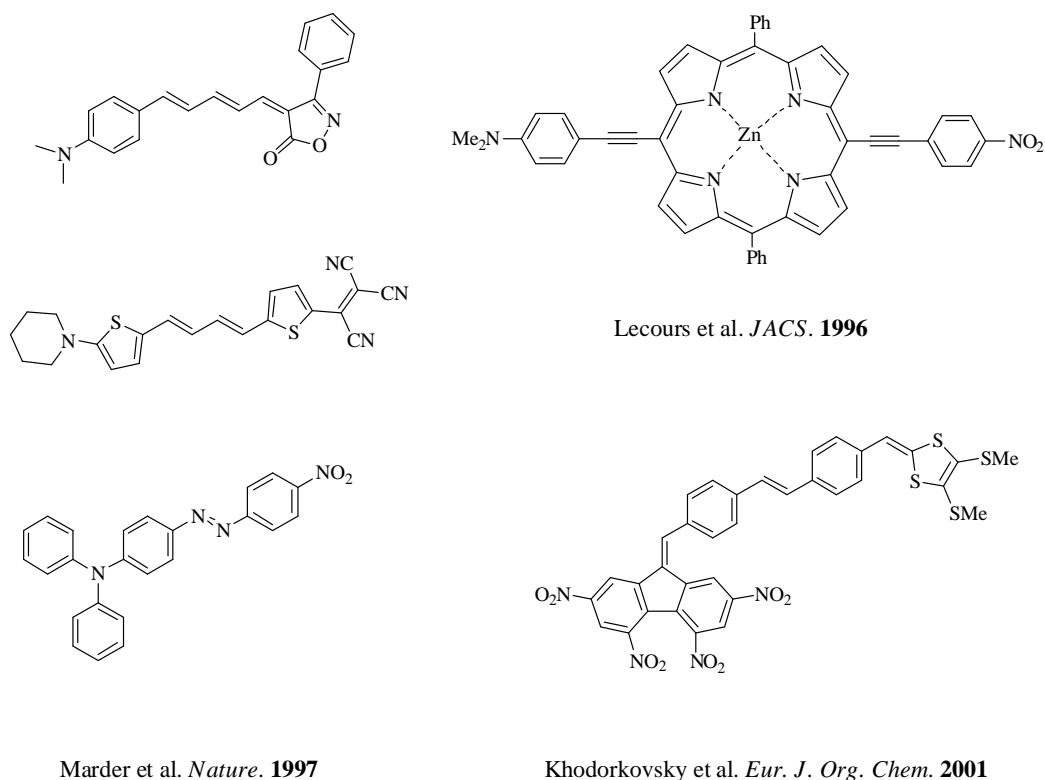


**Chart 1. Chemical structures of some push-pull chromophores.**<sup>5,6,20</sup>

During studies of structure-properties, it is considered that the asymmetric charge distribution of the  $\pi$ -electrons along the conjugated molecule results in the NLO response. The Oudar's two-state model (eq. 1) has been widely considered in designing organic NLO materials for the evaluation and modification of a given one dimensional organic compound with large hyperpolarizability ( $\beta$ ).<sup>24,25</sup> According to the equation, the hyperpolarizability ( $\beta$ ) is proportional to the changes in dipole moment ( $\mu$ ) between the ground ( $\mu_{gg}$ ) and excited states ( $\mu_{ee}$ ), and the square of the transition oscillator strength ( $\mu_{ge}$ ), while inversely proportional to the square of the energy gap ( $E_{ge}$ ) between these two states.<sup>6</sup> Therefore, the ( $\beta$ ) is intrinsically related to the molecular charge-transfer excited states.<sup>14,26</sup> However, it was also mentioned that simply increasing the donor/acceptor strength will not necessarily lead to enhanced hyperpolarizability even the two states are fully delocalized or localized,<sup>5,27</sup> but at some intermediate point where there is non-negligible overlap between the two states.<sup>14</sup> It was revealed that the overlapping between the HOMO and LUMO in the bridging region is necessary for obtaining the large hyperpolarizability ( $\beta$ ) in a push-pull system.<sup>28-30</sup> The theoretical and computational calculation studies,<sup>14,16,31-35</sup> which focus on developing new methods to adequately represent the push-pull chromophores in both ground and excited states, have been useful tool to accurately predict the molecular first hyperpolarizabilities ( $\beta$ ) and for acquiring a better understanding of such system.

$$\beta \propto (\mu_{ee} - \mu_{gg}) \frac{\mu_{ge}^2}{E_{ge}^2}$$

**Equation 1. Oudar's two-state model.**

Since recent years the two limit resonance forms (Figure 1) have been proposed and abundantly discussed in designing push-pull chromophores by Marder and co-workers.<sup>5,19,35-38</sup> It was considered that the bridges linking the donor and acceptor groups play an important role in molecular NLO response; different spacers (e.g. ethynyl, phenylene, small heteroaromatic ring, styrene building blocks, and a combination of two or more of these simple units); as well as larger chromophore such as porphyrine have been extensively employed in NLO materials synthesis.<sup>5,6,19,38-41</sup>

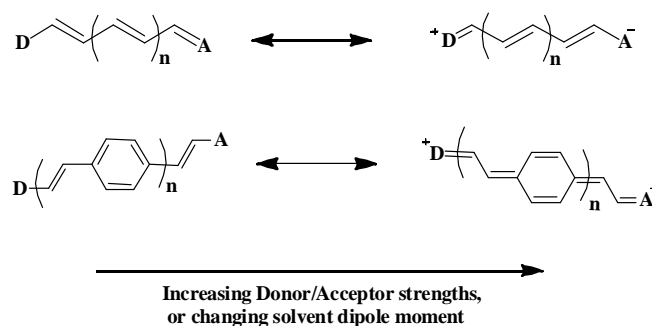


**Figure 1. Neutral (left) and zwitterionic (right) limiting resonance forms of the push-pull chromophores.**

### 1.1.2 New insight into BODIPY based push-pull chromophores

Over the last decade the main research attentions about push-pull system have been focused on the fundamental comprehension of structure-property relationship and engineering of molecular materials with large NLO responses. Recently, new researches using the push-pull chromophores in the field of electro-optics have been reported based on functionalized merocyanine dye for organic photovoltaics;<sup>8,42,43</sup> fluorene molecular probes for two photon absorption and NLO cell imaging,<sup>3,44,45</sup> which naturally attracted our attention.

The BODIPY dyes have been well known for their strong absorption bands in UV-visible; high solubility in common organic solvents; high fluorescence quantum yield and relatively long excitation life-time (1~5 ns); high chemical and photochemical stability of the  $\pi$ -system of the BODIPY core. All these remarkable properties make BODIPY a promising candidate for NLO applications. Moreover, the construction of the push-pull system upon the BODIPY scaffold will probably lead to some new electronic properties, such as chromism, charge transport properties,  $\pi$ -conjugated electronic states recombination, opto-electronic properties. These expected properties upon the BODIPY based push-pull system might also offer a new opportunity for the study of organic

photovoltaic devices.<sup>9,46</sup> Up to now only few functionalization of BODIPY based chromophores have been reported in the field of two photon absorption for cell imaging or telecommunications.<sup>21,22,47-49</sup> We however notice that the study of BODIPY based push-pull system is rather limited.<sup>7,11</sup>

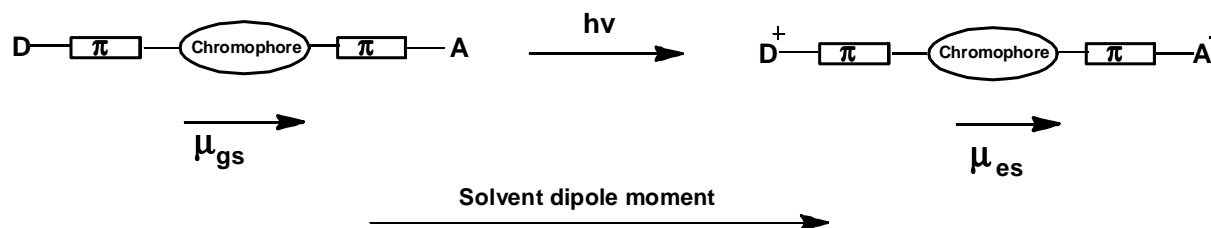


Figure 2. Push-pull Chromophore in the ground (l) and the excited (r) state,  $\mu$  represent for the dipole moment.

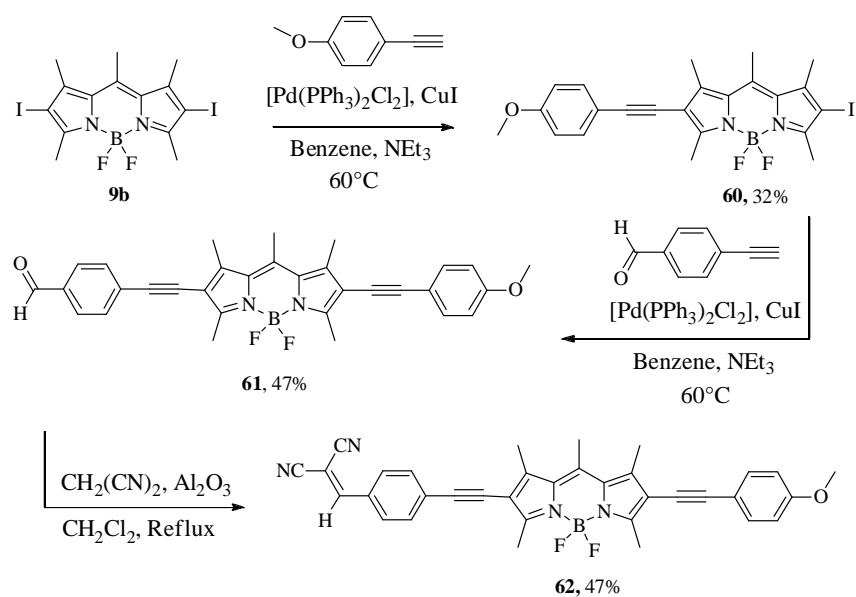
This is the main reason why we were motivated to the synthesis of fully conjugated BODIPY based push-pull system (Figure 2). Primarily, the BODIPY bridged push-pull system will be build from a functionalized BODIPY, by introducing of an electron donor group and an electron acceptor group through ethynyl linkers at both sides of the BODIPY core. The intramolecular charge transfer (ICT) properties of the conjugated BODIPY will then be investigated by UV-Vis absorption, fluorescence emission, electronic properties, as well as the measurement hyperpolarizability.

## 1.2 Synthesis of BODIPY-bridged push-pull chromophores

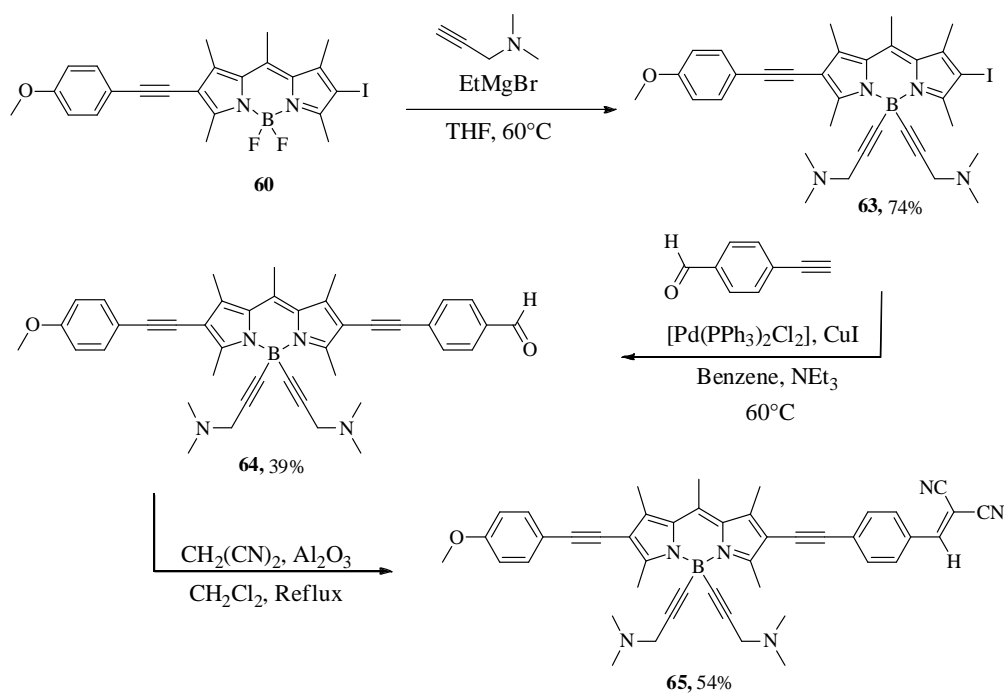
### 1.2.1 Synthesis of chromophores **62** and **65**.

Introduction of anisole or benzaldehyde groups onto the BODIPY **9b** at 2,6 position was performed by two successive Sonogashira coupling reactions under standard conditions (Scheme 1). The ethynyl groups are selected not only to attach the D/A groups to the chromophore, but also to extend the conjugation of the chromophore between the donor and the acceptor.<sup>6</sup> Then the dicyanomethylene group designed as electron withdrawing group was generated by a Knoevenagel condensation<sup>50</sup> of **61** with malononitrile in dichloromethane at reflux leading to the purple colored compound **62**.

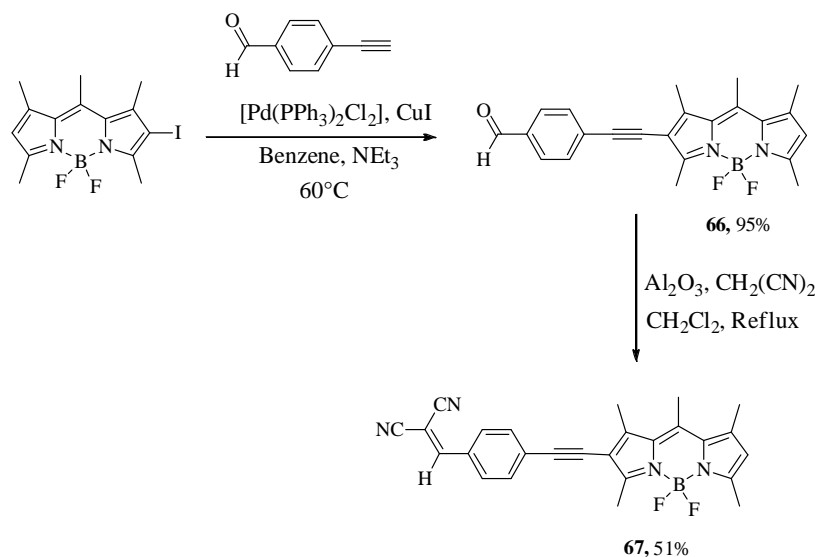
Some difficulties in the purification and identification of **62** were met during the synthesis, due to the poor solubility of **62** in common solvents. It is considered that the intermolecular aromatic  $\pi$ - $\pi$  stacking and anti-parallel dipole-dipole interactions in solution favor molecular aggregation. This is a common practical problem that has been widely discussed in push-pull chromophores synthesis.<sup>18,20,51</sup> Generally, the strategy often applied is to introduce bulky substituents onto the push-pull chromophore scaffold in order to increase the molecular sterical hindrance and prevent the formation of aggregation, and therefore providing a better solubility.<sup>18,51</sup> On the other hand, more elaborate molecules needs to be designed and with the risk to loose the intramolecular charge transfer efficiency with a significant reduction of the NLO response.



As discussed previously in Chapter III, introduction of diethynyl-groups on the boron atom of the BODIPY by using the appropriate Grignard reagents could efficiently prevent the formation of aggregates and to increase the solubility. Therefore, we designed a new synthetic route for the chromophore **65**, involving the replacement of the fluorides of **60** by the Grignard reagent of dimethylaminopropyne to give **63**, followed by a Sonogashira coupling reaction to give the benzaldehyde derivative **64**. Then a Knoevenagel condensation gave the dicyanomethylene derivative **65** (Scheme 2).



Finally, we synthesized compound **67**, according to Scheme 3 to compare the properties with compounds **62** and **65**. Compound **67** is less conjugated than **62** and therefore has a better solubility. Their optical properties will be discussed in the following section.



Scheme 3. Synthesis of compound **67**.

### 1.2.1.1 Optical properties of the push-pull chromophores

The optical properties of the push-pull chromophores **62**, **65**, **67** and the intermediates were evaluated in different solvents. The spectroscopic data were collected in Table 1. In solution, all compounds show a strong  $S_0 \rightarrow S_1$  ( $\pi \rightarrow \pi^*$ ) transition between  $\lambda \approx 540\text{-}570$  nm with an absorption coefficient in the  $12000\text{-}90000 \text{ M}^{-1}\text{cm}^{-1}$  range, unambiguously assigned to the boradiazaindacene chromophore.<sup>52</sup> At higher energy, two close and successive but resolvable, weaker and broad bands centered about 410 nm and 350 nm, can be attributed to the charge transfer absorption<sup>52</sup> and the  $S_0 \rightarrow S_2$  ( $\pi \rightarrow \pi^*$ ) transition of the BODIPY moiety, respectively.<sup>53</sup> The  $\pi \rightarrow \pi^*$  transitions with vibronic structures are observed at 230-320 nm for the phenyl groups. In  $\text{CH}_2\text{Cl}_2$ , the BODIPY dyes show emission maximum in the 561-611 nm range. The fluorescence quantum yields are in the 28-53% range, with the exception of the intermediate iodo-substituted compounds **60** and **63**, for which the fluorescence is dramatically reduced due to a faster nonradiative decay, suggesting that the intersystem crossing efficiency from the singlet excited state to the triplet state is favored by the internal heavy atom effect.<sup>54,55</sup> Interestingly, these D- $\pi$ -A type BODIPYs display larger Stokes shifts in the  $866\text{-}1915 \text{ cm}^{-1}$  range compared with common BODIPY dyes ( $300\text{-}900 \text{ cm}^{-1}$ ).<sup>52,56,57</sup>

The optical properties of the dicyanomethylene derivatives **62**, **65** and **67** were compared (Figure 4 and 5). The absorption spectra show intense absorption around 480-630 nm with molar absorption coefficients in the  $75000\text{-}94000 \text{ M}^{-1}\text{cm}^{-1}$  range. Compared with compound **62**, the

ethynyl-substituted derivative **65** shows small hypsochromic shifts about 5-10 nm in both absorption and emission. In absence of the anisole group, compound **67** has weaker absorption at shorter wavelength of 230-330 nm, and exhibits the hypsochromic shifts in both absorption and emission compared with compound **62** of 34 and 55 nm, respectively. In addition, we noticed that **67** has a relatively smaller Stokes shift ( $866\text{ cm}^{-1}$ ) with higher quantum yield (53%) and longer decay time (2.3 ns). However, it is noteworthy that, the absorption band centered about 420 nm with absorption coefficients in the  $15000\text{-}20000\text{ M}^{-1}\text{cm}^{-1}$  range, is likely attributed to the charge transfer absorption band.<sup>58</sup> This is unusual compared with the common BODIPYs where the CT absorption band usually largely overlaps with the  $S_0 \rightarrow S_1$  transition.<sup>52</sup> Furthermore, the absorption centered about 350 nm can be attributed to the  $S_0 \rightarrow S_2$  ( $\pi \rightarrow \pi^*$ ) transition with absorption coefficients in the range of  $15000\text{-}18000\text{ M}^{-1}\text{cm}^{-1}$ . This transition is also enhanced compared with common BODIPYs.<sup>52</sup>

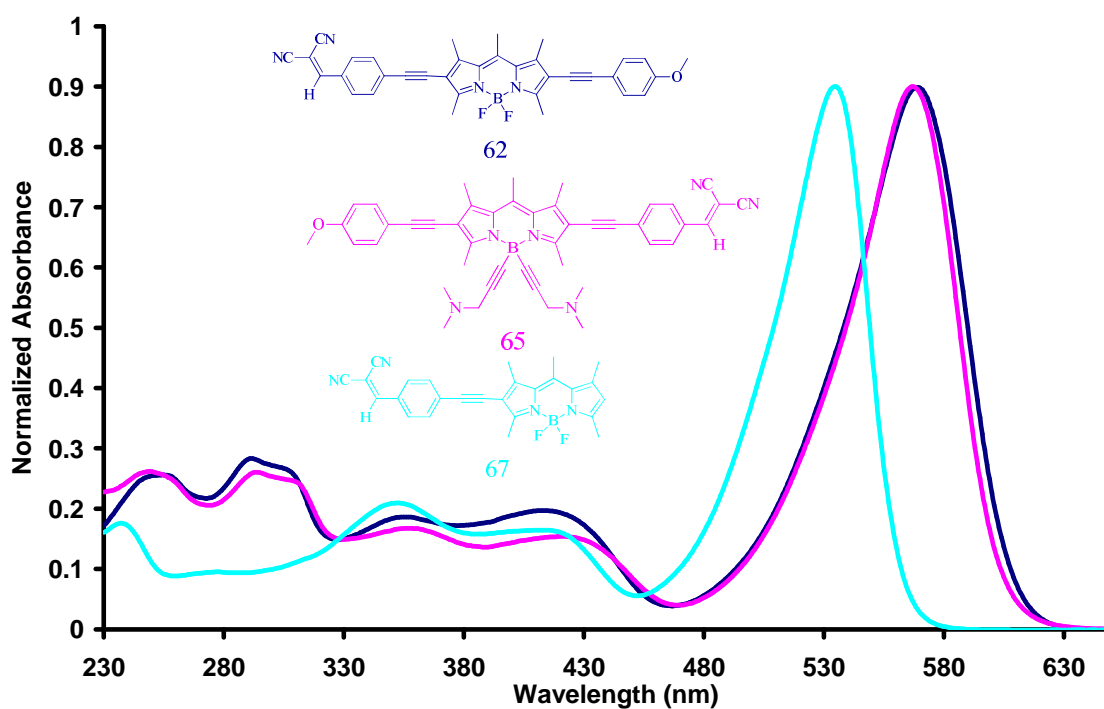


Figure 3. Normalized absorption spectra of compounds **62**, **65** and **67** in  $\text{CH}_2\text{Cl}_2$ .

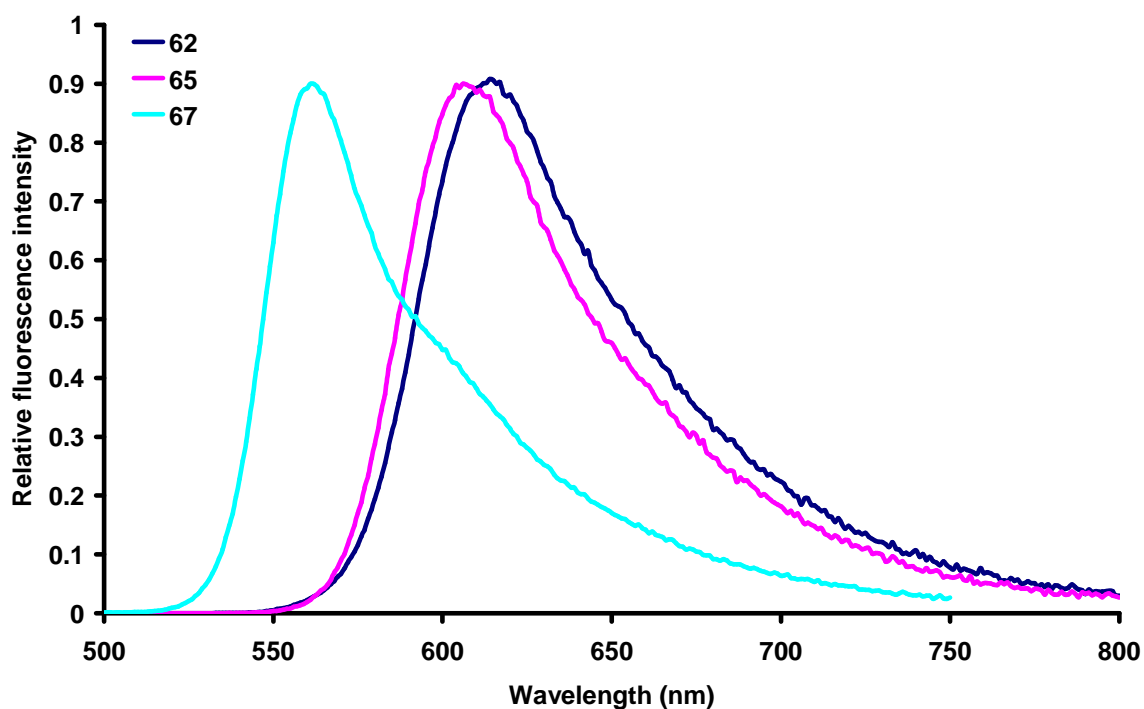


Figure 4. Normalized emission spectra of compounds **62**, **65** and **67** in  $\text{CH}_2\text{Cl}_2$ .

The solvatochromism induced by the electron withdrawing group of the push-pull system was also investigated (Figure 5). The difluoro-BODIPY (we call it here F-BODIPY) aldehyde **61** and dicyanomethylene **62** and their boron-ethynyl-substituted-BODIPY (E-BODIPY) analogues **64** and **65** were compared in dioxan,  $\text{CH}_2\text{Cl}_2$ , and ethanol (Figure 5 - 8). Subtle differences were observed in both absorption and emission spectra in solvents (Table 1). In the solvent with strong dipole moment, the absorption and fluorescence emission maximum of these compounds are slightly shifted to the red. The presence of the dicyanomethylene group from the formyl group leads to small bathochromic shifts ( $< 8$  nm) in both absorption and emission spectra in the corresponding solvents. Remarkably, in EtOH a dramatic decrease of the extinction coefficient for both formyl derivatives **61** and **64** were observed. This fact may be attributed to the poor solubility of the compounds in EtOH.

In comparison, a slight hypsochromic shift in absorption ( $\sim 5$  nm) and emission ( $\sim 10$  nm) appears for the E-BODIPY derivatives **64** and **65** according to the corresponding F-BODIPYs **61** and **62**. It is noteworthy that the E-BODIPY dyes show much better solubility in common solvents compared with the F-BODIPYs (but that is less evident at a concentration of  $10^{-6} \text{ M}^{-1}$ ). More quantitative experiments show the dependence of the quantum yield ( $\phi$ ) and lifetime of fluorescence ( $\tau$ ) of all these molecules upon the solvent polarity. Their quantum yields ( $\phi$ ) and lifetime ( $\tau$ ) decrease with increasing of solvent dipole moments. Conversely, the Stokes shifts slightly increase in more polar solvents (Table 1). For **65**, the quantum yield ( $\phi$ ) and lifetime ( $\tau$ ) decrease when the solvent changes from dioxan (0.73, 3.1 ns) to EtOH (0.15, 1.1 ns). The role of non-radiative decay  $k_{nr}$  increases (about

9 times) while the role of radiative decay  $k_n$  remains constant. The Stokes shifts of **65** slightly increase from  $1043\text{ cm}^{-1}$  to  $1127\text{ cm}^{-1}$ . The dependence of the Stokes shift upon the solvent dipole moments indicates that the dipole moments in the push-pull chromophores differ between the ground and excited states.<sup>52</sup> However, the small changes may indicate that the difference in dipole moments between the excited state and the ground state are relatively weak.<sup>58,59</sup>

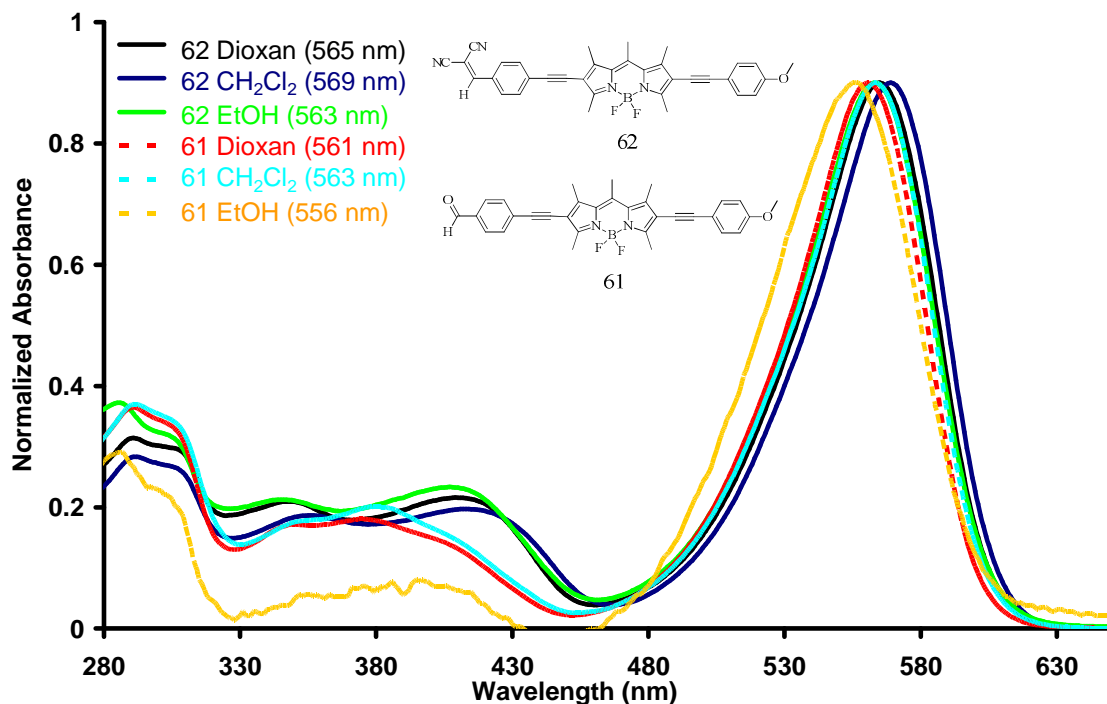


Figure 5. Normalized absorption spectra of compounds **62** and **61** in Dioxan,  $\text{CH}_2\text{Cl}_2$ , and EtOH, respectively.

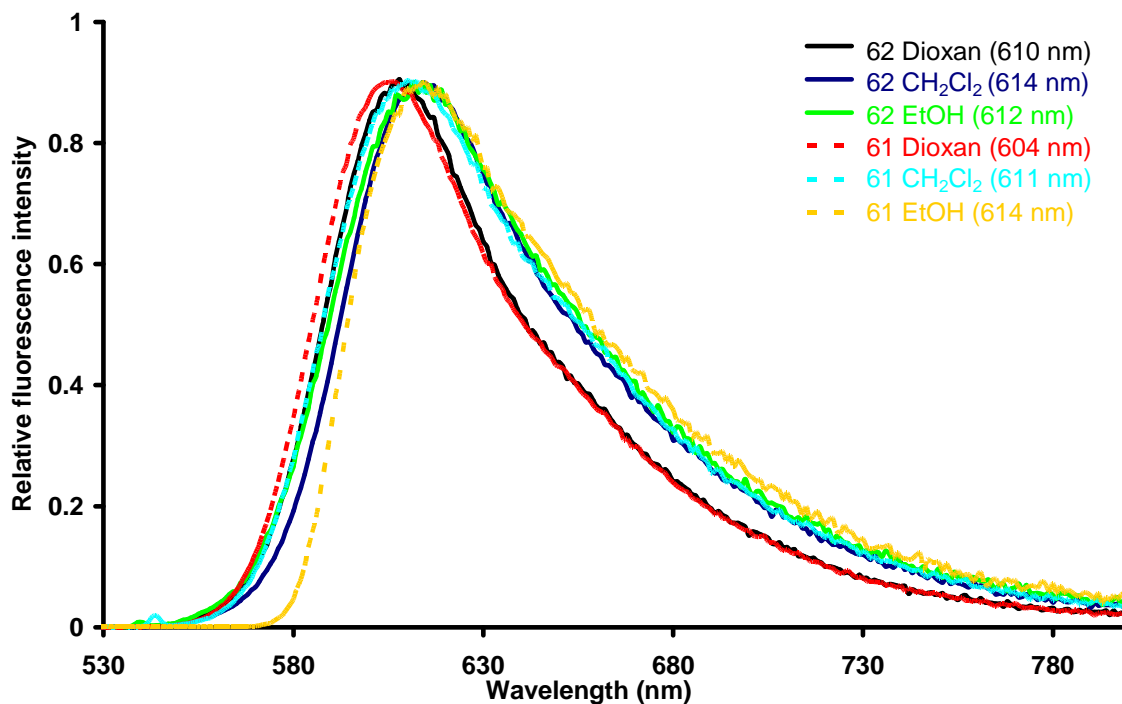


Figure 6. Normalized emission spectra of compound **62** and **61** in Dioxan,  $\text{CH}_2\text{Cl}_2$ , and EtOH, respectively.

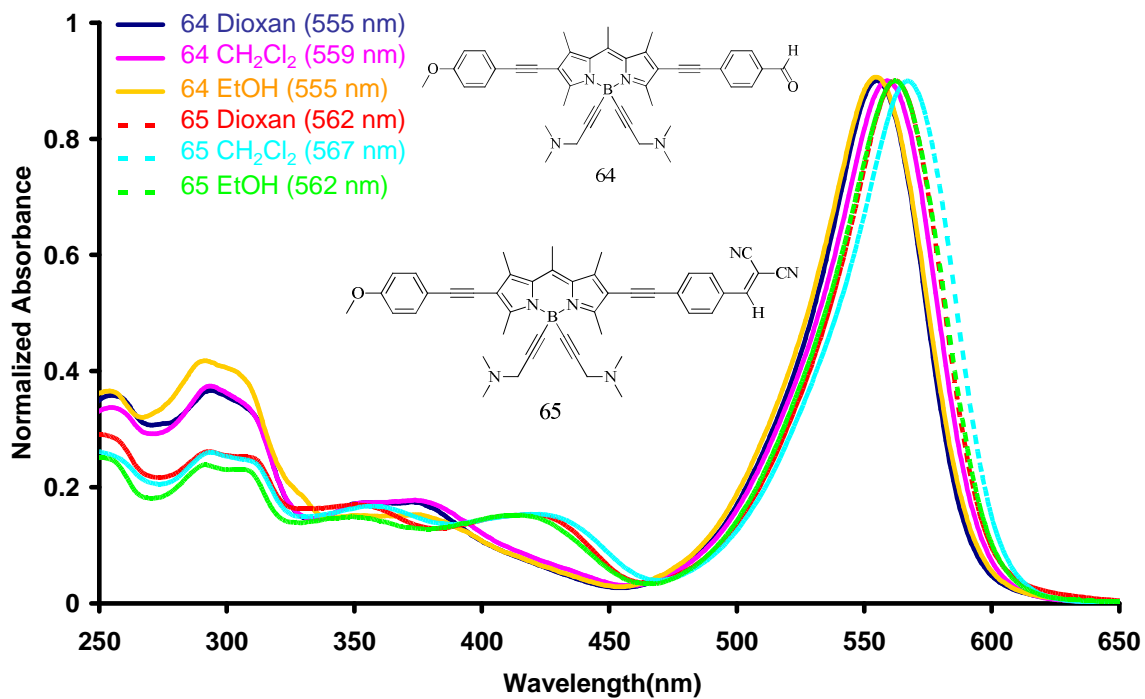


Figure 7. Normalized absorption spectra of compounds 64 and 65 in Dioxan, CH<sub>2</sub>Cl<sub>2</sub>, and EtOH, respectively.

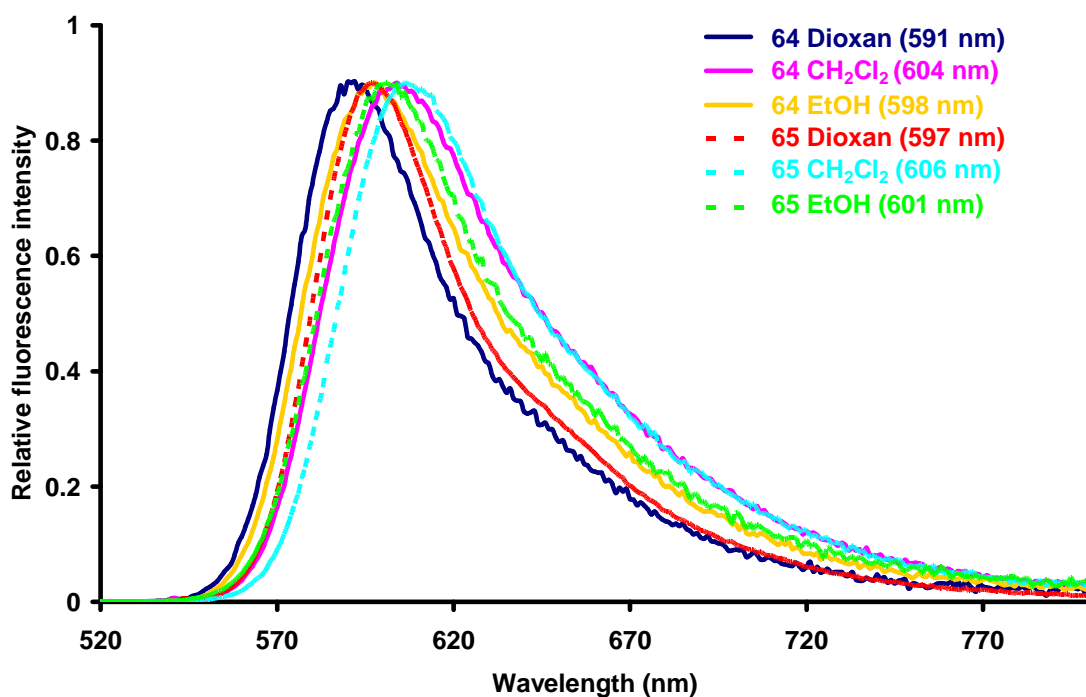


Figure 8. Normalized emission spectra of compounds 64 and 65 in Dioxan, CH<sub>2</sub>Cl<sub>2</sub>, and EtOH, respectively.

Table 1. Optical properties of the selected compounds.

| Compounds                                    | $\lambda_{\text{abs}}$ (nm) | $\epsilon$ ( $\text{M}^{-1} \cdot \text{cm}^{-1}$ ) | $\lambda_{\text{em}}$ (nm) | $\phi$ (%) <sup>a</sup> | $\tau$ (ns) | $k_r$ ( $10^7 \text{s}^{-1}$ ) <sup>b</sup> | $k_{nr}$ ( $10^7 \text{s}^{-1}$ ) <sup>b</sup> | $\Delta_s$ ( $\text{cm}^{-1}$ ) <sup>c</sup> |
|--|-----------------------------|---|----------------------------|-------------------------|-------------|---|--|--|
| <b>60</b> (CH <sub>2</sub> Cl <sub>2</sub> ) | 543                         | 57000   | 606                        | 6                       | 0.7         | 8.6   | 134.3  | 1915   |
| <b>61</b> (Dioxan)                           | 561                         | 80000   | 604                        | 42                      | 2.6         | 16.2  | 22.3   | 1269   |
| <b>61</b> (CH <sub>2</sub> Cl <sub>2</sub> ) | 563                         | 36000   | 611                        | 28                      | 1.7         | 16.5  | 42.4   | 1395   |
| <b>61</b> (EtOH)                             | 556                         | 12000   | 614                        | 16                      | 0.9         | 17.8  | 93.3   | 1699   |
| <b>62</b> (Dioxan)                           | 565                         | 73000   | 610                        | 46                      | 2.4         | 19.2  | 22.5   | 1306   |
| <b>62</b> (CH <sub>2</sub> Cl <sub>2</sub> ) | 569                         | 82000   | 616                        | 28                      | 1.7         | 16.5  | 42.4   | 1341   |
| <b>62</b> (EtOH)                             | 563                         | 74000   | 612                        | 16                      | 1.1         | 14.5  | 76.4   | 1422   |
| <b>63</b> (CH <sub>2</sub> Cl <sub>2</sub> ) | 539                         | 52000   | 600                        | 3                       | 1.4         | 2.1   | 69.3   | 1886   |
| <b>64</b> (Dioxan)                           | 555                         | 57000   | 591                        | 76                      | 3.2         | 23.8  | 7.5  | 1098   |
| <b>64</b> (CH <sub>2</sub> Cl <sub>2</sub> ) | 559                         | 65000   | 603                        | 36                      | 2.7         | 13.3  | 23.7   | 1305   |
| <b>64</b> (EtOH)                             | 555                         | 36000   | 598                        | 41                      | 2.5         | 16.4  | 23.6   | 1296   |
| <b>65</b> (Dioxan)                           | 562                         | 75000   | 597                        | 73                      | 3.1         | 23.5  | 8.7  | 1043   |
| <b>65</b> (CH <sub>2</sub> Cl <sub>2</sub> ) | 567                         | 85000   | 606                        | 32                      | 1.5         | 21.3  | 45.3   | 1135   |
| <b>65</b> (EtOH)                             | 562                         | 75000   | 600                        | 15                      | 1.1         | 13.6  | 77.3   | 1127   |
| <b>67</b> (CH <sub>2</sub> Cl <sub>2</sub> ) | 535                         | 94000   | 561                        | 53                      | 2.3         | 23.0  | 20.4   | 866  |

a) Quantum yield determined in dilute solution ( $1 \times 10^{-6} \text{M}$ ) using rhodamine 6G as reference ( $\phi_F = 0.78$  in water,  $\lambda_{\text{exc}} = 488 \text{ nm}$ ).<sup>60</sup> b) All  $\phi_F$  are corrected for changes in refractive index.  $K_r$  and  $k_{nr}$  were calculated using the following equations:  $k_r = \phi_F/\tau$ ,  $k_{nr} = (1-\phi_F)/\tau$ . c)  $\Delta_s$  = Stokes shift.

### 1.2.1.2 Electrochemical properties of compound **62**.

The electrochemical properties of compound **59** which was obtained as by-product of compound **60**, were evaluated by cyclic voltammetry (Figure 9). The measured oxidation/reduction potentials were gathered in Table 2 and compared with **62**. Both compounds are characterized by an irreversible oxidation wave at +1.01 and +1.09 V, corresponding to the one electron oxidation of the BODIPY moiety. On the reduction scans, a single reversible peak is observed at -1.10 V for **59** and -1.12 V for **62**, which can be unambiguously attributed to the formation of the  $\pi$ -radical anion of the BODIPY core.<sup>11,61,62</sup> For the mixed compound **62**, an additional irreversible reduction of the dicyanovinyl group is formed at -1.05 eV, this redox potential lies in the expected potential range as compared to analogue dicyanovinyl residue.<sup>63</sup>

In the next step, we synthesized and fully characterized the push-pull chromophores **62**, **65** and **67**. Their optical and electrochemical properties were evaluated. In the present design we use more efficient electron donor and electron withdrawing groups in order to improve the ICT strength along the BODIPY molecular axis. In addition, a good solubility of the resulting dyes is an important feature of that need to be taken into consideration in the synthesis design.

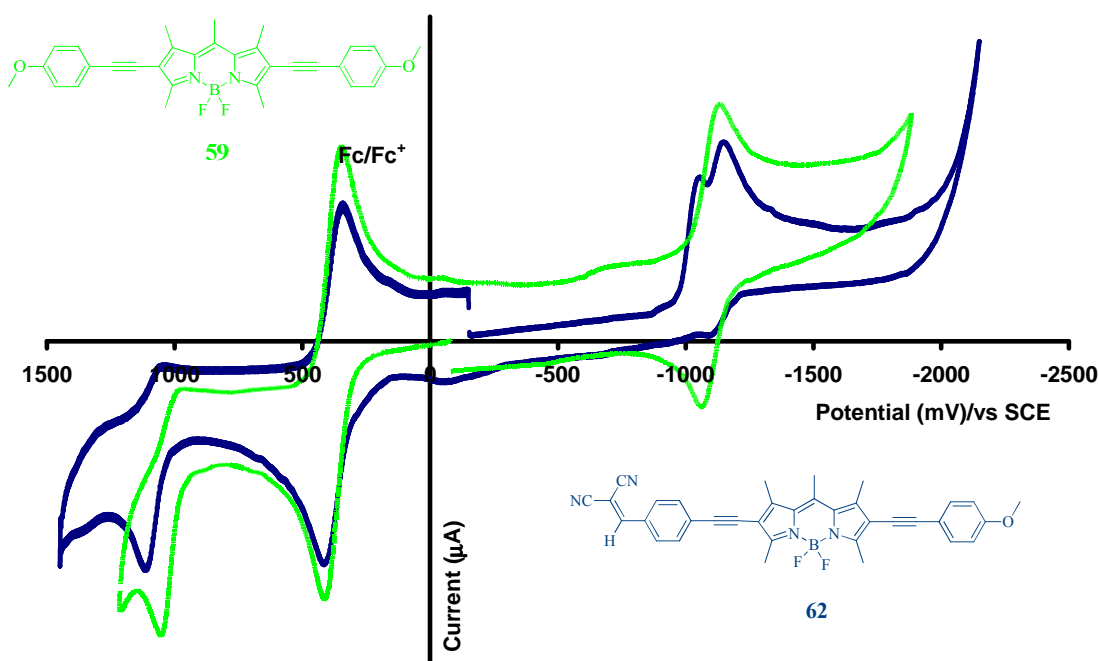


Figure 9. Cyclic voltammety spectra of 59 +ferrocene (green) and of 62 +ferrocene (blue).

Table 2. Electrochemical properties of 59 and 62.

| Compounds | $E^{\circ}_{ox}$ [V] ( $\Delta E$ [mV]) | $E^{\circ}_{red}$ [V] ( $\Delta E$ [mV]) |
|-----------|---|--|
| 59        | +1.01 (irrev)                           | -1.10 (96)                               |
| 62        | +1.09 (irrev)                           | -1.05 (irrev)<br>-1.12 (90)              |

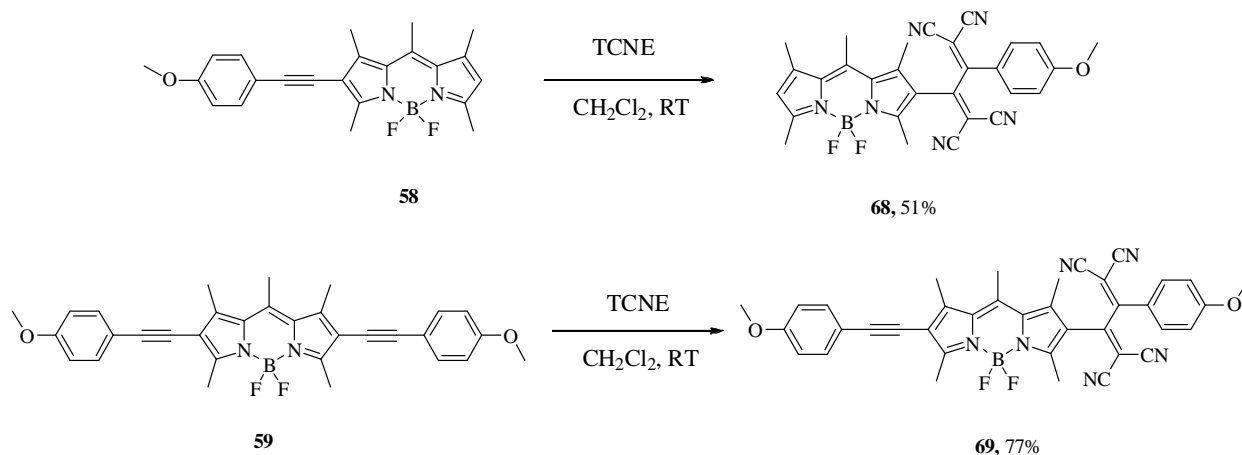
Cyclic voltammety carried out in deoxygenated  $\text{CH}_2\text{Cl}_2$  solutions, containing 0.1 M  $\text{TBAPF}_6$ , at a solute concentration range of  $1.5 \times 10^{-3} \text{M}$ , at  $20^\circ\text{C}$ . Potentials were standardized using added ferrocene (Fc) as internal reference and converted to SCE assuming that  $E_{1/2}(\text{Fc}/\text{Fc}^+) = +0.38\text{V}$  ( $\Delta E_p = 70 \text{ mV}$ ) versus SCE. Error in half-wave potentials is  $\pm 15\text{mV}$ . When the redox process is irreversible the peak potential ( $E_{ap}$  or  $E_{cp}$ ) is quoted.

### 1.2.2 Synthesis of tetracyanobuta-1,3-dienes (TCBDs) BODIPY

Therefore, a new synthetic strategy was applied according to the recent researches of Diederich and co-workers on the reaction of tetracyanoethene (TCNE) with alkynes derivatives.<sup>64-67</sup> The donor-substituted alkyne group undergo a [2+2] cycloaddition reaction with TCNE, followed by the formation of intermediate cyclobutene which subsequently undergoes ring opening leading to the 1,1,4,4-tetracyanobuta-1,3-dienes (TCBDs) derivatives. The TCBDs compounds exhibit a strong charge-transfer character and imports a good solubility in common solvents due to the non-planarity of the molecule which efficiently prevent the formation of aggregates.<sup>64,68</sup>

Therefore, we were interested in importing TCBDs group into the BODIPY bridged push-pull chromophore. Primarily, the BODIPYs **58** and **59** containing the ethynyl donor groups at 2,6 position

were selected to react with TCNE in dichloromethane at room temperature, leading to the amorphous donor-substituted TCBDs **68** and **69** in good yields. Interestingly, the reaction of **59** with TCNE in a proportion of 1:2.2 gives **69** in 77% of isolated yield. Despite the use of an excess of TCNE mono-insertion was observed, whereas no selectivity was observed in the following synthesis in Scheme 5.



Scheme 4. Synthesis of compounds **68** and **69**.

### 1.2.2.1 X-ray structure of compound **68**.

The single crystal of **68** suitable for X-ray analysis was grown by slow diffusion of Et<sub>2</sub>O vapor into a CH<sub>2</sub>Cl<sub>2</sub> solution. The X-ray structure of **68** shows pronounced nonplanarity of the BODIPY plan and the TCBDs moiety. The BODIPY core remains planar. Interestingly, the two dicyanovinyl (DCV) residues stretch in the opposite direction of each other with a dihedral angle (C24-C13-C12-C21) of 38.2°. The DCV moiety adjacent to the BODIPY twists backward out of the BODIPY platform with torsion angles (C5-C6-C12-C21) of 43.7°; while the other DCV moiety twists forward out of the BODIPY plan (C7-C6-C12-C13) of 43.5°. On the other side of the TCBDs, the torsion angles between the anisole ring and the adjacent DCV (C24-C13-C14-C19) are of 47.1° and (C12-C13-C14-C15) of 46.7° with the other DCV, respectively. Due to the strong electron withdrawing group TCBDs, the C7-C6 bond (1.41 Å) is relatively longer than that of the C2-C3 bond (1.36 Å).

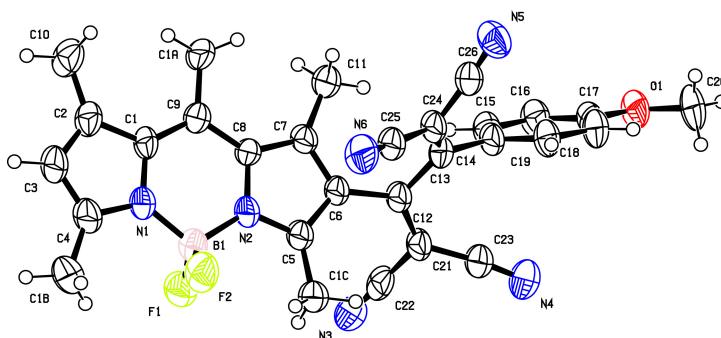
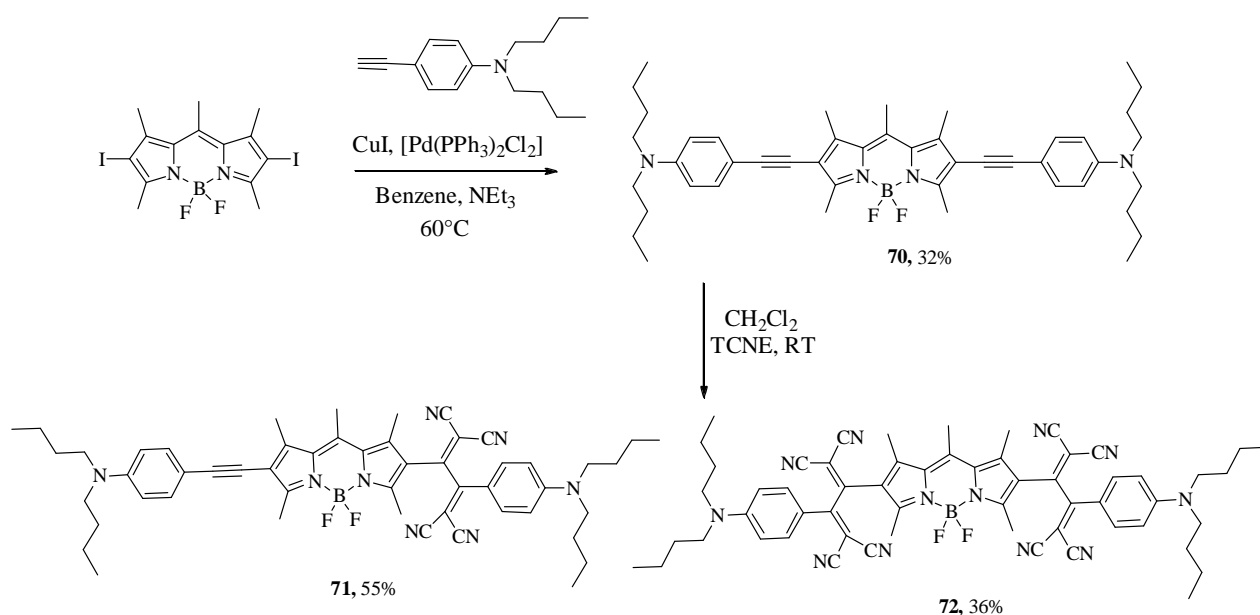


Figure 10. ORTEP view of **68**. Displacement ellipsoids are drawn at 30% probability level.

1.2.2.2 The synthesis of the TCBDs chromophores **71** and **72**.

According to the literature, compound **70** was synthesized by a the cross coupling reaction of the 2,6-diiodo-1,3,5,7-8- pendamethyl-4-bora-3a,4adiaza-s-indacene BODIPY with the *p*-(dibutylamino)phenylacetylene in standard condition.<sup>55</sup> In the second step, compound **70** reacts with TCNE in a proportion of 1:1.3 in the standard reaction conditions. However, the reaction leads to the mono and di-substituted derivatives **71** and **72**, with the yield of 55% and 36%, respectively. The fact indicated that TCNE was totally consumed in the reaction, indicating the dibutylamino moiety of **70** has a better reactivity with TCNE than the anisole of **59**.

Scheme 5. Synthesis of compounds **71** and **72**.

## 1.2.2.3 Optical properties of the TCBDs-BODIPYs

The optical properties of the TCBDs BODIPYs **69**, **71** and **72** were evaluated and the spectroscopic data were collected in Table 3. In solution, the TCBDs show high solubility in common solvents. The UV/Vis absorption spectra of all three molecules display the similar broad structureless band between 450-700nm, with the molar absorption coefficient in the 35000-80000 M<sup>-1</sup>cm<sup>-1</sup> range (Figure 11). In comparison with the parent BODIPY **59**, the lowest energy absorption maximum of **69** shows a bathochromic shift of 25 nm. For **71** and **72**, the formation of mono- and di-TCBDs moieties lead to a bathochromic shifts of 25 and 40 nm, respectively compared with **70**. The broad absorption band can be attributed to the strong ICT transition between the BODIPY core and the TCBDs residue. Interestingly, for **71** at shorter wavelength, two obvious overlapping absorption bands are observed between 260-400 nm, corresponding to the CT between amino group and the adjacent TCBDs; and the  $\pi$ - $\pi^*$  transition of the free alkylaminophenylethylene group, the latter disappeared in the case of

**72.** In more polar solvents, small blue shifts are observed about several nanometers for the TCBDs. However, the fluorescence of the TCBDs dyes **69**, **71**, and **72** is completely quenched, which can be attributed to the strong ICT process induced by the strong electron withdrawing TCBDs moieties.<sup>69</sup>

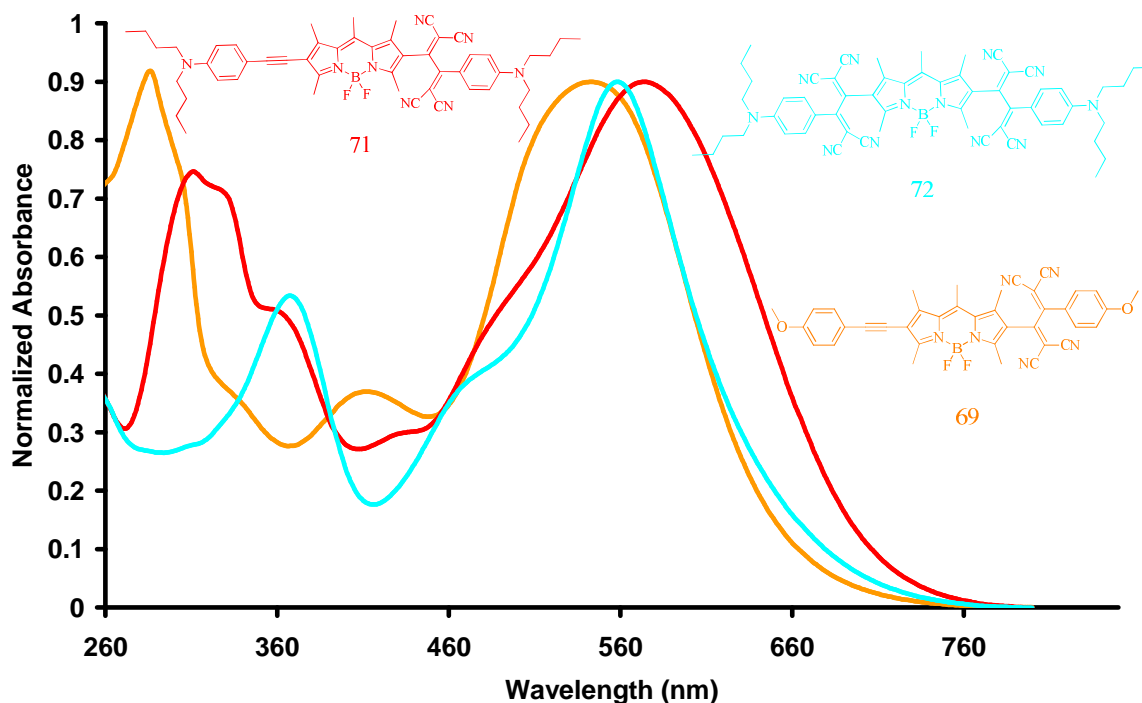


Figure 11. Normalized absorption spectra of **69**, **71** and **72** in Dioxan.

Table 3. Optical properties of the selected compounds.

| Compound                       | $\lambda_{\text{abs}}$ (nm) | $\epsilon$ ( $\text{M}^{-1} \cdot \text{cm}^{-1}$ ) |
|--------------------------------|-----------------------------|---|
| 59 in $\text{CH}_2\text{Cl}_2$ | 568                         | 50000   |
| 69 in Dioxan                   | 543                         | 36000   |
| 69 in EtOH                     | 540                         | 35000   |
| 70 in $\text{CH}_2\text{Cl}_2$ | 599                         | 40000   |
| 71 in Dioxan                   | 574                         | 60000   |
| 71 in EtOH                     | 575                         | 57000   |
| 72 in Dioxan                   | 558                         | 77000   |
| 72 in EtOH                     | 554                         | 74000   |

#### 1.2.2.4 Electrochemical properties of the TCBDs dyes

The electrochemical properties of the TCBDs dyes **69**, **71** and **72** were evaluated by cyclic voltammetry, and data were collected in Table 4.

For **69**, on the oxidation scans, an irreversible wave was observed at +1.27V and can be attributed to the BODIPY moiety undergoing one electron oxidation. Compared with the parent BODIPY **59**, it is clear that the TCBDs residue makes the BODIPY moiety more difficult to be oxidized by 250 meV.

On the reduction scans, interestingly, three successive reversible peaks are observed at -0.25V, -0.73V, and -1.48V, corresponding to the successive one electron reduction of the dicyanovinyl (DCV) groups and the BODIPY moiety, respectively. Due to the electrostatic effect, the second reduction of the DCV moiety is made more difficult by 480 meV. Clearly, the presence of the TCBDs makes also the reduction of the BODIPY moiety more difficult by 380 meV (Figure 12).

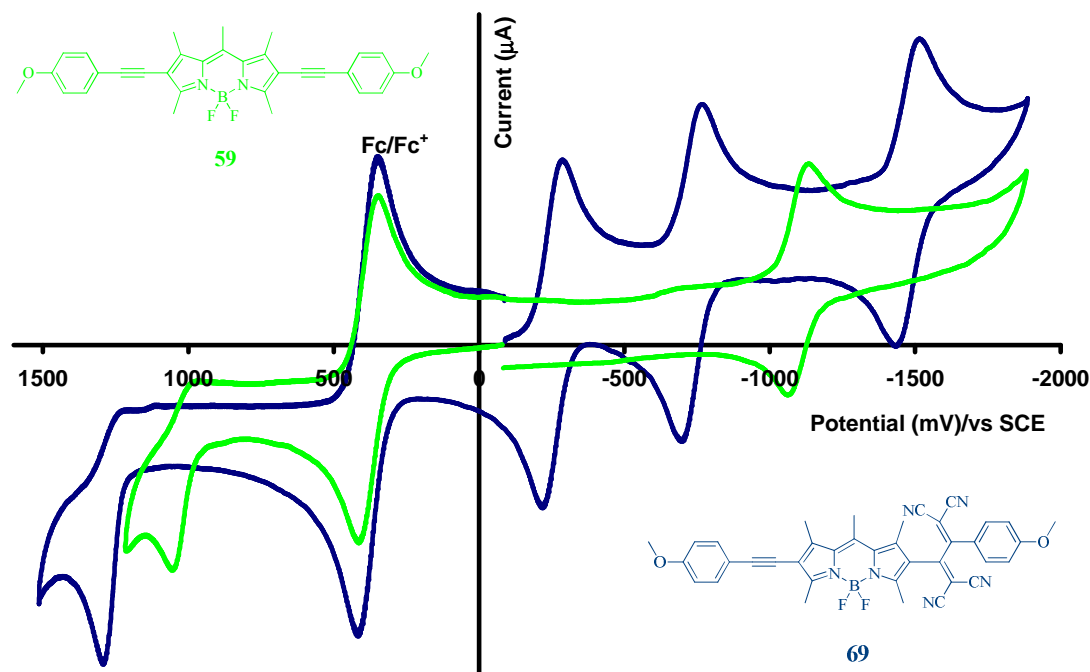


Figure 12. Cyclic voltammetry spectra of compound **69**.

The electrochemical properties of **70** were investigated in order to facilitate the analysis. On the oxidation scans, three irreversible oxidation steps are observed at +0.65V, +0.75V and +1.15V. The first two close but resolvable one electron oxidation waves can be attributed to the successive oxidation of the two dibutylamino moieties, indicating an effective electrostatic effect through the  $\pi$ -conjugated BODIPY core. The third irreversible oxidation wave can be attributed to the formation of the BODIPY radical cation. On the reduction scans, the reversible reduction peak observed at -1.16V corresponding to the formation of the BODIPY  $\pi$ -radical anion (Figure 13).

For **71**, on the oxidation scans, the first irreversible wave at +0.76V can be unambiguously assigned to the one electron oxidation of the free amino group at the other side of the TCBDs residue. It is clearly demonstrated that the TCBDs makes the oxidation of the adjacent amino group more difficult. However, the second reversible but not well resolved oxidation wave at +1.26 V is more difficult to be accurately determined. In comparison with **70**, the peak can be attributed either to the amino group adjacent to the TCBDs, or to the BODIPY oxidation to form the radical  $\pi$ -cation. On the reduction scans, according to **69**, two well resolved reversible reduction steps at -0.41V, -0.80V, and the third

quasi-reversible reduction step at -1.57V can be attributed to the successive one electron reduction of the dicyanovinyl (DCV) groups and the BODIPY moiety, respectively. The reduction of BODIPY core is made more difficult by the TCBDs residue by 410 meV.

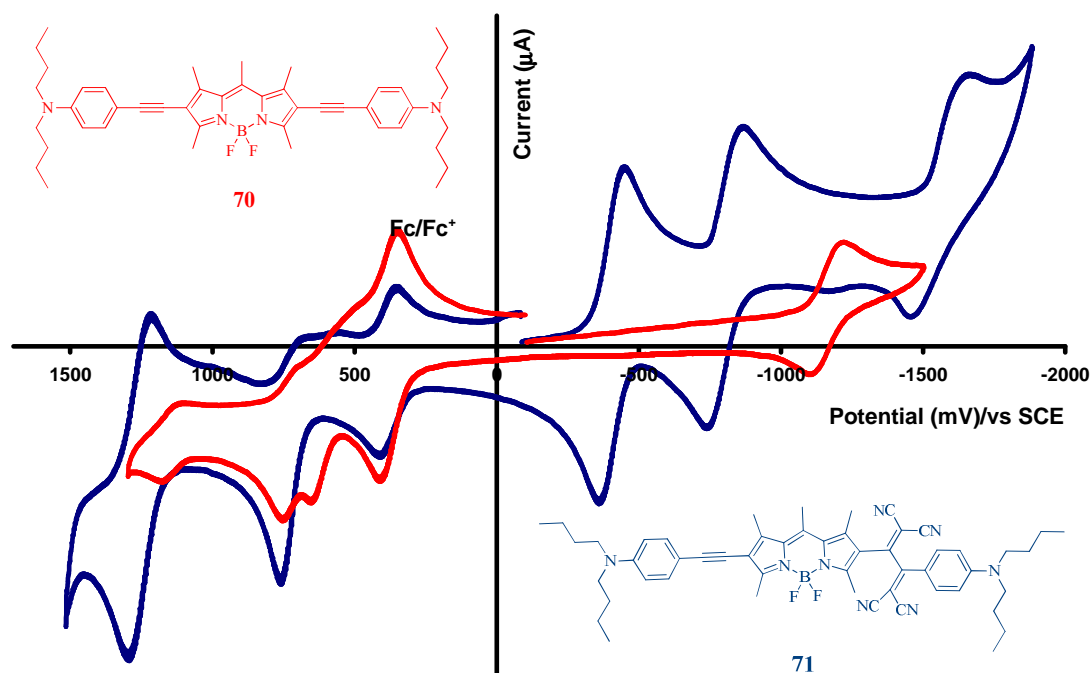


Figure 13. Cyclic voltammetry spectra of TCBDs dyes **70** and **71**.

More interestingly, for **72** (Figure 14), on the oxidation scans single reversible oxidation peak is observed at +1.27V. The fact that current integration of this peak at +1.27 V is double with respect to the first reduction peak at -0.29 V, speak in favor for the oxidation of both amino groups at this potential despite the obvious electrostatic effect. This might be considered as sterically enforced deconjugation induced by the TCBDs residues. Furthermore, in comparison with **71**, the oxidation of the BODIPY core will be shifted to a higher potential by the double TCBDs residues, hence it is more likely outside of the accessible electrochemical window (+1.6V vs SCE). On the reduction scans, the remarkable three reversible and the fourth quasi-reversible reductions steps observed at -0.29V, -0.42V, -0.81V, and -0.95V, respectively, corresponding to the successive one electron reduction of the four DCV moieties. The reduction of BODIPY core is obviously made more difficult by the double TCBDs residues, thus it might be outside of the accessible electrochemical window (-1.6V vs SCE).

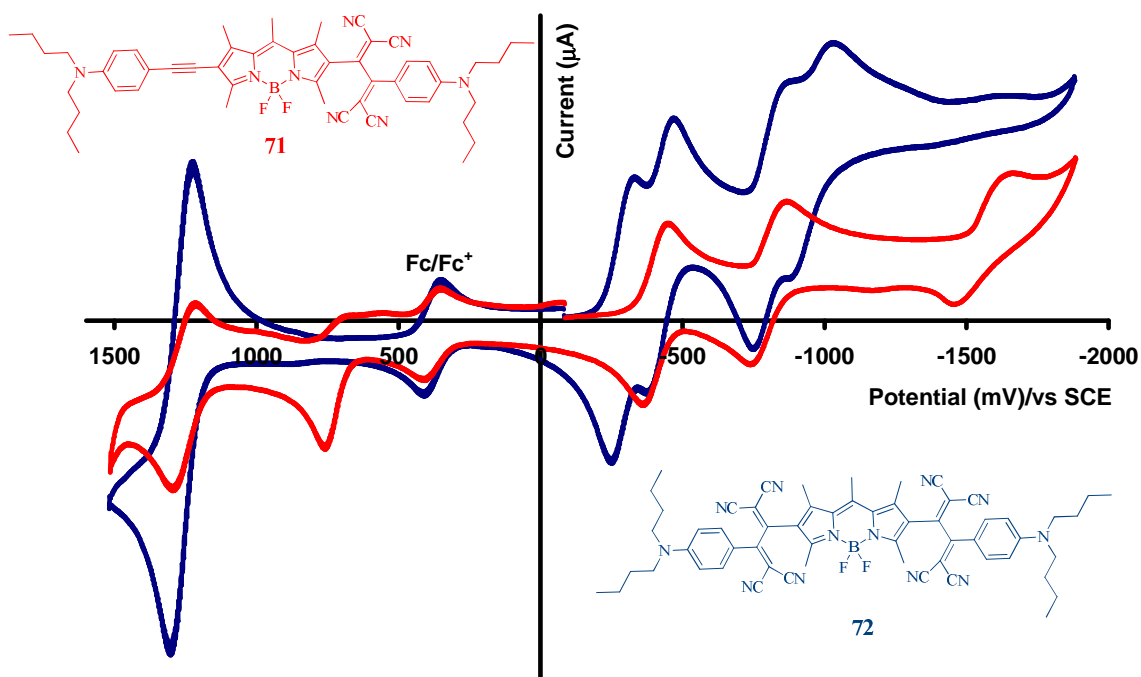


Figure 14. Cyclic voltammety spectra of compounds 71 and 72.

Table 4. Cyclic voltammety of the TCBDs BODIPYs.

| Compounds | $E^{\circ}_{ox}$ [V] ( $\Delta E$ [mV]) | $E^{\circ}_{red}$ [V] ( $\Delta E$ [mV]) |
|-----------|---|--|
| 59        | +1.01 (irrev)                           | -1.10 (96)                               |
| 69        | +1.27 (irrev)                           | -0.25 (64)                               |
|           |   | -0.73 (69)                               |
|           |   | -1.48 (78)                               |
| 70        | +0.65 (irrev)                           | -1.16 (106)                              |
|           | +0.75 (irrev)                           |  |
|           | +1.15 (76)                              |  |
| 71        | +0.76 (irrev)                           | -0.41 (83)                               |
|           | +1.26 (71)                              | -0.80 (quasi)                            |
|           |   | -1.57 (irrev)                            |
| 72        | +1.27 (80)                              | -0.29 (76)                               |
|           |   | -0.42 (85)                               |
|           |   | -0.81 (120)                              |
|           |   | -0.95 (quasi)                            |

Cyclic voltammety carried out in deoxygenated  $\text{CH}_2\text{Cl}_2$  solutions, containing 0.1 M  $\text{TBAPF}_6$ , at a solute concentration range of  $1.5 \times 10^{-3} \text{ M}$ , at  $20^\circ\text{C}$ . Potentials were standardized using added ferrocene (Fc) as internal reference and converted to SCE assuming that  $E_{1/2}(\text{Fc}/\text{Fc}^+) = +0.38 \text{ V}$  ( $\Delta E_p = 70 \text{ mV}$ ) versus SCE. Error in half-wave potentials is  $\pm 15 \text{ mV}$ . When the redox process is irreversible the peak potential ( $E_{ap}$  or  $E_{cp}$ ) is quoted.

### 1.2.3 Synthesis of mono-styryl BODIPY

In order to acquire more information of the BODIPY based push-pull chromophore, mono-styryl TCBDs BODIPY **74** was designed by a retrosynthetic analysis (Figure 15). Compound **74** can be

obtained by a cycloaddition reaction of **73** with TCNE, itself prepared via a Knoevenagel reaction of **58** with a benzaldehyde.<sup>11,70</sup>

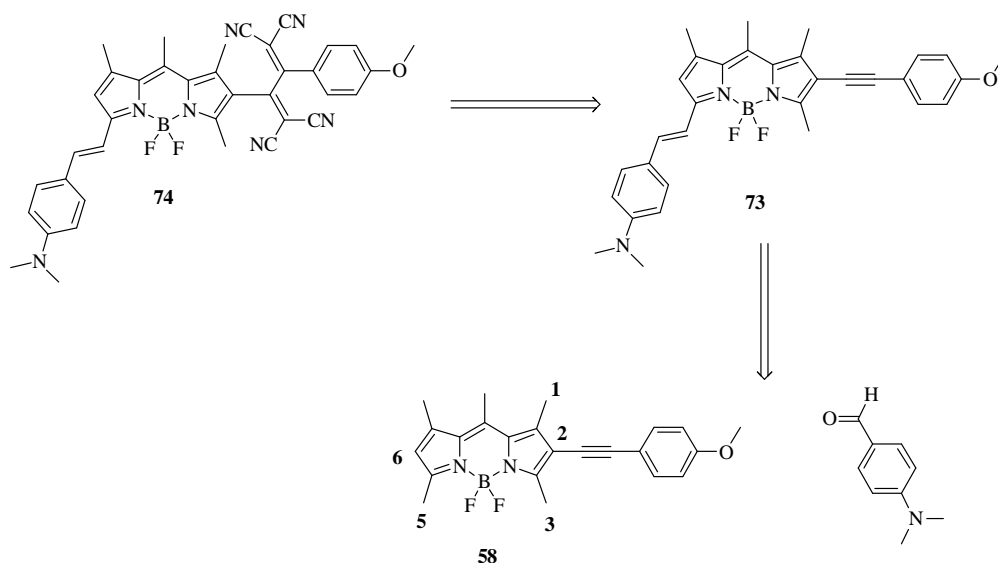
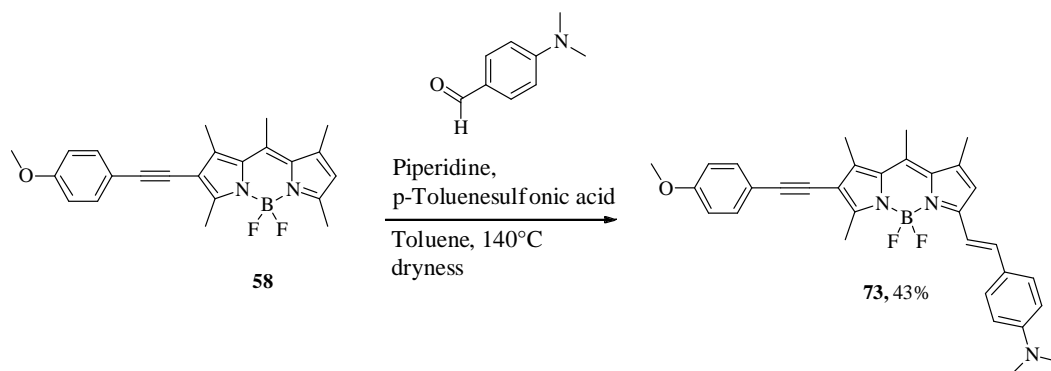


**Figure 15. Retrosynthetic analysis of compound 74.**

The key reaction is the regioselective Knoevenagel reaction carried out with compound **58** and dimethylaminobenzaldehyde under the standard conditions. Interestingly, only one mono-styryl product was isolated as the major substituted derivative. The condensation reaction is occurring principally at the 5-position and gave product **73** with 43% isolated yield (Scheme 6).



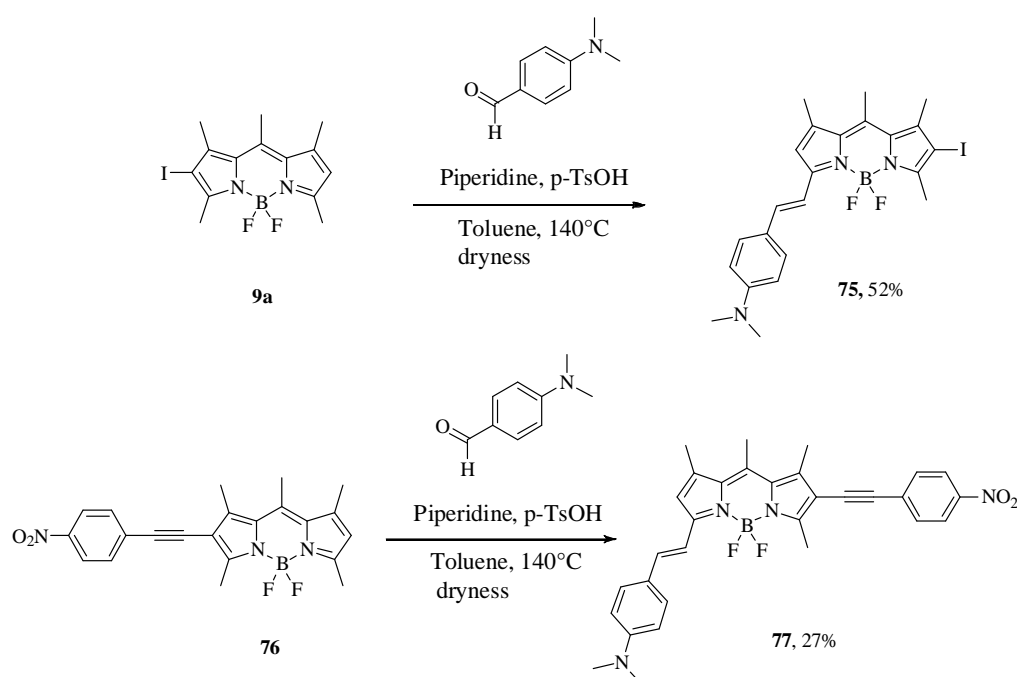
**Scheme 6. Knoevenagel reaction of compound 58.**

Other reactions were carried out with two more asymmetric BODIPY derivatives **9a**, **76**, in order to confirm such selectivity for the mono-styryl condensation (Scheme 7).

For **9a**, the iodine atom at the 2 position is considered as both electron donor (by conjugation) and electron acceptor (by induction). In this case, the condensation reaction gives principally the 5-mono-styryl derivative **75** in 52%, indicating a good selectivity and reactivity.

For **81**, the BODIPY core is conjugated with ethynyl-nitrobenzene, an electron withdrawing group. Once again, only the 5-mono-styryl compound **77** was obtained in a lower yield, due to the decrease of nucleophilicity of the 5-methyl group induced by the conjugated nitro group. It's worthnoting that when an excess amount of dimethylaminobenzaldehyde was used with longer reaction time, the green colored di-styryl compound can be obtained in trace amount after a long purification procedure. However, like all the large aromatic planar chromophore, a poor solubility of the di-styryl compound in common solvents makes identification rather difficult.

Therefore, we had successfully synthesized the mono-styryl BODIPY dyes **73**, **75** and **77** from the asymmetric BODIPY derivatives in acceptable yields. These novel compounds were fully characterized and their optical properties investigated in the follow section.



Scheme 7. Synthesis of monostyryl BODIPY dyes **75** and **77**.

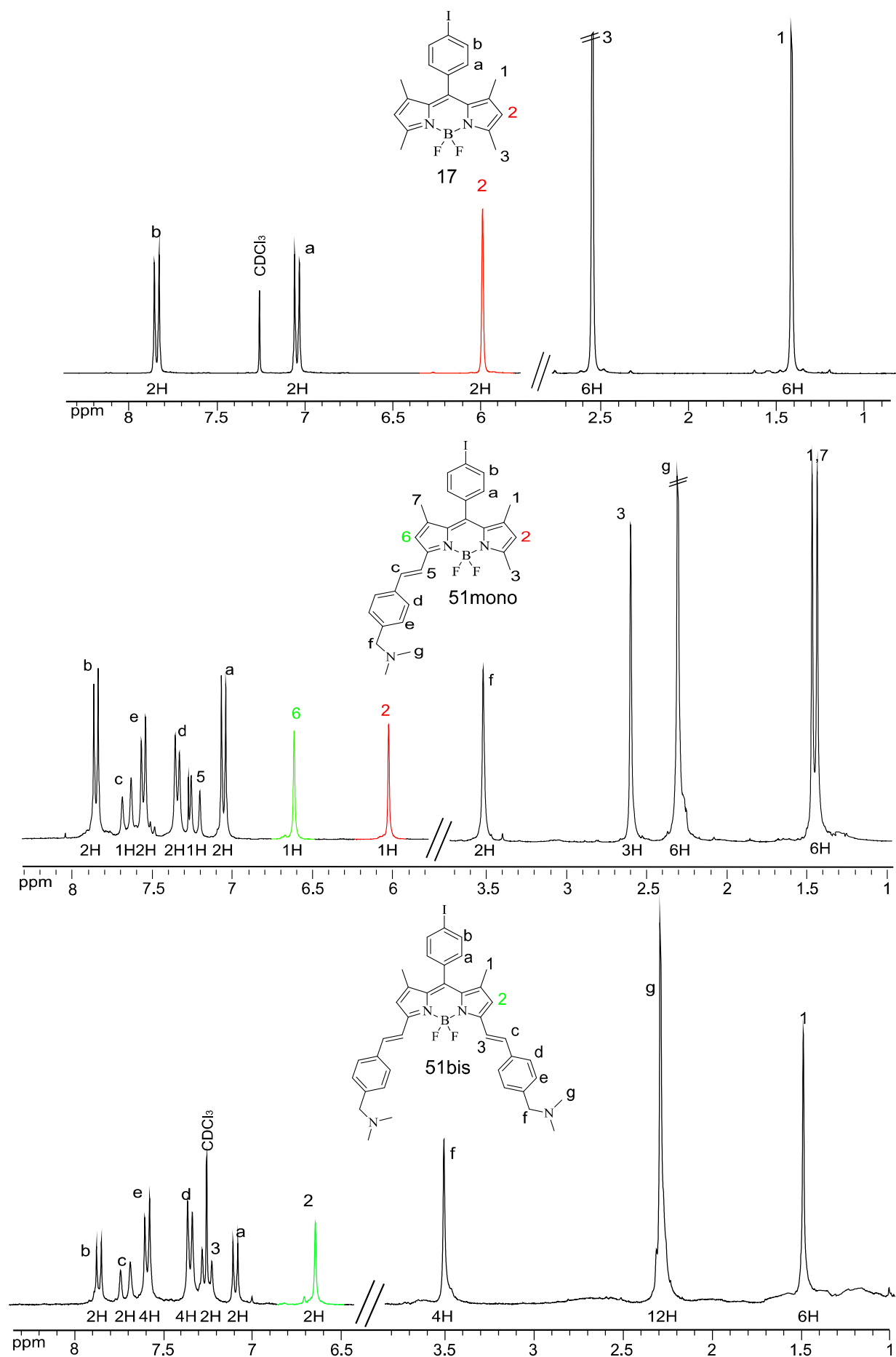
### 1.2.3.1 Identification of the mono-styryl BODIPYs

The 5-monostyryl BODIPY derivatives **73**, **75**, and **77** were fully characterized by  $^1\text{H}$  NMR,  $^{13}\text{C}$  NMR, mass spectroscopy analysis and element analysis. The  $^1\text{H}$  NMR analyses was used for the identification of the structures of the 5-monostyryl derivatives. In order to facilitate the interpretation, the spectra of their analogues **17**, **51mono**, and **51bis** were compared (Figures 16 and 17).

For **17**, the characteristic chemical shift of the identical  $\beta$ -pyrrolic protons (in red) is observed at 6.0 ppm. While for the mono-styryl **51mono**, one of the  $\beta$ -pyrrolic protons is shifted to 6.6 ppm, while the other remains at 6 ppm.

For di-styryl BODIPY **51bis**, both  $\beta$ -pyrrolic protons (in green) are both shifted at 6.6 ppm. Therefore, the spectra strongly indicate that the pyrrolic proton will be shifted downfield from 6.0 to 6.6 ppm during formation of the styryl group located at the same side.

For **58** and **73**, the chemical shift of the pyrrolic proton is shifted from 6.0 ppm for **58** (in red) to 6.6 ppm for **73** (in green), confirming that the monostyryl formation is localized at the 3-position. In addition, in all styryl-BODIPYs signals, the observed 16 Hz proton-proton coupling constant is in keeping with an *E* conformation of the double bonds.<sup>11</sup> It is worth noting that the chemical shifts of these compounds are changed in solvents with different dipole moments, due to the pronounced ICT process. The structures of **75** and **77** were identified as well by the same principles.

Figure 16.  $^1\text{H}$  NMR spectra of compounds 17, 51mono and 51bis in  $\text{CDCl}_3$ .

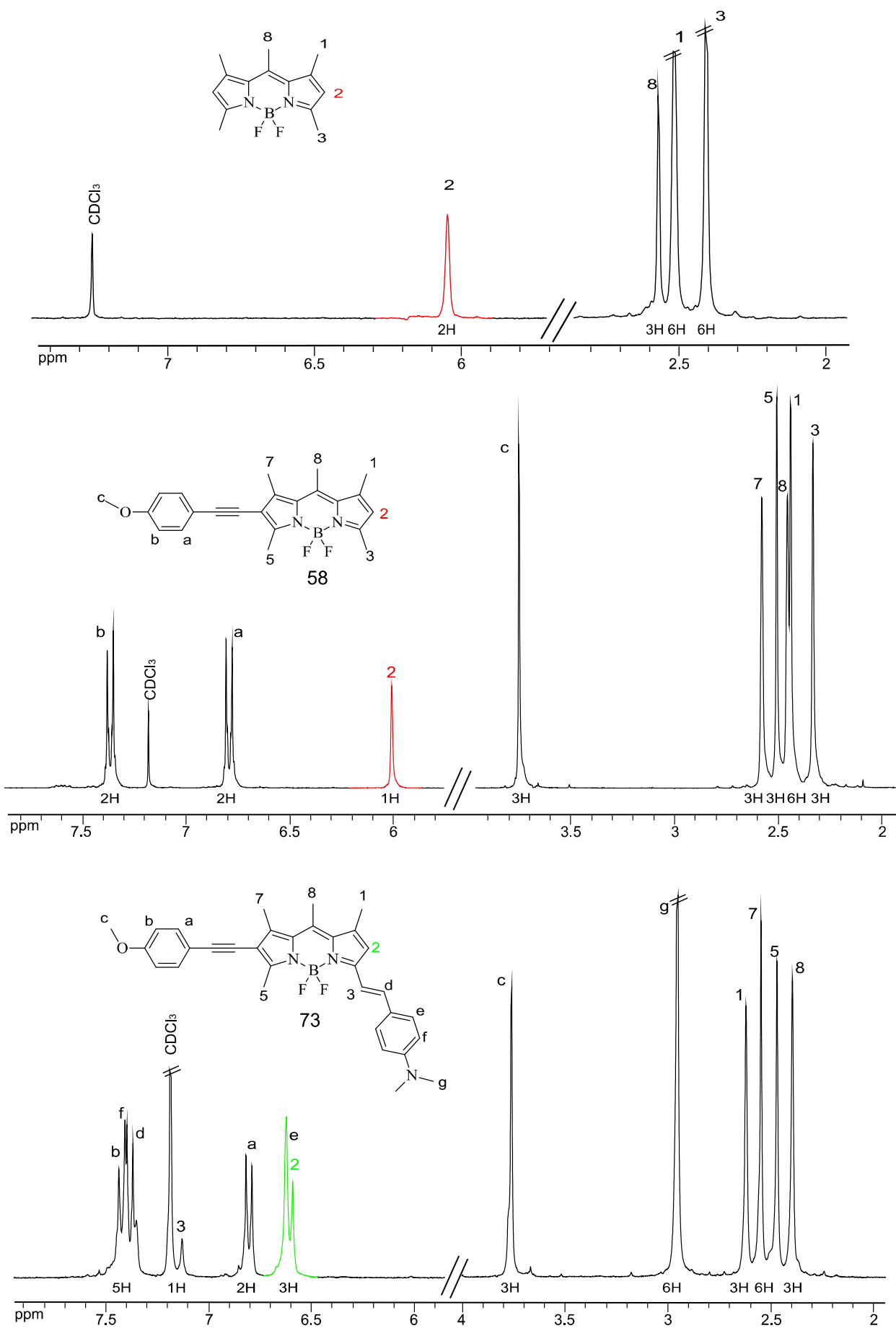
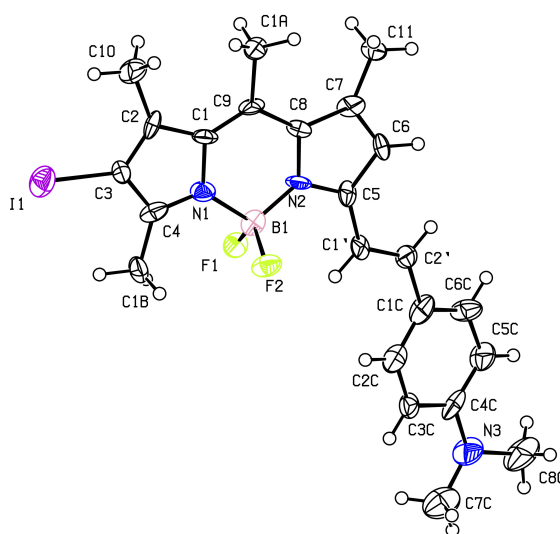


Figure 17.  $^1\text{H}$  NMR spectra of compounds pendamethylBODIPY, 58 and 73 in  $\text{CDCl}_3$ .

### 1.2.3.2 X-ray analysis of compound **75**.

In order to confirm the regioselectivity of the substitution reaction, single crystals of **75** were grown by slow diffusion of saturated Et<sub>2</sub>O vapor into a CH<sub>2</sub>Cl<sub>2</sub> solution. The X-ray analysis confirms the expected structure (Figure 18). Despite the presence of iodine atom at 2-position, the molecular conformation of the monostyryle BODIPY **75** is in good agreement with those monostyryl BODIPYs described in literature.<sup>11,71</sup> The BODIPY core of **75** remains planar, with the double bond slightly twists with the BODIPY plan with torsion angles (C6-C5-C1'-C2') of -8.67°; and the aniline ring slightly twists with the double bond (C1'-C2'-C1C-C6C) of -8.06°. The distance between atoms C1' and C2' is 1.342Å, between C3 and I1 is 2.060Å; between C4C and N3 is 1.386Å, respectively. These values are in keeping with C=C, C-I, and C-N bonds, respectively.<sup>70-73</sup>



**Figure 18.** ORTEP view of compound **75**. Displacement ellipsoids are drawn at the 30% probability level.

### 1.2.3.3 Optical properties of the asymmetric mono-styryls

The optical properties of **73** and **75** were evaluated in different solvents and the spectroscopic data were collected in Table 5. In solution, The UV-Vis absorption spectra of both styryl compounds are similar to those of mono-styryl BODIPYs described in literature (Figure 19 and 21).<sup>70,74</sup> Strong absorption band between 500-700 nm is observed with a absorption coefficient in the 70000-110000 M<sup>-1</sup>cm<sup>-1</sup> range, corresponding to S<sub>0</sub> → S<sub>1</sub> transition of the BODIPY core.<sup>71</sup> For **73** and **75**, the absorption maximum is centered at 617 ± 3 and 607 ± 5 nm, respectively. Weak solvent dependence is observed for both molecules in absorption. On the contrary, the fluorescence emission spectra of the both compounds are strongly dependent with the dipole moments of the solvent (Figure 20 and 22). For **73**, the emission maximum shifts from 660 nm in dioxan to 721 nm in acetonitrile. For **75**, the emission maximum shifts from 658 nm in dioxan to 705 nm in acetonitrile. The bathochromic shifts with concomitant decrease of fluorescence quantum yield (ϕ) and lifetime (τ) are observed for

the both molecules in more polar solvent. For **73**, the quantum yield ( $\phi$ ) and lifetime ( $\tau$ ) decrease from dioxan ( $\phi = 0.66$ ,  $\tau = 2.6$  ns) to  $\text{CH}_3\text{CN}$  ( $\phi = 0.09$ ,  $\tau = 1.1$  ns), accompanying with the increase of non-radiative decay  $k_{\text{nr}}$  (from 1.3 to  $8.3 \cdot 10^8 \text{ s}^{-1}$ ) and the decrease of radiative decay  $k_{\text{r}}$  (from 25.4 to  $8.2 \cdot 10^7 \text{ s}^{-1}$ ). The same phenomenon is also observed for **75**, which can be attributed to the acceleration of internal conversion as the energy gap between ground state and excited state decreases.<sup>74</sup> The protonation of **73** and **75** was used to “switch off” the ICT transition between the dimethylanilino group and the BODIPY moiety, by adding vapor of HCl into the solution of the mono-styryl derivatives. In absorption, the protonation results on a hypsochromic shift about 40 nm for **73** and **75**, which is independent to the solvent polarity. In emission, the protonation also results in a large hypochromic shift. The emission maximum is centered at  $618 \pm 7$  nm for **73** and  $580 \pm 7$  nm for **75**. For both molecules, small hypsochromic shift is observed in more polar solvents. However, instead of resulting in a higher fluorescence quantum yield by protonation as described in literatures,<sup>69-71,74</sup> rather low quantum yields ( $\phi$ ) are observed for **73** ( $\phi_{\text{f}}$  decrease from 0.12 to 0.02) and for **75** ( $\phi_{\text{f}}$  decrease from 0.20 decrease to 0.13), due to a faster non-radiative decay  $k_{\text{nr}}$ . The decrease of the lifetime in more polar solvent is also observed for both molecules. The solvent dependency of the protonated compounds **73** and **75** can be attributed to the ICT character between the BODIPY moiety and the substituent in 2-position. It is considered that after protonation, the amino group becomes the acceptor group while ethynylanisole moiety of **73** and the iodine atom of **75** act as donor group. The electronic signature moves from a push $\rightarrow\pi\leftarrow$ push situation to a pull $\leftarrow\pi\leftarrow$ push case.<sup>11</sup> But the CT character in both cases is rather modest, probably due to the weak electronic acceptor nature of the ammonium. In addition, in absorption spectra of the protonated **75**, an intramolecular CT transition can be assigned to the pronounced shoulder seen at 530 nm, while the lowest energy absorption band centered around 560 nm can be attributed to the BODIPY's  $S_0 \rightarrow S_1$  ( $\pi \rightarrow \pi^*$ ) transition (Figure 21).

**Table 5. Optical properties of dyes 73 and 75 under various solvent conditions.**

| Compound  | $\lambda_{\text{abs}}$ (nm) | $\epsilon$ ( $\text{M}^{-1}\cdot\text{cm}^{-1}$ ) | $\lambda_{\text{em}}$ (nm) | $\phi$ (%) | $\tau$ (ns) | $k_{\text{r}}$ ( $10^7\text{s}^{-1}$ ) | $k_{\text{nr}}$ ( $10^7\text{s}^{-1}$ ) | $\Delta_{\text{s}}$ ( $\text{cm}^{-1}$ ) |
|---|-----------------------------|---|----------------------------|------------|-------------|--|---|--|
| <b>73</b> (Dioxan)                                  | 620                         | 92400   | 660                        | 66         | 2.6         | 25.4                                   | 13.1                                    | 9775                                     |
| <b>73</b> (Dioxan + $\text{H}^+$ )                  | 582                         | 70100   | 628                        | 12         | 2.1         | 5.7                                    | 41.9                                    | 12586                                    |
| <b>73</b> (EtOH)                                    | 617                         | 88200   | 691                        | 21         | 2.1         | 10.0                                   | 37.6                                    | 17357                                    |
| <b>73</b> (EtOH + $\text{H}^+$ )                    | 580                         | 76200   | 625                        | 3          | 2.1         | 1.4                                    | 46.2                                    | 12414                                    |
| <b>73</b> ( $\text{CH}_3\text{CN}$ )                | 613                         | 71600   | 721                        | 9          | 1.1         | 8.2                                    | 82.7                                    | 24436                                    |
| <b>73</b> ( $\text{CH}_3\text{CN}$ + $\text{H}^+$ ) | 576                         | 73700   | 612                        | 2          | -           | -                                      | -                                       | 10212                                    |
| <b>75</b> (Dioxan)                                  | 606                         | 80300   | 658                        | 66         | 3.3         | 20.0                                   | 10.3                                    | 13041                                    |
| <b>75</b> (Dioxan + $\text{H}^+$ )                  | 566                         | 106000  | 587                        | 20         | 2.5         | 8.0                                    | 32.0                                    | 6321                                     |
| <b>75</b> (EtOH)                                    | 602                         | 94000   | 699                        | 14         | 2.1         | 6.7                                    | 41.0                                    | 23051                                    |
| <b>75</b> (EtOH + $\text{H}^+$ )                    | 563                         | 114700  | 574                        | 13         | 1.3         | 10.0                                   | 66.9                                    | 3404                                     |
| <b>75</b> ( $\text{CH}_3\text{CN}$ )                | 600                         | 92300   | 705                        | 9          | 2.5         | 3.6                                    | 36.4                                    | 24823                                    |
| <b>75</b> ( $\text{CH}_3\text{CN}$ + $\text{H}^+$ ) | 561                         | 94700   | 573                        | 17         | 1.2         | 14.2                                   | 69.2                                    | 3733                                     |

a) Quantum yield determined in dilute solution ( $1 \times 10^{-6} \text{M}$ ) using rhodamine 6G ( $\phi_F = 0.78$  in water,  $\lambda_{\text{exc}} = 488 \text{ nm}$ ), or cresyl violet as reference ( $\phi_F = 0.51$  in EtOH,  $\lambda_{\text{exc}} = 578 \text{ nm}$ ).<sup>60</sup> b) All  $\phi_F$  are corrected for changes in refractive index.  $K_r$  and  $k_{nr}$  were calculated using the following equations:  $k_r = \phi_F/\tau$ ,  $k_{nr} = (1-\phi_F)/\tau$ . c).  $\Delta s$  = Stokes shift.

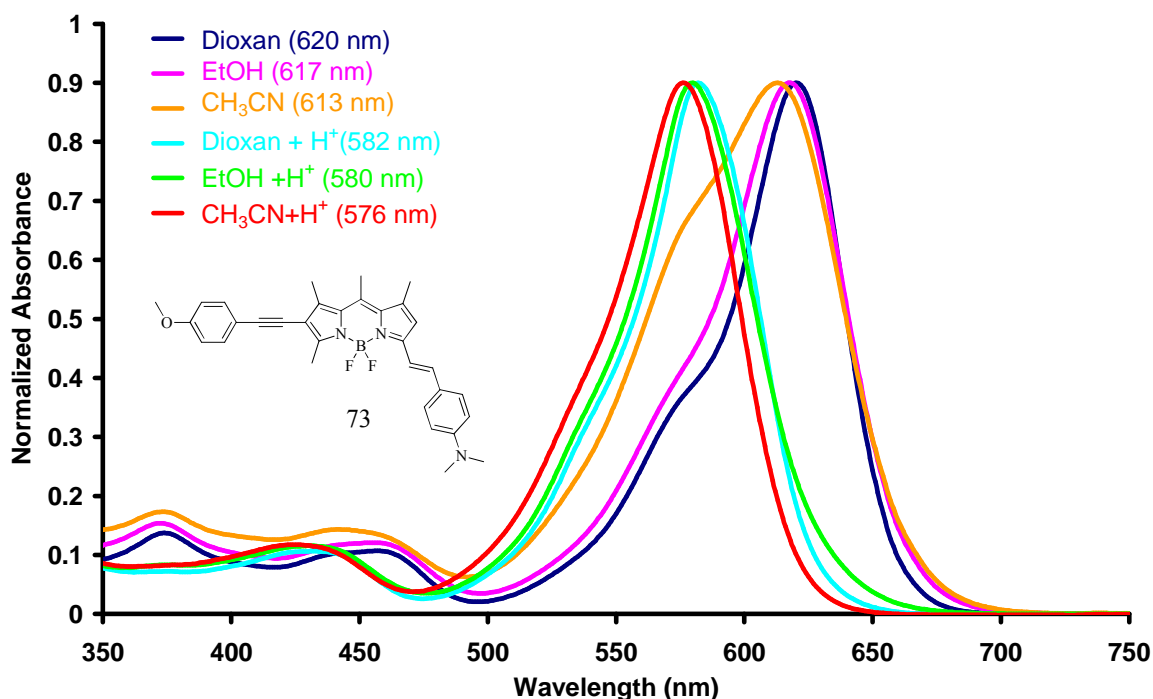


Figure 19. Normalized absorption spectra of 73 and the protonated 73 in Dioxan, EtOH and CH<sub>3</sub>CN, respectively.

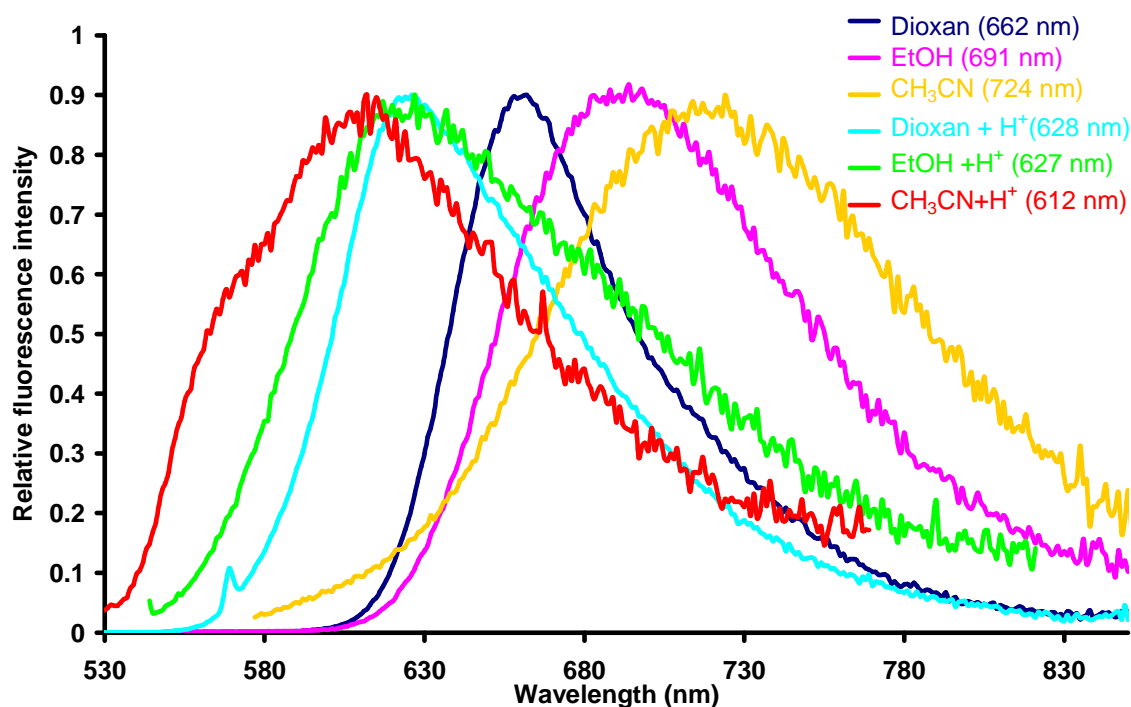


Figure 20. Normalized emission spectra of 73 and the protonated 73 in Dioxan, EtOH and CH<sub>3</sub>CN, respectively.

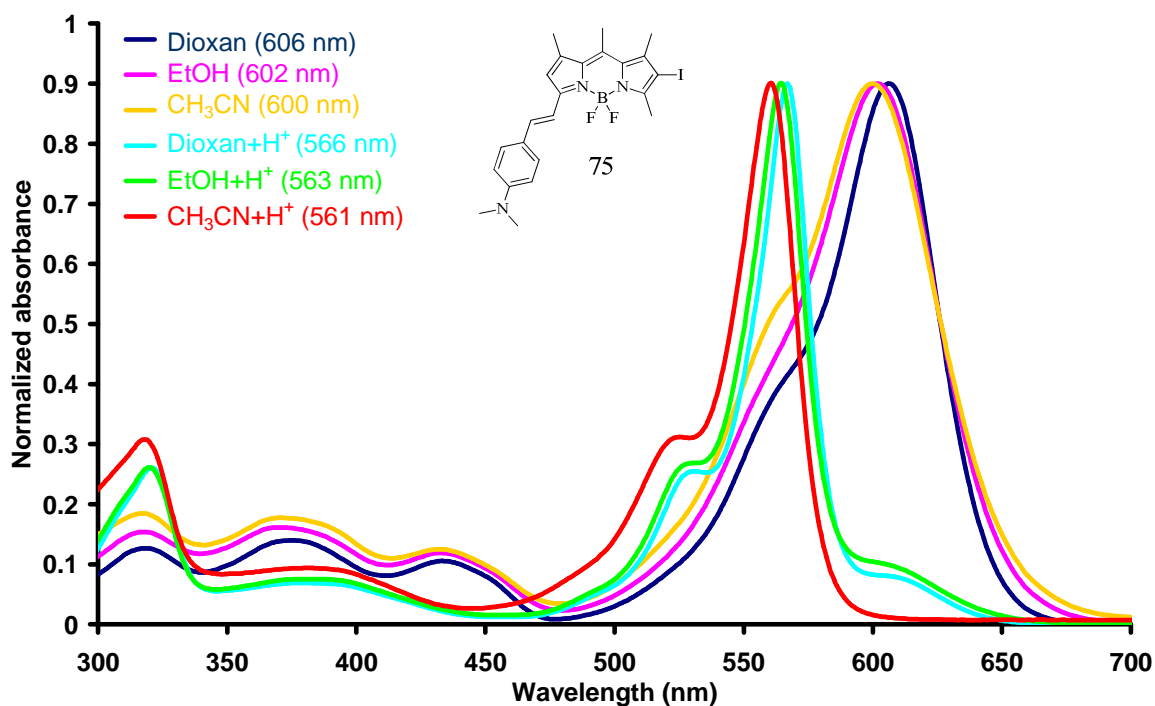


Figure 21. Normalized absorption spectra of **75** and the protonated **75** in Dioxan, EtOH and CH<sub>3</sub>CN, respectively.

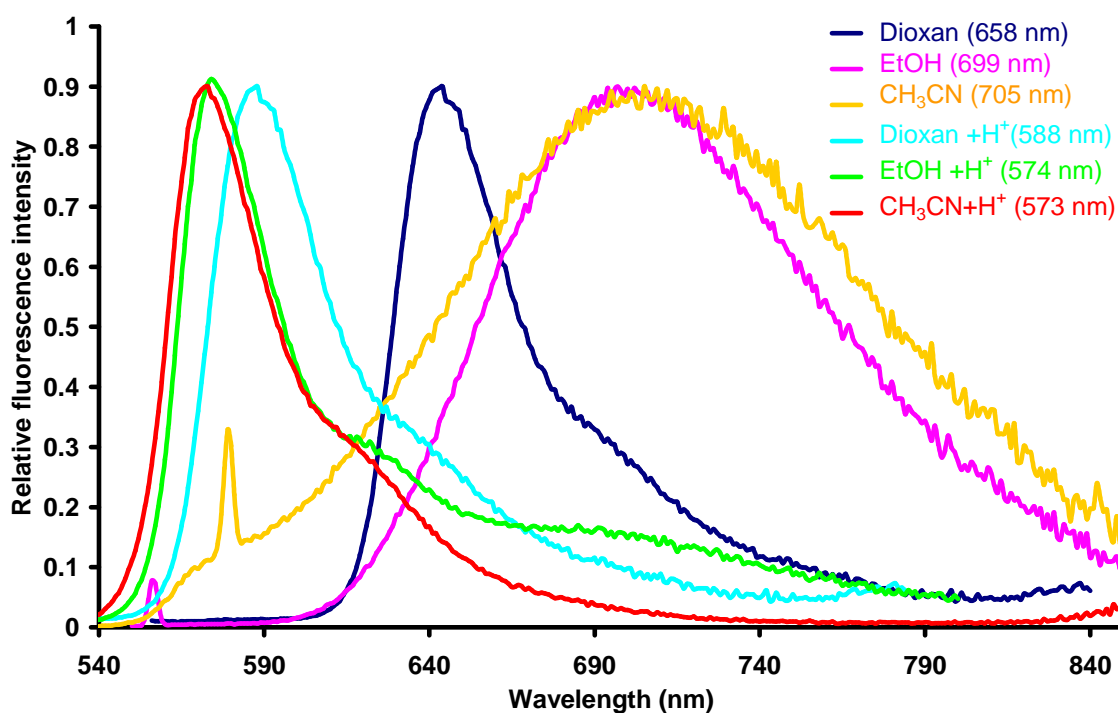
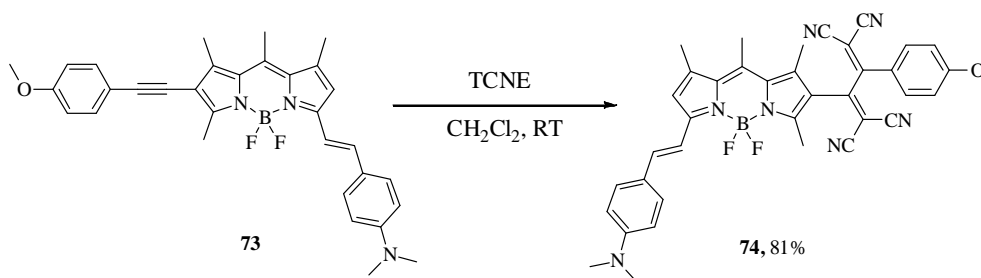


Figure 22. Normalized emission spectra of **75** and the protonated **75** in Dioxan, EtOH and CH<sub>3</sub>CN, respectively.

#### 1.2.4 Synthesis of TCBDs BODIPY **74**.

The [2+2] cycloaddition reaction of **73** with TCNE was carried out in standard condition. The purple colored amorphous product **74** was easily obtained by a flash chromatography, with yields between

84 and 94%. The TCBDs **74** was fully characterized, including optical and electrochemical properties, as well as nonlinear optical properties which will be discussed in the following section.



**Scheme 8. Synthesis of TCBDs BODIPY 74.**

#### 1.2.4.1 Optical properties of compound **74**.

The optical properties of **74** were evaluated in different solvents and the spectroscopic data were collected in Table 6. In solution, similar to the TCBDs analogues, the absorption spectra of **74** displays large broad CT character bands between 500-800 nm (Figure 23). The absorption maximum is centered at 600 nm with an extinction coefficient about  $45000 \text{ M}^{-1}\text{cm}^{-1}$ . Weak solvatochromism is observed in different polar solvent. Upon protonation, a hypsochromic shifts about 20 nm is observed in both solvents. However, the fluorescence of the chromophore is completely quenched as the other TCBDs BODIPYs, probably due to the photoinduced electron transfer (PET)<sup>75-77</sup> process induced by the strong dimethylamino group and the strong electron withdrawing group TCBDs.

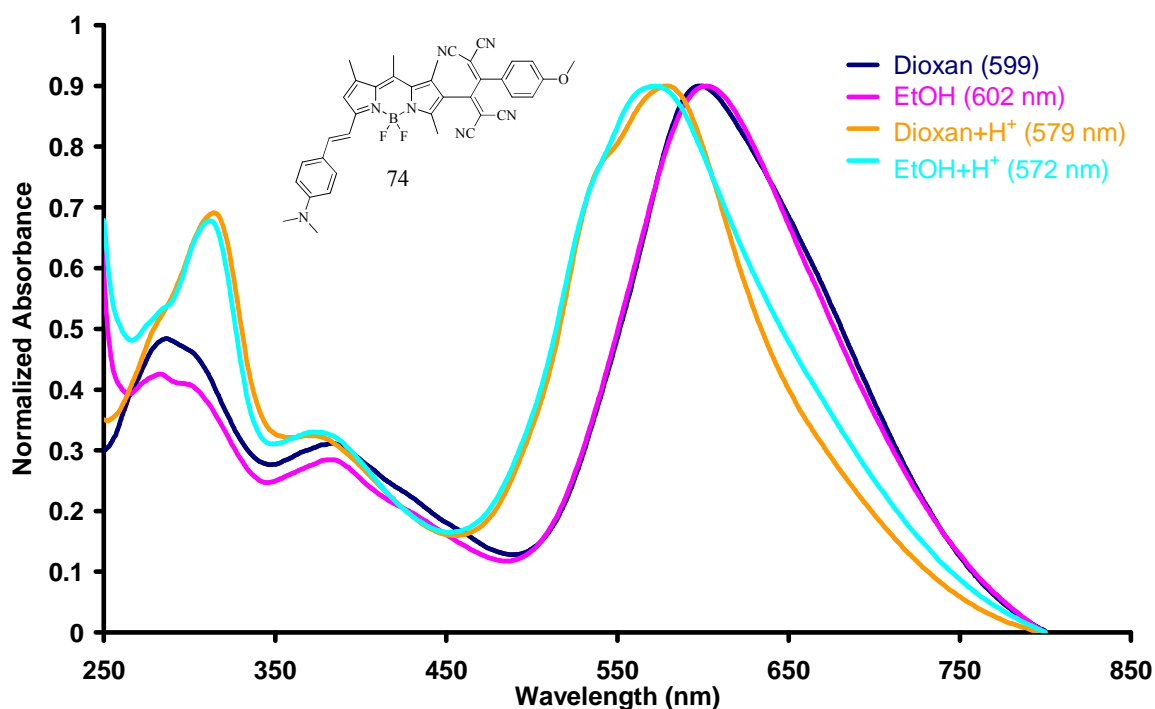


**Figure 23. Normalized absorption spectra of **74** and the protonated **74** in dioxan and EtOH.**

Table 6. Optical properties of compound **74**.

| Compound                           | $\lambda_{\text{abs}}$ (nm) | $\epsilon$ ( $\text{M}^{-1}\cdot\text{cm}^{-1}$ ) |
|------------------------------------|-----------------------------|---|
| <b>74</b> (Dioxan)                 | 599                         | 45500   |
| <b>74</b> (Dioxan + $\text{H}^+$ ) | 579                         | 39300   |
| <b>74</b> (EtOH)                   | 602                         | 44200   |
| <b>74</b> (EtOH + $\text{H}^+$ )   | 572                         | 36500   |

#### 1.2.4.2 Electrochemical properties of compounds **73** and **74**.

The electrochemical properties of **73** and **74** were investigated in deoxygenated  $\text{CH}_2\text{Cl}_2$  solution at rt. The data were collected in Table 7.

For **73**, on the oxidation scans, two irreversible oxidation steps at +0.56 V and +0.86V were observed, corresponding to successive one electron oxidation of dimethylamino group and BODIPY core, respectively. On the reduction scans, according to previous results, the reversible reduction step at -1.15 V can be attributed to the one electron reduction of the BODIPY core. For **74**, interestingly, the oxidation scans show two reversible oxidation steps at +0.72 and +1.04V corresponding to the oxidation of the aniline group and BODIPY moiety, respectively. The presence of the TCBDs group makes the oxidation of the amino group and BODIPY core more difficult by 160 meV and 180 meV, respectively. On the reduction scans, three well-resolved reversible reduction steps were observed, corresponding to two successive one electron reduction of the two DCV moieties at -0.32V and -0.78V; and the third reversible one electron reduction of the BODIPY moiety at -1.50V. The reduction of the BODIPY core is more difficult by 350 meV due to the TCBDs residue.

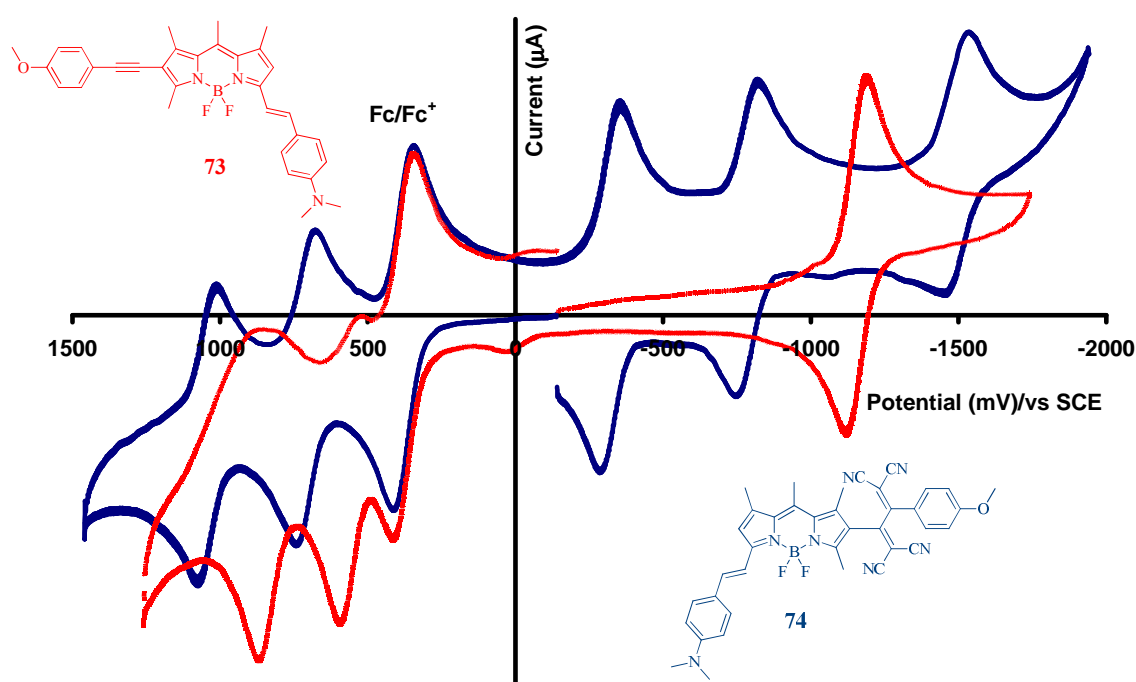
Figure 24. Cyclic voltammetry of compounds **73** and **74**.

Table 7. Cyclic voltammetry of the TCBDs BODIPYs.

| Compound | $E^{\circ}_{\text{ox}}$ [V]( $\Delta E^{\circ}$ [mV]) | $E^{\circ}_{\text{red}}$ [V]( $\Delta E^{\circ}$ [mV]) |
|----------|---|--|
| 73       | +0.56 (irrev)   | -1.15 (102)  |
|          | +0.86 (irrev)   |  |
| 74       | +0.72 (93)  | -0.32 (98)   |
|          | +1.04 (98)  | -0.78 (106)  |
|          |   | -1.50 (112)  |

Cyclic voltammetry carried out in deoxygenated  $\text{CH}_2\text{Cl}_2$  solutions, containing 0.1 M TBAPF<sub>6</sub>, at a solute concentration range of  $1.5 \times 10^{-3}$  M, at 20°C. Potentials were standardized using added ferrocene (Fc) as internal reference and converted to SCE assuming that  $E_{1/2}(\text{Fc}/\text{Fc}^+) = +0.38\text{V}$  ( $\Delta E_p = 70$  mV) versus SCE. Error in half-wave potentials is  $\pm 15$  mV. When the redox process is irreversible the peak potential ( $E_{\text{ap}}$  or  $E_{\text{cp}}$ ) is quoted.

### 1.2.5 The hyperpolarizabilities of the push-pull chromophores

The hyperpolarizability ( $\beta$ ) of the push-pull chromophores were investigated by using the Electric Field Induced Second-Harmonic Generation (EFISHG) technique and the results were gathered in Figure 25 and Table 8. These measurements were performed in collaboration with Prof. Alberto BARSELLA at *Department of ultrafast Optics and Nanophotonics (DON)* of IPCMS in Strasbourg. The EFISHG is a well established technique for the determination of molecular second order NLO response. In EFISHG, a fundamental laser beam is focused in a solution of the chromophore being analyzed, to which a strong static electric field is applied. The interaction of the field with the permanent dipoles moment of the molecules causes a bias in the average orientation of the molecules. The partial removal of the isotropy allows to second-harmonic generation to occur. From the intensity of the detected second-harmonic light the  $\mu\beta$  is determined. It represents the scalar product of the permanent dipole moment and the vectorial part of the hyperpolarizability.<sup>15,78,79</sup> The  $\beta$  can be extracted by a separate measurement of the permanent dipole moment.<sup>19,80</sup> The  $\mu\beta(2\omega)$  values and the static  $\mu\beta(0)$  values were calculated from the two-level model, the two-level model is used as an approximation to calculate the dispersion enhancement factor.<sup>19,81</sup> Since the  $\mu\beta(2\omega)$  values are significantly affected by dispersion enhancement, the experiments were carried out at 1.9  $\mu\text{m}$  in chloroform.

In EFISHG, a solvent concentration of  $10^{-3}\text{M}^{-1}$  minimum is need for the molecule being measured. As mentioned above, the poor solubility of the compound **62** in  $\text{CHCl}_3$  makes the measurement difficult to be realized. Nevertheless, the dye **67** is found highly soluble for the experiment, however the  $\mu\beta(0)$  value is rather weak.<sup>14</sup> Surprisingly, the dye **68** with strong electron withdrawing group TCBDs shows almost no NLO response. For **69**, the  $\mu\beta(0)$  value is comparable to that of **67**. Interestingly, conjugated with stronger electron donor group, the mono- and di- TCBDs **71** and **72** show high NLO response with the  $\mu\beta(0)$  of 870 and  $1233 \times 10^{-48}$  esu, respectively. The monostyryl **74** has the highest

$\mu\beta(0)$  value among the molecules of  $2237 \times 10^{-48}$  esu, which is almost three times as that of **71**. Upon the protonation of **74** with HCl vapor, the “switch off” of the donor character leads to dramatically reduce of NLO response to  $390 \times 10^{-48}$  esu. This response is totally reversible; the  $\mu\beta(0)$  value can be then restored by adding a drop of triethylamine into the protonated solution.

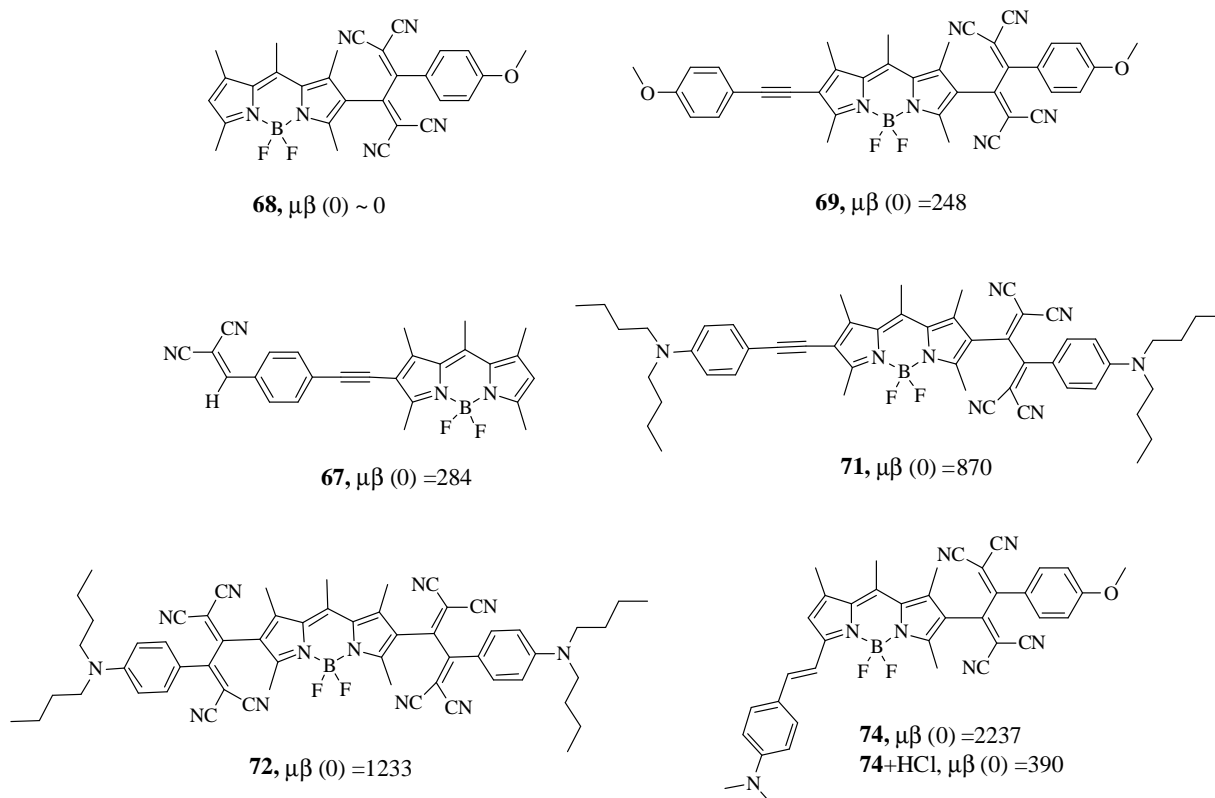
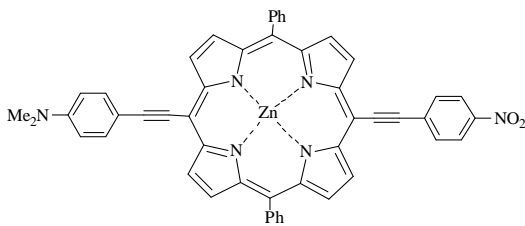
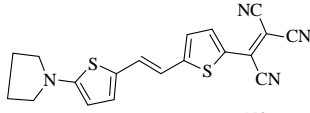
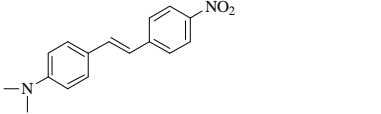
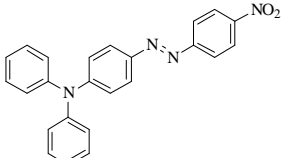
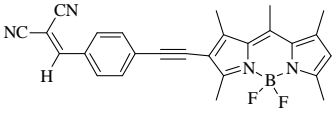
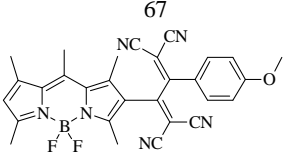
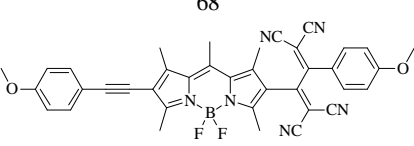
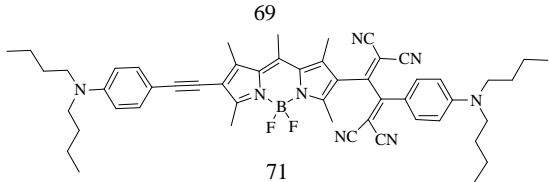
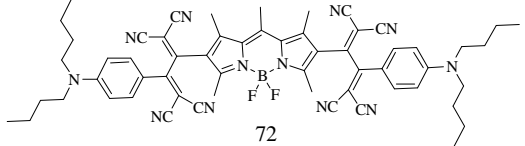
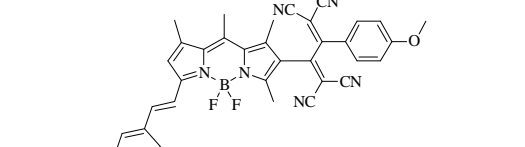


Figure 25. Hyperpolarizability of the push-pull chromophores in  $\text{CHCl}_3$  solution.

Table 8. EFISHG data of the BODIPY dyes and selected benchmark organic chromophores.

| compound  | $\lambda_{\text{max}}/\text{nm}$ | $\mu\beta(0)$ ( $10^{-48}$ esu) | $\mu\beta(2\omega)$ ( $10^{-48}$ esu) |
|---|----------------------------------|---------------------------------|---------------------------------------|
|          | 475                              | 9840                            | -                                     |
|          | 718                              | 2564                            | -                                     |
|          | 430                              | 363                             | -                                     |
|          | 486                              | 319                             | -                                     |
|         | 535                              | 284                             | 450                                   |
| 67<br> | 500                              | -                               | 90                                    |
| 68<br> | 543                              | 248                             | 400                                   |
| 69<br> | 574                              | 870                             | 1500                                  |
| 71<br> | 558                              | 1233                            | 2050                                  |
| 72<br> | 599                              | 2237                            | 4100                                  |
| 74<br> |                                  |                                 |                                       |

All data were collected in literatures.<sup>6,14,17,82</sup>

## 1.2.5.1 Studies of resonance effect on the hyperpolarizability of the TCBDs

In the study of structure-properties relationship of the push-pull compounds, a simple model has been proposed in which molecular hyperpolarizability is correlated with the degree of ground-state polarization.<sup>82</sup> The degree of ground-state polarization or, the degree of charge separation in the ground state (involves structure of the  $\pi$ -conjugated system or the strength of the donor and acceptor substituents) has large impact on the molecular hyperpolarizability.<sup>19</sup> To better understand this correlation, the molecular two limiting resonance structures have been largely considered in the donor-acceptor polyenes and porphyrine-based chromophore (Figure 26).<sup>5,6,17,83</sup> In those cases, an enhanced molecular hyperpolarizability was observed when the bridge connecting D to A is polarizable and manifests a large transition moment with considerable CT character.<sup>5,6,19</sup> Furthermore, as mentioned in the third paragraph : Simply increasing the donor/acceptor strength will not necessarily lead to enhanced the hyperpolarizability even the two states are fully delocalized or localized,<sup>5,27</sup> but at some intermediate point where there is non-negligible overlap between the two states.<sup>14</sup> It was revealed that the overlapping between the HOMO and LUMO in the bridging region is necessary for obtaining the large hyperpolarizability ( $\beta$ ) in a push-pull system.<sup>28-30</sup>

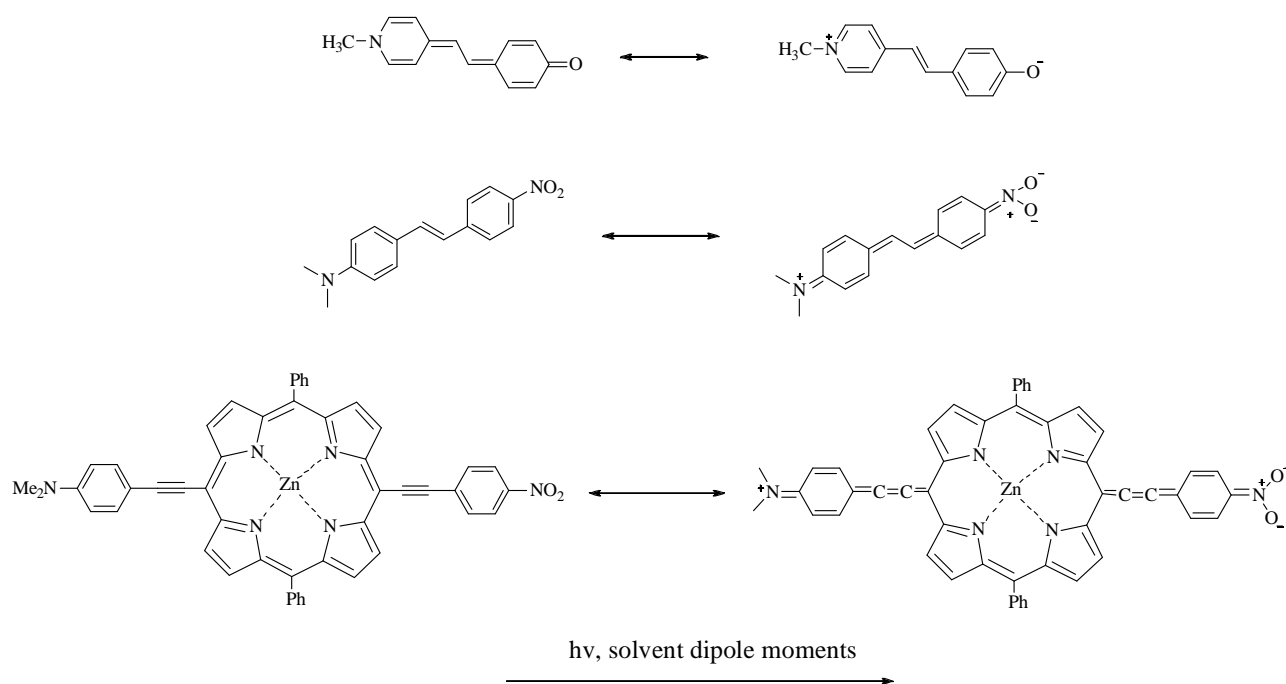


Figure 26. Structure of ground state and charge separated state for the selected compounds.<sup>5,6,17,83</sup>

Therefore, two limit resonance forms were also used here to evaluate the structure-polarizability of the synthesized BODIPY dyes. The negligible NLO response of **68** is probably due to the fully electron delocalization caused by the strong electron withdrawing character of TCBDs residue. While in the case of **69** and **71**, the modest NLO values can be explained by the inefficient  $\pi$ -electrons

delocalization represented in mesomeric forms of the TCBDs BODIPYs in Figure 27. In those mesomeric structures, the  $\pi$ -electrons couldn't be efficiently delocalized from donor group to the electron withdrawing group through the BODIPY core. Therefore for **69** and **71** the donor group plays a more important role in determination of the hyperpolarizability.<sup>20</sup>

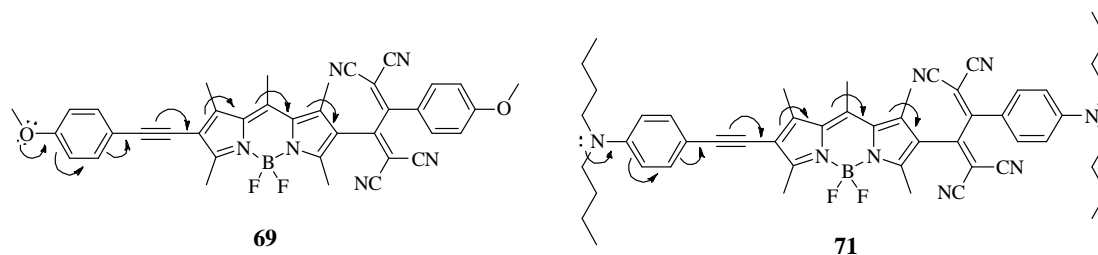


Figure 27. Electron delocalization of compounds **69** and **71**.

In the resonance forms of the monostyryl **74** (Figure 28), the  $\pi$ -electron is more likely efficiently delocalized along the whole molecule, and therefore a higher NLO value was obtained. In addition, the computational calculation studies are in process to get a better understanding about the structure-property relationship of TCBDs-BODIPY dyes.

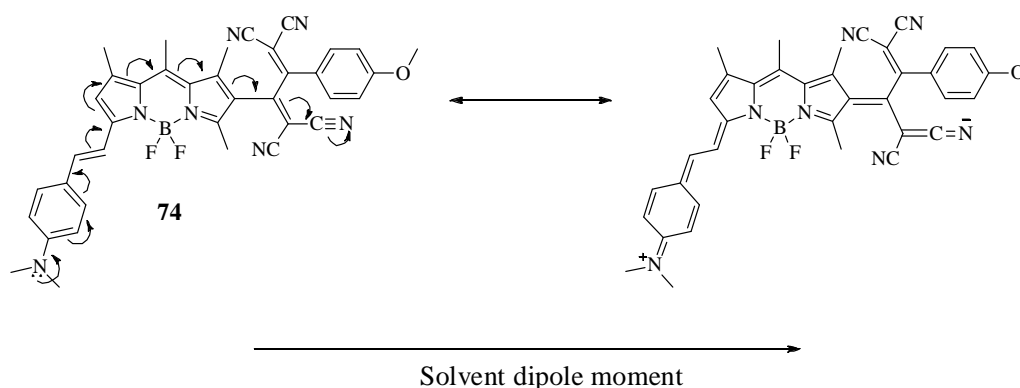


Figure 28. Resonance forms of compound **74**.

## 1.3 Conclusion

In the first part of the synthesis, several BODIPY bridged push-pull chromophores were designed and synthesized. Their optical, electrochemical properties were investigated. In thesecond part, undergoing [2+2] cyclo-addition and retro-ring-opening reactions, the amorphous TCBDs BODIPY derivatives were obtained in good yields from the reaction of symmetric BODIPYs with TCNE. In third part, we discovered that the 5-monostyryl BODIPYs can be selectively obtained from Knoevenagel condensation of a 2-position substituted BODIPY with an electron-rich benzaldehyde. The good reactivity and selectivity of the reaction were confirmed by a series of comparison. Ultimately, the TCBDs compound **74** was obtained in high yield from a second selective cycloaddition of the monostyryl BODIPY **73** with TCNE. The hyperpolarizability of the synthesized

compounds was evaluated by EFISHG measurement, the TCBDs compounds **72** and **74** show particular interesting NLO response, which might make them good candidates for the NLO materials. Moreover, the interesting electrochemical properties (especially in reduction steps); strong CT absorption band in the 500-700 nm range; as well as good solubility in common solvent, the TCBDs BODIPY dyes have already represented good candidates for the study of photovoltaic, and further investigation is on the list.

## References

- (1) Zhou, Y.; Xiao, Y.; Chi, S.; Qian, X. *Org. Lett.* **2008**, *10*, 633.
- (2) Dong, Y.; Bolduc, A. a.; McGregor, N.; Skene, W. G. *Org. Lett.* **2011**, *13*, 1844.
- (3) Barsu, C.; Cheaib, R.; Chambert, S.; Queneau, Y.; Maury, O.; Cottet, D.; Wege, H.; Douady, J.; Bretonniere, Y.; Andraud, C. *Org. Biomol. Chem.* **2010**, *8*, 142.
- (4) Lord, S. J.; Conley, N. R.; Lee, H.-I. D.; Samuel, R.; Liu, N.; Twieg, R. J.; Moerner, W. E. *J. Am. Chem. Soc.* **2008**, *130*, 9204.
- (5) Marder, S. R.; Kippelen, B.; Jen, A. K. Y.; Peyghambarian, N. *Nature (London)* **1997**, *388*, 845.
- (6) LeCours, S. M.; Guan, H.-W.; DiMagno, S. G.; Wang, C. H.; Therien, M. J. *J. Am. Chem. Soc.* **1996**, *118*, 1497.
- (7) Collado, D.; Casado, J.; González, S. R.; Navarrete, J. T. L.; Suau, R.; Perez-Inestrosa, E.; Pappenfus, T. M.; Raposo, M. M. M. *Chem. Eur. J.* **2011**, *17*, 498.
- (8) Burckstummer, H.; Kronenberg, N. M.; Meerholz, K.; Würthner, F. *Org. Lett.* **2010**, *12* (16), pp 3666.
- (9) Erten-Ela, S.; Yilmaz, M. D.; Icli, B.; Dede, Y.; Icli, S.; Akkaya, E. U. *Org. Lett.* **2008**, *10*, 3299.
- (10) Chu, T.-Y.; Lu, J.; Beaupré, S.; Zhang, Y.; Pouliot, J.-R. m.; Wakim, S.; Zhou, J.; Leclerc, M.; Li, Z.; Ding, J.; Tao, Y. *J. Am. Chem. Soc.* **2011**, *133*, 4250.
- (11) Ziessel, R.; Retailleau, P.; Elliott, K. J.; Harriman, A. *Chem. Eur. J.* **2009**, *15*, 10369.
- (12) Zhou, E.; Tan, Z. a.; Yang, Y.; Huo, L.; Zou, Y.; Yang, C.; Li, Y. *Macromolecules* **2007**, *40*, 1831.
- (13) Wakatsuki, Y.; Yamazaki, H.; Kobayashi, T.; Sugawara, Y. *Organometallics* **1987**, *6*, 1191.
- (14) Kanis, D. R.; Ratner, M. A.; Marks, T. J. *Chem. Rev.* **1994**, *94*, 195.
- (15) Levine, B. F. *Chem. Phys. Lett.* **1976**, *37*, 516.
- (16) Lalama, S. J.; Garito, A. F. *Phys. Rev. A* **1979**, *20*, 1179.
- (17) Verbiest, T.; Houbrechts, S.; Kauranen, M.; Clays, K.; Persoons, A. *J. Mater. Chem.* **1997**, *7*, 2175.
- (18) Würthner, F.; Wortmann, R.; Meerholz, K. *ChemPhysChem.* **2002**, *3*, 17.
- (19) Blanchard-Desce, M.; Alain, V.; Bedworth, P. V.; Marder, S. R.; Fort, A.; Runser, C.; Barzoukas, M.; Lebus, S.; Wortmann, R. *Chem. Eur. J.* **1997**, *3*, 1091.
- (20) Moore, Adrian J.; Chesney, A.; Bryce, Martin R.; Batsanov, Andrei S.; Kelly, Janet F.; Howard, Judith A. K.; Perepichka, Igor F.; Perepichka, Dmitrii F.; Meshulam, G.; Berkovic, G.; Kotler, Z.; Mazor, R.; Khodorkovsky, V. *Eur. J. Org. Chem.* **2001**, *2001*, 2671.

- 
- (21) Bouit, P. A.; Kamada, K.; Feneyrou, P.; Berginc, G.; Toupet, L.; Maury, O.; Andraud, C. *Advanced Materials* **2009**, *21*, 1151.
- (22) Didier, P.; Ulrich, G.; Mely, Y.; Ziessel, R. *Org. Biomol. Chem.* **2009**, *7*, 3639.
- (23) Bloembergen, N. *Selected Topics in Quantum Electronics, IEEE Journal of* **2000**, *6*, 876.
- (24) Ward, J. F. *Reviews of Modern Physics* **1965**, *37*, 1.
- (25) Oudar, J. L.; Le Person, H. *Opt. Commun.* **1975**, *15*, 258.
- (26) Zyss, J. *J. Non-Cryst. Solids* **1982**, *47*, 211.
- (27) Zerner, M. C.; Fabian, W. M. F.; Dworzak, R.; Kieslinger, D. W.; Kroner, G.; Junek, H.; Lippitsch, M. E. *Int. J. Quantum Chem.* **2000**, *79*, 253.
- (28) Yoshimura, T. *Phys. Rev. B* **1989**, *40*, 6292.
- (29) Yoshimura, T. *Molecular Crystals and Liquid Crystals Incorporating Nonlinear Optics* **1990**, *182*, 43
- (30) Yoshimura, T. *Appl. Phys. Lett.* **1989**, *55*, 534.
- (31) Sriyanka Mendis, B. A.; Nalin de Silva, K. M. *Journal of Molecular Structure: THEOCHEM* **2004**, *678*, 31.
- (32) Mendis, B. A. S.; de Silva, K. M. N. *Internet Electronic Journal of Molecular Design* **2005**, *4*, 226.
- (33) Sissa, C.; Parthasarathy, V.; Drouin-Kucma, D.; Werts, M. H. V.; Blanchard-Desce, M.; Terenziani, F. *Phys. Chem. Chem. Phys.* **2010**, *12*, 11715.
- (34) Albert, I. D. L.; Marks, T. J.; Ratner, M. A. *J. Phys. Chem* **1996**, *100*, 9714.
- (35) Albert, I. D. L.; Marks, T. J.; Ratner, M. A. *J. Am. Chem. Soc.* **1997**, *119*, 6575.
- (36) Marder, S. R.; Gorman, C. B.; Tiemann, B. G.; Perry, J. W.; Bourhill, G.; Mansour, K. *Science* **1993**, *261*, 186.
- (37) Meyers, F.; Marder, S. R.; Pierce, B. M.; Bredas, J. L. *J. Am. Chem. Soc.* **1994**, *116*, 10703.
- (38) Albert, I. D. L.; Marks, T. J.; Ratner, M. A. *Chem. Mater.* **1998**, *10*, 753.
- (39) Huijts, R. A.; Hesselink, G. L. J. *Chem. Phys. Lett.* **1989**, *156*, 209.
- (40) Varanasi, P. R.; Jen, A. K. Y.; Chandrasekhar, J.; Namboothiri, I. N. N.; Rathna, A. *J. Am. Chem. Soc.* **1996**, *118*, 12443.
- (41) Perepichka, I. F.; Perepichka, D. F.; Bryce, M. R.; Chesney, A.; Popov, A. F.; Khodorkovsky, V.; Meshulam, G.; Kotler, Z. *Synth. Met.* **1999**, *102*, 1558.
- (42) Frank, w.; Klaus, M. *Chem. Eur. J.* **2010**, *16*, 9366.
- (43) Kulinich, A. V.; Aleksandr, A. I. *Russ. Chem. Rev.* **2009**, *78*, 141.

- (44) Belfield, K. D.; Hagan, D. J.; Van Stryland, E. W.; Schafer, K. J.; Negres, R. A. *Org. Lett.* **1999**, *1*, 1575.
- (45) Belfield, K. D.; Schafer, K. J.; Mourad, W.; Reinhardt, B. A. *J. Org. Chem.* **2000**, *65*, 4475.
- (46) Kolemen, S.; Cakmak, Y.; Erten-Ela, S.; Altay, Y.; Brendel, J.; Thelakkat, M.; Akkaya, E. U. *Org. Lett.* **2010**, *12(17)*, pp 3812.
- (47) Zheng, Q.; Xu, G.; Prasad, P. *Chem. Eur. J.* **2008**, *14*, 5812.
- (48) Zhang, D.; Wang, Y.; Xiao, Y.; Qian, S.; Qian, X. *Tetrahedron* **2009**, *65*, 8099.
- (49) Zheng, Q.; He, G. S.; Prasad, P. N. *Chem. Phys. Lett.* **2009**, *475*, 250.
- (50) Knoevenagel, E. *Ber. Der. Deut. Chem. Gesell.* **1898**, *31*, 2596.
- (51) Würthner, F.; Yao, S. *Angew. Chem.* **2000**, *112*, 2054.
- (52) Qin, W.; Baruah, M.; Van der Auweraer, M.; De Schryver, F. C.; Boens, N. *J. Phys. Chem. A* **2005**, *109*, 7371.
- (53) Karolin, J.; Johansson, L. B. A.; Strandberg, L.; Ny, T. *J. Am. Chem. Soc.* **1994**, *116*, 7801.
- (54) Yogo, T.; Urano, Y.; Ishitsuka, Y.; Maniwa, F.; Nagano, T. *J. Am. Chem. Soc.* **2005**, *127*, 12162.
- (55) Bonardi, L.; Ulrich, G.; Ziessel, R. *Org. Lett.* **2008**, *10*, 2183.
- (56) Qin, W.; Rohand, T.; Dehaen, W.; Clifford, J. N.; Driesen, K.; Beljonne, D.; Van Averbeke, B.; Van der Auweraer, M.; Boens, N. *J. Phys. Chem. A* **2007**, *111*, 8588.
- (57) Loudet, A.; Burgess, K. *Chem. Rev.* **2007**, *107*, 4891.
- (58) Demeter, A.; Berces, T.; Zachariasse, K. A. *J. Phys. Chem. A* **2001**, *105*, 4611.
- (59) Druzhinin, S. I.; Kovalenko, S. A.; Senyushkina, T. A.; Demeter, A.; Januskevicius, R.; Mayer, P.; Stalke, D.; Machinek, R.; Zachariasse, K. A. *J. Phys. Chem. A* **2009**, *113*, 9304.
- (60) Olmsted, J. *J. Phys. Chem* **1979**, *83*, 2581.
- (61) Goze, C.; Ulrich, G.; Ziessel, R. *J. Org. Chem.* **2007**, *72*, 313.
- (62) Nepomnyashchii, A. B.; Cho, S.; Rossky, P. J.; Bard, A. J. *J. Am. Chem. Soc.* **2010**, *132*, 17550.
- (63) Liu, Y.; Zhou, J.; Wan, X.; Chen, Y. *Tetrahedron* **2009**, *65*, 5209.
- (64) Kato, S.-i.; Diederich, F. *Chem. Commun.* **2010**, *46*, 1994.
- (65) Kato, S. i.; Kivala, M.; Schweizer, W.; Boudon, C.; Gisselbrecht, J. P.; Diederich, F. *Chem. Eur. J.* **2009**, *15*, 8687.
- (66) Jarowski, P. D.; Wu, Y.-L.; Boudon, C.; Gisselbrecht, J.-P.; Gross, M.; Schweizer, W. B.; Diederich, F. *Org. Biomol. Chem.* **2009**, *7*, 1312.

- (67) Reutenauer, P.; Kivala, M.; Jarowski, P. D.; Boudon, C.; Gisselbrecht, J.-P.; Gross, M.; Diederich, F. *Chem. Comm.* **2007**, 4898.
- (68) Esembeson, B.; Scimeca, M. L.; Michinobu, T.; Diederich, F.; Biaggio, I. *Advanced Materials* **2008**, *20*, 4584.
- (69) Rurack, K.; Kollmannsberger, M.; Daub, J. *New J. Chem.* **2001**, *25*, 289.
- (70) Ziessel, R.; Ulrich, G.; Harriman, A.; Alamiry, M. A. H.; Stewart, B.; Retailleau, P. *Chem. Eur. J.* **2009**, *15*, 1359.
- (71) Yu, Y. H.; Descalzo, A.; Shen, Z.; Röhr, H.; Liu, Q.; Wang, Y. W.; Spieles, M.; Li, Y. Z.; Rurack, K.; You, X. Z. *Chem. Asian. J.* **2006**, *1*, 176.
- (72) Picou, C. L.; Stevens, E. D.; Shah, M.; Boyer, J. H. *Acta Crystallographica Section C* **1990**, *46*, 1148.
- (73) Burghart, A.; Kim, H.; Welch, M. B.; Thoresen, L. H.; Reibenspies, J.; Burgess, K.; Bergstrom, F.; Lennart, B. A. J. *J. Org. Chem* **1999**, *64*, 7813.
- (74) Rurack, K.; Kollmannsberger, M.; Daub, J. *Angew. Chem., Int. Ed.* **2001**, *40*, 385.
- (75) de Silva, A. P.; Gunaratne, H. Q. N.; McCoy, C. P. *J. Am. Chem. Soc.* **1997**, *119*, 7891.
- (76) Coskun, A.; Deniz, E.; Akkaya, E. U. *Org. Lett.* **2005**, *7*, 5187.
- (77) Fox, M. A. *Photochem. Photobiol.* **1990**, *52*, 617.
- (78) Maltey, I.; Delaire, J. A.; Nakatani, K.; Wang, P.; Shi, X.; Wu, S. *Adv. Mat. Opt. Elec* **1996**, *6*, 233.
- (79) Ferrighi, L.; Frediani, L.; Cappelli, C.; Salek, P.; Agren, H.; Helgaker, T.; Ruud, K. *Chem. Phys. Lett.* **2006**, *425*, 267.
- (80) Würthner, F.; Effenberger, F.; Wortmann, R.; Krämer, P. *Chem. Phys.* **1993**, *173*, 305.
- (81) Oudar, J. L. *J. Chem. Phys.* **1977**, *67*, 446.
- (82) Marder, S. R.; Cheng, L.-T.; Tiemann, B. G.; Friedli, A. C.; Blanchard-Desce, M.; Perry, J. W.; Skindhøj, J. *Science* **1994**, *263*, 511.
- (83) Karki, L.; Vance, F. W.; Hupp, J. T.; LeCours, S. M.; Therien, M. J. *J. Am. Chem. Soc.* **1998**, *120*, 2606.



---

## Conclusion and Perspective

In the beginning of this thesis, our main aim was to develop a new general strategy which allows improving the water solubility of BODIPY dyes. A two-step synthesis protocol was then developed to convert the hydrophobic BODIPY core to the hydrophilic one by introducing one pair of sulfobetaine groups onto the boron atom. This strategy can be applied in relatively mild conditions for most of *F*-BODIPY dyes to generate the corresponding *E*-BODIPY dyes with enhanced water-solubility. Moreover, this two step protocol has been proved to be compatible with other types of reactions before or even after the formation of sulfobetaine groups, depending on the requested reactions (such as carboalcoxylation, Sonogashira cross coupling). It is an important feature for the design and engineering of BODIPY dyes for different application purposes.

Later on, we applied this strategy with the distyryl BODIPY dyes in order to obtain water-soluble dyes that emit in the red region for bioconjugation applications. By combination of three water solubization approaches, including introducing the sulfobetain groups on styryl moieties; introduction of ethynyl groups (EG chains, sulfobetains ) onto boron atom; or introduction of polypeptide sulfonated linker at the pseudo-meso position. Ultimately, we obtained a series of water-soluble red-emitting dyes suitable for bioconjugation. The preliminary biological evaluation were performed by the conjugation with the BSA protein or antibody mAb and encouraging results were obtained; furthermore, two photon absorption cell imaging experiment on HeLa cells was also performed with our synthesized water-soluble red-emitting BODIPY dye. Up to now, encouraging results have been obtained, but more efforts must be invested in order to improve the optical performance of BODIPY dyes for bioconjugation applications.

We then moved onto the investigation of BODIPY bridged push-pull systems. By the construction of fully conjugated donor-BODIPY-acceptor systems, we were particularly interested in the role played by the donor and acceptor groups on the optical and electrochemical properties of the BODIPY core. Moreover, the  $\pi$ - electron asymmetric distribution induced nonlinear optical property of the chromophore which also attracted our attentions. Therefore, a series of push-pull BODIPY dyes were synthesized and investigated. Interesting electrochemical and NLO properties were discovered along with our research. It is also noteworthy that, during the synthesis, we discovered as well the interesting regio-selectivity of the Knoevenagel condensation reaction of 2 position substituted BODIPY dye with dimethylaminobenzaldehyde, which leads to principally 5-monostyryl BODIPY dyes. This observation may give some useful information for the future BODIPY molecular engineering and help to obtain a better understanding about structure-relationship of BODIPY dyes. Moreover, the interesting electrochemical properties of the TCBDs

BODIPY dyes may also contribute to the development of dye sensitized solar cells and photovoltaic devices.

In perspective, it might be useful to apply the two-step synthesis protocol to improve the water solubility of BODIPY dyes with different optical properties, in order to enable the dyes to be used not only for bioconjugation or cells imaging applications, but also as a tool for environmental detections purposes in aqueous media.

# Experimental part

## General Methods.

All reactions were performed under a dry atmosphere of argon using standard Schlenk tubes techniques. All chemicals were used as received from commercial sources without further purification. CH<sub>2</sub>Cl<sub>2</sub> was distilled from P<sub>2</sub>O<sub>5</sub> under an argon atmosphere. THF was distilled from sodium and benzophenone under an argon atmosphere. BF<sub>3</sub>OEt<sub>2</sub> has also been distilled. The 200 (<sup>1</sup>H), 300(<sup>1</sup>H), 50 (<sup>13</sup>C), 75 (<sup>13</sup>C) MHz NMR spectra were recorded at room temperature with perdeuterated solvents with residual protiated solvent signals providing internal references. Column chromatographic purification was conducted using 40-63 μm silica gel. Thin layer chromatography (TLC) was performed on silica gel plates coated with fluorescent indicator.

## 2) Spectroscopic Measurements.

UV-vis spectra were recorded using a Shimadzu UV-3600 dual-beam grating spectrophotometer with a 1 cm quartz cell. Fluorescence spectra were recorded on a HORIBA Jobin-Yvon fluoromax 4P spectrofluorimeter. All fluorescence spectra were corrected. The fluorescence quantum yield ( $\Phi_{\text{exp}}$ ) was calculated from eq (1).

$$\Phi_{\text{exp}} = \Phi_{\text{ref}} \frac{F\{1-\exp(-A_{\text{ref}} \ln 10)\}n^2}{F_{\text{ref}}\{1-\exp(-A \ln 10)\}n_{\text{ref}}^2} \quad (1)$$

Here, F denotes the integral of the corrected fluorescence spectrum, A is the absorbance at the excitation wavelength, and n is the refractive index of the medium. The reference system used were rhodamine 6G in methanol ( $\Phi_{\text{ref}} = 0.78$ ,  $\Phi_{\text{exc}} = 488$  nm) and cresyl violet in ethanol ( $\Phi_{\text{ref}} = 0.50$ ,  $\Phi_{\text{exc}} = 546$  nm) in air equilibrated water and deaerated solutions.<sup>1</sup> Luminescence lifetimes were measured on an Edinburgh Instruments spectrofluorimeter equipped with a R928 photomultiplier and a PicoQuant PDL 800-D pulsed diode connected to a G<sup>w</sup>Instect GFG-8015G delay generator. No filter was used for the excitation. Emission wavelengths were selected by a monochromator. Lifetimes were deconvoluted with FS-900 software using a light-scattering solution (LUDOX) for instrument response.

<sup>1</sup> Olmsted, J. J. *Phys. Chem* **1979**, 83, 2581.

## Reagents

Pyrrole, indole, Trimethylsilylacetylene,  $\text{BF}_3 \cdot \text{Et}_2\text{O}$ , copper iodide,  $\text{ICl}$ ,  $\text{K}_2\text{CO}_3$ ,  $\text{NaSO}_4$ , 1-dimethylamino-2-propyne, 1,3-propane sultone, iodobenzoyl chloride 2,6-Lutidine, Sodium hydride ( $\text{NaH}$ ),  $\text{KF}$ , tetracyanoethylene, malononitrile, 1-ethynyl-4-nitrobenzene, 4-ethynylbenzaldehyde, 1-ethynyl-4-methoxybenzene, 4'-ethynyl-2,2':6',2''-terpyridine, diethylene glycol monomethyl ether,  $\text{Al}_2\text{O}_3$ , 1,6-dibromopyrene, ethyl magnesiumbromide, NBS, p-(butylamino)phenylacetylene, 4-Bromo benzene sulfonyl chloride, and triethylamine ( $\text{Et}_3\text{N}$ ) were used as purchased.  $[\text{Pd}(\text{PPh}_3)_2\text{Cl}_2]$ ,<sup>2</sup>  $[\text{Pd}(\text{PPh}_3)_4]$ ,<sup>3</sup> 4-iodobenzyl bromide,<sup>4</sup> 4-[3-(dimethylamino)-1-propyn-1-yl]-benzaldehyde,<sup>5</sup> N-(4-iodobenzyl)-N,N-dimethylamine and 4-[(dimethylamino)methyl]-benzaldehyde,<sup>6</sup> were prepared according to literatures. Tetrahydrofuran, toluene, dichloromethane, dichloroethane, DMF and diethyl ether were dried over suitable reagents and distilled under argon atmosphere immediately prior to using.

## CHAPTER II

### 4-bromo -1-Isopropylsulfonatephenyl

To a solution of Benzenesulfonyl chloride (1 g, 3.91 mmol) in dry  $\text{C}_2\text{H}_4\text{Cl}_2$  was added the 2-methylpropan-1-ol (0.319 g, 4.30 mmol) and 2, 6-lutidine (0.460 g, 4.30mmol) at 0 °C for 10 minutes, then stirred at RT for 10 hours. The solvent was evaporated after the filtration. A chromatography on silica gel ( $\text{CH}_2\text{Cl}_2$ / petroleum ether, 4: 6) afforded the oil product (0.789 g, 77%).  $^1\text{H}$  NMR (200MHz,  $\text{CDCl}_3$ ):  $\delta$  7.73 (m, 4H), 3.82 (d, J = 6.72 Hz, 2H), 1.95(m, 1H), 0.88 (d, J = 6.72 Hz, 6H).

Follow the same procedure, the 4-Bromo -1-(N-sulfonylpyrrole)phenyl and 4-Bromo-1-(N-sulfonylindole)phenyl were prepared from pyrrole / indole treated with  $\text{NaH}$  in dry THF give the yield of 50% and 67%, respectively.

### 4-Bromo-1-(N-sulfonylpyrrole)phenyl

$^1\text{H}$  NMR (200MHz,  $\text{CDCl}_3$ ):  $\delta$  7.66 (m, 4H), 7.14 (t, J = 2.42 Hz, 2H), 6.31 (t, J = 2.42 Hz, 2H).

<sup>2</sup> N. Miyaura, A. Suzuki, *Org. Synth.* **1990**, 68, 130.

<sup>3</sup> Coulson, D. R. *Inorg. Chem.*, **1972**, 13, 121.

<sup>4</sup> Wilson, A. A.; Dannals, R. F.; Ravert, H. T.; Frost, J. J.; Wagner, H. N. *J. Med. Chem.* **1989**, 32, 1057.

<sup>5</sup> Lemhadri, M.; Doucet, H.; Santelli, M. *Synthesis* **2005**, 1359.

<sup>6</sup> Sheng, R.; Xu, Y.; Hu, C.; Zhang, J.; Lin, X.; Li, J.; Yang, B.; He, Q.; Hu, Y. *Eur. J. Med. Chem.* **2009**, 44, 7.

**4-Bromo-1-(N- sulfonylindole)phenyl**

$^1\text{H}$  NMR (300MHz,  $\text{CDCl}_3$ ):  $\delta$  7.89 (d,  $J = 8.28$  Hz, 1H), 7.64 (d,  $J = 6.96$  Hz, 2H), 7.50-7.44 (m, 4H), 7.22 (m, 3H), 6.60(d,  $J = 3.60\text{Hz}$ , 1H).

**4-[2-(trimethylsilyl)ethynyl]-1-(N-sulfonyl pyrrole)phenyl**

To a degassed solution of 4-Bromo-1-(N-sulfonylpyrrole)phenyl (0.841 g, 2.95 mmol), in benzene (3mL) and  $\text{NET}_3$  (2mL), was added  $[\text{Pd}(\text{PPh}_3)_2\text{Cl}_2]$  (0.128 g, 0.177 mmol), CuI (0.034 g, 0.177 mmol), Trimethylsilylacetylene (0.348 g, 3.94 mmol). The mixture was stirred at  $60^\circ\text{C}$  for 10 hours, until complete consumption of the starting material was observed by TLC. The mixture was then washed with water, brine then extracted with  $\text{CH}_2\text{Cl}_2$ , the organic layer was dried on  $\text{MgSO}_4$  then evaporated, followed by column chromatography of the residue on silica gel ( $\text{CH}_2\text{Cl}_2$ / petroleum ether, 2: 8) afforded (0.792 g, 88%).  $^1\text{H}$  NMR (200MHz,  $\text{CDCl}_3$ ):  $\delta$  7.77 (d,  $J = 8.86$  Hz, 2H), 7.53 (d,  $J = 8.60$  Hz, 2H), 7.13 (t,  $J = 1.88$  Hz, 2H), 6.26 (t,  $J = 2.16$  Hz, 2H), 0.24 (s, 9H).

Follow the same procedure, the compounds:

**4-[2-(trimethylsilyl)ethynyl]-1-ethylsulfonatephenyl** (yield 90%) ,

$^1\text{H}$  NMR (200MHz,  $\text{CDCl}_3$ ):  $\delta$  7.87 (d,  $J = 8.60$  Hz, 2H), 7.64 (d,  $J = 8.60$  Hz, 2H), 4.14 (q,  $J = 7.26$  Hz, 2H), 1.32 (t,  $J = 7.26$  Hz, 3H), 0.27 (s, 9H).

**4-[2-(trimethylsilyl)ethynyl]-1-isopropylsulfonatephenyl** (yield 86%),

$^1\text{H}$  NMR (200MHz,  $\text{CDCl}_3$ ):  $\delta$  7.84 (d,  $J = 8.86$  Hz, 2H), 7.60 (d,  $J = 8.60$  Hz, 2H), 3.79 (d,  $J = 6.46$  Hz, 2H), 1.58 (m,  $J = 6.94$  Hz, 1H), 0.88 (d,  $J = 6.72$  Hz, 6H), 0.27 (s, 9H).

**4-[2-(trimethylsilyl)ethynyl]-1-(N-sulfonylindole)phenyl** (yield 94%)

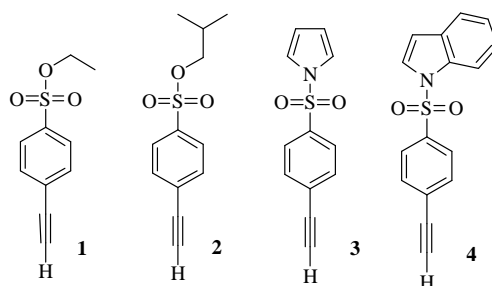
$^1\text{H}$  NMR (200MHz,  $\text{CDCl}_3$ ):  $\delta$  7.95 (d,  $J = 8.34$  Hz, 1H), 7.78 (d,  $J = 8.86$  Hz, 2H), 7.54-7.44 (m, 4H), 7.35-7.19 (m, 2H), 6.66 (d,  $J = 3.66\text{Hz}$ , 1H), 0.21 (s, 9H).

Were prepared from 4-Bromo-1-ethylsulfonatephenyl; 4-bromo -1-Isopropylsulfonatephenyl; 4-Bromo-1-(N-sulfonyl indole)phenyl respectively.

**Deprotection of trimethylsilyl**

4-[2-(trimethylsilyl)ethynyl]-1-ethylsulfonatephenyl; 4-[2-(trimethylsilyl)ethynyl]-1-isopropylsulfonatephenyl; 4-[2-(trimethylsilyl)ethynyl]-1-(N-sulfonylpyrrole)phenyl; 4-[2-

(trimethylsilyl)ethynyl]-1-(N-sulfonyl indole)phenyl with KF in MeOH / THF at RT gives the terminal alkynes derivatives 1 (yield 83%), 2 (yield 97%), 3 (yield 84%), and 4 (yield 91%).

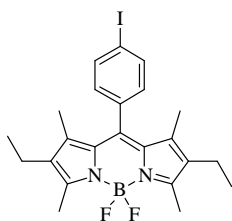


**Compound (1)** <sup>1</sup>H NMR (200MHz, CDCl<sub>3</sub>): δ 7.88 (d, J = 8.60 Hz, 2H), 7.64 (d, J = 8.60 Hz, 2H), 4.14 (q, J = 7.26 Hz, 2H), 3.29 (s, 1H), 1.31 (t, J = 7.26 Hz, 2H). <sup>13</sup>C NMR (75 MHz, CDCl<sub>3</sub>): δ =136.38, 132.85, 127.98, 127.85, 81.82, 81.43, 67.42, 14.82. MS (FAB<sup>+</sup>, m-NBA): m/z (%) = 210.0 [M + H]<sup>+</sup> (100). Anal. Calcd for C<sub>10</sub>H<sub>10</sub>O<sub>3</sub>S: C, 57.13; H, 4.79. Found: C, 56.82, H, 4.66.

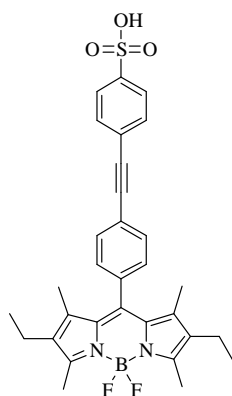
**Compound (2)** <sup>1</sup>H NMR (200MHz, CDCl<sub>3</sub>): δ 7.87 (d, J = 8.40 Hz, 2H), 7.64 (d, J = 8.78 Hz, 2H), 3.81 (d, J = 6.56 Hz, 2H), 3.29 (s, 1H), 1.95 (m, J = 6.94 Hz, 1H), 0.89 (d, J = 6.94 Hz, 6H). <sup>13</sup>C NMR (75 MHz, CDCl<sub>3</sub>): δ =136.28, 132.86, 127.97, 127.91, 81.87, 81.40, 76.87, 28.16, 18.67. MS (FAB<sup>+</sup>, m-NBA): m/z (%) =238.0 [M + H]<sup>+</sup> (100). Anal. Calcd for C<sub>12</sub>H<sub>14</sub>O<sub>3</sub>S: C, 60.48; H, 5.92. Found: C, 60.29, H, 5.77.

**Compound (3)** <sup>1</sup>H NMR (200MHz, CDCl<sub>3</sub>): δ 7.80 (d, J = 8.60 Hz, 2H), 7.58 (d, J = 8.60 Hz, 2H), 7.15(t, J = 1.88 Hz, 2H), 6.31(t, J = 2.16 Hz, 2H), 3.27 (s, 1H). <sup>13</sup>C NMR (75 MHz, CDCl<sub>3</sub>): δ = 138.98, 133.02, 128.19, 126.86, 120.96, 114.14, 81.74, 81.67. MS (FAB<sup>+</sup>, m-NBA): m/z (%) =231.0 [M + H]<sup>+</sup> (100). Anal. Calcd for C<sub>12</sub>H<sub>9</sub>NO<sub>2</sub>S: C, 62.32; H, 3.92; N, 6.06. Found: C, 62.04, H, 3.72;N, 6.17.

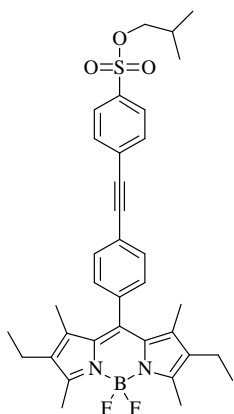
**Compound (4)** <sup>1</sup>H NMR (200MHz, CDCl<sub>3</sub>): δ 7.97 (d, J = 8.04 Hz, 1H), 7.82 (d, J = 8.78 Hz, 2H), 7.54-7.48 (m, 4H), 7.35-7.19 (m, 2H), 6.67 (d, J = 3.66Hz, 1H), 3.22 (s, 1H). <sup>13</sup>C NMR (75 MHz, CDCl<sub>3</sub>): δ = 138.12, 134.98, 132.92, 130.96, 128.17, 126.83, 126.35, 124.94, 123.72, 121.66, 113.64, 109.80, 81.72, 81.62. MS (FAB<sup>+</sup>, m-NBA): m/z (%) =281.1 [M + H]<sup>+</sup> (100)

**Compound (5)**

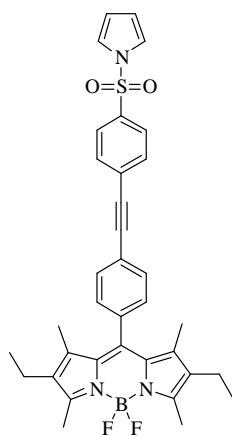
4-iodobenzoyl chloride (2 g, 7.5 mmol) was dissolved in freshly distilled dichloromethane (150 mL) under argon atmosphere. 2, 4-dimethyl-3-ethylpyrrole (2.2 mL, 16.5 mmol) was added and the mixture was stirred at room temperature for 7 days. Then triethylamine (6.3 mL) and  $\text{BF}_3 \cdot \text{Et}_2\text{O}$  (7.6 mL) were added. After stirring 3 h at room temperature, the mixture was treated with water and brine. The organic layer was concentrated to ~10 mL and silica gel was added before complete evaporation. The residue fixed over silica gel was purified by column chromatography on silica gel eluting with dichloromethane – petroleum ether (30/70). Recrystallization by slow evaporation of a dichloromethane / cyclohexane solution afforded 1.9 g (50%) of compound **5** as red crystals.  $^1\text{H}$  NMR (300MHz,  $\text{CDCl}_3$ ):  $\delta$  7.44 (AB sys,  $J_{\text{AB}} = 8.3$  Hz, 4H), 2.53 (s, 6H), 2.30 (q,  $J = 7.5$  Hz, 4H), 1.32 (s, 6H), 0.98 (t,  $J = 7.6$ Hz, 6H).  $^{13}\text{C}$  NMR (75 MHz,  $\text{CDCl}_3$ ):  $\delta = 12.1, 12.7, 14.7, 17.2, 94.6, 130.4, 130.6, 133.1, 135.5, 138.3, 138.4, 138.7, 154.3$ .

**Compound (6)**

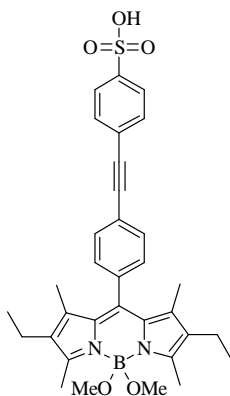
To a degassed solution of **5** (0.0746 g, 0.147 mmol) and **1** (0.031g, 0.147 mmol) in benzene (3 mL) and TEA (3 mL), was added  $[\text{Pd}(\text{PPh}_3)_4]$  (0.017 g, 0.0147 mmol ) under argon. The mixture was stirred at 60 °C for 10 hours until the complete consumption of the starting material was observed by TLC. The mixture was then evaporated, and a chromatography on silica gel ( $\text{CH}_2\text{Cl}_2$  100%, and then MeOH /  $\text{CH}_2\text{Cl}_2$ , 2: 8) afforded compound **6** (51 mg, 62%).  $^1\text{H}$  NMR (300MHz,  $\text{CDCl}_3/\text{CD}_3\text{OD}$ ):  $\delta$  7.84 (d,  $J = 8.4$  Hz, 2H), 7.64 (d,  $J = 8.2$  Hz, 2H), 7.56 (d,  $J = 8.4$  Hz, 2H), 7.27 (d, 2H), 2.49 (s, 6H), 2.27 (q,  $J = 7.3$ Hz, 4H), 1.29 (s, 6H), 0.95 (t,  $J = 7.3$ Hz, 6H).  $^{13}\text{C}$  NMR (75 MHz,  $\text{CDCl}_3/\text{CD}_3\text{OD}$ ):  $\delta = 153.9, 143.3, 138.9, 136.0, 132.8, 131.4, 130.3, 128.5, 125.9, 123.3, 90.3, 89.51, 48.5, 46.3, 16.8, 14.4, 12.3, 8.5$ . MS (FAB<sup>+</sup>, m-NBA):  $m/z$  (%) = 560.1  $[\text{M} + \text{H}]^+$  (100). Anal. Calcd for  $\text{C}_{31}\text{H}_{31}\text{BF}_2\text{N}_2\text{O}_3\text{S} + \text{H}_2\text{O}$ : C, 64.36; H, 5.75; N, 4.84. Found: C, 64.17; H, 5.62; N, 4.62.

**Compound (7)**

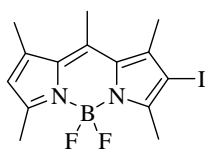
To a degassed solution of **5** (0.0286 g, 0.0565 mmol) and **2** (0.014g, 0.0565 mmol) in benzene (3 mL) and TEA (3 mL), was added  $[\text{Pd}(\text{PPh}_3)_4]$  ( 0.007 g, 0.00057 mmol ) under argon. The mixture was stirred at 60 °C for 10 hours until the complete consumption of the starting material was observed by TLC. The mixture was then evaporated, and a chromatography on silica gel ( $\text{CH}_2\text{Cl}_2$ / petroleum ether, 4: 6, and then  $\text{CH}_2\text{Cl}_2$  100%) afforded compound **7** (30 mg, 87%).  $^1\text{H}$  NMR (200MHz,  $\text{CDCl}_3$ ) :  $\delta$  7.91 (d,  $J = 8.40$  Hz, 2H), 7.71 (d,  $J = 8.40$  Hz, 2H), 7.68 (d,  $J = 8.04$  Hz, 2H), 7.33 (d,  $J = 8.04$  Hz, 2H), 3.85 (d,  $J = 6.58$  Hz, 2H), 2.54 (s, 6H), 2.30 (q,  $J = 7.68$  Hz, 4H), 1.97 (qt,  $J = 6.94$  Hz, 1H), 1.32 (s, 6H), 0.98 (t,  $J = 7.30$  Hz, 6H), 0.90 (d,  $J = 6.94$  Hz, 6H).  $^{13}\text{C}$  NMR (75 MHz,  $\text{CDCl}_3$ ):  $\delta = 154.3, 139.0, 138.2, 136.9, 135.84, 133.1, 132.5, 132.3, 130.6, 128.9, 128.8, 128.1, 122.9, 92.8, 88.8, 28.2, 18.7, 17.2, 14.7, 12.6, 12.0$ . MS ( $\text{FAB}^+$ , m-NBA):  $m/z$  (%) = 616.1 (80); 559.2 (100)  $[\text{M} + \text{H}]^+$ .

**Compound (8)**

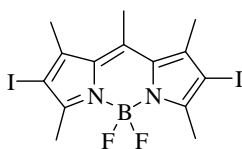
To a degassed solution of **5** (0.0547 g, 0.108 mmol) and **3** (0.025 g, 0.0108 mmol) in benzene (3 mL) and TEA (3 mL), was added  $[\text{Pd}(\text{PPh}_3)_4]$  ( 0.013 g, 0.0108 mmol) under argon. The mixture was stirred at 60 °C for 10 hours until the complete consumption of the starting material was observed by TLC. The mixture was then evaporated, and a chromatography on silica gel ( $\text{CH}_2\text{Cl}_2$ / petroleum ether, 4: 6) afforded compound **8** (60 mg, 91%).  $^1\text{H}$  NMR (200 MHz,  $\text{CDCl}_3$ ) :  $\delta$  7.85 (d,  $J = 8.76$  Hz, 2H), 7.65 (dd,  $J = 8.04$  Hz,  $J = 8.76$  Hz, 4H), 7.31 (d,  $J = 8.04$  Hz, 2H), 7.18 (t,  $J = 2.18$  Hz, 2H), 6.33 (t,  $J = 2.20$  Hz, 2H), 2.53 (s, 6H), 2.23 (q,  $J = 7.30$  Hz, 4H), 1.31 (s, 6H), 0.98 (t,  $J = 7.66$  Hz, 6H).  $^{13}\text{C}$  NMR (75 MHz,  $\text{CDCl}_3$ ):  $\delta = 154.4, 138.5, 136.5, 133.2, 132.5, 130.6, 129.1, 127.0, 122.9, 120.9, 114.1, 93.1, 88.7, 53.6, 29.8, 17.2, 14.7, 12.7$ . MS ( $\text{FAB}^+$ , m-NBA):  $m/z$  (%) = 609.1  $[\text{M} + \text{H}]^+$  (100). Anal. Calcd for  $\text{C}_{35}\text{H}_{34}\text{BF}_2\text{N}_3\text{O}_2\text{S}$ : C, 68.97; H, 5.62; N, 6.89. Found: C, 68.63; H, 5.44; N, 6.67.

**Compound (6')**

To a solution of **8** (0.02 g, 0.33 mmol) in THF (4 mL) and MeOH (2 mL) was added Cs<sub>2</sub>O<sub>3</sub> (0.03 g, 0.10 mmol), the The mixture was stirred at 50 °C for 10 hours until the complete consumption of the starting material was observed by TLC. The mixture was then evaporated, the residue was analyzed by mass spectrometry (FAB<sup>+</sup>, mode negative): m/z (%) = 583.2[M - H]<sup>-</sup> (100), and exact mass is 584.2

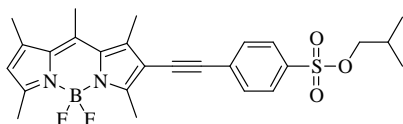
**Compound (9a)**

Compound **9a** was synthesized according to literature.<sup>7</sup> To a solution of 4,4-difluoro-1,3,5,7,8,-pentamethyl-4-bora-3a,4a,diaza-s-indacene (0.300 g, 1.14mmol) in MeOH / DMF (25mL / 25mL) was added a solution of ICl (1.2 equiv, 0.23mmol) in MeOH (5mL). A precipitate immediately formed, the mixture stirred at room temperature for about 45 minutes, and then the mixture was washed with saturated sodium thiosulphate solution (20 mL) then extracted with CH<sub>2</sub>Cl<sub>2</sub>. The organic layer was dried on MgSO<sub>4</sub> then evaporated. A chromatography on silica gel (CH<sub>2</sub>Cl<sub>2</sub>/ petroleum ether, 4: 6) afforded compound **9a** (330 mg, 75%). <sup>1</sup>H NMR (300MHz, CDCl<sub>3</sub>) : δ 6.12 (s, 1H), 2.60 (s, 6H), 2.53 (s, 3H), 2.45 (s, 3H ), 2.40 (s, 3H). <sup>13</sup>C NMR (75 MHz, CDCl<sub>3</sub>): δ = 156.2, 143.2, 141.3, 140.9, 84.4, 19.6, 17.7, 17.2, 15.9, 14.7.

**Compound (9b)**

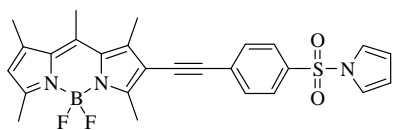
Compound **9b** was synthesized according to literature.<sup>7</sup> To a solution of 4,4-difluoro-1,3,5,7,8,-pentamethyl-4-bora-3a,4a,diaza-s-indacene (0.300 g, 1.14mmol) in MeOH / DMF (25mL / 25mL) was added a solution of ICl (3 equiv, 3.42mmol) in MeOH (10mL). A precipitate immediately formed, the mixture stirred at room temperature for about 30 minutes, and then the mixture was washed with saturated sodium thiosulphate solution (20 mL) then extracted with CH<sub>2</sub>Cl<sub>2</sub>. The organic layer was dried on MgSO<sub>4</sub> then evaporated. A chromatography on silica gel (CH<sub>2</sub>Cl<sub>2</sub>/ petroleum ether, 4: 6) afforded compound **9b** (340 mg, 58%). <sup>1</sup>H NMR (300MHz, CDCl<sub>3</sub>): 2.63 (s, 3H), 2.61 (s, 6H), 2.46 (s, 6H). <sup>13</sup>C NMR (75 MHz, CDCl<sub>3</sub>): δ = 155.2, 143.1, 132.3, 110.6, 105.5, 85.9, 20.0, 18.0, 16.2.

<sup>7</sup> Bonardi, L.; Ulrich, G.; Ziessel, R. *Org. Lett.* **2008**, *10*, 2183

**Compound (10)**

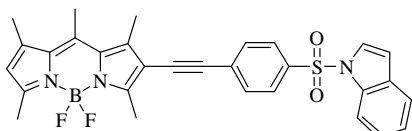
To a degassed solution of **9a** (0.040 g, 0.104 mmol) and **2** (0.0246g, 0.104 mmol) in benzene (3 mL) and TEA (3 mL) was added [Pd (PPh<sub>3</sub>)<sub>4</sub>] (0.012 g, 0.0104 mmol) under argon. The

mixture was stirred at 60 °C for 10 hours until the complete consumption of the starting material was observed by TLC. The solution was then evaporated, and a chromatography on silica gel (CH<sub>2</sub>Cl<sub>2</sub>/ petroleum ether, 4: 6) afforded compound **10** (33 mg, 64%). <sup>1</sup>H NMR (200 MHz, CDCl<sub>3</sub>): δ 7.87 (d, J = 8.40 Hz, 2H), 7.64 (d, J = 8.40 Hz, 2H), 6.15 (s, 2H), 3.82 (d, J = 6.58 Hz, 2H), 2.65 (d, 6H), 2.56 (s, 6H), 2.45 (s, 3H), 1.96 (m, 1H), 0.89 (d, J = 6.56 Hz, 6H). <sup>13</sup>C NMR (75 MHz, CDCl<sub>3</sub>): δ = 167.8, 157.2, 154.5, 143.6, 142.2, 140.3, 134.8, 131.2, 128.9, 122.9, 94.3, 87.2, 68.3, 38.9, 30.5, 29.0, 23.9, 18.7, 17.7, 16.8, 15.9, 14.8, 13.5, 11.1. MS (FAB<sup>+</sup>, m-NBA): m/z (%) = 498.2 [M + H]<sup>+</sup> (100). Anal. Calcd for C<sub>26</sub>H<sub>29</sub>BF<sub>2</sub>N<sub>2</sub>O<sub>3</sub>S: C, 62.66; H, 5.86; N, 5.62. Found: C, 62.44; H, 5.62; N, 5.43.

**Compound (11)**

To a degassed solution of **9a** (0.020 g, 0.052 mmol) and **3** (0.031g, 0.147 mmol) in benzene (3 mL) and TEA (3 mL), was added [Pd(PPh<sub>3</sub>)<sub>4</sub>] (0.017 g, 0.0147 mmol) under argon. The mixture

was stirred at 60 °C for 10 hours until the complete consumption of the starting material was observed by TLC. The mixture was then evaporated, and a chromatography on silica gel (CH<sub>2</sub>Cl<sub>2</sub>/ petroleum ether, 4: 6) afforded compound **11** (19 mg, 75%). <sup>1</sup>H NMR (300MHz, CDCl<sub>3</sub>): δ 7.80 (d, J = 8.60 Hz, 2H), 7.57 (d, J = 8.60 Hz, 2H), 7.16 (t, J = 2.42 Hz, 2H), 6.31 (t, J = 2.14 Hz, 2H), 6.14 (s, 1H), 2.63 (s, 6H), 2.54, 2.53 (ss, 6H), 2.44 (s, 3H). <sup>13</sup>C NMR (75 MHz, CDCl<sub>3</sub>): δ = 142.2, 140.3, 137.5, 131.8, 126.9, 120.9, 114.3, 94.2, 87.6, 68.3, 59.5, 38.9, 30.5, 17.7, 16.8, 14.8, 13.5. MS (EI neat matter): m/z (%) = 491.1 (100).

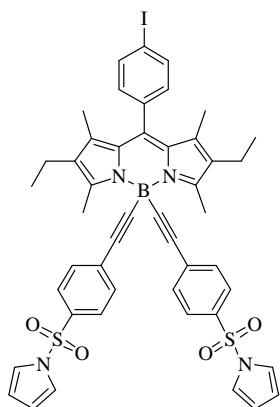
**Compound (12)**

To a degassed solution of **9a** (0.020 g, 0.052 mmol) and **4** (0.016g, 0.057 mmol) in benzene (3 mL) and TEA (3 mL), was added [Pd(PPh<sub>3</sub>)<sub>4</sub>] (0.006 g, 0.0052 mmol) under argon. The

mixture was stirred at 60 °C for 10 hours until the complete consumption of the starting material was observed by TLC. The mixture was then evaporated, and a chromatography on silica gel (CH<sub>2</sub>Cl<sub>2</sub>/ petroleum ether, 4: 6) afforded **12** (23 mg, 83%). <sup>1</sup>H NMR (200MHz, CDCl<sub>3</sub>): δ 7.99 (d, J = 6.72Hz, 1H), 7.82 (d, J = 8.88 Hz, 2H), 7.56-7.48 (m, 4H), 7.32-7.23 (m, 2H), 6.67 (d, J = 3.48Hz,

1H), 6.14 (s, 1H), 2.61 -2.44 (m, 15H). MS (EI neat matter):  $m/z$  (%) = 541.1 (100). Anal. Calcd for  $C_{30}H_{26}BF_2N_3O_2S$ : C, 66.55; H, 4.84; N, 7.76. Found: C, 66.39; H, 4.64; N, 7.52.

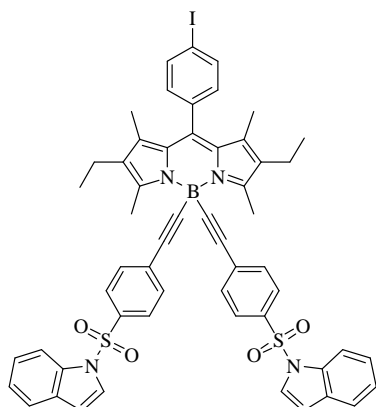
### Compound (13)



The compound **3** (0.114 g, 0.494 mmol) was dissolved in dry THF (4 mL) under argon in a schlenk flask, 1.0 M EtMgBr in THF (0.435 mL) was added and stirred at 60 °C for 1 hour. The resulting anion was then transferred via cannula to the solution of **5** (0.100 g, 0.198 mmol) in dry THF (3 mL) under argon. The mixture was stirred at 60 °C for about 15 minute, until complete consumption of the starting material was observed by TLC. H<sub>2</sub>O (2mL) was added, the mixture was then washed with water, brine then extracted with CH<sub>2</sub>Cl<sub>2</sub>, the organic layer was dried on MgSO<sub>4</sub> then evaporated. Then the crude product was purified by column

chromatography on silica gel (CH<sub>2</sub>Cl<sub>2</sub>/ petroleum ether, 6: 4) afforded compound **13** (132 mg, 72%). <sup>1</sup>H NMR (300MHz, CDCl<sub>3</sub>) : δ 7.84 (d, J = 8.48 Hz, 2H), 7.73 (d, J =8.66 Hz, 4H), 7.46 (d, J =8.67 Hz, 4H), 7.13 (t, J =2.26 Hz, 4H), 7.10 (d, J =8.48 Hz, 2H), 6.28 (t, J =2.26 Hz, 4H), 2.76 (s, 6H), 2.36 (q, J =7.35 Hz, 4H), 1.35 (s, 6H), 1.02 (t, J = 7.34 Hz, 6H). <sup>13</sup>C NMR (75 MHz, CDCl<sub>3</sub>): δ = 153.8, 138.7, 136.7, 135.4, 133.2, 132.1, 130.3, 128.7, 126.4, 120.6, 113.6, 94.4, 93.8, 76.9, 76.5, 17.2, 14.6, 12.1. MS (FAB<sup>+</sup>, m-NBA):  $m/z$  (%) = 928.1 [M + H]<sup>+</sup> (100). Anal. Calcd for C<sub>47</sub>H<sub>42</sub>BN<sub>4</sub>O<sub>4</sub>S<sub>2</sub>: C, 60.78; H, 4.56; N, 6.03; Found: C, 60.54; H, 4.35; N, 5.83.

### Compound (14)

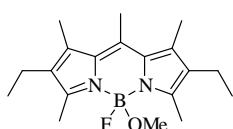


The compound **4** (0.139 g, 0.494 mmol) was dissolved in dry THF (4 mL) under argon in a schlenk flask, 1.0 M EtMgBr in THF (0.435 mL) was added and stirred at 60 °C for 1 hour. The resulting anion was then transferred via cannula to the solution of **5** (0.100 g, 0.198 mmol) in dry THF (3 mL) under argon. The mixture was stirred at 60 °C for about 15 minute, until complete consumption of the starting material was observed by TLC. H<sub>2</sub>O (2mL) was added, the mixture was then washed with water, brine then extracted with CH<sub>2</sub>Cl<sub>2</sub>, the organic layer was dried on MgSO<sub>4</sub>

then evaporated. Then the crude product was purified by column chromatography on silica gel (CH<sub>2</sub>Cl<sub>2</sub>/ petroleum ether, 4: 6) afforded **14** (135 mg, 66%). <sup>1</sup>H NMR (300MHz, CDCl<sub>3</sub>) : δ 7.98 (d, J = 8.29 Hz, 2H), 7.83 (d, J = 8.29 Hz, 2H), 7.75 (d, J =8.67 Hz, 4H), 7.54 (d, J =3.58 Hz, 2H), 7.52

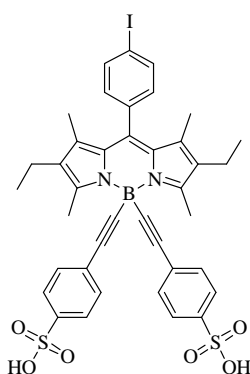
(s, 2H), 7.39 (d,  $J = 8.66\text{Hz}$ , 4H), 7.35-7.20 (m, 4H), 7.06 (d,  $J = 8.48\text{ Hz}$ , 2H), 6.66 (d,  $J = 3.58\text{ Hz}$ , 2H), 2.71 (s, 6H), 2.34 (q,  $J = 7.54\text{ Hz}$ , 4H), 1.34 (s, 6H), 1.01 (t,  $J = 7.53\text{ Hz}$ , 6H).  $^{13}\text{C}$  NMR (75 MHz,  $\text{CDCl}_3$ ):  $\delta = 153.8, 138.7, 136.6, 135.8, 134.7, 133.2, 131.9, 130.6, 128.7, 126.3, 124.5, 123.3, 121.3, 113.4, 109.3, 94.3, 93.7, 17.2, 14.5, 13.8, 12.0$ . MS ( $\text{FAB}^+$ , m-NBA):  $m/z$  (%) = 1028.1 [ $\text{M} + \text{H}$ ] $^+$  (100). Anal. Calcd for  $\text{C}_{55}\text{H}_{46}\text{BIN}_4\text{O}_4\text{S}_2$ : C, 64.21; H, 4.51; N, 5.45; Found: C, 64.09; H, 4.08; N, 5.19.

### Compound (15)



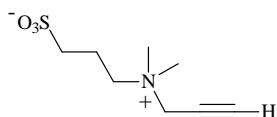
To a stirred solution of compound 2,6-diethyl-4,4-difluoro-1,3,5,7,8-pentamethyl-4-bora-3a,4a-diaza-s-indacene (0.030 g, 0.097 mmol) dissolved in 1,2-dichloroethane (4 mL) and methanol (3 mL) at  $70\text{ }^\circ\text{C}$  was added  $\text{Cs}_2\text{O}_3$  (90 mg, 0.201 mmol) and stirred for 10 hours. Then the solvent was removed, the crude product was purified by column chromatography on silica gel ( $\text{MeOH}/\text{CH}_2\text{Cl}_2$ , 1/99), afforded **15** (0.013g, 41%).  $^1\text{H}$  NMR (300MHz,  $\text{CDCl}_3$ ):  $\delta$  2.87 (s, 3H), 2.63(s, 3H), 2.52(s, 6H), 2.43 (q,  $J = 7.50\text{ Hz}$ , 4H), 2.36 (s, 6H), 1.06 (t,  $J = 7.60\text{ Hz}$ , 6H).  $^{13}\text{C}$  NMR (75 MHz,  $\text{CDCl}_3$ ):  $\delta = 152.0, 139.4, 135.4, 132.4, 49.1, 17.2, 17.0, 15.0, 14.4, 12.3, 12.2$ . MS ( $\text{FAB}^+$ , m-NBA):  $m/z$  (%) = 311.2 (100.0%) [ $\text{M}-\text{F}$ ] $^+$ . Anal. Calcd for  $\text{C}_{19}\text{H}_{28}\text{BFN}_2\text{O}$ : C, 69.10; H, 8.55; N, 8.48. Found: C, 69.37; H, 8.64; N, 8.64.

### Compound (16)



To stirred solution of compound **13** (0.030 g, 0.032 mmol) dissolved in 1, 2-dichloroethane (4 mL) and methanol (3 mL), was added  $\text{Cs}_2\text{O}_3$  (32 mg, 0.096 mmol) and stirred at  $70\text{ }^\circ\text{C}$  for 10 hours. Then the solvent was removed by evaporation, the crude product was purified by column chromatography on silica gel ( $\text{MeOH}/\text{CH}_2\text{Cl}_2$ , 10/90), afforded **16** (0.015g, 56%). MS ( $\text{FAB}^+$ , m-NBA):  $m/z$  (%) = 987.1(100.0%) [ $\text{M}+\text{Cs}+\text{Na}+\text{H}$ ] $^+$ , 853.1(35.0%) [ $\text{M}+\text{Na}$ ] $^+$ . Anal. Calcd for  $\text{C}_{39}\text{H}_{36}\text{BIN}_2\text{O}_6\text{S}_2$ : C, 56.40; H, 4.37; N, 3.37. Found: C, 56.22; H, 4.19; N, 3.19.

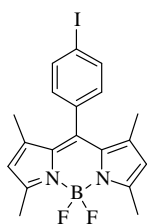
### sulfobetaine



To a degassed solution of 1-dimethylamino-2-propyne (0.5 g, 6.0 mmol) in dry toluene (3 mL) under argon, was added the 1, 3-propane sultone (0.8 g, 6.6 mmol). The mixture was stirred at RT for 10 hours, and then

centrifuged and washed with toluene (5mL) and pentane (5 mL). The powder was dried in vacuum, gave the compound (1.05 g, 85%).  $^1\text{H}$  NMR (300 MHz,  $\text{D}_2\text{O}$ ):  $\delta$  4.32 (s, 2H), 3.65 (m, 2H), 3.25 (s, 6H), 3.03 (t,  $J = 7.14$  Hz, 2H), 2.27 (m, 2H).  $^{13}\text{C}$  NMR (75 MHz,  $\text{D}_2\text{O}$ ):  $\delta = 81.2, 81.6, 62.9, 55.0, 51.0, 47.9, 18.9$ . MS (FAB<sup>+</sup>, m-NBA):  $m/z$  (%) = 206.1 [M + H]<sup>+</sup> (100). Anal. Calcd for  $\text{C}_8\text{H}_{15}\text{NO}_3\text{S}$ : C, 46.81; H, 7.37; N, 6.82. Found: C, 46.74; H, 7.11; N, 6.63.

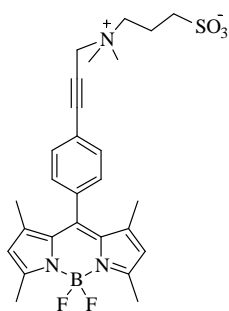
### Compound (17)



4-iodobenzoyl chloride (2.8 g, 10.5 mmol) was dissolved in freshly distilled dichloromethane (150 mL) under argon atmosphere. 2, 4-dimethyl-pyrrole (2.4 mL, 23 mmol) was added and the mixture was stirred at room temperature for 7 days. Then triethylamine (8.8 mL, 63 mmol) and  $\text{BF}_3 \cdot \text{Et}_2\text{O}$  (10.7 mL, 84 mL) were added. After stirring 3 h at room temperature, the mixture was treated with water and brine.

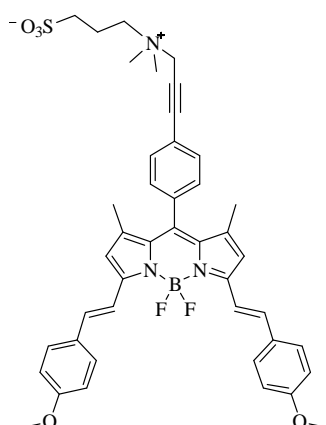
The organic layer was concentrated to ~10 mL and silica gel was added before complete evaporation. The residue fixed over silica gel was purified by column chromatography on silica gel eluting with dichloromethane – petroleum ether (30/70). Recrystallization by slow evaporation of a dichloromethane / cyclohexane solution afforded 1.2 g of compound **17** as red crystals in 25%.  $^1\text{H}$  NMR (300MHz,  $\text{CDCl}_3$ ):  $\delta$  7.44 (AB sys,  $J_{\text{AB}} = 8.3$  Hz, 4H), 5.99 (s, 2H), 2.55 (s, 6H), 1.42 (s, 6H).  $^{13}\text{C}$  NMR (75 MHz,  $\text{CDCl}_3$ ):  $\delta = 14.8, 94.9, 121.6, 130.6, 131.1, 134.5, 138.3, 140.2, 143.0, 156.0$ .

### Compound (18)

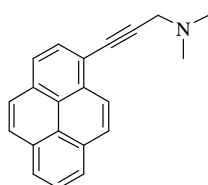


To a degassed solution of **17** (0.03 g, 0.067 mmol) in DMF (10 mL) and TEA (3 mL), was added  $[\text{Pd}(\text{PPh}_3)_4]$  ( 0.0077 g, 0.0067mmol ), and the sulfobetaine (0.0138 g, 0.0067mmol). The mixture was stirred at 80 °C for 10 hours under argon. The solution was then evaporated, and a chromatography on silica gel (MeOH /  $\text{CH}_2\text{Cl}_2$ , 20: 80) afforded compound **18** (26 mg, 74%).  $^1\text{H}$  NMR (400MHz,  $\text{CD}_2\text{Cl}_2$ ):  $\delta$  7.69 (d,  $J = 8.08$  Hz, 2H), 7.38 (d,  $J = 8.08$  Hz, 2H), 6.03 (s, 2H), 4.43 (s, 2H), 3.97 (t, 2H), 3.28 (s, 6H), 2.91 (t, 2H), 2.51 (s, 6H), 2.32 (m, 2H), 1.41(s, 6H).  $^{13}\text{C}$  NMR (75 MHz,  $\text{CDCl}_3 / \text{CD}_3\text{OD}$ ):  $\delta = 156.0, 142.7, 139.9, 136.8, 132.8, 130.9, 128.6, 121.1, 50.3, 49.6, 49.3, 49.0, 14.5$ . MS (FAB<sup>+</sup>, m-NBA):  $m/z$  (%) = 528.2 [M + H]<sup>+</sup> (100). Anal.

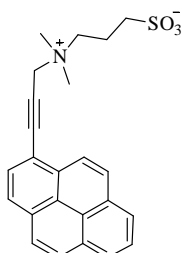
Calcd for  $\text{C}_{27}\text{H}_{32}\text{BF}_2\text{N}_3\text{O}_3\text{S}$ : C, 61.48; H, 6.12; N, 7.97. Found: C, 61.32; H, 5.82; N, 7.81.

**Compound (19)**

To a degassed solution of 8-iodophenyl-3,5-distyryl-methoxy BODIPY (0.050 g, 0.07 mmol) in DMF (5 mL) and TEA (3 mL), was added  $[\text{Pd}(\text{PPh}_3)_4]$  (0.0084 g, 0.0073 mmol) and the sulfobetaine (0.015 g, 0.07 mmol). The mixture was stirred at 80 °C for 10 hours under argon. The solution was then evaporated, and a chromatography on silica gel (MeOH/CH<sub>2</sub>Cl<sub>2</sub>, 20: 80) afforded **19** (16 mg, 30%). <sup>1</sup>H NMR (300 MHz, CDCl<sub>3</sub>/ CD<sub>3</sub>OD):  $\delta$  7.60 (d, J = 8.10 Hz, 2H), 7.50 (m, J = 8.08 Hz, 6H), 7.32 (d, J = 8.10 Hz, 2H), 7.15 (d, J = 16.2 Hz, 2H), 6.86 (d, J = 8.85 Hz, 4H), 6.56 (s, 2H), 4.44 (s, 2H), 3.77 (s, 6H), 3.70 (t, 2H), 3.28 (m, 2H), 3.19 (s, 6H), 2.87 (t, J = 8.85 Hz, 2H), 2.19 (m, 2H), 1.37 (s, 6H). <sup>13</sup>C NMR (75 MHz, CDCl<sub>3</sub>/ CD<sub>3</sub>OD):  $\delta$  = 160.4, 153.2, 141.4, 136.4, 132.8, 129.5, 120.8, 117.8, 114.3, 55.3, 47.1, 29.7, 26.8, 19.1, 14.8. MS (FAB<sup>+</sup>, m-NBA): m/z (%) = 763.2 [M + H]<sup>+</sup> (100). Anal. Calcd for C<sub>43</sub>H<sub>44</sub>BF<sub>2</sub>N<sub>3</sub>O<sub>5</sub>S · H<sub>2</sub>O: C, 66.07; H, 5.93; N, 5.38. Found: C, 65.82; H, 6.05; N, 5.22.

**Compound (20)**

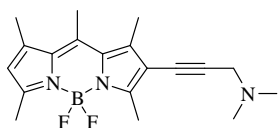
To a degassed solution of 2-bromo-pyrene (0.100 g, 0.356 mmol) in benzene (2 mL) and TEA (2 mL), was added  $[\text{Pd}(\text{PPh}_3)_2\text{Cl}_2]$  (0.015 g, 0.02 mmol), CuI (0.007 g, 0.036 mmol), and 1-dimethylamino-2-propyne (0.037 g, 0.534 mmol). The mixture was stirred at 60 °C for 10 hours under argon until the complete consumption of the starting material was observed by TLC. The mixture was washed with water, brine then extracted with CH<sub>2</sub>Cl<sub>2</sub>, the organic layer was dried on MgSO<sub>4</sub> then evaporated. Followed by column chromatography of the residue on silica gel (MeOH/CH<sub>2</sub>Cl<sub>2</sub>: 5/95) afforded compound **20** (63 mg, 62%). <sup>1</sup>H NMR (200 MHz, CDCl<sub>3</sub>):  $\delta$  8.57 (d, J = 9.50 Hz, 1H), 8.35-8.04 (m, 8H), 3.75 (s, 2H), 2.54 (s, 6H). <sup>13</sup>C NMR (75 MHz, CDCl<sub>3</sub>):  $\delta$  = 132.0, 131.3, 129.9, 128.3, 127.3, 126.3, 125.6, 124.5, 117.9, 90.1, 84.6, 49.1, 44.5.

**Compound (21)**

To a solution of **20** (0.040 g, 0.14 mmol) in dry toluene (2 mL) under argon was added the 1,3-propane sulfone (0.026 g, 0.21 mmol). The mixture was stirred at 40 °C for 10 hours, a precipitate formed. The residue was centrifuged and washed with toluene and pentane. The powder was dried in vacuum gave compound **21** (48.2 mg, 85%). <sup>1</sup>H NMR (300 MHz, DMSO):  $\delta$  8.51 (d, J = 9.42 Hz, 1H), 8.42-

8.13 (m, 8H), 4.85(s, 2H), 3.73(m, 2H), 3.27(s, 6H), 2.59 (t, J = 7.17 Hz, 2H), 2.19(m, 2H).  $^{13}\text{C}$  NMR (75 MHz, DMSO):  $\delta$  = 130.3, 129.3, 128.9, 127.2, 126.8, 124.7, 123.4, 114.6, 89.0, 83.3, 63.0, 54.6, 50.0, 47.7, 19.2. MS (FAB<sup>+</sup>, m-NBA): m/z (%) = 406.1 [M + H]<sup>+</sup> (100). Anal. Calcd for C<sub>24</sub>H<sub>23</sub>NO<sub>3</sub>S·H<sub>2</sub>O: C, 68.06; H, 5.95; N, 3.31. Found: C, 67.85; H, 5.72; N, 3.09.

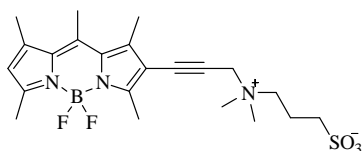
### Compound (22)



To a degassed solution of **9a** (0.050 g, 0.129 mmol) in benzene (2 mL) and TEA (2 mL), was added [Pd(PPh<sub>3</sub>)<sub>2</sub>Cl<sub>2</sub>] (0.010 g, 0.0129 mmol), CuI (0.003 g, 0.0129 mmol), and 1-Dimethylamino-2-propyne (0.010 g, 0.142 mmol).

The mixture was stirred at 60 °C for 10 hours under argon, until the complete consumption of the starting material was observed by TLC. The mixture was washed with water, brine then extracted with CH<sub>2</sub>Cl<sub>2</sub>, the organic layer was dried on MgSO<sub>4</sub> then evaporated, followed by column chromatography of the residue on silica gel (MeOH / CH<sub>2</sub>Cl<sub>2</sub>, 5: 95) afforded compound **22** (36.4 mg, 82%).  $^1\text{H}$  NMR (300MHz, CDCl<sub>3</sub>):  $\delta$  6.09 (s, 1H), 3.57 (s, 2H), 2.62-2.38 (m, 21H).  $^{13}\text{C}$  NMR (75 MHz, CDCl<sub>3</sub>):  $\delta$  = 154.6, 153.7, 141.5, 139.7, 132.0, 129.8, 121.1, 113.9, 89.0, 47.7, 28.7, 16.4, 15.6, 14.8, 12.3. MS (EI neat matter): m/z (%) = 343.1(100).

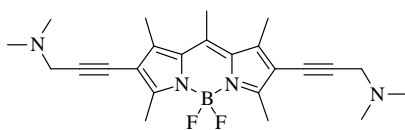
### Compound (23)



To a solution of **22** (0.027 g, 0.079 mmol) in dry toluene (2 mL) under argon, was added the 1,3-propane sultone (0.012 g, 0.094 mmol), then the mixture was stirred at 60 °C for 10 hours, and a precipitate formed. Then the mixture was centrifuged and washed

with toluene and pentane. The powder was dried in vacuum gave compound **23** (28.8 mg, 78%).  $^1\text{H}$  NMR (200MHz, D<sub>2</sub>O /DMSO):  $\delta$  6.40 (s, 1H), 4.64 (s, 2H), 3.12(s, 6H), 2.85(s, 6H), 2.67(s, 3H), 2.61(s, 2H), 2.16(s, 2H). MS (FAB<sup>+</sup>, m-NBA): m/z (%) = 466.1 [M + H]<sup>+</sup> (100). Anal. Calcd for C<sub>22</sub>H<sub>30</sub>BF<sub>2</sub>N<sub>3</sub>O<sub>3</sub>S·H<sub>2</sub>O: C, 54.66; H, 6.67; N, 8.69. Found: C, 54.44; H, 6.59; N, 8.42.

### Compound (24)

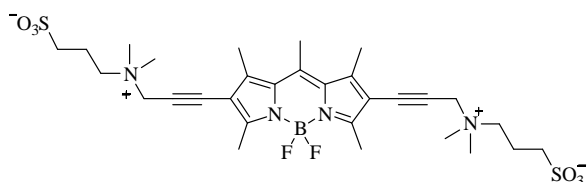


To a degassed solution of **9b** (0.100 g, 0.1946 mmol) in benzene (4 mL) and TEA ( 2 mL), was added [Pd(PPh<sub>3</sub>)<sub>2</sub>Cl<sub>2</sub>] (0.008 g, 0.0117 mmol), CuI (0.003 g, 0.0117 mmol), and 1-Dimethylamino-2-propyne (0.034 g, 0.486 mmol). The mixture

was stirred at 60 °C for 10 hours, until the complete consumption of the starting material was observed by TLC. The mixture was evaporated, followed by column chromatography of the residue

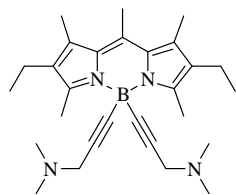
on silica gel (MeOH / CH<sub>2</sub>Cl<sub>2</sub>, 1: 9) afforded compound **24** (0.035 g, 42%). <sup>1</sup>H NMR (300 MHz, CDCl<sub>3</sub>): δ 3.55 (s, 4H), δ 2.61-2.58 (m, 9H), δ 2.49 (m, 6H), δ 2.38(s, 12H). <sup>13</sup>C NMR (75 MHz, CDCl<sub>3</sub>): δ =156.54, 142.30, 141.99, 131.67, 115.90, 90.99, 53.41, 48.79, 44.07, 16.88, 13.51. MS (FAB<sup>+</sup>, m-NBA): m/z (%) = 424.2 [M + H]<sup>+</sup> (100). Anal. Calcd for C<sub>24</sub>H<sub>31</sub>BF<sub>2</sub>N<sub>4</sub>: C, 67.93; H, 7.36; N, 13.20. Found: C, 67.72, H, 7.18, N, 12.93.

### Compound (25)

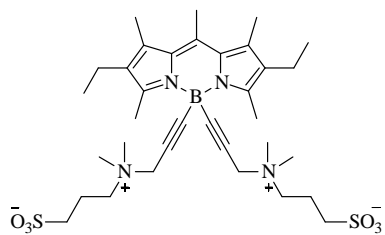


To a solution of **24** (0.035 g, 0.0825 mmol) in dry toluene (4 mL) under argon, was added the 1,3-propane sultone (0.025 g, 0.21 mmol), then the mixture was stirred at 60 °C for 3 days, until the complete consumption of the starting material was observed by TLC. The mixture was centrifuged and washed with toluene and pentane. The powder was dried in vacuum, gave compound **25** (32 mg, 58%). <sup>1</sup>H NMR (300 MHz, D<sub>2</sub>O): δ 4.58 (s, 4H), δ 3.67 (m, 4H), δ 3.25 (s, 12H), δ 2.98 (m, 4H), δ 2.41 (m, 19H). <sup>13</sup>C NMR (75 MHz, D<sub>2</sub>O): δ =156.9, 145.1, 131.3, 113.2, 83.6, 62.2, 60.2, 55.1, 50.6, 47.9, 42.1, 27.5, 18.5, 16.4, 12.7. MS (FAB<sup>+</sup>, m-NBA): m/z (%) = 335.1 (100, doubly charged) [M + 2H]<sup>+</sup> (100). Anal. Calcd for C<sub>30</sub>H<sub>43</sub>BF<sub>2</sub>N<sub>4</sub>O<sub>6</sub>S<sub>2</sub>·2H<sub>2</sub>O: C, 51.13; H, 6.72; N, 7.95; Found: C, 51.07, 6.50, 7.72.

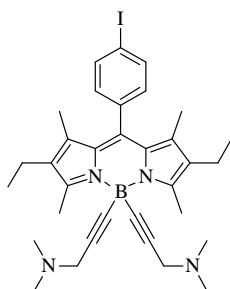
### Compound (26)



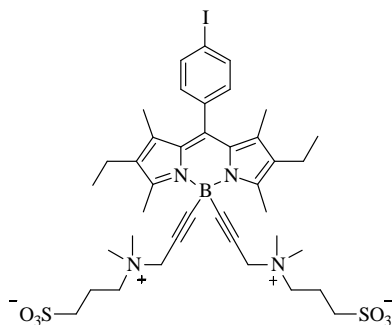
To a solution of 1-dimethylamino-2-propyne (0.043g, 0.63 mmol) in dry THF (5 mL) under argon in a schlenk flask, was added 1.0 M EtMgBr in THF (0.62 mL) and stirred at 60 °C for one hour. The resulting anion was then transferred via cannula to the solution of 2,6-diethyl-4,4-difluoro-1,3,5,7,8-pentamethyl-4-bora-3a,4a-diaza-s-indacene (0.100g, 0.31 mmol) in dry THF(3 mL) under argon. The mixture was stirred at 60 °C for about 15 minutes, then H<sub>2</sub>O (3mL) was added. The mixture was then washed with water, brine then extracted with CH<sub>2</sub>Cl<sub>2</sub>, the organic layer was dried on MgSO<sub>4</sub> then evaporated. The crude product was purified by column chromatography on silica gel (MeOH/ AcOEt, 1/9) afforded **26** (76 mg, 55%). <sup>1</sup>H NMR (300MHz, CDCl<sub>3</sub>): δ 3.30 (s, 4H), 2.71(s, 6H), 2.61(s, 3H), 2.41 (q, J = 7.54 Hz, 4H), 2.37 (s, 12H), 2.34 (s, 6H), 1.03 (t, J = 7.53 Hz, 6H). <sup>13</sup>C NMR (75 MHz, CDCl<sub>3</sub>): δ = 151.3, 139.6, 134.4, 132.5, 129.9, 87.7, 48.7, 43.6, 17.4, 14.9, 14.6. MS (FAB<sup>+</sup>, m-NBA): m/z (%) = 445.2 [M + H]<sup>+</sup> (100). Anal. Calcd for C<sub>28</sub>H<sub>41</sub>BN<sub>4</sub>: C, 75.66; H, 9.30; N, 12.61. Found: C, 75.44; H, 9.12; N, 12.32.

**Compound (27)**

To a solution of compound **26** (0.030 g, 0.068 mmol) in dry toluene (3 mL) under argon, was added the 1,3-propane sultone (0.020 g, 0.17 mmol). The mixture was stirred at 60 °C for 10 hours, a precipitate was formed. The crude was then centrifuged and washed with toluene and pentane. The powder was dried in vacuum afforded compound **27** (36.4 mg, 78%). <sup>1</sup>H RMN (D<sub>2</sub>O/CD<sub>3</sub>OD 300 MHz): 1.03 (t, 6H, <sup>3</sup>J = 5.46 Hz), 2,21 (m, 10H), 2.32 (s, 3H), 2.45 (m, 4H), 2,70 (s, 6H), 2,78 (t, 4H, <sup>3</sup>J = 5.64 Hz), 3,12 (s, 12H), 3,41 (m, 4H), 4,19 (s, 4H). <sup>13</sup>C RMN (D<sub>2</sub>O/CD<sub>3</sub>OD, 75 MHz): = 151.9, 141.7, 137.1, 134.1, 129.9, 83.2, 62.3, 60.6, 55.3, 50.9, 27.3, 24.6, 18.7, 17.1, 14.5, 13.9. MS (ESI-MS positive mode in using acetonitrile / H<sub>2</sub>O): m/z (%) = 345.1 (100, doubly charged) [M + 2H]<sup>+</sup> (100). Anal. Calcd for C<sub>34</sub>H<sub>53</sub>BN<sub>4</sub>O<sub>6</sub>S<sub>2</sub> · 2.5H<sub>2</sub>O: C, 55.65; H, 7.97; N, 7.64; Found: C, 55.84; H, 8.22; N, 7.40.

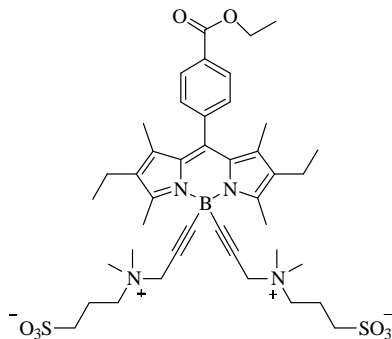
**Compound (28)**

To a solution of 1-dimethylamino-2-propyne (0.136 g, 1.976 mmol) in dry THF (5 mL) under argon in a schlenk flask, was added 1.0 M EtMgBr in THF (1.738 mL) and stirred at 60 °C for 1 hour. The resulting anion was then transferred via cannula to the solution of **5** (0.400g, 0.79 mmol) in anhydrous THF (5mL). The mixture was stirred at 60 °C for 15 minutes, then H<sub>2</sub>O (3mL) was added. The mixture was then washed with water, brine then extracted with CH<sub>2</sub>Cl<sub>2</sub>, the organic layer was dried on MgSO<sub>4</sub> then evaporated. The crude product was purified by column chromatography on silica gel [(CH<sub>2</sub>Cl<sub>2</sub>/ AcOEt, 50: 50), then (MeOH/CH<sub>2</sub>Cl<sub>2</sub>, 1/9)] afforded **28** (0.313 g, 63%). <sup>1</sup>H RMN (CDCl<sub>3</sub> 300 MHz): 0,97 (t, 6H, <sup>3</sup>J = 7,53 Hz), 1,30 (s, 6H), 2,32 (q, 4H, <sup>3</sup>J= 7,14Hz), 2,38 (s, 12H), 2.72 (s, 6H), 3,30 (s, 4H), 7,06 (AB sys, 2H, J<sub>AB</sub> = 8,31 Hz), 7,81 (AB sys, 2H, J<sub>AB</sub> = 8,31 Hz). <sup>13</sup>C RMN (CDCl<sub>3</sub>, 75 MHz): 12.1, 14.1, 17.3, 29.3, 43.7, 48.8, 94.3, 128.7, 130.5, 133.0, 135.8, 136.0, 138.5, 153.6. MS (FAB<sup>+</sup>, m-NBA): m/z (%) = 633.1 [M + H]<sup>+</sup> (100). Anal. Calcd for C<sub>33</sub>H<sub>42</sub>BN<sub>4</sub>I: C, 62.67; H, 6.69; N, 8.86. Found: C, 62.52; H, 6.51; N, 8.53.

**Compound (29)**

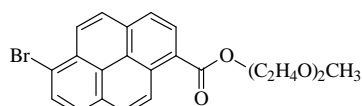
To a solution of **28** (0.100 g, 0.458 mmol) in dry toluene (3 mL) under argon, was added the 1,3-propane sultone (0.077 g, 0.63 mmol). The mixture was stirred at 60 °C for 10 hours. The precipitate formed was then centrifuged and washed with toluene and pentane, and recrystallized twice from methanol-acetone. The powder was dried in vacuum, gave compound **29** (0.086 g, 62%).

$^1\text{H}$  RMN ( $\text{CD}_3\text{OD}$  300 MHz): 0,99 (t, 6H,  $^3J = 7,53$  Hz), 1,37 (s, 6H), 2,20 (m, 4H), 2,39 (q, 4H,  $^3J = 7,53$  Hz), 2,72 (s, 6H), 2,82 (t, 4H,  $^3J = 6,99$  Hz), 3,14 (s, 12H), 3,56 (m, 4H), 4,30 (s, 4H), 7,13 (AB sys, 2H,  $J_{AB} = 8,28$  Hz), 7,93 (AB sys, 2H,  $J_{AB} = 8,28$  Hz);  $^{13}\text{C}$  RMN ( $\text{CD}_3\text{OD}$ , 75 MHz): = 10.9, 13.4, 16.6, 18.7, 29.3, 49.7, 55.2, 62.7, 94.1, 116.5, 128.7, 130.3, 133.6, 135.1, 137.2, 138.4, 139.6, 153.5. MS (FAB<sup>+</sup>, m-NBA):  $m/z$  (%) = 876.1  $[\text{M} + \text{H}]^+$  (100). Anal. Calcd for  $\text{C}_{39}\text{H}_{54}\text{BIN}_4\text{O}_6\text{S}_2 \cdot \text{H}_2\text{O}$ : C, 51.32; H, 6.40; N, 6.14; Found: C, 51.27; H, 6.28; N, 5.82.

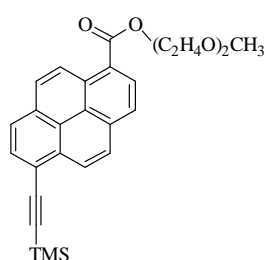
**Compound (30)**

To a stirred solution of compound **29** (0.040 g, 0.0457 mmol) dissolved in EtOH absolute (4 mL) and  $\text{NEt}_3$  (3 mL) was added  $\text{Pd}(\text{PPh}_3)_2\text{Cl}_2$  (4 mg, 0.046 mmol), the CO gas was bubbled for 4 hours at 70°C. After the solvent was removed, the crude product was purified by column chromatography on silica gel ( $\text{H}_2\text{O}/\text{EtOH}$ , 20: 80), then recrystallized from Methanol/ $\text{Et}_2\text{O}$  gave compound

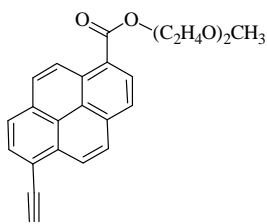
**30** (0.020 g, 53%).  $^1\text{H}$  RMN ( $\text{CD}_3\text{OD}$  300 MHz): 1.01 (t, 6H,  $J = 7,53$  Hz), 1,33 (s, 6H), 1,43 (t, 3H,  $J = 7,17$  Hz), 2,24 (m, 4H), 2,40 (q, 4H,  $J = 7,53$  Hz), 2,75 (s, 6H), 2,85 (m, 4H), 3,18 (s, 12H), 3,61 (m, 4H), 4,32 (s, 4H), 4,43 (q, 2H,  $J = 7,17$  Hz), 7,50 (d, 2H,  $J = 8,28$  Hz), 8,21 (d, 2H,  $J = 8,49$  Hz).  $^{13}\text{C}$  RMN ( $\text{CD}_3\text{OD}$ , 75 MHz):  $\delta = 7.6, 12.2, 14.9, 17.9, 20.1, 24.0, 51.1, 53.9, 54.8, 56.6, 62.5, 64.1, 129.5, 130.1, 130.5, 131.5, 132.5, 135.1, 138.6, 141.8, 155.1, 181.3$ . MS (FAB<sup>+</sup>, m-NBA):  $m/z$  (%) = 823.4  $[\text{M} + \text{H}]^+$  (100).

**Compound (31)**

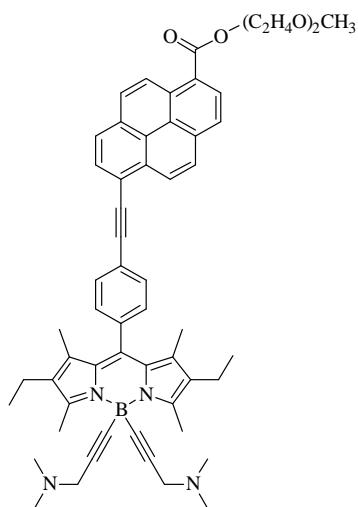
To a stirred solution of 1,6-dibromopyrene ( 1.62 g, 4.51 mmol) dissolved in toluene ( 80 mL) and  $\text{NEt}_3$  ( 30 mL) was added  $\text{Pd}(\text{PPh}_3)_2\text{Cl}_2$  (195 mg, 0.27 mmol) and Diethylene glycol monomethyl ether (3.79 mL, 35.6 mmol), the CO gas was bubbled at 90 °C for 48 hours. The carboalkoxylation was followed by TLC ( $\text{CH}_2\text{Cl}_2$  /AcOEt, 5/5). After the solvent was removed, the residue was separated by a chromatography on silica gel ( $\text{CH}_2\text{Cl}_2$ / Petroleum ether, 80:20), gave 568 mg of mono-substituted-ester-pyrene **31** with a yield of 30%.  $^1\text{H}$  NMR (300 MHz,  $\text{CDCl}_3$ ):  $\delta$  9.21 (d,  $J = 9.42$  Hz, 1H),  $\delta$  8.65 (d,  $J = 8.10$  Hz, 1H),  $\delta$  8.47 (d, ,  $J = 9.21$  Hz, 1H),  $\delta$  8.25-8.01 (m, 5H),  $\delta$  4.68 (t,  $J = 4.92$  Hz, 2H),  $\delta$  3.98 (t,  $J = 4.71$  Hz, 2H),  $\delta$  3.78 (t,  $J = 4.38$  Hz, 2H),  $\delta$  3.62 (t,  $J = 4.35$  Hz, 2H),  $\delta$  3.41(s, 3H).  $^{13}\text{C}$  NMR (75 MHz,  $\text{CDCl}_3$ ):  $\delta = 167.7, 133.9, 130.9, 129.7, 129.5, 128.6, 126.5, 125.3, 124.5, 124.1, 121.2, 71.9, 70.6, 69.3, 64.3, 59.1, 29.6$ . MS ( $\text{FAB}^+$ , m-NBA):  $m/z$  (%) = 426.0 [ $\text{M} + \text{H}$ ] $^+$  (100). Anal. Calcd for  $\text{C}_{22}\text{H}_{19}\text{BrO}_4$ : C, 61.84; H, 4.48. Found: C, 61.52; H, 4.22.

**Compound (32)**

To a degassed solution of **31** (0.50 g, 1.17 mmol), in benzene (3mL) and  $\text{NET}_3$  (2mL), was added  $[\text{Pd}(\text{PPh}_3)_4]$  (0.081 g, 0.070 mmol) and trimethylsilylacetylene (0.345 g, 3.51 mmol). The mixture was stirred at 90 °C for 10 hours, until complete consumption of the starting material was observed by TLC. The mixture was then evaporated, the residue was separated by column chromatography of the residue on silica gel (AcOEt / petroleum ether, 3: 7) afforded **32** (0.220 g, 42%).  $^1\text{H}$  NMR (400 MHz,  $\text{CDCl}_3$ ):  $\delta$  9.16 (d,  $J = 9.40$  Hz, 1H),  $\delta$  8.56 (dd,  $J = 8.16$  Hz,  $J = 8.28$  Hz, 2H),  $\delta$  8.15-8.02 (m, 5H),  $\delta$  4.67 (t,  $J = 4.48$  Hz, 2H),  $\delta$  3.96 (t,  $J = 4.88$  Hz, 2H),  $\delta$  3.76 (m, 2H),  $\delta$  3.60 (m, 2H),  $\delta$  3.40(s, 3H),  $\delta$  0.43(s, 9H).  $^{13}\text{C}$  NMR (75 MHz,  $\text{CDCl}_3$ ):  $\delta = 168.1, 134.4, 132.4, 131.4, 130.8, 129.4, 128.4, 127.9, 126.0, 125.8, 125.1, 124.6, 124.3, 124.1, 119.3, 104.3, 101.3, 72.4, 71.0, 69.8, 64.7, 59.5, 0.62$ . MS ( $\text{FAB}^+$ , m-NBA):  $m/z$  (%) = 467.1 [ $\text{M} + \text{Na}$ ] $^+$  (100). Anal. Calcd for  $\text{C}_{27}\text{H}_{28}\text{O}_4\text{Si}$ : C, 72.94; H, 6.35. Found: C, 73.17; H, 6.54.

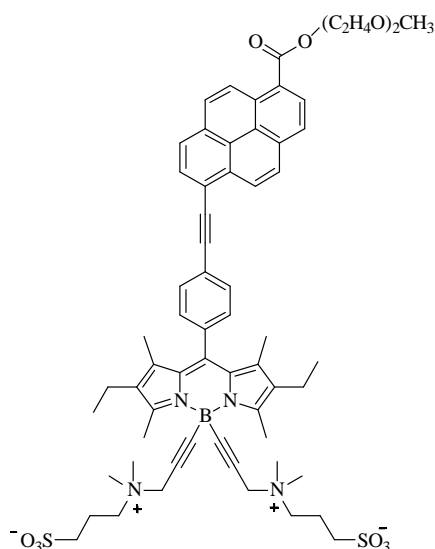
**Compound (33)**

To a stirred solution of compound **32** (0.213 g, 0.479 mmol) dissolved in MeOH ( 3 mL) and THF ( 3 mL) at room temperature was added KF (0.085mg, 1.439mmol) for 4 hours, followed by TLC (AcOEt / petroleum ether, 4: 6) until the starting material was complete consumed. After the solvent was removed, the residue was purified by a chromatography on silica gel (AcOEt / Petroleum ether, 3:7), gives 163 mg of compound **33** with yield of 91%. <sup>1</sup>H NMR (200 MHz, CDCl<sub>3</sub>): δ 9.28 (d, J = 9.40 Hz, 1H), δ 8.68 (m, 2H), δ 8.23-8.15 (m, 5H), δ 4.68 (t, J = 4.83 Hz, 2H), δ 3.98 (t, J = 4.71 Hz, 2H), δ 3.77 (m, 2H), δ 3.62 (m, 3H), δ 3.41(s, 3H). <sup>13</sup>C NMR (75 MHz, CDCl<sub>3</sub>): δ = 167.8, 134.1, 132.4, 131.2, 130.8, 129.1, 128.9, 127.4, 126.0, 125.5, 124.8, 83.2, 82.5, 64.4, 59.1. MS (FAB<sup>+</sup>, m-NBA): m/z (%) = 372.1 [M + H]<sup>+</sup> (100). Anal. Calcd for C<sub>24</sub>H<sub>20</sub>O<sub>4</sub>: C, 77.40; H, 5.41. Found: C, 77.18; H, 5.34.

**Compound (34)**

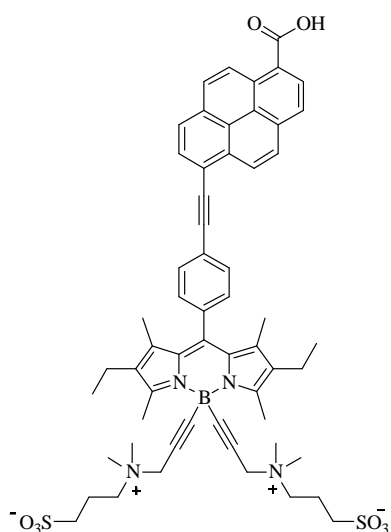
To a degassed solution of **33** (0.036 g, 0.097 mmol) and **28** (0.062 g, 0.098mmol), in benzene (3mL) and NET<sub>3</sub> (2mL), was added [Pd (PPh<sub>3</sub>)<sub>4</sub>] (0.010 g, 0.0087 mmol). The mixture was stirred at 60 °C for 10 hours, until complete consumption of the starting material was observed by TLC. The mixture was then evaporated, the residue was purified by column chromatography of the residue on silica gel [(CH<sub>2</sub>Cl<sub>2</sub> pure, then (MeOH/CH<sub>2</sub>Cl<sub>2</sub>, 1/9)] afforded **34** (0.075g, 87%). <sup>1</sup>H NMR (200 MHz, CDCl<sub>3</sub>): δ 9.22 (d, J = 9.40 Hz, 1H), δ 8.73 (d, J = 9.14 Hz, 1H), δ 8.63 (d, J = 8.06 Hz, 1H), δ 8.21-8.12 (m, 5H), δ 7.83 (d, J = 7.80 Hz, 2H), δ 7.38 (d, J = 8.06 Hz, 2H), δ 4.65 (t, J = 4.70 Hz, 2H), δ 3.94 (t, J = 4.71 Hz, 2H), δ 3.74 (m, 2H), δ 3.45 (s, 4H), δ 3.42(s, 3H), δ 2.76(s, 6H), δ 2.47(s, 12H), δ 2.36 (q, J = 7.52 Hz, 4H), δ 1.41(s, 6H), δ 0.99 (t, J = 6.98 Hz, 6H). <sup>13</sup>C NMR (50 MHz, CDCl<sub>3</sub>): δ = 167.8, 153.6, 139.4, 136.5, 134.1, 133.2, 132.9, 131.8, 130.6, 129.2, 128.9, 128.4, 128.2, 127.5, 125.9, 124.9, 123.8, 118.7, 95.2, 89.6, 64.4, 59.1, 48.8, 46.3, 43.6, 43.6, 17.4, 14.8, 14.3, 12.2, 8.7. MS (FAB<sup>+</sup>, m-NBA): m/z (%) = 877.3 [M + H]<sup>+</sup> (100). Anal. Calcd for C<sub>57</sub>H<sub>61</sub>BN<sub>4</sub>O<sub>4</sub>·H<sub>2</sub>O: C, 76.50; H, 7.10; N, 6.26. Found: C, 76.37; H, 6.79; N, 6.00.

**Compound (35)**



To a degassed solution of **33** (0.031 g, 0.082 mmol) and **29** (0.060 g, 0.068 mmol), in DMF (3mL) and NEt<sub>3</sub> (2mL), was added [Pd(PPh<sub>3</sub>)<sub>4</sub>] (0.008 g, 0.0068 mmol). The mixture was stirred at 80 °C for 10 hours. The mixture was then evaporated, the residue was separated by column chromatography of the residue on silica gel [MeOH/CH<sub>2</sub>Cl<sub>2</sub>, 1/9, then H<sub>2</sub>O/EtOH, 2/8] afforded compound **35** (0.040 g, 52%). <sup>1</sup>H NMR (400MHz, CD<sub>3</sub>OD): δ 9.11 (d, J = 9.50 Hz, 1H), δ 8.66 (d, J = 9.30 Hz, 1H), δ 8.56 (d, J = 8.30 Hz, 1H), δ 8.21-8.13 (m, 5H), δ 7.85 (d, J = 7.70 Hz, 2H), δ 7.38 (d, J = 7.80 Hz, 2H), δ 4.58 (t, J = 5.00 Hz, 2H), δ 4.25 (s, 4H), δ 3.89 (t, J = 4.80 Hz, 2H), δ 3.59-3.46 (m, 6H), δ 3.30 (s, 3H), δ 3.09 (s, 12H), δ 2.77 (t, J = 7.20 Hz, 4H), δ 2.68 (s, 6H), δ 2.34 (q, J = 8.70 Hz, 4H), δ 2.16 (m, 4H), δ 1.39 (s, 6H), δ 0.95 (t, J = 7.80 Hz, 6H).

### Compound (36)

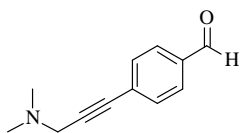


To a solution of **35** (0.060 g, 0.068 mmol), in EtOH (2mL) and H<sub>2</sub>O (1mL), was added NaOH (0.027 g, 0.68 mmol). The mixture was stirred at room temperature for 10 hours until complete consumption of the starting material was observed by TLC (H<sub>2</sub>O/EtOH, 20: 80). The solution was then added HCl (10%) until neutral, then evaporated. The crude product was purified by column chromatography on silica gel (H<sub>2</sub>O/EtOH, 10:90). The powder was dried in vacuum, gave compound **36** (0.020g, 30%). <sup>1</sup>H RMN (CD<sub>3</sub>OD 200 MHz) : 1.01 (t, 6H, J = 7,30 Hz), 1,45 (s, 6H), 2.04-2.22 (m, 8H), 2,74-2,86 (m, 9H), 3,14 (s, 12H), 3,59 (m, 5H), 4,30 (s, 4H), 7,43 (d, 2H, J = 8,40 Hz), 7,90 (d, 2H, J = 8,40 Hz), 8.10-8,27 (m, 6H), 8,66 (d, 1H, J = 9,14 Hz), 8,84 (d, 1H, J = 9,12 Hz). MS (FAB+, m-NBA): m/z (%) = 1041.46 [M + Na]<sup>+</sup> (100).

## CHAPTER III

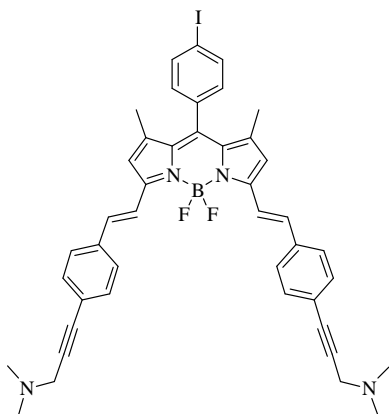
Compound **40** and **46** were prepared by laboratory of COBRA at Rouen University.

## 4-[3-(dimethylamino)-1-propyn-1-yl]-benzaldehyde



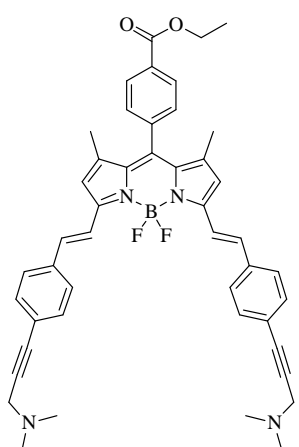
To a degassed solution of 4-bromobenzaldehyde (1.0 g, 5.40 mmol) in benzene (3 mL) and TEA (3 mL), were added  $[Pd(PPh_3)_4]$  (0.360 g, 0.324 mmol) and 1-dimethylamino-2-propyne (0.672 g, 8.10 mmol) under argon.

The mixture was stirred at 60 °C for 10 hours until the complete consumption of the starting material was observed by TLC. The mixture was then evaporated, and a chromatography on silica gel ( $CH_2Cl_2$  100%, and then MeOH /  $CH_2Cl_2$  ether, 3: 97,) afforded the compound (1.134 g, 100%).  $^1H$  NMR (200MHz,  $CDCl_3$ ):  $\delta$  10.00 (s, 1H), 7.82 (d,  $J = 8.26$  Hz, 2H), 7.58 (d,  $J = 8.28$  Hz, 2H), 3.54(s, 2H), 2.42 (s, 6H). MS (FAB<sup>+</sup>, m-NBA):  $m/z$  (%) = 188.1  $[M + H]^+$  (100). Anal. Calcd for  $C_{12}H_{13}NO$ : C, 76.98; H, 7.00; N, 7.48. Found: C, 76.64; H, 6.82; N, 7.17.

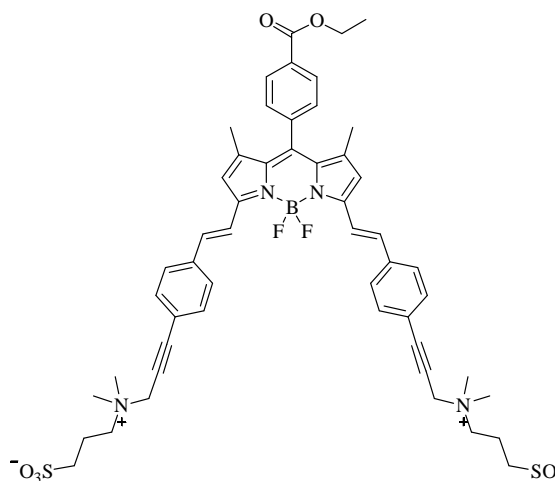
Compound (**37**)

A mixture of compounds **17** (500 mg, 1.11 mmol) and 4-[3-(dimethylamino)-1-propyn-1-yl]-benzaldehyde (415 mg, 2.22 mmol) solubilised in toluene (20 mL) and piperidine (0.5 mL) was heated at 140°C in a Dean–Stark apparatus for 2 h, then removed the Dean-stark apparatus and continued heating under Argon until the solvent was totally evaporated. The crude product was treated with saturated  $NaHCO_3$  solution and water, extracted with  $CH_2Cl_2$ .

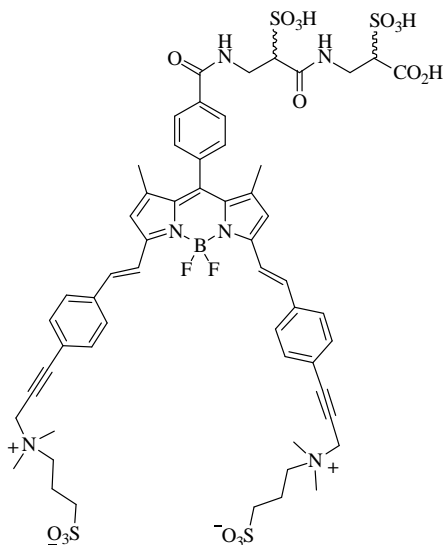
The organic layer was dried with  $MgSO_4$  then evaporated, a column Chromatography on silica gel (MeOH /  $CH_2Cl_2$ , 3: 97 to 7:93) afforded the compound **37** (193 mg, 22%).  $^1H$  NMR (300MHz,  $CDCl_3$ ):  $\delta$  7.86 (d,  $J = 7.7$  Hz, 2H), 7.71 (d,  $J = 16.3$  Hz, 2H), 7.56 (d,  $J = 7.9$  Hz, 4H), 7.46 (d,  $J = 7.8$  Hz, 4H), 7.22 (d,  $J = 16.4$  Hz, 2H), 7.08 (d,  $J = 7.7$  Hz, 2H), 6.65 (s, 2H), 3.52(s, 4H), 2.40 (s, 12H), 1.48(s, 6H).  $^{13}C$  NMR (75 MHz,  $CDCl_3$ ):  $\delta = 152.9, 142.2, 138.6, 136.4, 135.9, 134.8, 133.5, 130.6, 127.6, 123.8, 119.9, 118.4, 95.1, 86.7, 85.7, 48.9, 44.5, 15.2$ . MS (FAB<sup>+</sup>, m-NBA):  $m/z$  (%) = 788.2  $[M + H]^+$  (100). Anal. Calcd for  $C_{43}H_{40}BF_2IN_4$ : C, 65.50; H, 5.11, N, 7.11. Found: C, 65.22; H, 4.64; N, 6.82.

**Compound (38)**

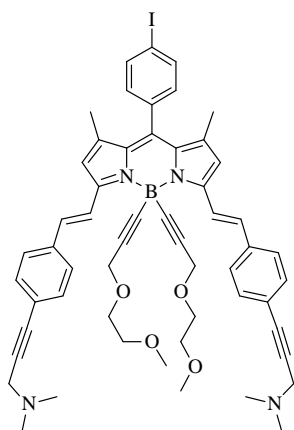
To a stirred solution of **37** (100mg, 0.124 mmol) dissolved in EtOH absolute (4 mL) and NEt<sub>3</sub> (3 mL) was added Pd(PPh<sub>3</sub>)<sub>2</sub>Cl<sub>2</sub> (9 mg, 0.012 mmol), the CO gas was bubbled for 4 hours at 60C° until the complete consumption of the starting material was observed by TLC. The mixture was treated with saturated NaHCO<sub>3</sub> solution and water, extracted with CH<sub>2</sub>Cl<sub>2</sub>. The organic layer was dried with MgSO<sub>4</sub>. The solvent was then removed and the crude product was purified by column chromatography on silica (MeOH/CH<sub>2</sub>Cl<sub>2</sub>, 7: 93), afforded the compound **38** (78 mg, 85%). <sup>1</sup>H NMR (300MHz, CDCl<sub>3</sub>): δ 8.18 (d, J = 8.1 Hz, 2H), 7.70 (d, J = 16.4 Hz, 2H), 7.54 (d, J = 8.1 Hz, 4H), 7.43 (d, J = 8.1 Hz, 4H), 7.42 (d, J = 7.7 Hz, 2H), 7.20 (d, J = 16.2 Hz, 2H), 6.62(s, 2H), 4.41 (q, J = 7.2 Hz, 2H), 3.51(s, 4H), 2.39 (s, 12H), 1.42 (t, J = 7.3 Hz, 3H), 1.40(s, 6H). <sup>13</sup>C NMR (75 MHz, CDCl<sub>3</sub>): δ = 166.2, 152.9, 142.2, 139.9, 137.9, 136.4, 133.4, 132.3, 131.4, 130.5, 128.9, 127.6, 123.7, 120.0, 118.5, 86.3, 85.9, 61.6, 48.9, 46.4, 44.4, 15.0, 14.5. MS (FAB<sup>+</sup>, m-NBA): m/z (%) = 735.4 [M + H]<sup>+</sup> (100).

**Compound (39)**

To a solution of **38** (62mg, 0.084 mmol) in dry DMF (3 mL), the 1,3-propane sultone (103 mg, 0.844mmol) was added, then the mixture was stirred at 60°C over night, until the complete consumption of the starting material was observed by TLC (H<sub>2</sub>O/EtOH, 20: 80). The mixture was then centrifuged, the crude product was purified by column chromatography on silica gel (H<sub>2</sub>O/EtOH, 30: 70) and recrystallized from methanol/ AcOEt afforded **39** (36 mg, 60%). <sup>1</sup>H NMR (300MHz, MeOH/CDCl<sub>3</sub>): δ = 8.03 (d, J = 8.2 Hz, 2H), 7.56 (d, J = 16.3 Hz, 4H), 7.44 (d, J = 8.1 Hz, 4H), 7.36 (d, J = 8.3 Hz, 4H), 7.29 (d, J = 8.2 Hz, 2H), 7.08 (d, J = 16.2 Hz, 4H), 6.52(s, 2H), 4.31 (s, 4H), 4.27(m, 2H), 3.05(s, 12H), 2.75(m, 4H), 2.09(m, 4H), 1.27(m, 9H). MS (FAB<sup>+</sup>, m-NBA): m/z (%) = 979.4 [M + H]<sup>+</sup> (100).

**Compound (40)**

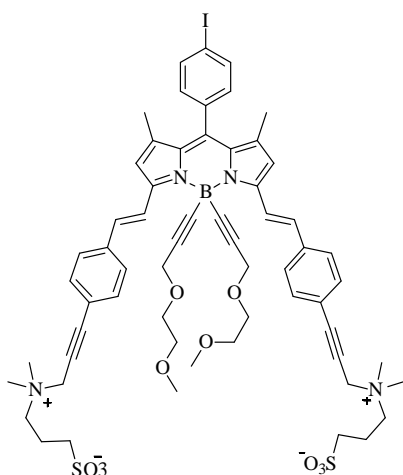
Synthesis was accomplished at COBRA.

**Compound (41)**

To a solution of 3-(2-methoxyethoxy)-1-propyne, (68 mg, 0.60 mmol) in dry THF (5 mL) under argon in a schlenk flask, was added 1.0 M EtMgBr in THF (0.52 mL) and stirred at 60 °C for one hour. The resulting anion was then transferred via cannula to the solution of **37** (120mg, 0.15 mmol) dissolved in a separate schlenk flask in dry THF (3 mL) under argon. The mixture was stirred at 60 °C for about 15 minutes, until complete consumption of the starting material was observed by TLC, then H<sub>2</sub>O (3mL) was added. The mixture was then washed with water, brine then extracted with CH<sub>2</sub>Cl<sub>2</sub>, the organic layer was dried on MgSO<sub>4</sub> then evaporated. The

crude product was purified by column chromatography on silica gel (MeOH/CH<sub>2</sub>Cl<sub>2</sub>, 7: 93) afforded **41** (104 mg, 70%). <sup>1</sup>H NMR (300MHz, CDCl<sub>3</sub>): δ 8.21 (d, J = 16.5 Hz, 2H), 7.86 (d, J = 7.7 Hz, 2H), 7.58 (d, J = 8.0 Hz, 4H), 7.48 (d, J = 8.1 Hz, 4H), 7.13 (m, 4H), 6.66(s, 2H), 4.15(s, 4H), 3.56(s, 4H), 3.49(m, 4H), 3.20(s, 6H), 3.16(m, 4H), 2.43(s, 12H), 1.47(s, 6H). <sup>13</sup>C NMR (75 MHz, CDCl<sub>3</sub>): δ = 152.0, 140.7, 138.5, 137.0, 135.1, 133.8, 132.5, 130.7, 127.4, 123.4, 121.8, 118.7, 92.1, 86.0, 68.5, 59.0, 48.7, 44.2, 29.9, 15.4. MS (FAB<sup>+</sup>, m-NBA): m/z (%) = 977.2 [M + H]<sup>+</sup> (100). Anal. Calcd for C<sub>55</sub>H<sub>58</sub>BN<sub>4</sub>O<sub>4</sub>·H<sub>2</sub>O: C, 66.40; H, 6.08; N, 5.63. Found: C, 66.12; H, 5.74; N, 5.44.

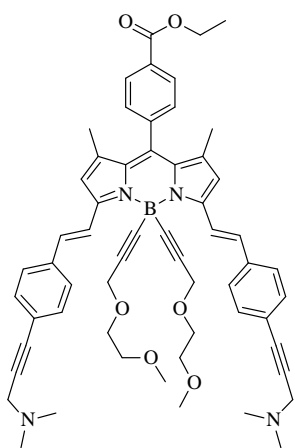
## Compound (42)



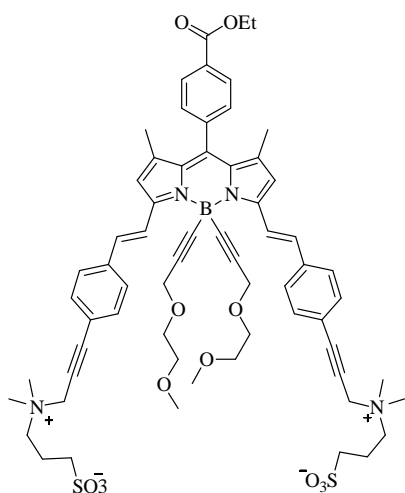
To a solution of **41** (50mg, 0.050 mmol) in dry toluene (3 mL), the 1,3-propane sultone (30 mg, 0.2mmol) was added, then the mixture was stirred at 60°C for 10 hours, until the complete consumption of the starting material was observed by TLC (H<sub>2</sub>O/EtOH, 20: 80). The mixture was centrifuged and then washed with ethyl ether, the residue was recrystallized twice from methanol/ AcOEt. The powder was dried in vacuum, afforded **42** (30 mg, 47%). <sup>1</sup>H NMR (300MHz, MeOH/CDCl<sub>3</sub>): δ 8.24 (d, J = 16.4 Hz, 2H), 7.85 (d, J = 8.3 Hz, 2H), 7.62 (d, J = 8.3 Hz, 4H), 7.54 (d, J = 8.4 Hz, 4H), 7.14

(d, J = 16.3 Hz, 4H), 7.09 (d, J = 8.3 Hz, 2H), 6.67(s, 2H), 4.47(s, 4H), 4.09(s, 4H), 3.69(m, 4H), 3.42 (m, 4H), 3.21 (s, 12H), 3.14 (m, 10H), 2.91 (m, 4H), 2.24 (m, 4H), 1.46 (s, 6H). <sup>13</sup>C NMR (75 MHz, MeOH/CDCl<sub>3</sub>): δ = 151.9, 141.4, 138.7, 133.1, 130.7, 127.7, 123.1, 122.0, 120.2, 119.1, 111.3, 95.2, 92.6, 59.6, 58.8, 57.3, 55.8, 42.5, 19.4, 15.3. MS (ESI-MS positif mode): m/z (%) = 1221.2 (100), 611.2 (25, doubly charged). Anal. Calcd for: C<sub>61</sub>H<sub>70</sub>BN<sub>4</sub>O<sub>10</sub>S<sub>2</sub>·H<sub>2</sub>O: C, 59.13; H, 5.86; N, 4.52; Found: C, 59.04; H, 5.61; N 4.47.

## Compound (43)

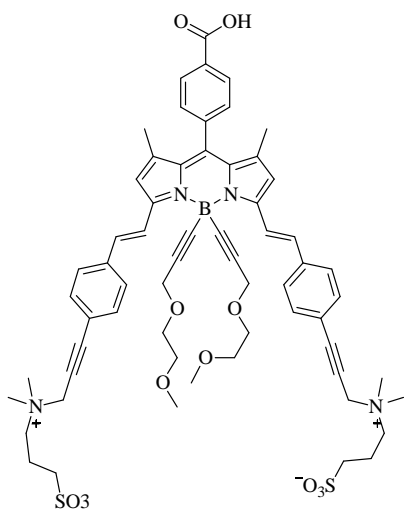


To stirred solution of compound **41** (104mg, 0.105 mmol) in EtOH absolute (4 mL) and NEt<sub>3</sub> (3 mL) was added Pd(PPh<sub>3</sub>)<sub>2</sub>Cl<sub>2</sub> (8 mg, 0.01 mmol), and the CO gas was bubbled at 60°C for 5 hours. Then the solvent was removed, and a column chromatography on silica gel (MeOH/CH<sub>2</sub>Cl<sub>2</sub>, 7: 93) afforded **43** (116 mg, 100%). <sup>1</sup>H NMR (300MHz, CDCl<sub>3</sub>): δ 8.24 (d, J = 16.3 Hz, 2H), δ 8.19 (d, J = 8.5 Hz, 2H), 7.58 (d, J = 8.3 Hz, 4H), 7.48 (d, J = 8.3 Hz, 4H), 7.46 (d, J = 7.9 Hz, 2H), 7.13 (d, J = 16.5 Hz, 2H), 6.65(s, 2H), 4.43 (q, J = 7.2 Hz, 2H), 4.15(s, 4H), 3.59(s, 4H), 3.49(m, 4H), 3.20(s, 6H), 3.16(m, 4H), 2.46(s, 12H), 1.45 (t, J = 7.3 Hz, 3H), 1.41(s, 6H). <sup>13</sup>C NMR (75 MHz, CDCl<sub>3</sub>): δ = 166.2, 152.1, 140.7, 140.3, 138.3, 132.5, 131.3, 130.4, 129.1, 127.4, 123.2, 121.9, 118.8, 92.1, 86.4, 85.4, 61.6, 59.6, 59.0, 48.7, 46.0, 44.1, 29.9, 15.2, 14.5, 8.8. MS (FAB<sup>+</sup>, m-NBA): m/z (%) = 922.4 [M + H]<sup>+</sup> (100). Anal. Calcd for C<sub>58</sub>H<sub>63</sub>BN<sub>4</sub>O<sub>6</sub>·H<sub>2</sub>O: C, 74.03; H, 6.96; N, 5.95; Found: C, 73.78, H, 6.70, N, 5.66.

**Compound (44)**

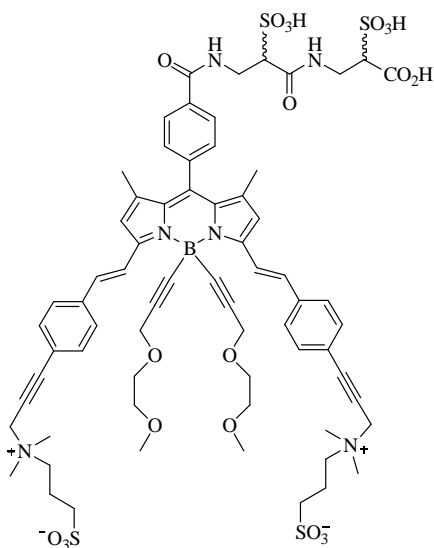
To a solution of **43** (50mg, 0.054 mmol) in dry  $C_2H_4Cl_2$  (3 mL) under argon, the 1,3-propane sultone (66 mg, 0.542mmol) was added, then the mixture was stirred at  $60^\circ C$  over night, until the complete consumption of the starting material was observed by TLC ( $H_2O/EtOH$ , 20: 80). The mixture was then centrifuged, the crude product was purified by column chromatography on silica gel ( $H_2O/EtOH$ , 30:70) and recrystallized from methanol/AcOEt afforded **44** (36 mg, 60%).  $^1H$  NMR (300MHz, MeOH/ $CDCl_3$ ):  $\delta$  8.24 (d,  $J = 16.4$  Hz, 2H),  $\delta$  8.16 (d,  $J = 8.1$  Hz, 2H), 7.61 (d,  $J = 8.2$  Hz, 4H), 7.55 (d,  $J = 8.2$  Hz, 4H), 7.44 (d,  $J = 8.3$  Hz, 2H), 7.14 (d,

$J = 16.2$  Hz, 2H), 6.67(s, 2H), 4.49 (s, 4H), 4.39 (q,  $J = 7.3$  Hz, 2H), 4.09(s, 4H), 3.69(m, 4H), 3.28(m, 4H), 3.21(s, 12H), 3.14(m, 10H), 2.90(m, 4H), 2.24(m, 4H), 1.39(m, 9H).  $^{13}C$  NMR (75 MHz, MeOH/ $CDCl_3$ ):  $\delta = 166.2, 151.5, 140.8, 139.8, 138.5, 132.9, 131.5, 130.9, 130.1, 128.7, 127.2, 122.5, 119.9, 118.6, 91.8, 67.9, 63.1, 61.4, 59.1, 58.2, 55.3, 41.9, 18.7, 14.7, 13.9$ . MS (FAB<sup>+</sup>, m-NBA):  $m/z$  (%) = 1167.5 [M + H]<sup>+</sup> (100).

**Compound (45)**

To a solution of compound **44** (36mg, 0.03 mmol), in EtOH (2mL) and  $H_2O$  (1mL), were added NaOH (12 mg, 0.3 mmol). The mixture was stirred at RT over night, until complete consumption of the starting material was observed by TLC ( $H_2O/EtOH$ , 30: 70). To the solution was added HCl (2%) until neutral, then addition of AcOEt led to precipitation and then centrifuged. The crude was recrystallized twice from methanol/AcOEt, gave **45** (30 mg, 88%).  $^1H$  NMR (200MHz, MeOH/ $CDCl_3$ ):  $\delta$  8.35-8.14 (m, 4H),  $\delta$  7.65 (m, 8H), 7.40-7.24 (m, 4H), 6.79 (s, 2H), 4.63 (s, 4H), 4.11 (s, 4H), 3.72 (m, 4H),

3.48 (m, 4H), 3.28 (m, 12H), 3.15 (m, 10H), 2.90 (m, 4H), 2.30 (m, 4H), 1.43 (m, 6H).  $^{13}C$  NMR (50 MHz, MeOH/ $CDCl_3$ ):  $\delta = 152.8, 142.2, 140.0, 133.8, 128.3, 124.8, 92.8, 72.4, 70.3, 69.1, 59.9, 56.3, 30.3, 26.4, 20.0, 15.2$ . MS (ESI-MS positif mode):  $m/z$  (%) = 1139.3(100) [M + H]<sup>+</sup>; 570.2 (35 doubly charged). Anal. Calcd for:  $C_{62}H_{71}BN_4O_{12}S_2 \cdot H_2O$ : C, 64.35; H, 6.36; N, 4.84; Found: C, 64.62; H, 6.38; N, 4.72.

**Compound (46)**

The synthesis was accomplished at laboratory COBRA. (a) Preparation of N-hydroxysuccinimidyl ester: BODIPY carboxylic acid **45** (6.2 mg, 4.5  $\mu\text{mol}$ ) was dissolved in dry NMP (200  $\mu\text{L}$ ). 350  $\mu\text{L}$  of a solution of TSTU reagent in dry NMP (10.0 mg, 33.2  $\mu\text{mol}$ ) and 9  $\mu\text{L}$  of a 2.0 M solution of DIEA in dry NMP (18  $\mu\text{mol}$ ) were added and the resulting reaction mixture was protected from light and stirred at room temperature for 1 h. The reaction was checked for completion by RP-HPLC (system B) and ESI-MS. The resulting N-hydroxysuccinimidyl ester was used in the next coupling step

without purification. HPLC (system B):  $t_R = 16.3$  min (compared to  $t_R = 15.1$  min for BODIPY carboxylic acid **45**); MS (ESI<sup>+</sup>):  $m/z$  1236.47 [M + H]<sup>+</sup>, calcd for C<sub>66</sub>H<sub>74</sub>BN<sub>5</sub>O<sub>14</sub>S<sub>2</sub> :1236.27.

(b) Coupling reaction:  $\alpha$ -sulfo- $\beta$ -alaninyl- $\alpha$ -sulfo- $\beta$ -alanine (22 mg, 40.7  $\mu\text{mol}$ ) was dissolved in 0.24 M aq. NaHCO<sub>3</sub> buffer (pH 8.2, 500  $\mu\text{L}$ ) and the resulting solution was cooled to 4 °C. The crude solution of N-hydroxysuccinimidyl ester in NMP was added dropwise to this stirred solution. The resulting reaction mixture was left at 4°C overnight. The reaction was checked for completion by RP-HPLC. (System C). Finally, the reaction mixture was quenched by dilution with aq. TEAB (50 mM, pH 7.5) and purified by RP-HPLC (system D, 1 injection,  $t_R = 22.7$ -25.0 min). The product-containing fractions were lyophilised to give the TEA salt of water-soluble BODIPY **46**. Desalting by ion-exchange chromatography (followed by lyophilisation) afforded the acid form of **46** as a blue amorphous powder (3.0 mg, yield 47%, mixture of two racemic diastereomers).  $\delta$ H(300 MHz; DMSO-d<sub>6</sub>) 8.17 (2 H, d, J 16.3, -CH=CH-BODIPY), 7.97 (2 H, m, Ph-BODIPY), 7.70 (10 H, m, Ph-BODIPY), 7.55 (m, 4 H, -CH=CH-BODIPY and Ph-BODIPY), 7.02 (2 H, s, pyrrole-BODIPY), 4.64 (4 H, s, 2  $\times$  N-CH<sub>2</sub>-C $\equiv$ C-), 4.05 (4 H, s, 2  $\times$  O-CH<sub>2</sub>-C $\equiv$ C-), 3.79-3.37 (14 H, m, 2  $\times$  CH<sub>2</sub>-CH(SO<sub>3</sub>H)-CO-, 2  $\times$  N-CH<sub>2</sub>-(CH<sub>2</sub>)<sub>2</sub>-SO<sub>3</sub>- and 2  $\times$  O-CH<sub>2</sub>-CH<sub>2</sub>-O), 3.15 (12 H, s, 2  $\times$  -N(CH<sub>3</sub>)<sub>2</sub>-(CH<sub>2</sub>)<sub>2</sub>-SO<sub>3</sub>-), 3.12 (4 H, m, 2  $\times$  O-CH<sub>2</sub>-CH<sub>2</sub>-O), 3.06 (6 H, s, 2  $\times$  OCH<sub>3</sub>), 2.54 (4 H, m, 2  $\times$  N-(CH<sub>2</sub>)<sub>2</sub>-CH<sub>2</sub>-SO<sub>3</sub>-), partially masked by DMSO peak), 2.05 (4 H, m, 2  $\times$  N-CH<sub>2</sub>-CH<sub>2</sub>-CH<sub>2</sub>-SO<sub>3</sub>-), 1.41 (6 H, s, 2  $\times$  CH<sub>3</sub>, BODIPY); (ESI<sup>+</sup>):  $m/z$  1442.07 [M + H]<sup>+</sup>, MS (ESI<sup>-</sup>):  $m/z$  1439.40 [M - H]<sup>-</sup>, calcd for C<sub>68</sub>H<sub>81</sub>BN<sub>6</sub>O<sub>20</sub>S<sub>4</sub> : 1441.47; HPLC (system C):  $t_R = 9.7$  min, purity 92%;  $\lambda_{\text{max}}$ (PBS)/nm 368 ( $\epsilon/\text{dm}^3 \text{ mol}^{-1} \text{ cm}^{-1}$  76,860), 642 ( $\epsilon/\text{dm}^3 \text{ mol}^{-1} \text{ cm}^{-1}$  55,080).

Fluorescent labelling of proteins.

(a) Conversion of water-soluble BODIPY **46** into amine-reactive derivative: the water-soluble BODIPY dye carboxylic acid (0.54 mg, 0.37  $\mu\text{mol}$ , weighed in a 0.5 mL Eppendorf tube) was dissolved in deionised water (50  $\mu\text{L}$ ). 30  $\mu\text{L}$  of an aq. solution of water-soluble carbodiimide (EDC, 1-ethyl-3-(3-dimethylaminopropyl) carbodiimide hydrochloride, 1.06 mg, 5.55  $\mu\text{mol}$ ) and 10  $\mu\text{L}$  of an aq. solution of sulfo-NHS (0.17 mg, 0.78  $\mu\text{mol}$ ) were sequentially added and the resulting reaction mixture was protected from light and periodically vortexed. The reaction was checked for completion by RP-HPLC (system C). The resulting N-hydroxysulfosuccinimidyl ester was used in the next labelling step without purification. HPLC (system C):  $t_R = 10.3$  min (compared to  $t_R = 9.7$  min for water-soluble BODIPY carboxylic acid **45**).

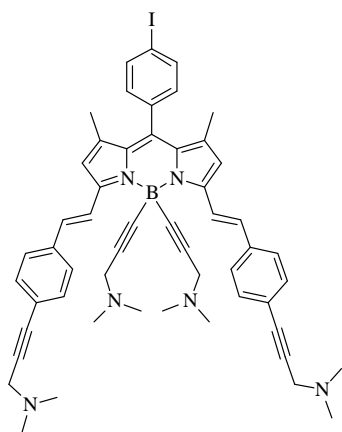
(b) Labelling of antibodies: 45  $\mu\text{L}$  of the solution of N-hydroxysulfosuccinimidyl ester (vide supra, 185 nmol, 31-fold excess) was added to a 500  $\mu\text{L}$  solution of anti-HA antibodies (1.8 mg/mL, 6 nmol) in phosphate buffer (pH 7.4). The resulting mixture was protected from the light and periodically vortexed. The reaction was left at 4  $^\circ\text{C}$  overnight. Thereafter, BODIPY-mAb conjugate was purified by size-exclusion chromatography (vide supra). The number of BODIPY per antibody (molar ratio, F/P) was determined spectrophotometrically by measuring their absorbance at 280 and 642 nm and inserting the measured values into the following equation:

$$F/P = A_{\text{max}}^P \epsilon_{280} / (A_{280}^F \epsilon_{\text{max}} + A_{\text{max}}^F \epsilon_{280})$$

Where  $A_{280}$  is the absorbance of the protein at 280 nm,  $P\epsilon_{280}$  is the extinction coefficient of the protein at 280 nm,  $A_{\text{max}}$  is the absorbance of the BODIPY label as its absorption maximum,  $F\epsilon_{\text{max}}$  is the extinction coefficient of the fluorophore at the absorption maximum, and  $F\epsilon_{280}$  is the extinction coefficient of the fluorophore at 280 nm. Anti-HA antibodies have an extinction coefficient at 280 nm of  $2.95 \times 10^5 \text{ dm}^3 \text{ mol}^{-1} \text{ cm}^{-1}$ .

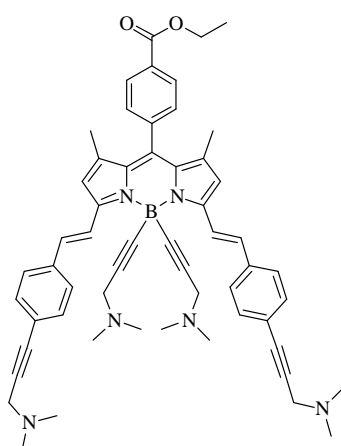
(c) Labelling of BSA: 45  $\mu\text{L}$  of the solution of N-hydroxysulfosuccinimidyl ester (vide supra, 185 nmol, 13-fold excess) was added to a 500  $\mu\text{L}$  solution of BSA (1.8 mg/mL, 13 nmol) in phosphate buffer (pH 7.4). The resulting mixture was protected from the light and periodically vortexed. The reaction was left at 4  $^\circ\text{C}$  overnight. Thereafter, BODIPY-BSA conjugate was purified by size-exclusion chromatography (vide supra). The BODIPY per protein ratio (F/P) was determined spectrophotometrically by measuring their absorbance at 280 and 642 nm and using the same equation described above. BSA protein has an extinction coefficient at 280 nm of  $43\,824 \text{ dm}^3 \text{ mol}^{-1} \text{ cm}^{-1}$ .

Further fluorescent labelling experiments were performed with sulfoindocyanine dye Cy 5.0 ( $F\epsilon_{\text{max}} = 2.5 \times 10^5 \text{ dm}^3 \text{ mol}^{-1} \text{ cm}^{-1}$ ) under the same conditions.

**Compound (47)**

To stirred solution of 1-dimethylamino-2-propyne (52 mg, 0.62 mmol) in dry THF (3 mL) under argon in a schlenk flask, was added 1.0 M EtMgBr in THF (0.435 mL) and stirred at 60 °C for one hour. The resulting anion was then transferred via cannula to the solution of **37** (100 mg, 0.124 mmol) dissolved in a separate schlenk flask in dry THF (3 mL) under argon. The mixture was stirred at 60 °C for 15 minutes until the complete consumption of the starting material was observed by TLC. Then the mixture was treated with water and brine, and then extracted with CH<sub>2</sub>Cl<sub>2</sub>. The

organic layer was dried with MgSO<sub>4</sub> then evaporated. The crude product was purified by column chromatography on aluminium oxide (MeOH/CH<sub>2</sub>Cl<sub>2</sub>, 3: 97) afforded **47** (114 mg, 100%). <sup>1</sup>H NMR (300MHz, CDCl<sub>3</sub>): δ 8.39 (d, J = 16.4 Hz, 2H), δ 7.86 (d, J = 8.2 Hz, 2H), δ 7.61 (d, J = 8.2 Hz, 4H), 7.47 (d, J = 8.0 Hz, 4H), 7.15 (d, J = 16.6 Hz, 2H), 7.11 (d, J = 8.1 Hz, 2H), 6.67 (s, 2H), 3.53 (s, 4H), 3.20 (s, 4H), 2.42(s, 12H), 2.20 (s, 12H), 1.47 (s, 6H). <sup>13</sup>C NMR (75 MHz, CDCl<sub>3</sub>): δ = 151.8, 140.3, 138.2, 137.8, 136.8, 135.1, 133.4, 132.1, 131.8, 130.6, 127.2, 123.3, 122.0, 118.5, 94.8, 90.8, 86.5, 85.4, 48.9, 48.7, 44.3, 34.1, 29.7, 22.4, 15.2, 14.1. MS (FAB<sup>+</sup>, m-NBA): m/z (%) = 915.2 [M + H]<sup>+</sup> (100). Anal. Calcd for C<sub>53</sub>H<sub>56</sub>BN<sub>6</sub>·H<sub>2</sub>O: C, 66.95; H, 6.36; N, 8.84. Found: C, 66.78, H, 6.21, N, 8.64.

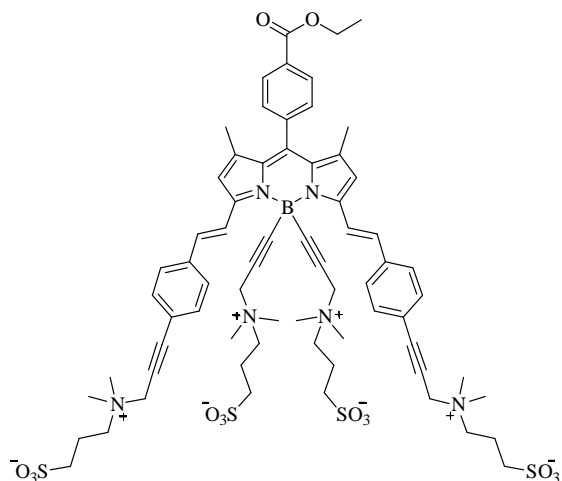
**Compound (48)**

To stirred solution of compound **47** (100 mg, 0.109 mmol) in EtOH absolute (4 mL) and NEt<sub>3</sub> (3 mL) was added Pd(PPh<sub>3</sub>)<sub>2</sub>Cl<sub>2</sub> (8 mg, 0.011 mmol), the CO gas was bubbled for 5 hours at 60°C until the complete consumption of the starting material was observed by TLC. The mixture was treated with saturated NaHCO<sub>3</sub> solution and water, extracted with CH<sub>2</sub>Cl<sub>2</sub>. The organic layer was dried with MgSO<sub>4</sub>. After the solvent was removed, the crude product was purified by column chromatography on

aluminium oxide (MeOH/CH<sub>2</sub>Cl<sub>2</sub>, 3: 97) afforded the compound **48** (80 mg, 85%). <sup>1</sup>H NMR (300MHz, CDCl<sub>3</sub>): δ 8.35 (d, J = 16.3 Hz, 2H), δ 8.17 (d, J = 8.1 Hz, 2H), 7.57 (d, J = 8.4 Hz, 4H), 7.43 (dd, 6H), 7.06 (d, J = 16.3 Hz, 2H), 6.64 (s, 2H), 4.41 (q, J = 7.4 Hz, 2H), 3.49 (s, 4H), 3.17 (s, 4H), 2.37(s, 12H), 2.17 (s, 12H), 1.42 (t, J = 7.2 Hz, 3H), 1.39 (s, 6H). <sup>13</sup>C NMR (75 MHz, CDCl<sub>3</sub>):

$\delta = 166.0, 151.9, 140.3, 138.0, 136.8, 133.4, 132.1, 131.5, 128.9, 127.2, 123.3, 122.0, 118.5, 90.7, 86.6, 85.4, 61.4, 48.9, 44.3, 29.7, 15.0, 14.3$ . MS (FAB<sup>+</sup>, m-NBA):  $m/z$  (%) = 860.3 [M + H]<sup>+</sup> (100). Anal. Calcd for C<sub>56</sub>H<sub>61</sub>BN<sub>6</sub>O<sub>2</sub>·H<sub>2</sub>O: C, 76.52; H, 7.22; N, 9.56; Found: C, 76.22, H, 6.89, N, 9.37.

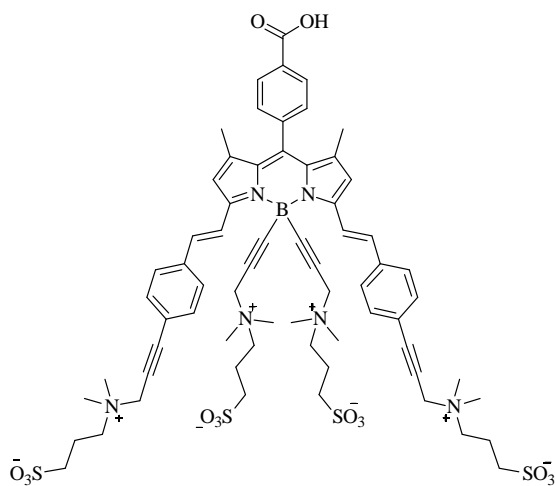
### Compound (49)



To a solution of **48** (88mg, 0.102 mmol) in distilled DMF (2mL), was added the 1,3-propane sultone (250 mg, 2.05 mmol). The mixture was stirred at 60°C for 10 hours. Then addition of AcOEt led to precipitation and then centrifuged. The residue was purified by column chromatography on silica C18, (THF/H<sub>2</sub>O, 15: 85), afforded **49** (60 mg, 43%). <sup>1</sup>H NMR (400MHz, CD<sub>3</sub>OD/D<sub>2</sub>O, internal reference : *t*-BuOH):  $\delta$  8.31 (d, J = 8.40 Hz, 2H),

8.22 (d, J = 16.20 Hz, 2H), 7.84 (s, 8H), 7.58 (d, J = 16.2 Hz, 2H), 7.04 (s, 2H), 4.66 (s, 4H), 4.50 (q, J = 7.20 Hz, 2H), 4.36 (s, 4H), 3.82(m, 4H), 3.50 (m, 4H), 3.35 (s, 12H), 3.04 (s, 16H), 2.70 (m, 4H), 2.39 (m, 4H), 2.14 (m, 4H), 1.56 (s, 6H), 1.50 (t, J = 7.20 Hz, 3H). <sup>13</sup>C NMR (100MHz, CD<sub>3</sub>OD/D<sub>2</sub>O):  $\delta = 153.0, 143.5, 139.1, 136.3, 134.5, 132.9, 131.6, 130.2, 128.6, 122.7, 120.5, 92.6, 79.2, 64.2, 63.8, 62.8, 56.6, 20.1, 15.2, 14.6$ . MS (FAB<sup>+</sup>, m-NBA):  $m/z$  (%) = 1349.6 [M + H]<sup>+</sup> (100).

### Compound (50)

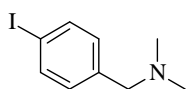


To a solution of compound **49** (60mg, 0.04 mmol), in EtOH (2mL) and H<sub>2</sub>O (0.5mL), was added NaOH (18 mg, 0.4 mmol). The mixture was stirred at RT for 10 hours until complete consumption of the starting material was observed by TLC (H<sub>2</sub>O/EtOH, 30: 70). The solution was then added HCl solution (2%) until neutral, then addition of AcOEt led to precipitation and then centrifuged, the residue was purified by column chromatography on silica C18, (THF/H<sub>2</sub>O, 5: 95), afforded **50** (15 mg, 25%).

<sup>1</sup>H NMR (200MHz, CD<sub>3</sub>OD/D<sub>2</sub>O, internal reference : *t*-BuOH):  $\delta$  8.26 (d, J = 16.2 Hz, 2H), 8.20 (d, J = 7.9 Hz, 2H), 7.98 (s, 8H), 7.61(d, J = 16.2 Hz, 2H), 7.41(d, J = 8.3 Hz, 2H), 6.99 (s, 2H), 4.67 (s, 4H), 4.37 (s, 4H), 3.80(m, 4H), 3.51 (m, 4H), 3.46 (s, 12H),

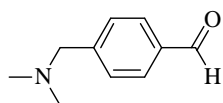
3.04 (s, 16H), 2.72 (m, 4H), 2.39 (m, 4H), 1.54 (s, 6H).  $^{13}\text{C}$  NMR (50MHz,  $\text{CD}_3\text{OD}/\text{D}_2\text{O}$ ):  $\delta$  = 153.2, 144.1, 142.3, 139.6, 138.0, 136.5, 135.0, 133.6, 131.8, 129.5, 123.1, 120.8, 93.0, 79.7, 64.6, 64.3, 57.1, 20.6, 15.6. MS (ESI-MS positif mode):  $m/z$  (%) = 1321.3  $[\text{M} + \text{H}]^+$  (100), 660.6 (50, double charged). Anal. Calcd for  $\text{C}_{66}\text{H}_{81}\text{BN}_6\text{O}_{14}\text{S}_4 \cdot \text{H}_2\text{O}$ : C, 59.18; H, 6.25; N, 6.27; Found: C, 58.99; H, 5.92; N 5.99.

### N-(4-iodobenzyl)-N,N-dimethylamine



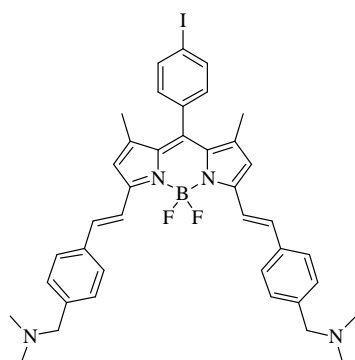
To a solution of 4-iodobenzyl bromide (2g, 6.7 mmol) dissolved in distilled THF (50 mL) under argon atmosphere, was added dimethylamine (1.7 mL, 0.01 mmol) and  $\text{K}_2\text{CO}_3$  (13.8g, 0.1 mmol). The mixture was stirred at reflux for 2 hours then cooled and filtered. The filtrate was treated with water and brine, the organic layer was extracted with  $\text{CH}_2\text{Cl}_2$  then dried. The solvent was removed to leave a white solid, which was purified by column chromatography on silica gel [ $(\text{CH}_2\text{Cl}_2$  pure, then  $(\text{MeOH}/\text{CH}_2\text{Cl}_2, 1/9)$ ] afforded the compound (1.63g, 93%).  $^1\text{H}$  NMR (200MHz,  $\text{CDCl}_3$ ):  $\delta$  7.64 (d,  $J = 8.4$  Hz, 2H),  $\delta$  7.06 (d,  $J = 8.04$  Hz, 2H), 3.35 (s, 2H), 2.22(s, 6H).

### 4-[(dimethylamino)methyl]-benzaldehyde



The compound N,N-dimethyl-N-(4-iodobenzyl)amine (500 mg, 1.92 mmol), dried sodium formate (156 mg, 2.30 mmol) and  $\text{Pd}(\text{PPh}_3)_2\text{Cl}_2$  (69 mg, 0.096 mmol) were dissolved in distilled DMF (10 mL), the mixture was stirred at  $96^\circ\text{C}$  for 4 hours under bubbled of CO gas at atmospheric pressure. Then the mixture was washed with water 3 times (200 mL), then extracted with AcOEt then dried with  $\text{MgSO}_4$ . After evaporation, the crude product was purified by column chromatography on aluminium oxide ( $\text{CH}_2\text{Cl}_2$  pure) afforded the compound (283 mg, 91%).  $^1\text{H}$  NMR (200MHz,  $\text{CDCl}_3$ ): 9.93(s, 1H),  $\delta$  7.77 (d,  $J = 8.04$  Hz, 2H),  $\delta$  7.42 (d,  $J = 8.04$  Hz, 2H), 3.43 (s, 2H), 2.20 (s, 6H).

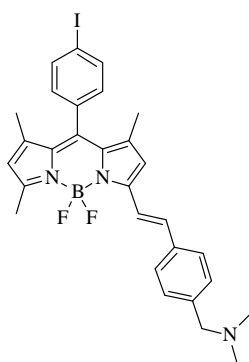
### Compound (51bis)



Compound **17** (450 mg, 0.696mmol) and 4-[(dimethylamino)methyl]-benzaldehyde (227 mg, 1.39 mmol) were dissolved in toluene (5 mL), and piperidine (0.5 mL) in a Dean-stark apparatus, the mixture was heated at  $140^\circ\text{C}$  for 2 h, then removed the Dean-stark apparatus and continued heating under argon until the solvent was totally evaporated. The crude product was treated with saturated  $\text{NaHCO}_3$  solution and water, extracted with  $\text{CH}_2\text{Cl}_2$ . The organic layer was dried with  $\text{MgSO}_4$  then evaporated. The residue was

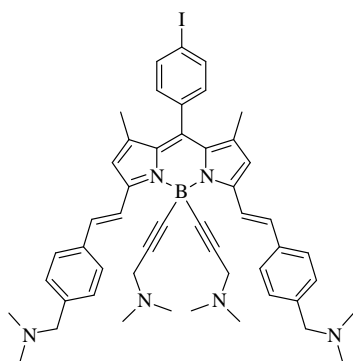
purified by column chromatography on aluminium oxide ( $\text{CH}_2\text{Cl}_2$  pure), afforded **51bis** (210 mg, 40%).  $^1\text{H}$  NMR (300MHz,  $\text{CDCl}_3$ ):  $\delta$  7.84 (d,  $J = 8.3$  Hz, 2H), 7.70 (d,  $J = 16.6$  Hz, 2H), 7.57 (d,  $J = 8.3$  Hz, 4H), 7.33 (d,  $J = 8.2$  Hz, 4H), 7.24 (d,  $J = 16.4$  Hz, 2H), 7.08 (d,  $J = 8.2$  Hz, 2H), 6.63(s, 2H), 3.49 (s, 4H), 2.27 (s, 12H), 1.47 (s, 6H).  $^{13}\text{C}$  NMR (75 MHz,  $\text{CDCl}_3$ ):  $\delta = 142.1, 138.5, 136.5, 135.8, 134.9, 130.7, 127.8, 119.2, 118.3, 64.0, 45.3, 29.9, 22.9, 15.2, 14.3$ . MS (FAB+, m-NBA):  $m/z$  (%) = 740.2  $[\text{M} + \text{H}]^+$  (100).

### Compound 51(mono)



Compounds 17 (355 mg, 0.79 mmol) and **50** (283 mg, 1.74 mmol) was dissolved in toluene 10 mL and piperidine 0.5 mL in a Dean–Stark apparatus, the mixture was heated at  $140^\circ\text{C}$  for 3 h, then removed the Dean-stark apparatus and continued heating under Argon until the solvent was totally evaporated. The crude product was treated with saturated  $\text{NaHCO}_3$  solution and water, extracted with  $\text{CH}_2\text{Cl}_2$ . The organic layer was dried with  $\text{MgSO}_4$  then evaporated. The crude product was purified by column Chromatography on silica gel ( $\text{CH}_2\text{Cl}_2$  pure, then  $\text{MeOH} / \text{CH}_2\text{Cl}_2$ , 3: 97) afforded **51** (94mg, 20%), and then ( $\text{MeOH} / \text{CH}_2\text{Cl}_2$ , 10: 90) afforded **51mono** (123 mg, 22%).  $^1\text{H}$  NMR (300MHz,  $\text{CDCl}_3$ ):  $\delta$  7.89 (d,  $J = 8.3$  Hz, 2H), 7.70 (d,  $J = 16.5$  Hz, 1H),  $\delta$  7.59 (d,  $J = 8.1$  Hz, 2H),  $\delta$  7.38 (d,  $J = 8.2$  Hz, 2H), 7.27 (d,  $J = 16.5$  Hz, 1H), 7.09 (d,  $J = 8.3$  Hz, 2H), 6.65(s, 1H), 6.06 (s, 1H), 3.56 (s, 2H), 2.63 (s, 3H), 2.34 (s, 6H), 1.50 (s, 3H), 1.47 (s, 3H).  $^{13}\text{C}$  NMR (75 MHz,  $\text{CDCl}_3$ ):  $\delta = 156.1, 153.1, 142.9, 139.0, 138.5, 136.2, 135.8, 134.7, 132.7, 131.8, 130.3, 129.9, 127.7, 121.8, 119.1, 118.0, 95.0, 63.9, 45.6, 29.9, 15.1, 14.9$ . MS (FAB $^+$ , m-NBA):  $m/z$  (%) = 595.2  $[\text{M} + \text{H}]^+$  (100). Anal. Calcd for  $\text{C}_{29}\text{H}_{29}\text{BF}_2\text{IN}_3$ : C, 58.51; H, 4.91; N, 7.06. Found: C, 58.22, H, 4.66, N, 6.82.

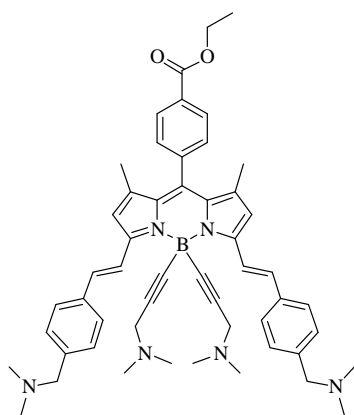
### Compound (52)



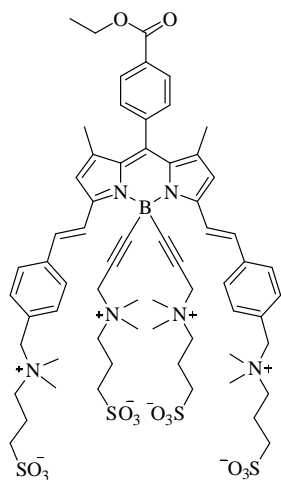
The 1-dimethylamino-2-propyne (121 mg, 1.46 mmol) was dissolved in dry THF (3 mL) under argon in a schlenk flask, was added and stirred 1.0 M  $\text{EtMgBr}$  in THF (1.28 mL) at  $60^\circ\text{C}$  for one hour. The resulting anion was then transferred via cannula to the solution of **51** (260mg, 0.35 mmol) dissolved in a separate schlenk flask in dry THF (3 mL) under argon. The mixture was stirred at  $60^\circ\text{C}$  for about 15 minutes until the complete consumption of the starting material was observed by TLC. Then the mixture was treated with water and brine, and then extracted with  $\text{CH}_2\text{Cl}_2$ . The organic layer was dried with  $\text{MgSO}_4$  then evaporated. the crude product

was purified by column chromatography on aluminium oxide ( $\text{CH}_2\text{Cl}_2$  pure to  $\text{MeOH}/\text{CH}_2\text{Cl}_2$ , 1: 99) afforded **52** (247 mg, 81%).  $^1\text{H}$  NMR (300MHz,  $\text{CDCl}_3$ ):  $\delta$  8.34 (d,  $J = 16.3$  Hz, 2H),  $\delta$  7.80 (d,  $J = 8.3$  Hz, 2H), 7.57 (d,  $J = 8.0$  Hz, 4H), 7.29 (d,  $J = 8.3$  Hz, 4H), 7.13 (d,  $J = 16.4$  Hz, 2H), 7.06 (d,  $J = 8.4$  Hz, 2H), 6.61 (s, 2H), 3.42 (s, 4H), 3.17 (s, 4H), 2.23 (s, 12H), 2.15 (s, 12H), 1.43 (s, 6H).  $^{13}\text{C}$  NMR (75 MHz,  $\text{CDCl}_3$ ):  $\delta = 152.2, 140.2, 139.8, 138.3, 137.6, 136.2, 135.4, 134.1, 131.6, 130.8, 129.6, 127.5, 121.4, 118.4, 94.7, 90.7, 64.3, 49.0, 45.5, 44.3, 15.3$ . MS (FAB<sup>+</sup>, m-NBA):  $m/z$  (%) = 866.2  $[\text{M} + \text{H}]^+$  (100). Anal. Calcd for  $\text{C}_{49}\text{H}_{56}\text{BIN}_6 \cdot 2\text{H}_2\text{O}$ : C, 65.19; H, 6.70; N, 9.31. Found: C, 64.84, H, 6.62, N, 9.04.

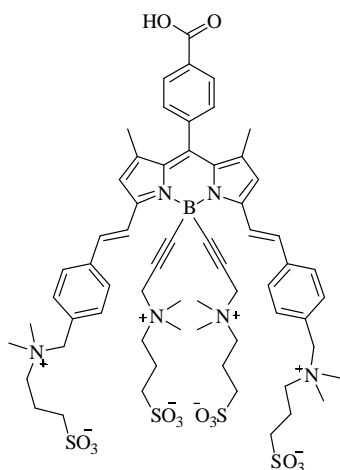
### Compound (53)



To stirred solution of compound **52** (100mg, 0.115 mmol) dissolved in EtOH absolute (4 mL) and  $\text{NEt}_3$  (3 mL), was added  $\text{Pd}(\text{PPh}_3)_2\text{Cl}_2$  (8 mg, 0.011 mmol), and the CO gas was bubbled for 5 hours at  $60^\circ\text{C}$  until the complete consumption of the starting material was observed by TLC. The mixture was treated with saturated  $\text{NaHCO}_3$  solution and water, extracted with  $\text{CH}_2\text{Cl}_2$ . The organic layer was dried with  $\text{MgSO}_4$ . After the solvent was, a column chromatography on aluminium oxide ( $\text{CH}_2\text{Cl}_2$  pure to  $\text{MeOH}/\text{CH}_2\text{Cl}_2$ , 1: 99) afforded **53** (80 mg, 85%).  $^1\text{H}$  NMR (300MHz,  $\text{CDCl}_3$ ):  $\delta$  8.34 (d,  $J = 16.4$  Hz, 2H),  $\delta$  8.16 (d,  $J = 8.2$  Hz, 2H), 7.58 (d,  $J = 8.1$  Hz, 4H), 7.43 (d,  $J = 8.4$  Hz, 2H), 7.30 (d,  $J = 8.4$  Hz, 4H), 7.14 (d,  $J = 16.5$  Hz, 2H), 6.62 (s, 2H), 4.41 (q,  $J = 7.1$  Hz, 2H), 3.43 (s, 4H), 3.18 (s, 4H), 2.24 (s, 12H), 2.16 (s, 12H), 1.41 (t,  $J = 7.2$  Hz, 3H), 1.38 (s, 6H).  $^{13}\text{C}$  NMR (75 MHz,  $\text{CDCl}_3$ ):  $\delta = 166.3, 152.3, 140.6, 139.8, 137.8, 136.2, 134.2, 131.4, 130.3, 129.6, 127.5, 121.4, 118.5, 90.6, 64.3, 61.5, 53.6, 49.0, 45.6, 44.1, 15.2, 14.5$ . MS (FAB<sup>+</sup>, m-NBA):  $m/z$  (%) = 813.5  $[\text{M} + \text{H}]^+$  (100).

**Compound (54)**

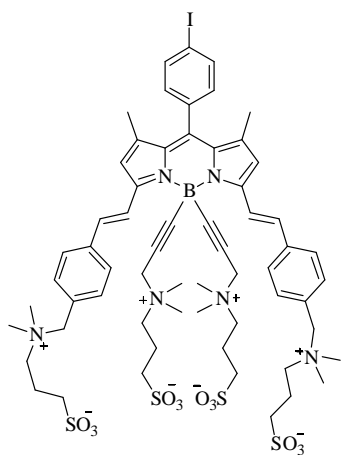
To a solution of **53** (80mg, 0.098 mmol) in distilled DMF (2mL), was added the 1,3-propane sultone (240 mg, 1.97 mmol). The mixture was stirred at 60°C for 12 hours. Then addition of AcOEt led to precipitation and then centrifuged, the residue was purified by column chromatography on silica C18, (THF/H<sub>2</sub>O, 15: 85) afforded **54** (82 mg, 64%). <sup>1</sup>H NMR (300MHz, CD<sub>3</sub>OD/D<sub>2</sub>O, internal reference : *t*-BuOH): δ 8.31 (d, J = 7.2 Hz, 2H), 8.28 (d, J = 16.1 Hz, 2H), 7.93 (d, J = 7.3 Hz, 4H), 7.84 (d, J = 7.3 Hz, 4H), 7.61 (d, J = 16.4 Hz, 2H), 7.05 (s, 2H), 4.69 (s, 4H), 4.50 (q, J = 6.9 Hz, 2H), 4.38 (s, 4H), 3.62 (m, 4H), 3.54 (m, 4H), 3.21 (s, 12H), 3.07 (s, 12H), 3.02 (m, 4H), 2.64 (m, 4H), 2.41 (m, 4H), 2.15 (m, 4H), 1.56 (s, 6H), 1.50 (t, J = 6.6 Hz, 3H). <sup>13</sup>C NMR (75 MHz, CD<sub>3</sub>OD/D<sub>2</sub>O): δ = 167.9, 153.2, 143.7, 140.8, 136.3, 135.6, 132.9, 131.7, 130.3, 129.8, 122.3, 120.6, 85.4, 69.4, 63.8, 56.8, 51.2, 50.0, 49.7, 20.1, 15.3, 14.8. MS (FAB<sup>+</sup>, m-NBA): m/z (%) = 1301.3 [M + H]<sup>+</sup> (100), 651.2(55, doubly charged). Anal. Calcd for C<sub>64</sub>H<sub>85</sub>BN<sub>6</sub>O<sub>14</sub>S<sub>4</sub>·1.5H<sub>2</sub>O: C, 57.86; H, 6.68; N, 6.33. Found: C, 57.52, H, 6.53, N, 6.69.

**Compound (55)**

To a solution of compound **54** (70 mg, 0.05 mmol), in EtOH (2 mL) and H<sub>2</sub>O (0.5 mL), was added NaOH (21 mg, 0.5 mmol). The mixture was stirred at RT for 10 hours until complete consumption of the starting material was observed by TLC. To the solution the HCl solution (2%) was added until the pH was neutral. Then addition of AcOEt led to precipitation and then centrifuged. The residue was purified by column chromatography on silica C18, (THF/H<sub>2</sub>O 5: 95 then 10: 90) afforded **55** (60 mg, 88%). <sup>1</sup>H NMR (300MHz, CD<sub>3</sub>OD/D<sub>2</sub>O, internal reference : *t*-BuOH): δ 8.26 (d, J = 16.3 Hz, 2H), 8.21 (d, J = 8.3 Hz, 2H), 7.92 (d, J = 8.2 Hz, 4H), 7.83 (d, J = 8.2 Hz, 4H), 7.58 (d, J = 16.2 Hz, 2H), 7.44 (d, J = 8.3 Hz, 2H), 7.01 (s, 2H), 4.66 (s, 4H), 4.36 (s, 4H), 3.64 (m, 4H), 3.51 (m, 4H), 3.21 (s, 12H), 3.06 (s, 12H), 3.03 (m, 4H), 2.65 (t, J = 6.8 Hz, 4H), 2.42 (m, 4H), 2.14 (m, 4H), 1.53 (s, 6H). <sup>13</sup>C NMR (75MHz, CD<sub>3</sub>OD/D<sub>2</sub>O): δ = 152.9, 143.8, 139.9, 135.5, 133.0, 131.6, 129.7, 122.2, 120.5, 85.3, 80.2, 69.3, 67.1, 63.7, 56.8, 51.1, 20.0, 15.3. MS (FAB<sup>+</sup>, m-NBA): m/z (%) = 1273.4 [M + H]<sup>+</sup> (100), 637.2 (35, doubly charged). Anal. Calcd for C<sub>62</sub>H<sub>81</sub>BN<sub>6</sub>O<sub>14</sub>S<sub>4</sub>·2.5H<sub>2</sub>O: C,

56.48; H, 6.57; N, 6.37. Found: C, 56.18, H, 6.29, N, 6.76.

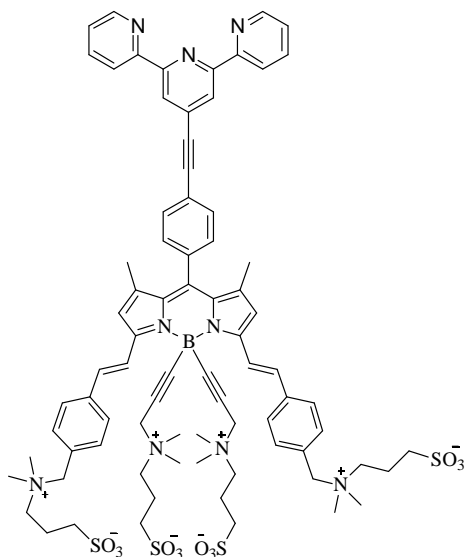
### Compound (56)



To a solution of **52** (60mg, 0.069 mmol) in distilled DMF (2mL), was added the 1,3-propane sultone (169 mg, 1.39 mmol). The mixture was stirred at 60°C for 10 hours. Then addition of AcOEt led to precipitation and then centrifuged. the residue was purified by column chromatography on silica C18, (THF/H<sub>2</sub>O, 15: 85), afforded **56** (79 mg, 84%). <sup>1</sup>H NMR (300MHz, CD<sub>3</sub>OD/D<sub>2</sub>O, internal rerefence : *t*-BuOH): 8.22 (d, J = 16.4 Hz, 2H), δ 8.01 (d, J = 8.2 Hz, 2H), 7.91 (d, J = 8.4 Hz, 4H), 7.82 (d, J = 8.4 Hz, 4H), 7.61 (d, J = 16.4 Hz, 2H), 7.18 (d, J = 8.2 Hz, 2H), 7.01 (s, 2H), 4.68 (s,

4H), 4.34 (s, 4H), 3.62 (m, 4H), 3.45 (m, 4H), 3.21 (s, 12H), 3.0 (s, 16H), 2.62 (m, 4H), 2.42 (m, 4H), 2.11 (m, 4H), 1.57 (s, 6H). <sup>13</sup>C NMR (75 MHz, CD<sub>3</sub>OD/D<sub>2</sub>O): δ = 153.0, 143.7, 140.7, 139.7, 136.4, 135.5, 133.0, 131.6, 129.7, 129.0, 121.9, 120.6, 96.3, 85.2, 63.6, 56.7, 51.2, 19.9, 15.4. MS (FAB<sup>+</sup>, *m*-NBA): *m/z* (%) = 1355.3 [M + H]<sup>+</sup> (100), 678.2 (40, doubly charged).

### Compound (57)



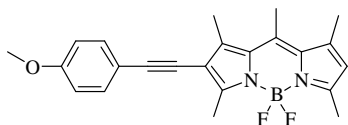
To a degassed solution of **56** (0.040 g, 0.044 mmol) and 4'-ethynyl-2,2':6',2''-terpyridine (0.017 g, 0.066 mmol) in DMF (3 mL) H<sub>2</sub>O (3 mL) and NEt<sub>3</sub> (1 mL), was added [Pd (PPh<sub>3</sub>)<sub>4</sub>] (0.008 g, 0.0068 mmol). The mixture was stirred at 60 °C for 10 hours until the complete consumption of the starting material was observed by TLC (EtOH/H<sub>2</sub>O, 70: 30). The mixture was cooled to room temperature, and then to the solution addition of AcOEt (50 mL) led to precipitation, then the crude was filtered through cotton wool and washed with AcOEt and H<sub>2</sub>O. The residue was

resolved with MeOH/H<sub>2</sub>O/CH<sub>2</sub>Cl<sub>2</sub> then evaporated. The crude product was Recrystallized twice from methanol/H<sub>2</sub>O/THF afforded **57** (0.032g, 52%). <sup>1</sup>H NMR (300MHz, CDCl<sub>3</sub>/CD<sub>3</sub>OD/D<sub>2</sub>O): δ 8.28-8.20 (m, 5H), δ 8.09 (m, 2H), δ 7.83 (d, J = 16.2 Hz, 2H), δ 7.56 (t, J = 7.8 Hz, 2H), δ 7.43 (d, J = 8.2 Hz, 4H), δ 7.34 (d, J = 8.2 Hz, 4H), δ 7.10-6.99 (m, 6H), δ 6.50 (s, 2H), δ 4.17 (s, 4H), δ 3.86 (s, 4H), δ 3.17 (m, 4H), δ 2.72 (s, 12H), δ 2.65 (m, 4H), δ 2.59 (s, 12H), δ 2.52 (m, 4H), δ 2.25 (t, J = 6.6 Hz, 4H), δ 1.89 (m, 4H), δ 1.70 (m, 4H), δ 1.19 (s, 6H). <sup>13</sup>C NMR (75 MHz,

CD<sub>3</sub>OD/D<sub>2</sub>O/CDCl<sub>3</sub>):  $\delta$  =155.4, 155.0, 151.2, 148.6, 141.9, 138.3, 137.1, 133.8, 132.4, 131.5, 128.4, 127.4, 124.0, 123.3, 122.3, 122.1, 121.4, 120.8, 118.8, 62.2, 61.7, 55.6, 53.0, 49.4, 18.5, 14.3. MS (FAB<sup>+</sup>, m-NBA): m/z (%) = 742.7 (55, doubly charged), 495.5 (100, triply charged). Anal. Calcd for C<sub>78</sub>H<sub>90</sub>BN<sub>9</sub>O<sub>12</sub>S<sub>4</sub>·2.5H<sub>2</sub>O: C, 61.24; H, 6.26; N, 8.24. Found: C, 60.89; H, 6.17; N, 8.67.

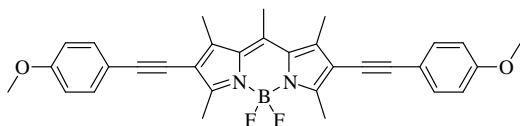
## CHAPTER IV

## Compound (58)



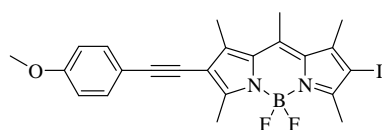
To a degassed solution of **9a** (0.100 g, 0.258 mmol) and the 1-ethynyl-4-methoxybenzene (0.051 g, 0.384 mmol) in benzene (3 mL) and TEA (3 mL), was added  $[\text{Pd}(\text{PPh}_3)_2\text{Cl}_2]$  (0.011 g, 0.0129 mmol), CuI (0.003 g, 0.0129 mmol) under argon. The mixture was stirred at 60 °C for 12 hours until the complete consumption of the starting material was observed by TLC. The mixture was then evaporated, and a chromatography on silica gel ( $\text{CH}_2\text{Cl}_2$ / petroleum ether, 6: 4) afforded **58** (96 mg, 95%).  $^1\text{H}$  NMR (300MHz,  $\text{CDCl}_3$ ):  $\delta$  7.42 (d,  $J$  = 8.9 Hz, 2H), 6.85 (d,  $J$  = 8.8 Hz, 2H), 6.07 (s, 1H), 3.81 (s, 3H), 2.64 (s, 3H), 2.56 (s, 3H), 2.51 (s, 3H), 2.50 (s, 3H), 2.39 (s, 3H).  $^{13}\text{C}$  NMR (75 MHz,  $\text{CDCl}_3$ ):  $\delta$  = 159.7, 155.6, 142.6, 140.5, 133.2, 131.3, 122.2, 116.0, 115.6, 114.2, 95.9, 80.9, 55.5, 17.7, 16.8, 14.8, 13.7. MS ( $\text{FAB}^+$ , m-NBA):  $m/z$  (%) = 392.1  $[\text{M} + \text{H}]^+$  (100). Anal. Calcd for  $\text{C}_{23}\text{H}_{23}\text{BF}_2\text{N}_2\text{O}$ : C, 70.43; H, 5.91; N, 7.14. Found: C, 70.27, H, 5.67, N, 6.84.

## Compound (59)

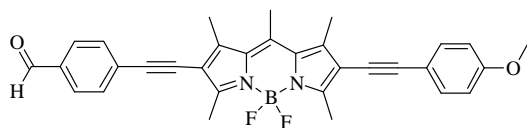


To a degassed solution of **9b** (0.200 g, 0.39 mmol) and the 1-ethynyl-4-methoxybenzene (0.051g, 0.39 mmol) in benzene (6 mL) and TEA (3 mL), was added  $[\text{Pd}(\text{PPh}_3)_2\text{Cl}_2]$  (0.017 g, 0.023 mmol), CuI (0.005 g, 0.023 mmol), under argon. The mixture was stirred at 60 °C for 10 hours until the complete consumption of the starting material was observed by TLC. The mixture was then evaporated, and a chromatography on silica gel ( $\text{CH}_2\text{Cl}_2$ /petroleum ether 4: 6 to 6: 4) afforded **59** (45 mg, 22 %) along with mono-coupled compound **60** (65mg, 32%).  $^1\text{H}$  NMR (300MHz,  $\text{CDCl}_3$ ):  $\delta$  7.43 (d,  $J$  = 8.8 Hz, 4H), 6.86 (d,  $J$  = 8.6 Hz, 4H), 3.83 (s, 3H), 2.67 (s, 9H), 2.56 (s, 6H).  $^{13}\text{C}$  NMR (75 MHz,  $\text{CDCl}_3$ ):  $\delta$  = 133.1, 132.4, 128.8, 114.3, 55.6, 29.9, 22.9, 16.3, 14.3, 13.8. MS ( $\text{FAB}^+$ , m-NBA):  $m/z$  (%) = 523.4  $[\text{M} + \text{H}]^+$  (100). Anal. Calcd for  $\text{C}_{32}\text{H}_{29}\text{BF}_2\text{N}_2\text{O}_2$ : C, 73.57; H, 5.60; N, 5.36. Found: C, 73.37, H, 5.44, N, 5.24.

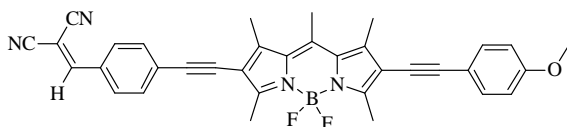
## Compound (60)



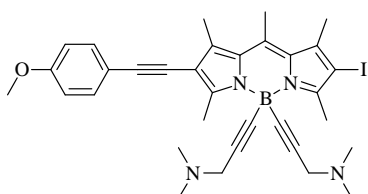
$^1\text{H}$  NMR (300MHz,  $\text{CDCl}_3$ ):  $\delta$  7.43 (d,  $J$  = 8.9 Hz, 2H), 6.86 (d,  $J$  = 8.8 Hz, 2H), 3.82 (s, 3H), 2.65 (s, 3H), 2.63 (s, 3H), 2.60 (s, 3H), 2.53 (s, 3H), 2.45 (s, 3H).  $^{13}\text{C}$  NMR (75 MHz,  $\text{CDCl}_3$ ):  $\delta$  = 133.1, 114.3, 61.2, 55.6, 19.9, 17.6, 16.5.

**Compound (61)**

To a degassed solution of **60** (0.060 g, 0.126 mmol) and the 4-ethynylbenzaldehyde (0.019 g, 0.151 mmol) in benzene (4 mL) and TEA (3 mL), was added [Pd(PPh<sub>3</sub>)<sub>2</sub>Cl<sub>2</sub>] (0.005 g, 0.007 mmol), CuI (0.002 g, 0.007 mmol), under argon. The mixture was stirred at 60 °C for 12 hours until the complete consumption of the starting material was observed by TLC. The mixture was then evaporated, and a chromatography on silica gel (CH<sub>2</sub>Cl<sub>2</sub>/ petroleum ether 6: 4) afforded **61** (31 mg, 47 %). <sup>1</sup>H NMR (300MHz, CDCl<sub>3</sub>): δ 10.00 (s, 1H), 7.84 (d, J = 8.2 Hz, 2H), 7.63 (d, J = 8.3 Hz, 2H), 7.44 (d, J = 8.7 Hz, 2H), 6.87 (d, J = 8.8 Hz, 2H), 3.82 (s, 3H), 2.67 (s, 9H), 2.56 (s, 6H). <sup>13</sup>C NMR (75 MHz, CDCl<sub>3</sub>): δ =135.2, 132.9, 131.7, 129.6, 114.1, 55.3, 16.6, 15.6. MS (EI neat matter): m/z (%) = 520.2(100). Anal. Calcd for C<sub>32</sub>H<sub>27</sub>BF<sub>2</sub>N<sub>2</sub>O<sub>2</sub>·0.5H<sub>2</sub>O: C, 72.60; H, 5.33; N, 5.29. Found: C, 72.93, H, 5.72, N, 5.18.

**Compound (62)**

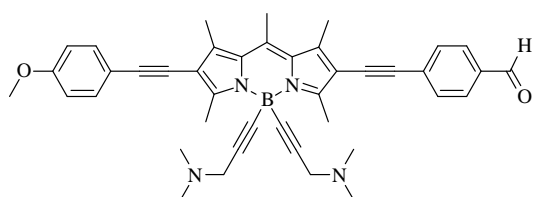
To a stirred solution of **61** (26 mg, 0.05 mmol) in distilled CH<sub>2</sub>Cl<sub>2</sub> (6 mL), was added malononitrile (8 mg, 0.10 mmol) and Al<sub>2</sub>O<sub>3</sub> (10 mg, 0.1 mmol). The mixture stirred and at 38 °C for 3 hours until the complete consumption of the starting material was observed by TLC, then cooled and filtered. The solvent was removed to evaporated, and a column chromatography on silica gel (CH<sub>2</sub>Cl<sub>2</sub> 80%) afforded **62** (20mg, 70%). <sup>1</sup>H NMR (300MHz, CDCl<sub>3</sub>): δ 7.87 (d, J = 8.4 Hz, 2H), 7.70 (s, 1H), δ 7.59 (d, J = 8.6 Hz, 2H), δ 7.44 (d, J = 8.8 Hz, 2H), δ 6.87 (d, J = 8.8 Hz, 2H), 3.82 (s, 3H), 2.66 (s, 9H), 2.55 (s, 6H). MS (EI neat matter): m/z (%) = 568.2(100). Anal. Calcd for C<sub>35</sub>H<sub>27</sub>BF<sub>2</sub>N<sub>4</sub>O: C, 73.95; H, 4.79; N, 9.86. Found: C, 73.64; H, 4.39; N, 9.59.

**Compound (63)**

To a stirred solution of 1-Dimethylamino-2-propyne (96 mg, 1.16 mmol) in dry THF (3 mL) under argon in a schlenk flask, was added 1.0 M EtMgBr in THF (0.77 mL) and stirred at 60 °C for one hour. The resulting anion was then transferred via cannula to the solution of **60** (196mg, 0.39 mmol) dissolved in a separate schlenk flask in dry THF (3 mL) under argon. The mixture was stirred at 60 °C for 15 minutes until the complete consumption of the starting material was observed by TLC. Then the mixture was treated with water and brine, and then extracted with

CH<sub>2</sub>Cl<sub>2</sub>. The organic layer was dried with MgSO<sub>4</sub> then evaporated. The crude product was purified by column chromatography on aluminium oxide (CH<sub>2</sub>Cl<sub>2</sub> pure then MeOH/CH<sub>2</sub>Cl<sub>2</sub>, 1: 99) afforded **63** (183 mg, 74%). <sup>1</sup>H NMR (300MHz, CDCl<sub>3</sub>): δ 7.43 (d, J = 8.7 Hz, 2H), 6.89 (d, J = 8.8 Hz, 2H), 3.82 (s, 3H), 3.25 (s, 4H), 3.17 (s, 4H), 2.86 (s, 3H), 2.64 (s, 3H), 2.55 (s, 3H), 2.47 (s, 3H), 2.33 (s, 12H). <sup>13</sup>C NMR (75 MHz, CDCl<sub>3</sub>): δ = 159.6, 156.5, 153.8, 142.5, 141.4, 140.5, 133.6, 132.8, 129.9, 124.1, 116.9, 114.4, 96.7, 55.6, 49.0, 44.1, 20.3, 18.0, 17.9, 16.8, 15.6.

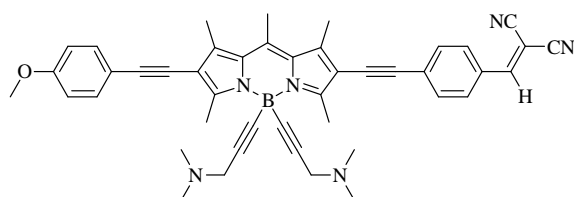
### Compound (64)



To a degassed solution of **63** (0.090 g, 0.14 mmol) and the 4-ethynylbenzaldehyde (0.027 g, 0.21 mmol) in THF (4 mL) and TEA (3 mL), was added [Pd(PPh<sub>3</sub>)<sub>2</sub>Cl<sub>2</sub>] (0.006 g, 0.007 mmol), CuI (0.003 g, 0.007 mmol)

under argon. The mixture was stirred at 60 °C for 10 hours, until the complete consumption of the starting material was observed by TLC. The mixture was then evaporated, and a chromatography on silica gel (CH<sub>2</sub>Cl<sub>2</sub> pure to MeOH/CH<sub>2</sub>Cl<sub>2</sub>, 3: 97) afforded **64** (46 mg, 51 %). <sup>1</sup>H NMR (300MHz, CDCl<sub>3</sub>): δ 9.99 (s, 1H), 7.84 (d, J = 8.2 Hz, 2H), 7.63 (d, J = 8.2 Hz, 2H), 7.44 (d, J = 8.8 Hz, 2H), 6.87 (d, J = 8.8 Hz, 2H), 3.82 (s, 3H), 3.25 (s, 4H), 2.89 (s, 6H), 2.67 (s, 3H), 2.58 (s, 3H), 2.57 (s, 3H), 2.32 (s, 12H). <sup>13</sup>C NMR (75 MHz, CDCl<sub>3</sub>): δ = 191.3, 157.4, 142.2, 140.6, 135.1, 132.8, 131.6, 130.1, 129.6, 117.2, 115.6, 114.1, 96.7, 95.7, 55.4, 48.8, 43.9, 29.7, 17.2, 16.5, 15.4. MS (EI neat matter): m/z (%) = 646.2(100). Anal. Calcd for C<sub>42</sub>H<sub>43</sub>BN<sub>4</sub>O<sub>2</sub>·0.3H<sub>2</sub>O: C, 77.29; H, 6.74; N, 8.58. Found: C, 77.39, H, 6.92, N.8.39.

### Compound (65)

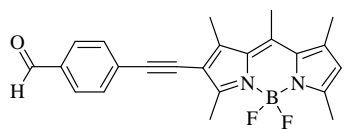


To a stirred solution of **64** (60 mg, 0.093 mmol) in distilled CH<sub>2</sub>Cl<sub>2</sub> (6 mL), was added malononitrile (12 mg, 0.19 mmol) and Al<sub>2</sub>O<sub>3</sub> (20 mg, 0.19 mmol). The mixture was stirred at 38 °C

for 2 hours until the complete consumption of the starting material was observed by TLC. Then cooled and filtered. Then the solvent was removed, and a column chromatography on silica gel (CH<sub>2</sub>Cl<sub>2</sub>) afforded **62** (35mg, 54%). <sup>1</sup>H NMR (300MHz, CDCl<sub>3</sub>): δ 7.86 (d, J = 8.5 Hz, 2H), 7.69 (s, 1H), δ 7.59 (d, J = 8.4 Hz, 2H), δ 7.44 (d, J = 8.9 Hz, 2H), δ 6.87 (d, J = 8.9 Hz, 2H), 3.82 (s, 3H), 3.21 (s, 4H), 2.90 (s, 6H), 2.65 (s, 3H), 2.55 (s, 6H), 2.29 (s, 12H). <sup>13</sup>C NMR (75 MHz, CDCl<sub>3</sub>): δ = 158.4, 155.5, 154.1, 142.2, 140.9, 139.7, 132.8, 131.8, 130.8, 114.1, 96.8, 95.9, 90.1, 89.7, 55.4, 53.4, 48.9, 44.1, 17.2, 16.6, 15.5, 15.3. MS (EI neat matter): m/z (%) = 694.2(100). Anal. Calcd for

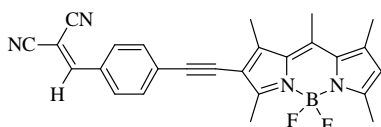
$C_{45}H_{43}BN_6O$ : C, 77.80; H, 6.24; N, 12.10. Found: C, 77.78, H, 5.94, N, 11.84.

### Compound (66)



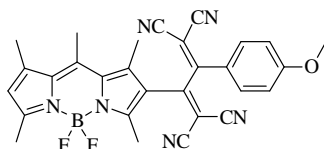
To a degassed solution of **9a** (0.050 g, 0.129 mmol) and the 4-ethynylbenzaldehyde (0.021 g, 0.155 mmol) in benzene (3 mL) and TEA (3 mL), was added  $[Pd(PPh_3)_2Cl_2]$  (0.006 g, 0.008 mmol), CuI (0.003 g, 0.007 mmol) under argon. The mixture was stirred at 60 °C for 10 hours until the complete consumption of the starting material was observed by TLC. The solvent was then removed, and a chromatography on silica gel ( $CH_2Cl_2$ / petroleum ether, 6: 4) afforded **66** (49 mg, 98%).  $^1H$  NMR (200MHz,  $CDCl_3$ ):  $\delta$  9.99 (s, 1H), 7.84 (d,  $J = 8.8$  Hz, 2H), 7.62 (d,  $J = 8.8$  Hz, 2H), 6.13 (s, 1H), 2.67 (s, 3H), 2.61 (s, 3H), 2.54 (s, 6H), 2.43 (s, 3H). MS (EI neat matter):  $m/z$  (%) = 390.2 (100).

### Compound (67)



To a stirred solution of **66** (23 mg, 0.06 mmol) in distilled  $CH_2Cl_2$  (4 mL), was added malononitrile (8 mg, 0.12 mmol) and  $Al_2O_3$  (12 mg, 0.12 mmol). The mixture was stirred at 38 °C for 2 hours until the complete consumption of the starting material was observed by TLC. Then cooled and filtered. The solvent was evaporated, and the crude was purified by column chromatography on silica gel ( $CH_2Cl_2$ , 80%) afforded **67** (13 mg, 51%).  $^1H$  NMR (200MHz,  $CDCl_3$ ):  $\delta$  7.89 (d,  $J = 8.02$  Hz, 2H), 7.72 (s, 1H),  $\delta$  7.60 (d,  $J = 8.40$  Hz, 2H), 6.16 (s, 1H), 2.67 (s, 3H), 2.64 (s, 3H), 2.56 (s, 6H), 2.46 (s, 3H). MS (EI neat matter):  $m/z$  (%) = 438.0(100). Anal. Calcd for  $C_{26}H_{21}BF_2N_4$ : C, 71.25; H, 4.83; N, 12.78. Found: C, 71.08, H, 4.59, N, 12.54.

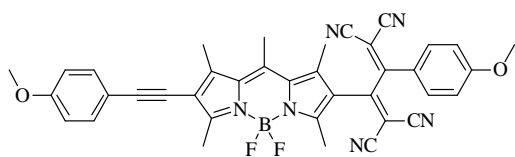
### Compound (68)



To a stirred solution of **58** (20 mg, 0.05 mmol) in distilled  $CH_2Cl_2$  (4 mL), was added tetracyanoethylene (8 mg, 0.06 mmol). The mixture was stirred at room temperature for 8 hours until the complete consumption of the starting material was observed by TLC. The solvent was then removed, and the crude was purified by column chromatography on silica gel ( $CH_2Cl_2$ , 100%) afforded **68** (14 mg, 51%).  $^1H$  NMR (300 MHz,  $CDCl_3$ ):  $\delta$  7.67 (d,  $J = 9.0$  Hz, 2H),  $\delta$  7.05 (d,  $J = 9.0$  Hz, 2H), 6.28 (s, 1H), 3.90 (s, 3H), 2.67 (s, 3H), 2.57 (s, 3H), 2.51 (s, 3H), 2.47 (s, 6H).  $^{13}C$  NMR (75 MHz,  $CDCl_3$ ):  $\delta = 167.0, 165.0, 162.6, 149.6, 147.2, 143.1, 137.0, 136.1, 132.9, 125.5, 115.8, 113.3, 111.6, 89.3, 85.9, 56.1, 53.6, 29.9, 18.2, 17.7, 15.3, 14.1$ . MS (EI neat matter):  $m/z$  (%) = 520.1(100). Anal.

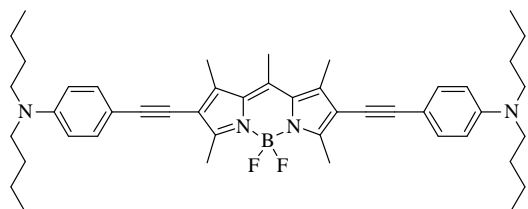
Calcd for  $C_{29}H_{23}BF_2N_6O$ : C, 66.94; H, 4.46; N, 16.15. Found: C, 66.77, H, 4.18, N, 15.84.

### Compound (69)

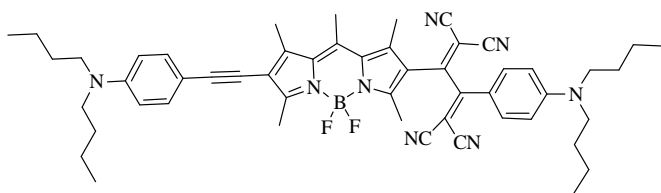


To a stirred solution of **59** (50 mg, 0.10 mmol) in distilled  $CH_2Cl_2$  (4 mL), was added tetracyanoethylene (27 mg, 0.21 mmol). The mixture stirred at room temperature for 8 hours until the complete consumption of the starting material was observed by TLC. The solvent was removed, then the crude was purified by column chromatography on silica gel ( $CH_2Cl_2$ , 100%) afforded **69** (48 mg, 77 %).  $^1H$  NMR (300MHz,  $CDCl_3$ ):  $\delta$  7.67 (d,  $J$  = 9.0 Hz, 2H), 7.45 (d,  $J$  = 8.9 Hz, 2H), 7.06 (d,  $J$  = 8.9 Hz, 2H), 6.88 (d,  $J$  = 8.9 Hz, 2H), 3.91 (s, 3H), 3.83 (s, 3H), 2.73 (s, 3H), 2.71 (s, 3H), 2.59 (s, 3H), 2.52 (s, 3H), 2.49 (s, 3H).  $^{13}C$  NMR (75 MHz,  $CDCl_3$ ):  $\delta$  = 166.8, 165.1, 163.5, 161.8, 160.3, 150.4, 145.8, 143.6, 138.0, 135.2, 133.3, 132.9, 125.4, 115.9, 114.9, 113.2, 111.6, 99.0, 89.8, 85.9, 79.2, 56.1, 55.6, 18.0, 17.4, 14.3, 14.2. MS (EI neat matter):  $m/z$  (%) = 650.1(100). Anal. Calcd for  $C_{38}H_{29}BF_2N_6O_2$ : C, 70.16; H, 4.49; N, 12.92. Found: C, 70.04, H, 4.19, C, 12.77.

### Compound (70)

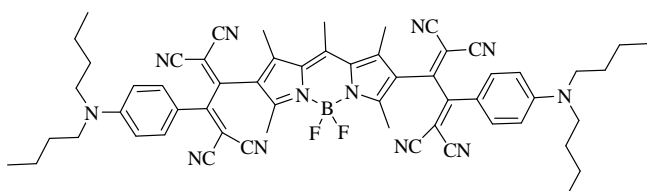


To a degassed solution of **9b** (0.160 g, 0.31 mmol) and the *p*-(butylamino)phenylacetylene (0.157 g, 0.69 mmol) in benzene (6 mL) and TEA (3 mL), was added  $[Pd(PPh_3)_2Cl_2]$  (0.013 g, 0.019 mmol), CuI (0.003 g, 0.02 mmol), under argon. The mixture was stirred at 60 °C over night, until the complete consumption of the starting material was observed by TLC. The mixture was then evaporated, a chromatography on silica gel ( $CH_2Cl_2$ / petroleum ether 4:6) afforded **70** (71 mg, 32 %).  $^1H$  NMR (300 MHz,  $CDCl_3$ ):  $\delta$  7.33 (d,  $J$  = 8.9 Hz, 4H), 6.56 (d,  $J$  = 9.0 Hz, 4H), 3.27 (t,  $J$  = 7.3 Hz, 8H), 2.56 (s, 6H), 2.61 (s, 3H), 2.51 (s, 6H), 1.56 (quin,  $J$  = 8.2 Hz, 8H), 1.34 (sext,  $J$  = 7.7 Hz, 8H), 0.95 (t,  $J$  = 7.3 Hz, 12H).  $^{13}C$  NMR (75 MHz,  $CDCl_3$ ):  $\delta$  = 156.5, 148.1, 141.5, 140.8, 132.9, 117.1, 111.5, 109.2, 97.7, 79.4, 50.9, 29.6, 22.8, 20.7, 17.1, 16.2, 14.2, 13.8. MS (EI neat matter):  $m/z$  (%) = 716.3 (100).

**Compound (71)**

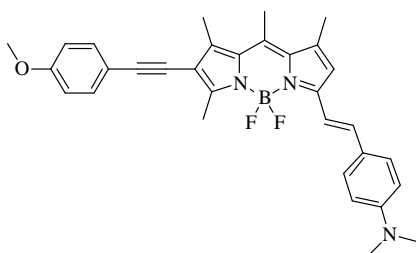
To a stirred solution of **70** (60 mg, 0.08 mmol) in distilled  $\text{CH}_2\text{Cl}_2$  (4 mL), was added tetracyanoethylene (14 mg, 0.10 mmol). The mixture was stirred at room temperature for 8

hours until the complete consumption of the starting material was observed by TLC. The solvent was removed, then the crude product was purified by column chromatography on silica gel ( $\text{CH}_2\text{Cl}_2$ , 100%) gave the mono-substituted compound **71** (40 mg, 55 %), and bis compound **72** (30 mg, 36%).  $^1\text{H}$  NMR (300 MHz,  $\text{CDCl}_3$ ):  $\delta$  7.68 (d,  $J = 9.3$  Hz, 2H), 7.34 (d,  $J = 9.0$  Hz, 2H),  $\delta$  6.70 (d,  $J = 9.4$  Hz, 2H), 6.57 (d,  $J = 9.0$  Hz, 2H), 3.39 (t,  $J = 7.6$  Hz, 4H), 3.28 (t,  $J = 7.4$  Hz, 4H), 2.73 (s, 3H), 2.70 (s, 3H), 2.58 (s, 3H), 2.52 (s, 3H), 2.49 (s, 3H), 1.59 (m, 8H), 1.37 (m, 8H), 0.98 (t,  $J = 7.2$  Hz, 6H), 0.95 (t,  $J = 7.3$  Hz, 6H).  $^{13}\text{C}$  NMR (75 MHz,  $\text{CDCl}_3$ ):  $\delta = 164.4, 163.7, 153.3, 150.9, 148.5, 144.6, 143.0, 138.4, 135.1, 133.7, 132.9, 120.2, 115.4, 113.6, 112.4, 111.9, 108.2, 100.5, 88.5, 53.6, 51.4, 50.9, 29.6, 20.5, 18.0, 17.8, 16.9, 14.3, 14.2$ . MS (EI neat matter):  $m/z$  (%) = 844.3(100). Anal. Calcd for  $\text{C}_{52}\text{H}_{59}\text{BF}_2\text{N}_8$ : C, 73.92; H, 7.04; N, 13.26. Found: C, 73.79, H, 6.82, N, 13.00.

**Compound (72)**

$^1\text{H}$  NMR (300 MHz,  $\text{CDCl}_3$ ):  $\delta$  7.65 (d,  $J = 8.7$  Hz, 4H), 6.71 (d,  $J = 8.6$  Hz, 4H), 3.40 (t,  $J = 7.4$  Hz, 8H), 2.85 (s, 3H), 2.58 (s, 6H), 2.54 (s, 6H), 1.63 (m, 8H), 1.39 (sext,  $J = 7.3$  Hz, 8H),

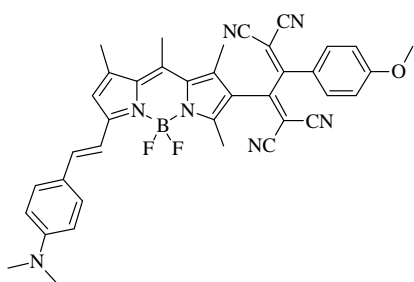
0.98 (t,  $J = 7.2$  Hz, 12H).  $^{13}\text{C}$  NMR (75 MHz,  $\text{CDCl}_3$ ):  $\delta = 162.9, 155.8, 153.5, 148.3, 144.8, 134.6, 133.6, 128.1, 119.8, 115.1, 113.6, 112.8, 111.2, 91.7, 75.4, 51.5, 29.6, 20.4, 19.1, 18.7, 14.5, 14.0$ . MS (EI neat matter):  $m/z$  (%) = 972.4 (100). Anal. Calcd for  $\text{C}_{58}\text{H}_{59}\text{BF}_2\text{N}_{12}$ : C, 71.60; H, 6.11; N, 17.27. Found: C, 71.42, H, 5.80, N, 16.92.

**Compound (73)**

Compound **58** (100 mg, 0.255mmol) and 4-dimethylaminobenzaldehyde (46 mg, 0.31 mmol) were dissolved in toluene (5 mL) and piperidine (0.5 mL) in a Dean-Stark apparatus. The mixture was heated at  $140^\circ\text{C}$  for 2 h, then removed the Dean-stark apparatus, continued heating under Argon until the solvent was totally evaporated. The residue was

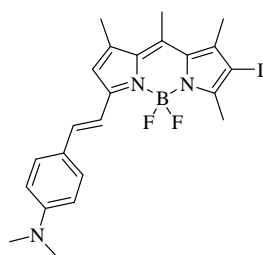
purified by column chromatography on silica gel ( $\text{CH}_2\text{Cl}_2$ / petroleum ether, 6: 4 then 8:2) gave **73** (57 mg, 43%).  $^1\text{H}$  NMR (300 MHz,  $\text{CDCl}_3$ ) : 7.42-7.35 [m, (7.42, d,  $J = 9.3$  Hz, 2H), (7.39, d,  $J = 9.3$  Hz, 2H), 5H], 7.16 (d, 1H), 6.81 (d,  $J = 8.6$  Hz, 2H), 6.61 [m, (6.61, d,  $J = 9.3$  Hz, 2H), 3H], 3.76 (s, 3H), 2.96 (s, 6H), 2.62 (s, 3H), 2.55 (s, 3H), 2.47 (s, 3H), 2.40 (s, 3H).  $^{13}\text{C}$  NMR (75 MHz,  $\text{CDCl}_3$ ):  $\delta = 151.4, 142.3, 138.6, 133.0, 129.6, 124.8, 118.7, 114.2, 112.2, 95.4, 55.6, 40.5, 27.1, 25.6, 18.0, 16.7, 16.0, 13.8, 12.6$ . MS (EI neat matter):  $m/z$  (%) = 523.1(100). Anal. Calcd for  $\text{C}_{32}\text{H}_{32}\text{BF}_2\text{N}_3\text{O}$ : C, 73.43; H, 6.16; N, 8.03. Found: C, 73.17, H, 6.00; N, 7.82.

### Compound (74)

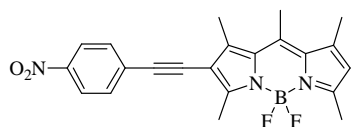


To a stirred solution of **73** (18 mg, 0.03 mmol) in distilled  $\text{CH}_2\text{Cl}_2$  (4 mL), was added tetracyanoethylene (6 mg, 0.4 mmol). The mixture was stirred at room temperature for about 8 hours until the complete consumption of the starting material was observed by TLC. Then the solvent was removed, then the crude product was purified by column chromatography on silica gel ( $\text{CH}_2\text{Cl}_2$ , 100%) afforded **74** (18 mg, 81 %).  $^1\text{H}$  NMR (300MHz,  $\text{CDCl}_3$ ):  $\delta$  7.68 (d,  $J = 8.9$  Hz, 2H), 7.51 (d,  $J = 8.8$  Hz, 2H), 7.39 (s, 2H), 7.04 (d,  $J = 9.0$  Hz, 2H), 6.85 (s, 1H), 6.68 (d,  $J = 8.9$  Hz, 2H), 3.90 (s, 3H), 3.05 (s, 6H), 2.65 (s, 3H), 2.54 (s, 3H), 2.49 (s, 3H), 2.46 (s, 3H).  $^{13}\text{C}$  NMR (50 MHz,  $\text{CDCl}_3$ ):  $\delta = 164.8, 159.7, 152.1, 143.5, 132.8, 131.6, 130.5, 129.9, 125.6, 123.8, 121.7, 115.6, 112.1, 55.9, 40.3, 29.8, 18.3, 17.3, 16.8, 14.1$ . MS (EI neat matter):  $m/z$  (%) = 651.2 (100). Anal. Calcd for  $\text{C}_{38}\text{H}_{32}\text{BF}_2\text{N}_7\text{O}$ : C, 70.05; H, 4.95; N, 15.05. Found: C, 69.78; H, 4.77; N, 14.82.

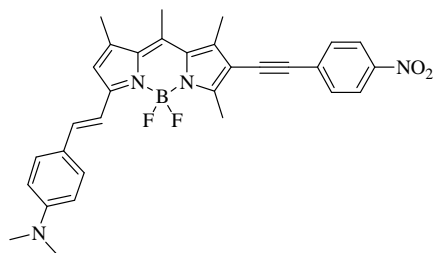
### Compound (75)



Compound **9a** (50 mg, 0.129 mmol) and 4-dimethylaminobenzaldehyde (20 mg, 0.142 mmol) were dissolved in toluene (5 mL) and piperidine (0.5 mL) in a Dean–Stark apparatus. The mixture was heated at  $140^\circ\text{C}$  for 2 h, then removed the Dean-stark apparatus and continued heating under Argon until the solvent was totally evaporated. The residue was purified by column chromatography on silica gel ( $\text{CH}_2\text{Cl}_2$ /petroleum ether, 6: 4), afforded **75** (35 mg, 52%).  $^1\text{H}$  NMR (300 MHz, DMSO) : 7.55 (d,  $J = 16.3$  Hz, 1H), 7.45 (d,  $J = 8.9$  Hz, 2H), 7.20 (d,  $J = 16.6$  Hz, 1H), 7.08 (s, 1H), 6.78 (d,  $J = 8.9$  Hz, 2H), 3.01 (s, 6), 2.65 (s, 3H), 2.44 (s, 3H).  $^{13}\text{C}$  NMR (50 MHz, DMSO):  $\delta = 151.3, 129.1, 123.3, 112.2, 54.9, 18.7, 17.4, 16.6$ . MS (EI neat matter):  $m/z$  (%) = 519.1(100). Anal. Calcd for  $\text{C}_{23}\text{H}_{25}\text{BF}_2\text{IN}_3$ : C, 53.21; H, 4.85; N, 8.09. Found: C, 52.93; H, 4.56; N, 7.77.

**Compound (76)**

To a degassed solution of **9a** (0.100 g, 0.258 mmol) and the 1-ethynyl-4-nitrobenzene (0.057 g, 0.387 mmol) in benzene (3 mL) and TEA (3 mL), was added [Pd(PPh<sub>3</sub>)<sub>2</sub>Cl<sub>2</sub>] (0.011 g, 0.0129 mmol), CuI (0.003 g, 0.0129 mmol) under argon. The mixture was stirred at 60 °C for 12 hours until the complete consumption of the starting material was observed by TLC. The mixture was then evaporated, and purified by a chromatography on silica gel (CH<sub>2</sub>Cl<sub>2</sub>/petroleum ether, 5: 5). Then the recrystallisation from toluene affords **76** (20 mg, 21%). <sup>1</sup>H NMR (200 MHz, CDCl<sub>3</sub>): δ 8.21 (d, J = 8.6 Hz, 2H), 7.62 (d, J = 8.9 Hz, 2H), 6.16 (s, 1H), 2.67 (s, 3H), 2.65 (s, 3H), 2.58 (s, 6H), 2.46 (s, 3H). MS (EI neat matter): m/z (%) = 407.1 (100). Anal. Calcd for C<sub>22</sub>H<sub>20</sub>BF<sub>2</sub>N<sub>3</sub>O<sub>2</sub>: C, 64.89; H, 4.95; N, 10.32. Found: C, 64.59, H, 4.72, N, 10.06.

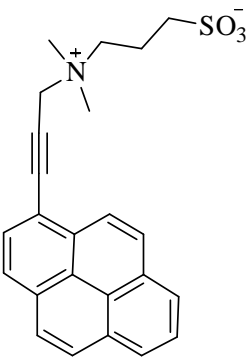
**Compound (77)**

Compound **76** (20 mg, 0.049 mmol) and 4-dimethylaminobenzaldehyde (8 mg, 0.054 mmol) were dissolved in toluene (5 mL) and piperidine (0.5 mL) in a Dean–Stark apparatus. The mixture was heated at 140°C for 2 h, then removed the Dean-stark apparatus and continued heating under Argon until the solvent was totally evaporated. The residue was purified by column chromatography on silica gel (CH<sub>2</sub>Cl<sub>2</sub>/ petroleum ether, 6: 4), afforded **77** (7 mg, 27%). <sup>1</sup>H NMR (200 MHz, CDCl<sub>3</sub>): δ 8.20 (d, J = 8.8 Hz, 2H), 7.61 (d, J = 8.7 Hz, 2H), 7.50 (d, J = 8.8 Hz, 2H), 7.44 (d, J = 15.3 Hz, 1H), 6.72 (d, J = 16.1 Hz, 1H), 6.68 (d, J = 8.4 Hz, 2H), 3.04 (s, 6), 2.70 (s, 3H), 2.64 (s, 3H), 2.56 (s, 3H), 2.49 (s, 3H). MS (EI neat matter): m/z (%) = 538.1(100). Anal. Calcd for C<sub>31</sub>H<sub>29</sub>BF<sub>2</sub>N<sub>4</sub>O<sub>2</sub>: C, 69.16; H, 5.43; N, 10.41. Found: C, 68.92, H, 5.35, N, 10.27.

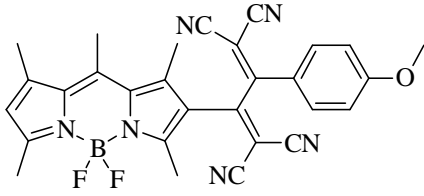
# Appendix

## A. Crystallographic data

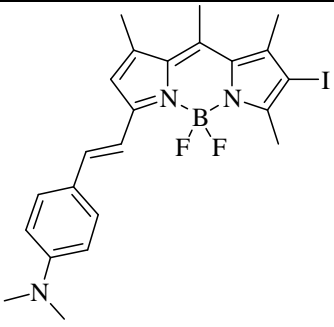
### Compound 21

|                      |  |   |
|----------------------|--|---|
| Formula sum          | $C_{24} H_{25} N O_4 S$  |  |
| Formula weight       | 423.51   |   |
| Crystal system       | orthorhombic   |   |
| Space group          | $P b c a$ (no. 61)   |   |
| Unit cell dimensions | $a = 7.517(2) \text{ \AA}$<br>$b = 19.331(3) \text{ \AA}$<br>$c = 28.791(4) \text{ \AA}$ |   |
| Cell volume          | $4183.65(140) \text{ \AA}^3$   |   |
| Z                    | 8  |   |
| Density, calculated  | $1.345 \text{ g/cm}^3$   |   |
| $R_{All}$            | 0.098  |   |
| Pearson code         | oP440  |   |
| Formula type         | NOP4Q24R25...  |   |
| Wyckoff sequence     | $c^{55}$   |   |

## Compound 68

|                      |   |  |
|----------------------|---|--|
| Formula sum          | $C_{29} H_{23} B F_2 N_6 O$   |  |
| Formula weight       | 520.34  |  |
| Crystal system       | monoclinic  |  |
| Space group          | $P 1 21/c 1$ (no. 14)   |  |
| Unit cell dimensions | $a = 7.0970(4) \text{ \AA}$<br>$b = 28.4679(13) \text{ \AA}$<br>$c = 14.2999(8) \text{ \AA}$<br>$\beta = 114.65(0)^\circ$ |  |
| Cell volume          | $2625.72(20) \text{ \AA}^3$   |  |
| Z                    | 4   |  |
| Density, calculated  | $1.316 \text{ g/cm}^3$  |  |
| $R_{All}$            | 0.144   |  |
| Pearson code         | mP248   |  |
| Formula type         | NO2P6Q23R29...  |  |
| Wyckoff sequence     | $e^{62}$  |  |

## Compound 75

|                      |   |   |
|----------------------|---|---|
| Formula sum          | $C_{23} H_{25} B F_2 I N_3$   |  |
| Formula weight       | 519.17  |   |
| Crystal system       | monoclinic  |   |
| Space group          | $P 1 21/c 1$ (no. 14)   |   |
| Unit cell dimensions | $a = 8.429(7) \text{ \AA}$<br>$b = 9.844(7) \text{ \AA}$<br>$c = 27.51(2) \text{ \AA}$<br>$\beta = 105.68(5)^\circ$ |   |
| Cell volume          | $2197.7(30) \text{ \AA}^3$  |   |
| Z                    | 4   |   |
| Density, calculated  | $1.569 \text{ g/cm}^3$  |   |
| $R_{All}$            | 0.071   |   |
| Pearson code         | mP220   |   |
| Formula type         | NO2P3Q23R25...  |   |
| Wyckoff sequence     | $e^{55}$  |   |

## B. Publication/Patent produced during the thesis

Water-solubilization and bio-conjugation of a red-emitting BODIPY marker.

Song Lin Niu, Cédrik Massif, Gilles Ulrich, Raymond Ziessel, Pierre-Yves Renard, and Anthony Romieu. *Org. Biomol. Chem.* **2010**, *9*, 66-69.

New insights into the solubilization of Bodipy dyes.

Song-Lin Niu, Gilles Ulrich, Pascal Retailleau, Jack Harrowfield and Raymond Ziessel. *Tetrahedron Letters.*, **2009**, *50* (27), 3840-3844.

Water-Soluble BODIPY Derivatives.

SongLin Niu, Gilles Ulrich, Raymond Ziessel, Agneta Kiss, Pierre-Yves Renard and Anthony Romieu. *Org. Lett.*, **2009**, *11* (10), 2049–2052.

Composés fluorescents hydrophiles à base de dipyrrométhène-bore.

Ulrich, G.; Ziessel, R.; Niu, Song-lin.; Haefele, A.; Bura, T.;  
French patent, PCT/FR2009/052606, 2009.